ISSN 1977-5296

ESARDA

European Safeguards Research and Development Association

Bulletin

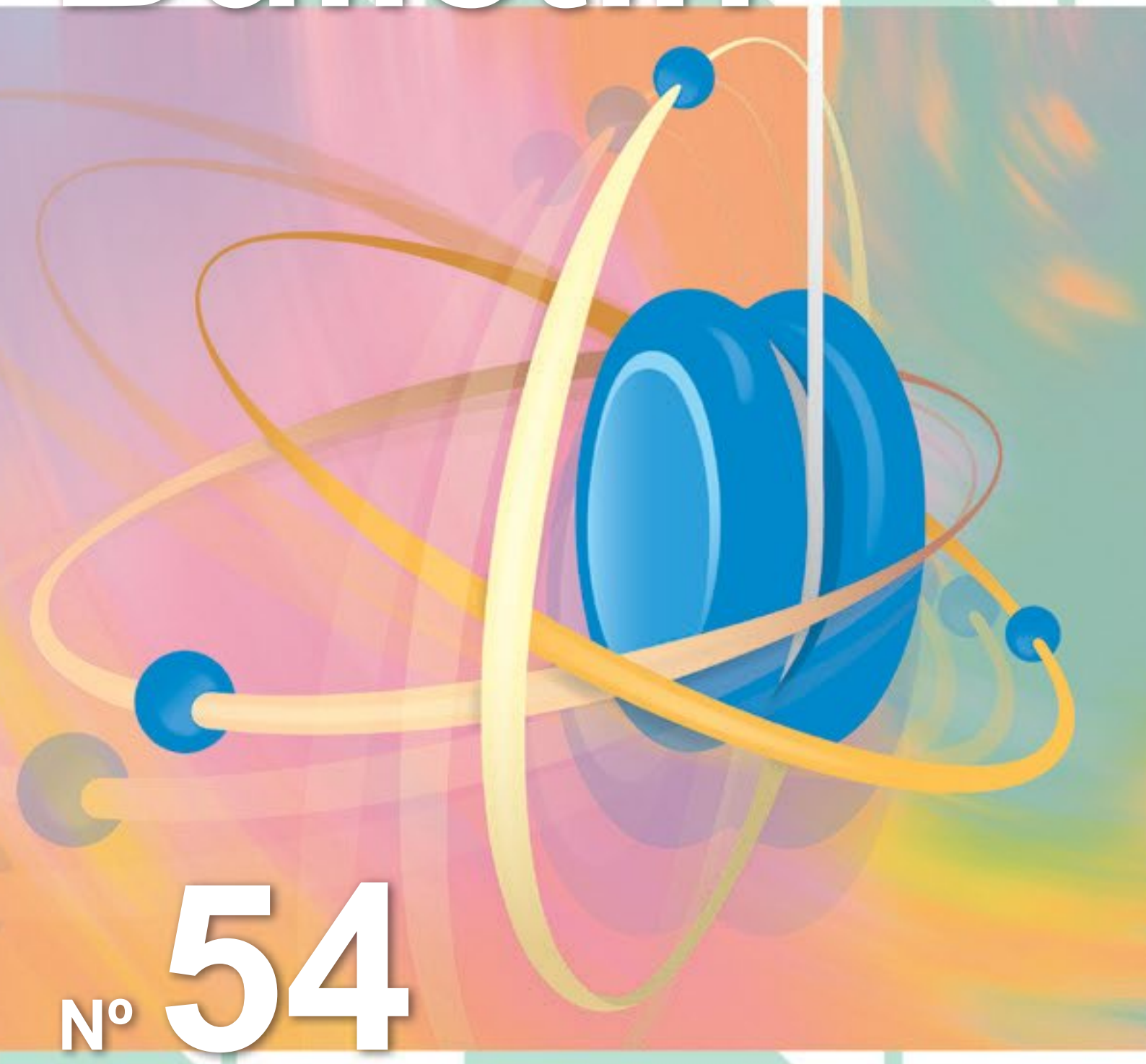

Nº 54

June 2017

ISSN 1977-5296

Number 54

June 2017

Editor

Elena Stringa and Hamid Tagziria

European Commission, Joint Research Centre,

ITU - Nuclear Security Unit

T.P. 800, I-21027 Ispra (VA), Italy

Tel. +39 0332-786182

Elena Stringa@ec.europa.eu

Hamid.Tagziria@ec.europa.eu

Cover designed by Laura Spirito, (JRC Ispra in Italy),

Printed by
IMPRIMERIE CENTRALE, Luxembourg

ESARDA

European Safeguards Research and Development Association

Bulletin

Table of Content Issue n° 54

Editorial

Hamid Tagziria

Dear colleagues,

As the ESARDA prepares to celebrate its 50th Anniversary in 2019 on the Lago di Maggiore in Italy, its journal resumes its strides to improve its quality and value to its readership and members by consolidating its peer review section while still reflecting an even wider and richer area of activities which are of interest to our communities.

We are pleased to present you with Issue 54, following a successful 39th ESARDA Symposium held in Dusseldolf (Germany) from 16th to 18th May 2017 and which had 19 sessions as diverse as:

- Implementation of Safeguards
- Non-destructive Analysis - Gamma measurements
- International collaborations
- Geoscientific methods
- Arms control and Nuclear Disarmament Verification I+II
- Geological repositories
- Non-destructive analysis: Neutron I+II
- Destructive Analysis I + II
- Spent Fuel Verification and Spent Fuel Transfer
- Training and Knowledge Management
- Non-destructive Analysis: Tomography
- Evaluation
- Containment & Surveillance
- Nuclear Security
- Process Monitoring
- Statistical Methodologies

The 39th ESARDA symposium was marked by a lively panel discussion “Reflecting on ESARDA’s future strategy direction” which will be followed by a dedicated meeting in Berlin in October 2017. A round table discussion on “20 years of the Additional Protocol” also took place in addition to the well-established and important ESARDA Working Group meetings.

As in previous issues of the journal, the papers of issue 54 resulted from those judged best in each session during Esarda symposium in addition to those independently submitted by their authors. All chairpersons had access to the papers in their session prior to the symposium allowing them to best select up to two best papers. Peer reviewing was carried out by independent experts in the field including members of the editorial committee where appropriate. At least two reviewers were used wherever possible. I am grateful to the authors for their contributions and to the reviewers for their great efforts in improving the quality of each paper published. The papers will be published in issue 54 and issue 55 depending on their progress with the review process. The bulletins can be downloaded from our newly redesigned web site and hard copies are posted to more than 1100 institutions, universities, libraries and individuals, free of charge.

Authors and experts are very much encouraged to:

1. Submit their work anytime during the year to EC-ESARDA-BULLETIN@ec.europa.eu using the ESARDA template (see https://esarda.jrc.ec.europa.eu) and giving the names and e-mail addresses of two potential independent reviewers
2. Cite the work published in the journal in order to increase the visibility, the citation and impact indexes of the journal which is most important to any evaluation process we may undertake.
3. Volunteer as potential reviewers by sending me an email to that effect specifying one’s area of expertise.

I am very pleased to announce that my colleague Elena Stringa had kindly agreed to join the ESARDA editorial committee and act as my co-editor to support the endeavor. I would like to thank Elena for her great support and dedication in the processes to produce this issue.

On behalf of the editorial committee, Elena and I would like to thank all authors and reviewers for their great work which allowed the publication of this important journal to continue with its new developments and improvements.

I am also pleased to announce that from 17-18th may 2018, the ESARDA Non-Destructive Assay (NDA) Working Group is organising an international workshop on the topics of computer simulation applied to the modelling of NDA instrumentation and methods for nuclear safeguards applications. The two days event aims at covering a broad range of topics and presents a unique opportunity for the safeguards community interested in recent advances and in lessons learned from practical cases. You are invited to present your work in the field of numerical modelling (details on https://esarda.jrc.ec.europa.eu)

Wish you all a very good and fruitful year.

Hamid Tagziria
Co-Editor and Editorial Committee Chairman
Website: https://esarda.jrc.ec.europa.eu

Contacts:
EC-ESARDA-BULLETIN@ec.europa.eu
elena.stringa@ec.europa.eu
hamid.tagziria@ec.europa.eu

Muon Tomography for spent nuclear fuel control

P. Checchia[1], F. Gonella[1], A. Rigoni[2], S. Vanini[2], G. Zumerle[2]

[1] INFN sezione di Padova Padova Italy
[2] Department of Physics and Astronomy, University of Padova, Padova, Italy

Abstract:

At present no validated methods to verify the content of Dry Storage Containers exist. The investigation profiting of cosmic muons may constitute a very effective method to detect or exclude the presence of spent fuel bundles. The layout of a possible detector and the techniques to provide the relevant information are described. A specific proposal to evaluate effects of surrounding radioactivity on detector performance is presented.

Keywords: muons tomography; spent fuel control; muon detectors

1. Introduction

Cosmic rays at sea level consist mainly of charged elementary particles called muons. Muons are produced by the decay of several types of very short-lived elementary particles, created in the upper part of the atmosphere by the interactions of primary cosmic rays, mainly protons or alpha particles, with atoms or molecules. Primary cosmic rays originate from galactic processes and thus their flux on earth is constant and isotropically distributed. At sea level the muon flux is about $10^4/m^2$/minute, with maximum intensity in the vertical direction and an approximate dependence on the zenith angle θ as $\cos\theta^2$. The cosmic muon energy spectrum is quite broad, with an average value of several GeV. Energetic muons can cross very thick layers of dense materials since they do not undergo nuclear interactions.

The use of the highly penetrative properties of cosmic-ray muons to explore inaccessible volumes has been proposed in the past [1], [2] and recently many efforts have been produced to demonstrate the potential of muon tomography in many application fields [3],[4]. A detailed review of possible applications can be found in [5].

2. Spent nuclear fuel inspection with cosmic muons

In the particular case of the dry storage containers (DSC), the approach to explore their content can profit of different physical processes occurring when muons cross the container. Firstly, since all the charged particles travelling in a medium lose energy as a function of the medium density, a fraction of muons is stopped inside the container. In addition, depending on the density and the atomic number of the crossed material, the muon trajectories undergo detectable deviations from the initial direction (multiple Coulomb scattering). These phenomena would give a threefold information on the content of the material inside the hidden volume provided a set of muon detectors could be installed around the container. In detail, cylindrical detectors can be placed around the lateral surface of the containers. They should measure the position and direction of the muons entering in the container. They should also measure position and direction of the particles that exit crossing the lateral surface of the container as shown in Figure 1.

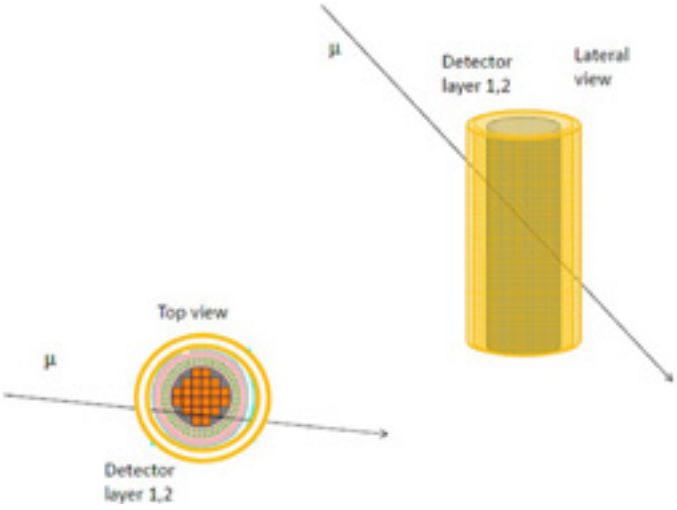

Figure 1: Sketch of a Muon Tomography station (not in scale) Top and lateral view.

With this configuration it is possible to know: i) the most probable path of muons that pass through the container; ii) most probable path of muons that should exit from the lateral surface but are absorbed; iii) the scattering angle of the passing-through muons.

The first two items contain a complementary information. Indeed, the abundance of passing-through particles is connected to spatial regions with light material (e.g. air), while the absorbed particles are located in correspondence to dense regions. In case of an inhomogeneous

material distribution (e.g. because a fuel bundle is missing) the first set of data would show an excess of particles with a path crossing a large fraction of the light material region. At the opposite, the absorbed particles whose trajectory points to the light material region would be less copious, since they have a smaller probability to stop inside the container.

The measurement of the muon scattering angle allows to determine a two or three-dimensional image of the container. The image reproduces the spatial distribution of a quantity, the linear scattering density, that is roughly proportional to the product of the material density times its atomic number. This method requires a complex formalism and noise filtering techniques as described in [6], [7].

In more detail, to obtain a three-dimensional distribution of the material linear scattering density in the inspected volume, the space is divided into finite volume elements called voxels. The density is assumed to be uniform in the single voxel. It is important to stress that the particular geometry of the inspected volume and the well-known shape of the fuel bundles, allow the choice of voxels with vertically-elongated geometry. This results in a small size set of voxels, high statistics as regards muons per voxel, and low inspection time required.

2.1 Results with simulated data

It is possible to produce a realistic simulation of an inspection system and to obtain simulated cosmic-muon data in a situation similar to the one sketched above. The simulation software chain is based on GEANT4 package that is designed for modeling a broad range of particle processes and their interaction with matter and it is used in a variety of applications, including High Energy Physics (HEP), nuclear physics experiments, astrophysics, space science and medical physics [8]. In the present environment, the simulation includes the generation of cosmic-muon spectrum, the description of the muon detectors and the tracking of muons through a DSC. Several sets of data can be produced simulating different detectors and different containers. For each configuration, datasets with the presence of all the foreseen fuel bars and others with missing bars can be produced.

Using GEANT4, a complete CASTOR® container with and without a missing bar placed in different positions has been simulated. The simulated container is approximately a 4.9 height cylinder with a 2.3 m diameter exposed to cosmic muons with vertical axis. The main container material is steel, while the fuel bars are assumed to be bundles of zirconium cylindrical tubes filled up with Uranium Oxides. The simulation includes a cylindrical detector placed around the CASTOR, covering its entire lateral surface.

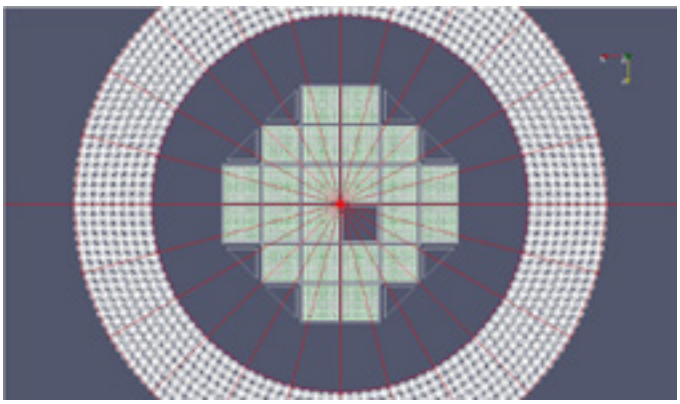

Figure 2: Top- view of a drift tube detector placed around a CASTOR® container with a missing fuel bar.

The detector is composed by 8 layers of cylindrical drift tubes. Figure. 2 shows the top view sketch of the simulated CASTOR.

In this paper the analysis of the simulated data used a very simple algorithm based on weighted count of muons crossing each voxel Results about the detection of a missing bar in a CASTOR container, for simulated samples corresponding to three hours of cosmic-muons data taking, are shown in Figure 3. On the left there is the reconstructed CASTOR density average along vertical axis, obtained using information from absorbed muons. They are particles which are detected before entering the container with a precise trajectory reconstruction but which are not releasing any signal in correspondence to their expected position at the exit. The right image shows the result obtained with the complementary set of data when muons releasing signals on the opposite sides of the container are analyzed. The figures are the difference between the images obtained from the CASTOR under examination and reference images, obtained analysing a container without missing bars The images are obtained by averaging over the vertical axis 2 cm size voxels. This comparison with reference images is not strictly necessary but it is used to improve the contrast. The missing bar is clearly visible with both techniques and it can be seen with poorer resolution also with one hour data taking. Given the large size of CASTOR containers, comparable or even better results can be reasonably expected for other types of containers. Reconstructions based on more sophisticated algorithms or on scattering measurement are not considered in this analysis. The eventual addition of scattering-based results would improve the reliability of the technique.

These results are based on the simulation of a DSC without any nuclear activity and radioactivity emission. In real case, canisters with spent nuclear material emit gamma and neutrons that could interfere with the cosmic muons detection.

Figure 3: Top-view of the reconstructed CASTOR® density, averaged over vertical axis, obtained using absorbed muon (left) and passing-through muon information (right). The simulated container has one missing bar. Both images are the difference between the images obtained from the CASTOR under examination and reference images, obtained analysing a container without missing bars. The container structure including the bar grid is added for reference.

3. An operative proposal

While the perspectives of a system based on cosmic-muon tracking used to provide an effective control are encouraging, several concerns could arise from the environmental radioactivity in proximity of a DSC and the consequences on the muon detector response.

3.1 Detector layout for canister inspection

It has been shown that one of the cheapest way to provide muon detection with good tracking capability and large area coverage is based on drift tube technology [9],[10],[5].

As sketched in Figure 2, an ideal detector could be realised by several circular layers of drift tubes surrounding the cylindrical container. Muons crossing the tubes before entering the container and, if not absorbed, after exiting, release with large efficiency a hit in each crossed tube. It is then possible to have a good tracking of particles with a hit multiplicity that can be as large as twice the number of circular layers.

However, the presence of an intense radioactivity produced inside the container and reaching the detector can induce a number of signals with a frequency and an occupancy that could, in principle, spoil the detector performance. To quantify this effect, it is necessary to quantify the activity and the impact of its components on the detector. It is therefore not straightforward to clarify this point until several details will be available. In particular, to include the radioactivity in the GEANT4 simulation would require a precise model of the emission rate and energy, to be validated with measurements.

In any case, even if it has been demonstrated that the proposed type of detectors can be operative in presence of high radioactivity, the best way to prove their response in problematic environmental conditions is to perform a dedicated test.

3.2 A detector for a dedicated test

The proposed test consists in producing a small prototype of drift tube detector with a reasonable number of channels to measure properly a cosmic muon track and sufficiently light to be moved and transported in proximity of a DCS. The detector should be capable to self trigger the data recording in the event of a muon passage. Once positioned in proximity of a DSC, the response of the prototype in presence of the radioactivity could be easily monitored. In particular, it could be proved that the tracking capability is maintained even with the coincidence of several additional hits induced by photon conversion or nucleon interactions in some of the tubes of the detector.

The design of such a prototype is shown in Figure 4 and consists of 8 layers of 8 drift tubes each for a total of 64 channels. Each drift tube is realised with a 50 mm diameter Al tube, 1.5 mm thick and a length of 2 meters which is sufficient for the proposed test. The tubes are equipped with a 100 μm anodic wire, connected to a High Voltage supply (~3000 V), to produce a radial electric field and the necessary multiplication of the charges released by incident muons. The collected signal is then amplified and shaped by the front end (FE) electronics and then processed (time digitalization, trigger and remote transmission) by the readout block. The tubes are operated with a gas mixture (*Ar*85%/$CO_2$15%) that should not present any safety issue.

The total size of the prototype, including mechanical supports, would be about 0.6 m x 0.5m x 2 m, with a total mass of about 100 kg. A sufficient number of tubes have been produced so far by the Padova group in the INFN National Laboratory of Legnaro (LNL), as shown in Figure 5. To complete the prototype, it is then sufficient to assembly the cells and to equip the detector with HV and FE electronics and to complete the gas distribution system. A read-out system based on field-programmable gate array

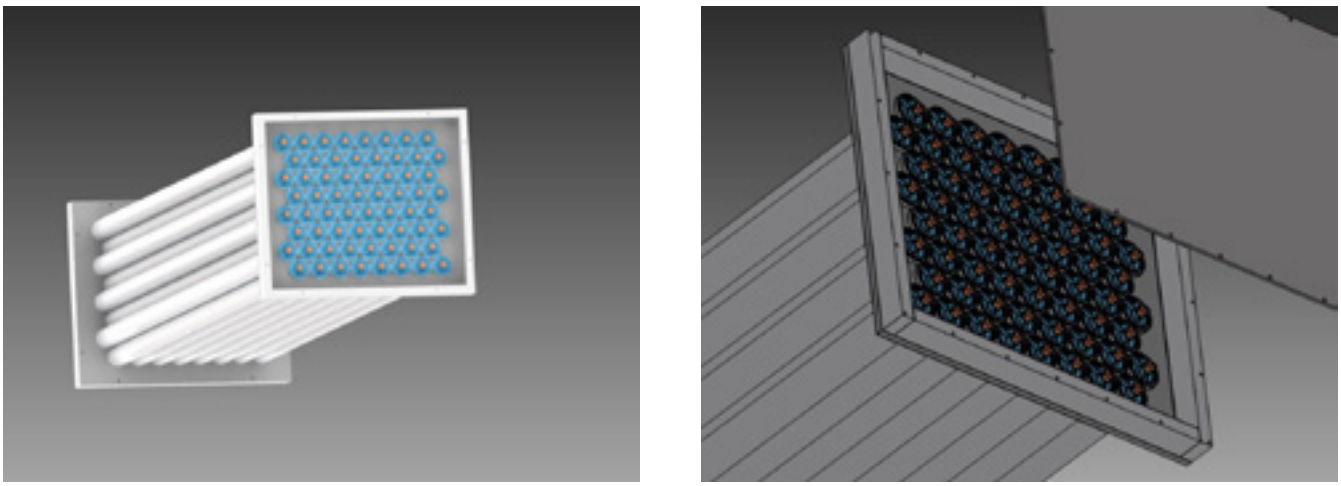

Figure 4: Schematic view of a drift tube prototype detector (left). A detail of the front-end side of the tubes (right).

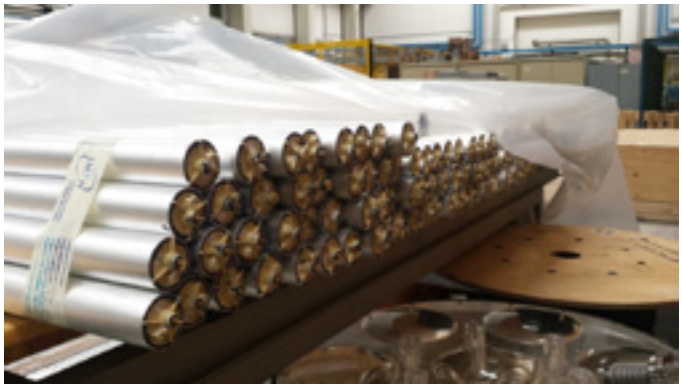

Figure 5: Set of 2m long drift tubes produced in LNL INFN laboratory.

(FPGA) circuits installed in the detector and remote data transmission to an on-line computer is foreseen. The whole electronic chain has been developed for the muon chambers produced for the CMS experiment at CERN-LHC [11] and is available to realize the prototype. Although not strictly necessary for the proposed test, the detector can be instrumented to measure also the coordinate parallel to the wire direction, as required by a complete detector devoted also to 3D imaging reconstruction.

The time needed for an "on site" test would require a couple of days for far (low radioactivity) and near DSC data taking.

4. Conclusions

The volume reconstruction using cosmic muons represents a promising technique for spent nuclear fuel control inside Dry Storage Canisters. It could ensure an effective inspection of the content of disposal canisters after closure. Remaining doubts about the detector capability to operate in presence of radioactivity can be quickly understood with a simple test in proximity of a real canister. A detector prototype for this kind of tests is proposed.

5. Acknowledgements

The authors would like to acknowledge the important help received from Paolo Peerani and Hamid Tagziria, respectively, at the early and at the present stage of this work. This work has been supported by the INFN_E project of INFN.

6. References

[1] E.P. George, *Cosmic rays measure overburden of tunnel*, *Commonwealth Engineer* (1955) 455.

[2] L.W. Alvarez et al., *Search for Hidden Chambers in the Pyramids*, *Science* **167** (1970) 832.

[3] K.R. Borozdin et al., *Surveillance: Radiographic imaging with cosmic-ray muons*, *Nature* **422** (2003) 277.

[4] S. Pesente et al., *First results on material identification and imaging with a large-volume muon tomography prototype*, *Nucl. Instrum. Meth.* **A 604** (2009) 738.

[5] P. Checchia, *Review of possible applications of cosmic muon tomography, JINST* **11** C12072 (2017)

[6] L.J. Schultz et al., *Statistical reconstruction for cosmic ray muon tomography*, *IEEE Trans. Image Process.* **16** (2007) 1985.

[7] M. Benettoni et al., *Noise reduction in muon tomography for detecting high density objects*, 2013 *JINST* **8** P12007

[8] GEANT4 Collaboration, "*GEANT 4 – a simulation toolkit*", *Nucl. Instrum. Meth. A* **506** (2003) 250

[9] https://www.decisionsciences.com/

[10] http://mutomweb.pd.infn.it:5210/

[11] CMS collaboration, *The CMS experiment at the CERN LHC*, 2008 *JINST* **3** S08004.

A Comparison of Approaches to Determine Dead Time Parameters Using a Boron-Coated-Straw High-Level Neutron Coincidence Counter

A.T. Simone[1, 2], S. Croft[2], A. Favalli[3], and J. P. Hayward[1, 2]

[1] University of Tennessee, Department of Nuclear Engineering, 308 Pasqua Engineering Building, Knoxville, TN 37996, USA.
[2] Safeguards & Security Technology, Nuclear Security and Isotope Technology Division, Oak Ridge National Laboratory, One Bethel Valley Road, PO Box 2008, MS-6166, Oak Ridge, TN 37831-6166, USA.
[3] Safeguards Science & Technology Group, Non-proliferation and Nuclear Engineering Division, Los Alamos National Laboratory, MS E540, Los Alamos, NM 87545, USA.

Abstract:

When characterizing a neutron coincidence counter for use in international safeguards, it is important to understand the dead time of the system. With current data acquisition in the form of shift register logic, there are several options to determine effective dead time model parameters. A customary approach consists of incrementally overwhelming the detection system with various sources to generate different count rates for analysis. An empirical fit to these data can then produce a dead time parameter. This method makes use of the expectation that the doubles to singles count rate ratio, after dead time correction, should remain fixed. In our measurements, we begin with a single ^{252}Cf source and successively combine it with 1, 2, 3, and 4 AmLi (α,n) sources. The time-correlated fission neutrons from the ^{252}Cf are detected by the neutron coincidence counter, and the random-in-time neutrons produced from the multiple AmLi sources provide excess counts to trigger on. Another recently reported approach [12] consists of utilizing the neutron-count number distribution, for a number of counting cycles, to permit a statistical analysis and subsequent determination of the dead time along with a robust estimate of the statistical uncertainty. Moments of several orders can be used; therefore, several estimates of the effective dead time parameter are obtained. In the results reported here, two and four AmLi sources are measured simultaneously within the well of the counter for a number of cycles. We have selected 24 cycles of 300 s each, with predetermined timing gates, where detected neutron multiplicities can range up to approximately 10 neutrons per cycle. These two methods were tested at Oak Ridge National Laboratory using a Boron Coated Straw High-Level Neutron Coincidence Counter, but the methods are also applicable to ^{3}He counters. In this paper, we compare the results of these approaches and discuss the relevance of both.

Keywords: Dead time correction; boron coated straws; high-level neutron coincidence counter; neutron coincidence counting; shift register

1. Introduction

Neutron coincidence counting is widely used in international safeguards applications for the nondestructive assay of nuclear material. Common thermal neutron coincidence and multiplicity counters take the form of an annular body filled with a moderator and populated with ^{3}He tubes, which surround a central well used for sample loading. When a sample undergoes fission, each event produces a simultaneous release of neutrons, the average number of which are characteristic of the sample's isotopics, which travel through the well of the detector and into the moderating body. These time-correlated neutrons are slowed in the moderator, spreading out this distribution over a longer period of time; this time is related to the neutron die-away time. The die-away time is characteristic of the geometry of the detector, and it cannot be altered. These thermalized neutrons are then captured in the ^{3}He tubes and can be detected, by software, in coincidence and higher order multiplicities using appropriate timing gates. The total number of neutron events measured is recorded as the singles count rate. The doubles count rate corresponds to two related neutrons detected within a specified time gate, and the triples count rate corresponds to three related neutrons within that gate. However, in addition to these fission neutrons, background and (α, n) neutrons can also be detected within these timing gates, generating artificial multiplicities mistaken as multiplicities related to fissions in the sample.

Each neutron interaction produces a pulse in the electronics connected to the ^{3}He tube, and the tube system is then dead for some amount of time. This means that any neutrons captured during this dead period are not counted and do not contribute to the total neutron pulse train. The dead period is related to the processing and recovery time of the electronics used and applies to each of the tube and electronic systems. Because the signals from each system are summed together in a total output, a total detector system dead time can be determined. For systems with several detector bank channel outputs, dead times for the individual channels can also be determined.

Neutron coincidence and multiplicity counting depend on the accurate measurement of these fission neutrons as a function of time to correctly determine the quantity of nuclear material within the measured sample [1, 2]. These distributions of neutrons are perturbed due to this dead time, thereby influencing assay values. Because detection systems cannot be 100% efficient, nor will every

emitted neutron travel towards the moderated detector body, corrections are applied for neutron losses. In addition, another correction for the dead time related losses in the system is required. This value must be well-known to accurately adjust the measured neutron multiplicity rates for the true multiplicity rates.

Previous work has been done to determine the dead time of neutron coincidence counting systems and to characterize how this affects the incoming neutron pulse trains. The long-standing and widely used approach is extended to higher order multiplicities by Dytlewski [3] and is applied to safeguards systems, including High Level Neutron Coincidence Counter designs [4, 5], assuming a paralyzable (or updating) dead time model. The paralyzable model assumes that not only will a neutron captured during the dead period of the tube not be counted towards the total neutron pulse train, but that neutron event will extend the dead period. Although this model has been assumed for neutron coincidence counting, it has not been fully verified. The common experimental approach to measure the dead time uses multiple ^{252}Cf sources of increasing strength to determine two dead time parameters, which will be explained in detail later. Another approach utilizes random-in-time neutrons produced by AmLi (α, n) sources— in conjunction with a single ^{252}Cf spontaneous fission neutron source— to increase the uncorrelated single neutron events while maintaining the doubles neutron rate; this method was employed for this paper. Many others have built upon these methods by deriving alternative approaches to singles dead time corrections [6, 7] and investigating the effect of correlation in the neutron pulse train due to varying sources [8, 9], while also trying to simplify the theory and expressions for easy adaptation. However, the final expressions and implementation of the theory to experiment are complex, and as a result have not been adopted in favor of older simplifications.

Using the approach laid out by Menaa [10], based on the theory outlined by Foglio Para and Bettoni [11], random-in-time neutrons produced by AmLi sources are used to obtain a neutron-count distribution. Then, using the methodology outlined in [12], a statistical analysis is performed on this distribution over many cycles. With this analysis, the dead time parameters for second, third, and fourth order factorial moments can be determined, enabling an inter-comparison of values from a single data acquisition. These multiple samplings also allow for a robust estimate of the statistical uncertainty.

The importance of this method from a safeguards inspection perspective relates to the availability of sources for in-field measurements; AmLi sources are present for active interrogation in neutron coincidence or multiplicity counters. Meanwhile, it is not uncommon for a facility under inspection to not have ^{252}Cf at that location. Compared to the traditional method, the AmLi sources allow for shorter acquisition times with similar precision, and they do not have to be replaced as frequently due to the long half-life of Am isotopes. This work summarizes both the traditional approach and the new statistical approach and compares the two using data obtained using a boron-coated-straw (BCS) High-Level Neutron Coincidence Counter (HLNCC).

2. Experimental Setup

The BCS HLNCC was built by Proportional Technologies, Inc. (PTI) as a prototype ^{3}He alternative neutron coincidence counter. This prototype was designed to meet the specifications and performance objectives set for evaluation against other systems at an international workshop searching for a drop-in ^{3}He replacement [13]. Because of this, the BCS HLNCC was built as an aluminium-encased cylindrical high density polyethylene (HDPE) body measuring 34 cm in diameter and 68.2 cm in height (Figure 1a), preserving the dimensions of the ^{3}He-based HLNCC-II. The sample well is 17 cm in diameter and 41 cm in height and is sealed with top and bottom end plugs made of HDPE and aluminium. The main differences between the standard system and BCS system are a 6 kg increase in mass and the use of ^{10}B rather than ^{3}He for the neutron capture reaction.

The 18 ^{3}He tubes from the standard HLNCC-II were substituted for 804 ^{10}B straws, each measuring 4.4 mm in diameter, evenly dispersed throughout the HDPE body. The 96% enriched $^{10}B_4C$ coats a 2 μm thickness on the inside of aluminium or copper tubes, which are filled with a mixture of CO_2 (10%) and Ar (90%) at 1 atm [14-16]. The incident neutrons interact with the ^{10}B, releasing an alpha particle and ^{7}Li ion, which ionize the gas as they travel. Because this method of charge collection is similar to the method exploited in ^{3}He tubes, similar electronics and software can be used for both technologies. There are six detector banks, of 134 tubes each, connected and processed by six amplifiers. A conversion box consisting of inputs (Figure 1b), outputs (Figure 1c), and a field-programmable gate array (FPGA) module shapes the incoming pulses and amplifies them to produce the correct form for an output signal trigger to be used with shift register or list mode acquisition software (Figure 1d). An external power supply provides the +5 V needed for the detector.

A list mode data acquisition system, Pulse Train Recorder-32 (PTR-32) [18], was used with the BCS HLNCC to bias, record, and analyze the neutron pulse train for each of the detector bank channels (Figure 1d). Because previous data taken with the PTR-32 have shown to be in agreement [19] with data taken with a JSR-15 shift register [20], the two were used interchangeably. PTR-32 can produce output files in a form similar to those output by

Figure 1a-1d. Left to right: The BCS HLNCC showing (a) the six detector bank outputs; (b) the BCS HLNCC-specific conversion box containing electronics to shape and amplify the output signals, resting on the external power supply used for the +5 V; (c) the output signal cables of the conversion box; and (d) PTR-32. See text for details.

the International Atomic Energy Agency (IAEA) Neutron Coincidence Counting (INCC) Program, including a neutron count distribution per every cycle recorded, in addition to neutron multiplicity analysis. PTR-32 can perform analysis using shift register logic when the user specifies predelay, gate width, and long delay time windows. As an added benefit, PTR-32 can perform this analysis for each individual detector channel connected to 1 of the 32 inputs on the board from a single measurement. The BCS HLNCC was biased to the standard setting of +850 V, and PTR-32 was set to analyze using the previously-determined optimal timing gates of 2 μs for the predelay, 48 μs for the gate width, and 4096 μs for the long delay for these measurements.

3. Traditional Dead Time Approach

As previously mentioned, the traditional and most commonly used approach for determining detector dead time was established decades ago, and extended to greater multiplicities by Dytlewski in 1990 [3], assuming a paralyzable dead time model. This methodology was then applied for use in neutron coincidence counters such as the ^{3}He-based HLNCC models [4, 5]. The combination of these works implement the following equations for the doubles (D) and singles (S) dead time correction factors (CF):

$$CF_D = e^{\delta_R \cdot S_m} = e^{(a+b \cdot S_m) \cdot S_m} \quad (1)$$

$$CF_S = e^{\delta_T \cdot S_m} = e^{\frac{1}{4}(a+b \cdot S_m) \cdot S_m} = CF_D^{\,1/4} \quad (2)$$

where δ_R is the dead time for the doubles, δ_T is the dead time for the singles, S_m is the measured singles rate, and *a* and *b* are the dead time parameters which are empirically determined for a specific detection system. Equation 1 represents the dead time correction factor for the doubles rate, and Equation 2 represents the dead time correction factor for the singles rate. The free parameters *a* and *b* are determined by a quadratic fit to doubles count rate data as a function of increasing singles rate. It is common for detectors of the same model to keep the ratio of a/b constant across all production, aiding in this analysis. The dead time-corrected rates can then be found by multiplying the measured rate for the respective multiplicity by the appropriate correction factor.

Data can be obtained using multiple ^{252}Cf sources of increasing strength, or with a single ^{252}Cf source in combination with random-in-time neutrons produced by AmLi sources to provide a range of count rates. The number and/or strength of the sources chosen should correlate with the full count range expected to be measured. Because the first method uses only ^{252}Cf point-like sources, there is no significant multiplication nor (α, n) contribution, and so the multiplicity ratios of triples to doubles (T/D), triples to singles (T/S), and doubles to singles (D/S) should all be constant and independent of the source strength once dead time corrected. This allows the dead time parameters to be determined and adjusted by minimizing the chi-squared value from each of these ratios.

For an uncorrelated neutron source, where the emitted neutrons have no time-dependent pattern (as a fissionable source would have), there is a very low probability that emitted neutrons will be counted in doubles or triples. Therefore, the (Reals + Accidentals) count rate should be approximately equal to the (Accidentals) count rate illustrated in the Rossi-Alpha distribution below (Figure 2). The second experimental approach to the traditional method uses a number of AmLi sources with a single ^{252}Cf source to incrementally overwhelm the detection system to generate different singles count rates for a similar analysis. This method benefits from the convenience and availability of using one ^{252}Cf source, while still having the ability to determine the dead time corrections for both the singles rate and the doubles rate. This is the method used in this section for analysis.

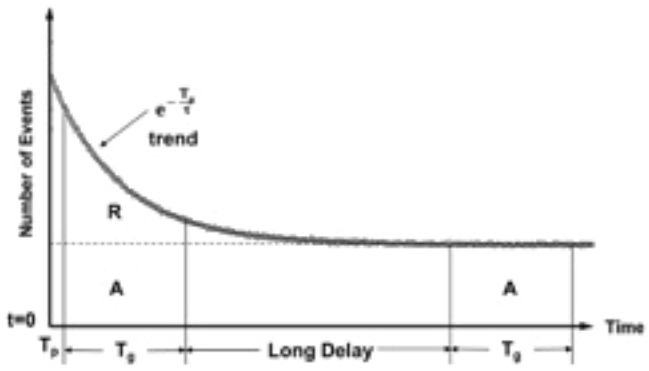

Figure 2: A Rossi-Alpha distribution illustrating the various gates used in shift register analysis and their chronological positions on the neutron pulse train.

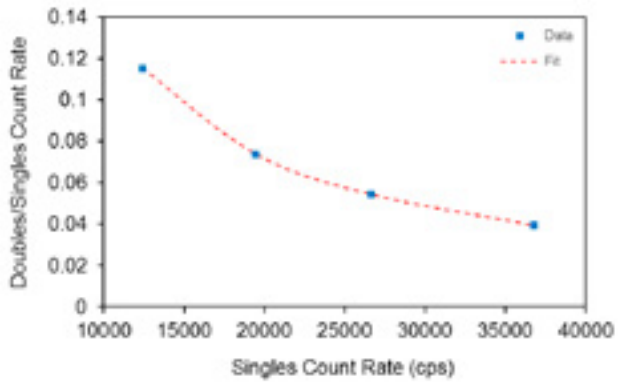

Figure 3: A plot of the measured Doubles to Singles count rate ratio as a function of the measured singles count rate. An empirical fit used to determine the dead time parameters is shown as the dotted red curve. The error bars are smaller than the markers.

A newly-acquired NIST-traceable ^{252}Cf source, with a known neutron emission rate around 94,000 cps and 1.10% relative standard error, was placed in the center of the BCS HLNCC. Two different metal cans were used to hold the ^{252}Cf and the AmLi sources: the ^{252}Cf was placed just below the middle plane of the BCS for optimal efficiency, and a second, slightly taller, metal can was placed over this and served as a stand for the AmLi sources. The ^{252}Cf source and the metal cans remained stationary throughout the entire experiment to ensure that no associated systematic errors were introduced. Using the experimental setup described here, a 120 minute acquisition, using only the ^{252}Cf source, was obtained to ensure good counting statistics on the doubles count rate. The total detector signal was collected along with the six individual channel neutron pulse trains, as a result of using the PTR-32. In this work, we only analyze the total detector signal, but the same procedure would apply when analyzing each of the channels. The next measurement taken was of ^{252}Cf along with two AmLi sources. These two AmLi sources had measured strengths around 7,300 cps with a count rate uncertainty of 0.11% with the selected timing gates. Because of the greater singles count rate, the acquisition time for this data collection was reduced to 30 minutes. A third AmLi, with a measured strength around 10,200 cps and a count rate uncertainty of 0.11%, was then added. Data were taken again for 30 minutes. A fourth, and final, AmLi source, with similar strength to the third, was then added. For this run, the acquisition time was increased to 45 minutes to give a greater certainty of the count rate, as this is crucial for producing an accurate fit.

These files were then analyzed in PTR-32 with the standard 2 μs predelay, 48 μs gate width, and 4096 μs long delay in order to find the singles and doubles count rates for each of these runs. This method is the same as the analysis performed using a shift register. Figure 3 shows a plot of the ratio of doubles to singles count rates as a function of singles count rate with the dotted empirical fit reflecting the ratio of the dead time-corrected rates using Equations 1 and 2 above.

The method described above is not robust under our experimental conditions, as it relies on the user to manipulate the terms by hand to produce the best fit. This method is also sensitive to the number of data points acquired, thereby increasing the total experimental time and number of sources needed for a more accurate result. Because of this, there can be several values which minimize the sum of squared errors of the deviation between the dead time corrected doubles to singles ratio to the uncorrected ratio with respect to a and b. For a set of standard counters, the ratio of b / a has typically been determined previously using a large number of ^{252}Cf sources; but for this new BCS HLNCC, there is no predetermined ratio. Instead, assuming that $b = \frac{a^2}{4}$ as outlined in the literature [6,7], the fitting parameters were found to be $a = 6.53 \cdot 10^{-8}$ and $b = 1.066 \cdot 10^{-15}$, resulting in an average dead time of (0.0653 ± 0.0054) μs. The uncertainty in this value was determined through chi squared analysis of minimizing the sum of squared error and is relatively large due to the reasons discussed previously. Next, b was constrained to 0 and a was found to be $6.199 \cdot 10^{-8}$ producing a dead time of (0.0620 ± 0.0077) μs. The dead time values found are within error using the different empirical approaches, due to the insensitivity of the equations to b over a wide range of values.

A note to the reader: in the first work characterizing the BCS HLNCC [17], it was stated that the dead time parameters were $a = 0.55 \cdot 10^{-6}$ and $b = 0$ using ^{252}Cf sources. For the sources measured at PTI, these values were selected as the best fit for the D/S ratio allowing a constant value, independent of the source strength, once dead time corrected. However, only three sources of a limited count rate range were used, therefore influencing the accuracy of the fit. Also, these values applied to a measurement using only a single detector bank rather than the total six banks combined for the total detector output. As expected, when the whole system was measured for this paper, the total detector dead time decreased.

4. Neutron Count Distribution Dead Time Approach

Menaa et al [10] outlined and experimentally justified an alternative method to the traditional approach. It was proposed that dead time could also be experimentally estimated using random-in-time neutrons produced by a source such as AmLi, to generate an uncorrelated neutron count distribution. The equations presented in [11], under the assumption of a paralyzable not-free (the system starts counting the initial neutron pulse while it may be dead) detector, represent the mean value of the count distribution and the variance of that distribution. They are then used by Menaa et al. to derive expressions for the dead time, δ, in terms of the gate width, T_g, and the statistics of the neutron count distribution:

$$\varphi = 1 - \sqrt{1 - \left[\frac{\langle i\rangle - \sigma_i^2}{\langle i\rangle^2}\right]}; \varphi = \frac{\delta}{T_g} \tag{3}$$

with i representing the mean value of the neutron count distribution as

$$\langle i\rangle = \frac{\sum_i i \cdot A_i}{\sum_i A_i} \tag{4}$$

and σ_i^2 representing the variance of the distribution as

$$\sigma_i^2 = \frac{\sum_i [i - \langle i\rangle]^2 \cdot A_i}{\sum_i A_i}. \tag{5}$$

Through simple measurement of an AmLi source, all necessary variables can be obtained in a short period of time.

Croft et al. [12] reviewed this method in detail, and built upon this work to extend the same methodology to higher order moments of the neutron count distribution. The expressions derived for the third and fourth reduced factorial moments,

$$\varphi = \frac{1}{2}\left[1 - \sqrt[3]{\frac{\langle i(i-1)(i-2)\rangle}{\langle i\rangle^3}}\right] \tag{6}$$

and

$$\varphi = \frac{1}{3}\left[1 - \sqrt[4]{\frac{\langle i(i-1)(i-2)(i-3)\rangle}{\langle i\rangle^4}}\right] \tag{7}$$

respectively, can all be determined from a single measurement. It was proven that the dead times determined from each of these expressions were consistent within counting precision. All three values are reported below.

Because the bias,

$$Bias = 100\left[\frac{\langle i\rangle_{R+A}}{\langle i\rangle_A} - 1\right], \% , \tag{8}$$

should be approximately zero for an uncorrelated neutron source, the neutron count distributions should be roughly equal between the (Reals + Accidentals), or (R + A), and the (Accidentals), or (A), gates (as illustrated in Figure 2). To test this theory, the (R+A) and (A) neutron count distributions were analyzed separately to produce individual dead time values, checked for bias, and then combined into a single 48 cycle data set for an additional dead time determination.

Twenty-four cycles of 300 s data acquisition runs were taken to randomly sample the neutron count distribution, produced by the AmLi sources previously listed, a large number of times. The AmLi sources were centered vertically and radially within the well to load an approximately even count rate on each of the six detector banks. Two separate acquisition runs were taken, one using two AmLi sources for a combined measured singles count rate of approximately 14,000 cps with a standard error of 0.02%, and the other using all four AmLi sources for a combined measured singles count rate of 33,500 cps with a standard error of 0.016%. The optimal detector parameters were set at 2 μs for the predelay, 48 μs for the gate width, and 4096 μs for the long delay. The total neutron pulse train recorded in PTR-32 was exported to INCC format to produce the count distributions. As is customary with shift register electronics and INCC software, the neutron distributions in each of the cycles are reported as a function of multiplicity for both the (R+A) and (A) gates. These count distributions were analyzed using the second, third, and fourth order moment expressions to determine the dead time and the bias. The results are reported below in Tables I-III.

Number of Sources	δ(R+A) (μs)	±	δ(A) (μs)	±	δ(Combined) (μs)	±	Bias (%)	±
2	0.0669	0.0050	0.0657	0.0054	0.0663	0.0036	0.0008	0.0197
4	0.0641	0.0015	0.0652	0.0018	0.0646	0.0012	0.0060	0.0069
Average	0.0655	0.0052	0.0654	0.0057	0.0654	0.0038	0.0034	0.0209

Table I: Total detector dead time values calculated using the second order factorial moment

As expected, there is less uncertainty in the dead time calculated for the measurement using four AmLi sources rather than just two sources, due to better counting statistics. However, as is typical for in-field measurements, two AmLi sources may be more readily available and still provide accurate evaluations of the detector dead time. The bias is consistent with 0, the individually calculated dead time values are consistent within counting precision across sources, and therefore, the average dead time values between (R+A), (A), and combined gates are also in agreement.

Number of Sources	δ(R+A) (μs)	±	δ(A) (μs)	±	δ(Combined) (μs)	±
2	0.0639	0.0069	0.0723	0.0063	0.0681	0.0047
4	0.0632	0.0019	0.0635	0.0018	0.0634	0.0013
Average	0.0635	0.0071	0.0679	0.0065	0.0657	0.0049

Table II: Total detector dead time values calculated using the third order factorial moment

Number of Sources	δ(R+A) (μs)	±	δ(A) (μs)	±	δ(Combined) (μs)	±
2	0.0603	0.0111	0.0711	0.0086	0.0657	0.0072
4	0.0598	0.0029	0.0609	0.0026	0.0604	0.0020
Average	0.0600	0.0115	0.0660	0.0090	0.0630	0.0075

Table III: Total detector dead time values calculated using the fourth order factorial moment

As the ordered factorial moments increase, the uncertainty in the dead time parameter increases due to the lower precision of higher neutron multiplicity rates. Because an uncorrelated source is used, higher order multiplicities are not likely to be detected with this count rate. Despite this, all three expressions result in values that are in agreement within counting precision. This result verifies, using another detector model than was used by Croft et al. [12], that this approach is robust and appropriate for estimating the dead time of a system.

5. Conclusion

The comparison of dead times determined from both the traditional and statistical methods are shown below in Table IV. The traditional approach values are reported for two different empirical fits: where $b = \frac{a^2}{4}$ and when b was constrained to zero. The second order (R+A) and (A) combined gate average dead time value, obtained from both the two source and four source measurements, are reported for this comparison. The values are in agreement within uncertainties. It is evident that the uncertainty in the neutron count distribution analysis approach is much less than the uncertainty associated with the traditional approach. This is due to the insensitivity of the equations to b over a wide range of values and the number of experimental data points used to find the empirical fit.

Method	δ (μs)	±
Traditional- $b=a^2/4$	0.0653	0.0054
Traditional- b=0	0.0620	0.0077
Statistical- 2 sources	0.0663	0.0036
Statistical- 4 sources	0.0646	0.0012
Statistical- Average	0.0654	0.0038

Table IV: Comparison of total detector dead time values using the traditional method and the statistical approach

Both methods have been previously used with ^{3}He-based neutron multiplicity counters, and are shown here to apply to BCS as well. The neutron count distribution approach allows for a quick, robust, and convenient way to determine the dead time of a system. The availability of AmLi sources in facilities also serves as another benefit to the traditional approach. Multiple dead time values can be calculated with a single data acquisition run using the higher order factorial moment expressions, allowing for a cross-verification.

In this work, it has been shown that both approaches return similar dead time values. We have discussed the underlying theories of both methods, while acknowledging many other works over the last few decades. This list is certainly not exhaustive, and it illustrates the revived drive

to accurately, precisely, and easily represent detector dead times based on true physical models. This comparison was performed to show the capabilities of both approaches, while justifying the newly proposed analysis with another detector system. The statistical approach provides an experimentally determined approximation to the neutron multiplicity counter's dead time which may be more simple to grasp and implement, returning values with greater confidence due to the robust uncertainty calculations. Future work may include extending this analysis to each of the detector channels, in addition to quantifying the impact these dead time determinations have on the uncertainty in the final calculated mass values of an assay.

6. Acknowledgments

This work was sponsored by the U.S. Department of Energy (DOE), National Nuclear Security Administration (NNSA), Office of Nonproliferation Research and Development (NA-22).

7. References

[1] N. Ensslin, W.C. Harker, M.S. Krick, D.G. Langner, M.M. Pickrell, and J.E. Stewart, "Application guide to neutron multiplicity counting," Los Alamos National Laboratory Report LA-UR-98-4090, 1998.

[2] S. Croft, A. Favalli, D.K. Hauck., D. Henzlova, P.A. Santi, "Feynman variance-to-mean in the context of passive neutron coincidence counting*," Nucl. Instrum. and Meths. in Phys*. Res A686 (2012)136-144.

[3] N. Dytlewski "Dead-time corrections for multiplicity counters," *Nuclear Instruments and Methods in Physics Research Section A: Accelerators, Spectrometers, Detectors and Associated Equipment,* 305, no. 2 (1991): 492-494.

[4] M. S. Krick, H. O. Menlove, *The High-Level Neutron Coincidence Counter (HLNCC): User's Manual*, Los Alamos Scientific Laboratory Report LA-7779-M, June 1979.

[5] J. E. Swansen "Deadtime reduction in thermal neutron coincidence counter*," Nuclear Instruments and Methods in Physics Research Section B: Beam Interactions with Materials and Atoms* 9, no. 1 (1985): 80-88.

[6] S. Croft, L.G. Evans, D. K. Hauck, M. T. Swinhoe, P. A. Santi, "Testing an alternative singles rate dead time correction algorithm for use in neutron multiplicity analysis," in: 52nd Annual Meeting of the Institute of Nuclear Materials Management, 17-21 July, 2011.

[7] L. G. Evans, M. T. Swinhoe, S. Croft, D. K. Hauck, and P. A. Santi, "Extension of ESARDA NDA Multiplicity Benchmark," No. LA-UR-11-03052; LA-UR-11-3052. Los Alamos National Laboratory (LANL), 2011.

[8] W. Hage and D. M. Cifarelli, "Correlation analysis with neutron count distribution for a paralyzing dead-time counter for the assay of spontaneous fissioning material," *Nuclear science and engineering,* 112, no. 2 (1992): 136-158.

[9] D. K. Hauck, S. Croft, L. G. Evans, A. Favalli, P. A. Santi, and J. Dowell. "Study of a theoretical model for the measured gate moments resulting from correlated detection events and an extending dead time." *Nuclear Instruments and Methods in Physics Research Section A: Accelerators, Spectrometers, Detectors and Associated Equipment,* 719 (2013): 57-69.

[10] N. Menaa, S. Croft, S. C. Kane, S. Philips, M. Villani, and L. G. Evans. "Experimental Determination of the Multiplicity Deadtime Parameter." WM Symposia, 1628 E. Southern Avenue, Suite 9-332, Tempe, AZ 85282 (United States), 2008.

[11] A. Foglio Para and M.M. Bettoni, "Counting statistics of nuclear detectors," *Nuclear Instruments and Methods,* 70 (1969): 52-56.

[12] S. Croft, S. Cleveland, A. Favalli, R. D. McElroy, and A. T. Simone. "Estimating the Effective System Dead Time Parameter for Correlated Neutron Counting." *Nuclear Instruments and Methods in Physics Research Section A: Accelerators, Spectrometers, Detectors and Associated Equipment* (2017).

[13] D. Henzlova, R. Kouzes, R. McElroy, P. Peerani, M. Aspinall, K. Baird, A. Bakel et al. "Current Status of 3He Alternative Technologies for Nuclear Safeguards." *Final report from series of workshops on ^{3}He alternatives, LA-UR-15-21201 ver*, vol. 3. 2015.

[14] J. L. Lacy, A. Athanasiades, L. Sun, C. S. Martin, G. J. Vazquez-Flores, and S. Mukhopadhyay, "Performance of a straw-based portable neutron coincidence/multiplicity counter," Nuclear Science Symposium and Medical Imaging Conference (NSS/MIC), IEEE (2011): 529-532.

[15] J. L. Lacy, A. Athanasiades, C. S. Martin, L. Sun, and G. J. Vazquez-Flores, "Design and performance of high-efficiency counters based on boron-lined straw detectors," *Proceedings of the 53rd Annual Meeting of Institute of Nuclear Materials Management* (INMM), 2012.

[16] J. L. Lacy, A. Athanasiades, L. Sun, C. S. Martin, and G. J. Vazquez-Flores," A Straw Based HLNCC Multiplicity Counter with Improved FOM in Same Form Factor," *Proceedings of the 55th Annual*

Meeting of Institute of Nuclear Materials Management (INMM), Atlanta, GA, 2014.

[17] A. T. Simone, S. Croft, R. D. McElroy Jr., L. Sun, J. L. Lacy, A. Athanasiades, and J. P. Hayward, "Performance of a Boron-Coated-Straw-Based HLNCC for International Safeguards Applications," submitted to *IEEE Transactions on Nuclear Science*, July 2017.

[18] "32-channel list mode instrument with channel number handling," Multi channel list mode instrument. Accessed April 05, 2017. http://www.iki.kfki.hu/radsec/groups/mcl_en.shtml.

[19] S. L. Cleveland, J. A. Chapman, S. Croft, and R. D. McElroy, Jr. "Comparison of Pulse Train Recorder Module (PTR) and Shift Register Multiplicity Measurements Using the Large Active Well Coincidence Counter (LV-AWCC)," *Proceedings of the 56th Annual Meeting of the Institute of Nuclear Materials Management*, July 12-16, 2015, Indian Wells, California.

[20] "Instrumentation." Instrumentation – CANBERRA Industries. Accessed April 05, 2017. http://www.canberra.com/products/waste_safeguard_systems/instrumentation.asp

Revisiting Currie's Minimum Detectable Activity for Non-Destructive Assay By Gamma Detection Using Tolerance Intervals

E. Agboraw[1], E. Bonner[1], T. Burr[1], S. Croft[2], J.M. Kirkpatrick[3], T. Krieger[4], C. Norman[1], P. Santi[1], S.Walsh[1]

1 International Atomic Energy Agency, Vienna Austria;
2 Oak Ridge National Laboratory, USA ;
3 Mirion Technologies (Canberra), Inc., USA
4 Forschungszentrum Jülich GmbH, Inst. Energy and Climate Research, Jülich, Germany

Abstract

Currie's paper [1] on estimating the minimum detectable activity (MDA) applied a Gaussian approximation to either Gaussian or Poisson data and remains the standard method to estimate radiological detection limits. This paper revisits the Currie method with attention to the false alarm probability (FAP) in Poisson and Gaussian data in non-destructive assay (NDA) by gamma (denoted as γ) detection. The Currie detection limit L_D is an estimate of the smallest net signal count rate λ_N that can be detected with high probability and low FAP in the presence of non-zero background count rate λ_B that has been previously estimated. The MDA is the sample activity or mass corresponding to λ_N, defined as $MDA = \frac{L_D}{\nu}$, where in the case of γ-based NDA, the calibration factor ν (a product of γ-ray yield, detector and geometric efficiency, counting time, and other factors) has measurement error that introduces systematic error in the estimate of the MDA. Kirkpatrick et al. [2] showed how to account for systematic uncertainties in the estimate of $MDA = \frac{L_D}{\nu}$ using a modified version of Currie estimation [2,3]. The present paper combines the approach in [2] with a tolerance interval approach. It is shown that the FAP in signal detection can be significantly different from the nominal FAP if the nominal FAP is not based on a tolerance interval, and if the nominal FAP is based on a tolerance interval, then the MDA will be larger than Currie's estimated MDA.

1. Introduction

The Currie detection limit L_D is an estimate of the smallest net signal count rate λ_N that can be reliably detected with low FAP in the presence of non-zero background count rate λ_B [1]. The MDA is the sample activity (or mass through a conversion) corresponding to λ_N, defined as $MDA = \frac{L_D}{\nu}$, where the calibration factor ν (a product of γ-ray yield, detector and geometric efficiency, counting time, and other factors) has measurement error that can introduce systematic error in the estimate of the MDA. Kirkpatrick et al. [2] showed how to account for such systematic uncertainties in the estimate of $MDA = \frac{L_D}{\nu}$ using a modified version of the Currie estimation [2,3]. The MDA can be used prior to data collection to compare different instruments and measurement scenarios, and can also be used as a quantitative measure on an item-specific basis after data collection. In γ-ray spectroscopy, the background is often estimated from the continuum beneath the peak(s) of interest, so the MDA is specific to the measurement conditions (including what other nuclides are present).

This paper revisits L_D with attention to the FAP (denoted α) in Poisson and Gaussian data, by using a tolerance interval approach [4,5]. Section 2 provides background, motivation, and example tolerance intervals. Section 3 provides a simulation approach and results for both Gaussian and Poisson data. Section 4 uses results from Section 3 to estimate the MDA while allowing for random and systematic errors in the calibration factor ν in $MDA = \frac{L_D}{\nu}$. Section 5 is a discussion. Section 6 is a summary.

2. Background

Currie [1] provided approximate MDA calculations for the desired FAP based on the assumption that the measurement data has a Gaussian distribution with mean μ and variance σ^2, denoted $X \sim N(\mu, \sigma^2)$. In γ-ray spectroscopy, the measurement data are γ-ray counts at certain energies, which are often well modeled with a Poisson distribution, which for a large mean count rate is well approximated by a Gaussian distribution. Because μ and σ must be estimated, the well-known frequentist approach to a confidence interval for μ from n measurements $x_1, x_2, \ldots, x_n$ is $\bar{x} \pm t_{1-\alpha,(n-1)} s/\sqrt{n} = \hat{\mu} \pm t_{1-\alpha,(n-1)} \hat{\sigma}/\sqrt{n}$, where $t_{1-\alpha,(n-1)}$ denotes the (1-α) quantile of the t distribution with n-1 degrees of freedom, $\bar{x} = \sum_{i=1}^{n} x_i / n$, and $s^2 = \hat{\sigma}^2 = \sum_{i=1}^{n} (x_i - \bar{x})^2 / (n-1)$ [1,4,5].

In nuclear safeguards (Sections 3 and 4), background measurements are often used to estimate an alarm threshold that has a small nominal α, such as α = 0.05. So, instead of requiring a confidence interval for μ, the need is to estimate a threshold (the 0.95 quantile of the distribution of X), denoted $T_{0.95}$, that corresponds to α= 0.05. The threshold $T_{0.95}$ is the upper limit of a one-sided interval of the distribution of X if doing one-sided testing for a positive mean shift. In contrast to a confidence interval, a tolerance interval is an interval that bounds a fraction of a probability

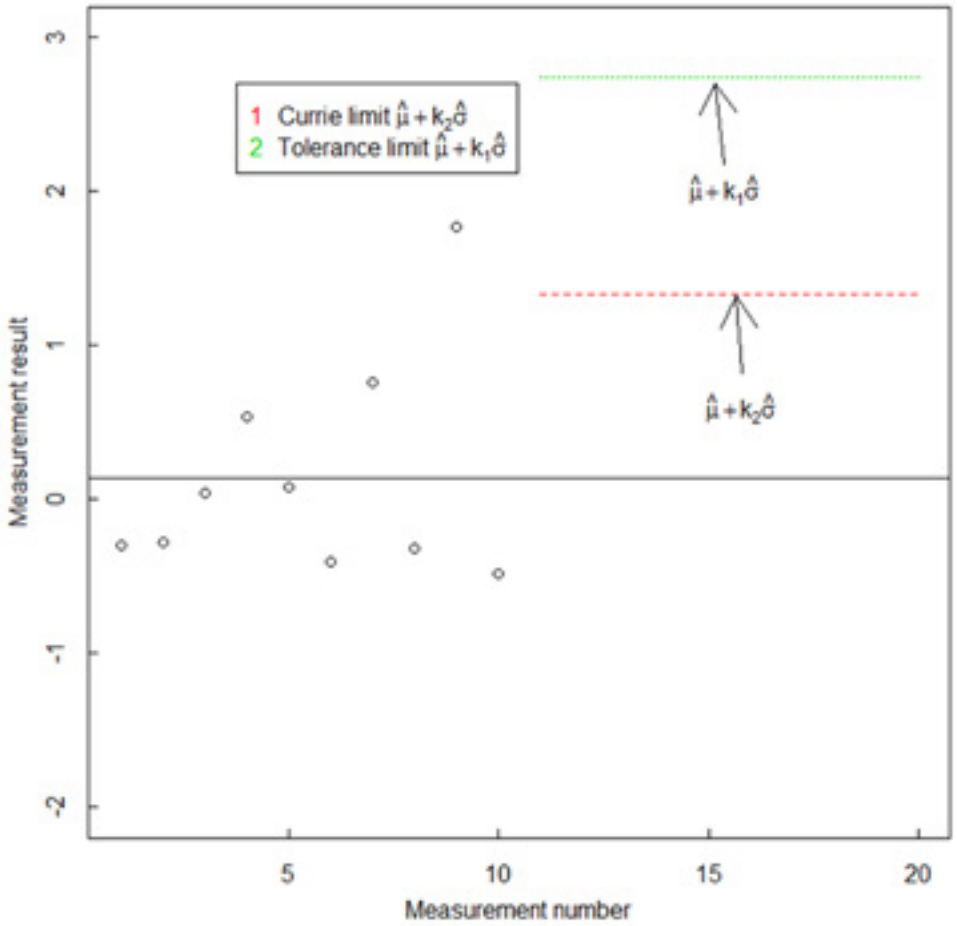

Fig. 1: Illustration of the tolerance limit $k_1 = 3.7$ compared to the Currie limit $k_2 = 1.7$ for future data in the case of using 10 Gaussian observations to estimate μ and σ and the corresponding Gaussian quantile, $\hat{T}_{0.95} = \hat{\mu} + k\hat{\sigma}$.

distribution with a specified confidence (frequentist) or probability (Bayesian approach) [4,5]. Both frequentist and Bayesian tolerance interval approaches will be presented in this paper. The frequentist tolerance interval estimators presented have the form $\hat{T}_{0.95} = \hat{\mu} + k\hat{\sigma}$, where k is the coverage factor that depends on n. The goal in both the frequentist and Bayesian approaches is to achieve $P(\hat{T}_{0.95} \geq T_{0.95}) = p$, where p is a user-specified probability (the frequentist confidence level), such as $p = 0.99$ [4,5]. In the Bayesian approach, μ and σ are random unknown parameters so $P(\hat{T}_{0.95} \geq T_{0.95}) = P_{\mu,\sigma}(\hat{T}_{0.95} \geq T_{0.95})$ is computed with respect to μ and σ. In the frequentist approach, $\hat{\mu}$ and $\hat{\sigma}$ are random while μ and σ are fixed unknowns so $P(\hat{T}_{0.95} \geq T_{0.95}) = P_{X_1,X_2,\ldots,X_n}(\hat{T}_{0.95} \geq T_{0.95})$ is computed with respect to random samples of size n.

In any frequentist approach, probabilities such as α are calculated with respect to the distribution of X for fixed μ and σ. A frequentist tolerance interval has an associated confidence, which is the long-run relative frequency (probability) that an interval such as $(0, \hat{T}_{0.95} = \hat{\mu} + k\hat{\sigma})$ will include a future observation X from the same distribution as the training data used to estimate $\hat{\mu}$ and $\hat{\sigma}$. In any Bayesian approach, probabilities are calculated with respect to the joint posterior distribution $f_{posterior}(\mu, \sigma)$ for fixed X [5].

To illustrate the frequentist approach, assume that $n = 10$ measurements are used to construct an upper limit that bounds at least $p = 0.95$ ($\alpha \leq 0.05$) of future data with probability $p = 0.99$. Fig. 1 plots a single realization of the $n = 10$ measurements and compares the Currie limit to the tolerance interval limit. To achieve a user-specified α for future measurements aimed to detect whether any signal is present in a background measurement, Currie [1] used the detection threshold $\hat{T} = \hat{\mu}_B + k_{1-\alpha}\hat{\sigma}_B$ where $k_{1-\alpha}$ is the (1-α) quantile of the Gaussian distribution, and $\hat{\sigma}_B = \sqrt{\hat{\sigma}^2 + \hat{\sigma}^2/n}$, and the term $\hat{\sigma}^2/n$ is the estimated variance of the estimate of the unknown mean μ_B. Regarding notation, in this paper, the subscript B denotes background, and the subscript N denotes net, and both the B and N subscripts will sometimes be omitted, depending on the context, to avoid cluttering the notation. Currie regarded this value of $\hat{T}$ as an approximate value if the underlying data is non-Gaussian (such as Poisson; see Section 3). If one uses $k_{1-\alpha} = t_{n-1}(\delta)/\sqrt{n}$ instead of the (1-α) quantile of the Gaussian distribution in Currie's calculation $\hat{T} = \hat{\mu}_B + k_{1-\alpha}\hat{\sigma}_B$, with noncentrality parameter $\delta = z_p\sqrt{n}$ where z_p is the 1-p quantile of the standard Gaussian, then the calculation is exact if the underlying data has a Gaussian distribution [4].

Perhaps surprisingly, an exact expression for a tolerance interval is only available in the one-sided Gaussian case just described [4-7]. However, good approximate expressions for many other cases are available [5-7]. Alternatively, and in the approach taken in this paper, tolerance intervals can be well estimated using simulation to approximate an alarm threshold that is designed to contain at least $1-\alpha$ percent of future observations with a specified coverage probability p. Currie did not consider the probability $p$and note from Fig. 1, that for $p = 0.99$, the decision limit is much larger than Currie's limit, with $k_1 = 3.7$ (tolerance) versus $k_2 = 1.7$(Currie). As shown in Section 3, using the value $k_1 = 3.7$ corresponds to $p = 0.99 = P(\hat{T}_{0.95} \geq T_{0.95})$, while using $k_2 = 1.7$ gives $p = 0.52$.

Fig. 2 plots $P(\hat{T}_{0.95} \geq T_{0.95})$ (Fig. 2a) and the true average FAP (Fig. 2b) for a range of sample sizes n if the data is Gaussian for both the tolerance method (using $p = 0.99$) and the Currie method. The tolerance value for k_1 (which depends on n), $P(\hat{T}_{0.95} \geq T_{0.95})$, and the true FAP are easily calculated using simulation in R [8] as shown in Section 3.

A Bayesian analysis specifies a prior probability for parameter(s) θ, a likelihood (such as Gaussian or Poisson in this paper) $P(X \mid q)$, and then finds the posterior distribution of θ, $f_{posterior}(\theta)$. Bayesian tolerance interval construction then finds an estimate $\hat{T}_{1-\alpha}$ such that $P(X < \hat{T}_{1-\alpha} \mid \theta) = 1-\alpha$ with specified coverage probability p. In the Gaussian case with unknown μ and σ, $\theta = (\mu, \sigma)$. In the Poisson case, $\theta = (\lambda_G, \lambda_B)$ if both a gross count rate and background count rate are required, and $\theta = (\lambda)$ if the count rate at a single region of interest is required. For Gaussian and Poisson data, conjugate prior pdfs are available, which have the convenient property that the posterior pdf is in the same family as the prior, but with updated parameters. For example, the conjugate prior for the Gaussian with unknown μ and σ is the Gaussian-inverse-Gamma and the conjugate prior for the Poisson is the Gamma distribution [5].

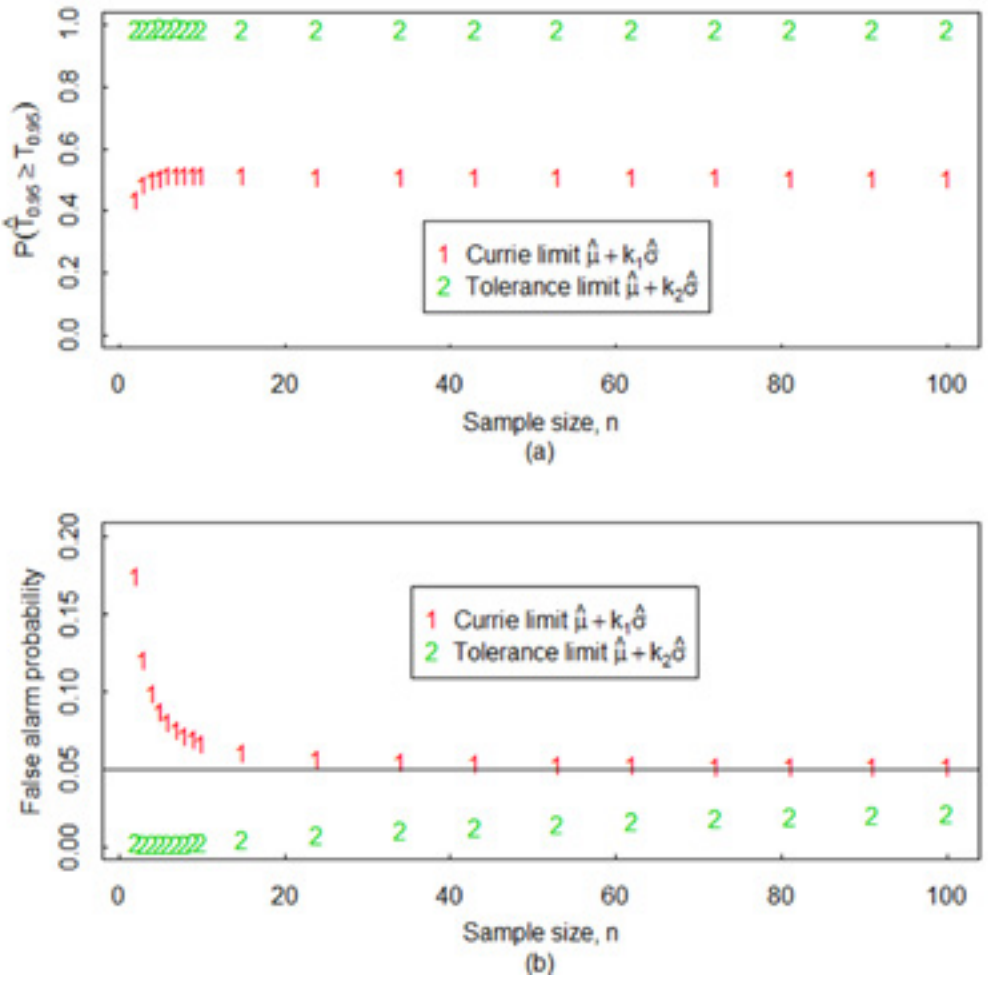

Fig. 2: The true value of $P(\hat{T}_{0.95} \geq T_{0.95})$ in (a) and true FAP in (b) if data is Gaussian. The tolerance interval method is conservative, so has a FAP that is smaller than 0.05 by construction. The Currie method has FAP much larger than 0.05 for small sample sizes.

3. Simulation to estimate $\hat{T}_{0.95}$

The user seeks $\hat{T}_{1-\alpha}$ such that $P(X < \hat{T}_{1-\alpha} \mid \theta) = 1-\alpha$ with specified coverage probability p.

3.1 A simulation-based trial-and-error frequentist approach for Gaussian data

The simulation-based trial-and-error frequentist approach to estimate k is as follows.

1. Specify n, μ, σ.
2. For each of many (typically 10^5 or more) simulations, generate $X_i \sim N(\mu,\sigma^2)$, *for* $i = 1, 2, \ldots, n$
3. Compute $\hat{\mu}+k\hat{\sigma}$ for a grid of trial values for k using $\hat{\mu} = \bar{x} = \sum_{i=1}^{n} x_i \Big/ n$, $\hat{\sigma} = \sqrt{\sum_{i=1}^{n}(x_i-\bar{x})^2 \Big/ (n-1)}$.
4. Select the trial value of k that includes at least 95% of the population (of future X values) with probability $p = 0.99$; that is, $P(\hat{T}_{0.95} \geq T_{0.95}) = 0.99$, where $\hat{T}_{0.95} = \hat{\mu}+k\hat{\sigma}$.

For example, with $n = 10$ and for any values of μ and σ, the exact result is $k = 3.738$, and the simulation-based result in R [8] is $k = 3.74$, which is within the small simulation error in a large but finite number (10^5) or simulations. Similarly, simulation can also estimate the probability that the Currie-based k value bounds at least 95% of the probability density function (pdf) of X (so the FAP is 0.05 or less), and in this example with $n = 10$, there is a probability of approximately 0.52 that the Currie-based value of k has a FAP of 0.05 or less.

One nuclear safeguards application for tolerance intervals for Gaussian data is inspector (i) measurements of operator (o) declarations of n items sampled for verification. In each of n values of the operator-inspector difference statistic $d_j = (o_j - i_j)/o_j$, if $|d_j| > k\delta$ (in two-sided testing), then the j-th item selected for verification leads to an alarm, where $\delta_T = \sqrt{\delta_R^2 + \delta_S^2}$, (with δ_T the total RSD, δ_S the between-period short-term systematic error RSD, and δ_R the within-period reproducibility) and $k = 3$ is a common choice that corresponds to a small α of approximately 0.001. The null hypothesis is $\mu = 0$, and δ_T can be estimated by applying analysis of variance (ANOVA) [9-12]. If one assumes $\hat{\delta}_T = \delta_T$ then choosing $k = 1.65$ corresponds to $\alpha = 0.05$ (Gaussian approximation); however, as an example, if $n = 10$ paired measurements in each of 3 prior inspection periods are available, and $\delta_S = \delta_R = 0.03$ [9 12], then choosing k= 1.65 leads to an actual FAP of 0.05 or less with probability 0.38. If one desires a high probability $p = 0.99$ that the actual FAP is as small as the nominal FAP, then simulation [9,12] indicates that instead of k = 1.65, one must choose, for example, k = 2.58 for 5 groups of 10 measurements, k = 2.94 for 3 groups of 10 measurements and k = 4.35 for 2 groups of 5 measurements. Unlike the single-component Gaussian case, these values of k depend on the values of the ratio δ_S/δ_R, which is unknown, so approximate frequentist or Bayesian methods are needed. Note that any Bayesian method can be regarded as approximate because one almost never knows the exact prior probability distribution. The accuracy of these approximate methods can be assessed using simulation and/or by analysis of historical data.

3.2 Poisson data

Fig. 3 shows that the true FAP of Currie's method can be quite different from the nominal FAP, so tolerance interval construction should be considered. In Fig. 3, the simulated data is n = 1 observation of $X \sim$ Poisson(λ), with λ = 1, 10, or 100. A count time of t = 1 second is used to estimate the background and to test whether a subsequent measurement corresponds to the same background rate λ (See Section 5.1). For comparison, $P\left(X_{test}/t = \hat{\lambda}_{test} > T\right)$ of the corresponding Gaussian distribution is shown, where $\hat{T}_{0.95} = \hat{\lambda} + k\sqrt{\hat{\lambda}(1+1/n)/t}$, which is Currie's [1] approach to estimate T by using the Gaussian approximation for both Gaussian and Poisson data, and using the factor $\sqrt{1+1/n}$ to quantify the impact of uncertainty in the estimated mean on the estimated background standard deviation. Note (Fig. 3b) that for large values of λ (and/or large count times) such as $\lambda \geq 100$, then the Gaussian approximation (with the factor $\sqrt{1+1/n}$ but without the notion of a tolerance interval) to the Poisson is adequate. The reason for this good accuracy is that the variance of the Poisson distribution is equal to its mean λ, so the Poisson standard deviation can be estimated with less uncertainty than that of the Gaussian.

Recall from Example 3.1 that estimating the standard deviation of the Gaussian requires $n > 1$, and that the notion of tolerance intervals is needed; the estimated threshold T is much too small if uncertainties in $\hat{\mu},\hat{\sigma}$ are not accounted for properly. Without using tolerance intervals, references [2, 13-14] extended Currie's treatment of Poisson data [1] by using the Poisson distribution rather than an approximating Gaussian. Particularly when count rates and/or count times are small, it is prudent to use the Poisson distribution rather than the approximating Gaussian. As an example (also used in Section 4), let n = 5, $\mu = 10$, and $x_1, x_2, \ldots, x_5$ are 10,12,10,10,8, so $\bar{x}$ = 10 and Currie's $\hat{T}_{0.95} = \hat{\mu}_B + k_{1-\alpha}\hat{\sigma}_B = 12.5$, which is rounded up to 13 (and in 93% of 10^5 simulations, test measurements exceed the 13 limit, so the FAP can be much larger than 0.05). In the same example, a one-sided tolerance interval using the R code in Section 3.3 below leads to $\hat{T}$= 21.5, rounded up to 22 for 99% confidence that the FAP is 0.05 or smaller. Also for the same example, a Bayesian tolerance interval approach is illustrated in Section 3.3 using a prior probability density $f_{prior}(\lambda) = Gamma(\alpha_{prior} = 1, \beta_{prior} = .075)$ (the conjugate prior for the Poisson, and this particular prior has mean $\alpha_{prior}/\beta_{prior} = 1/0.075 = 13.3$ and standard deviation $\sqrt{\alpha/\beta^2} = 1/0.075 = 13.3$) has $f_{posterior}(\lambda) = Gamma(\alpha_{prior} + \sum_{i=1}^{n} x_i, \beta_{prior} + n) = Gamma(1+50, 0.075+5)$, which has

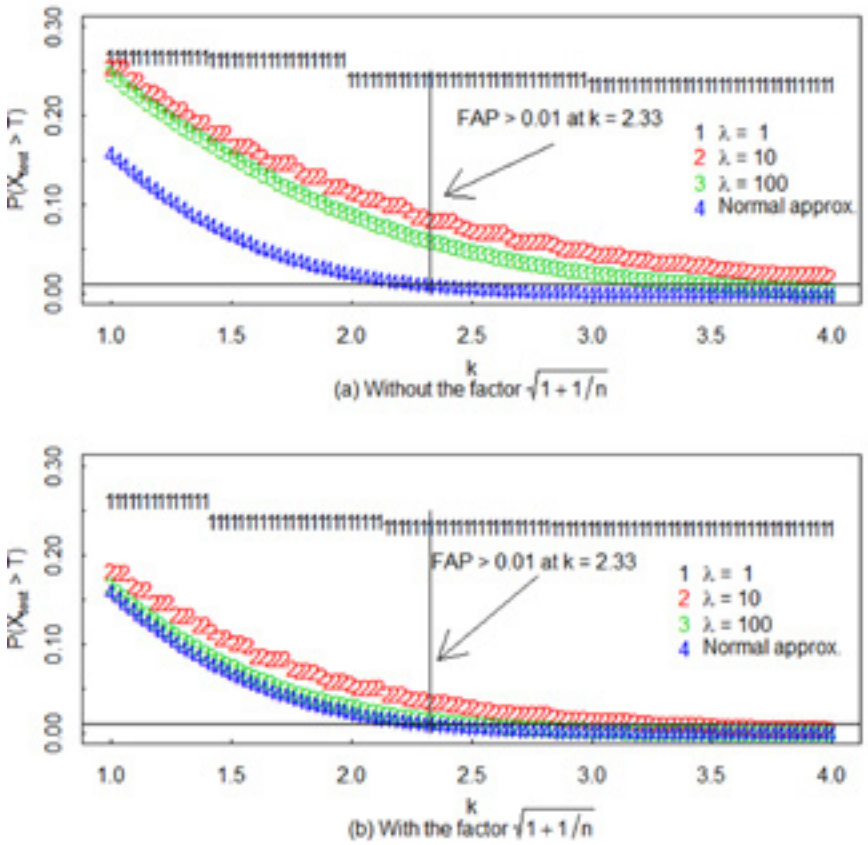

Fig. 3: The probability $P\left(X_{test}/t=\hat{\lambda}_{test}>T\right)$ versus k for $\lambda=1$, 10, and 100. The normal approximation is also plotted. Currie's factor $\sqrt{1+1/n}=\sqrt{2}$ is ignored in (a), included in (b).

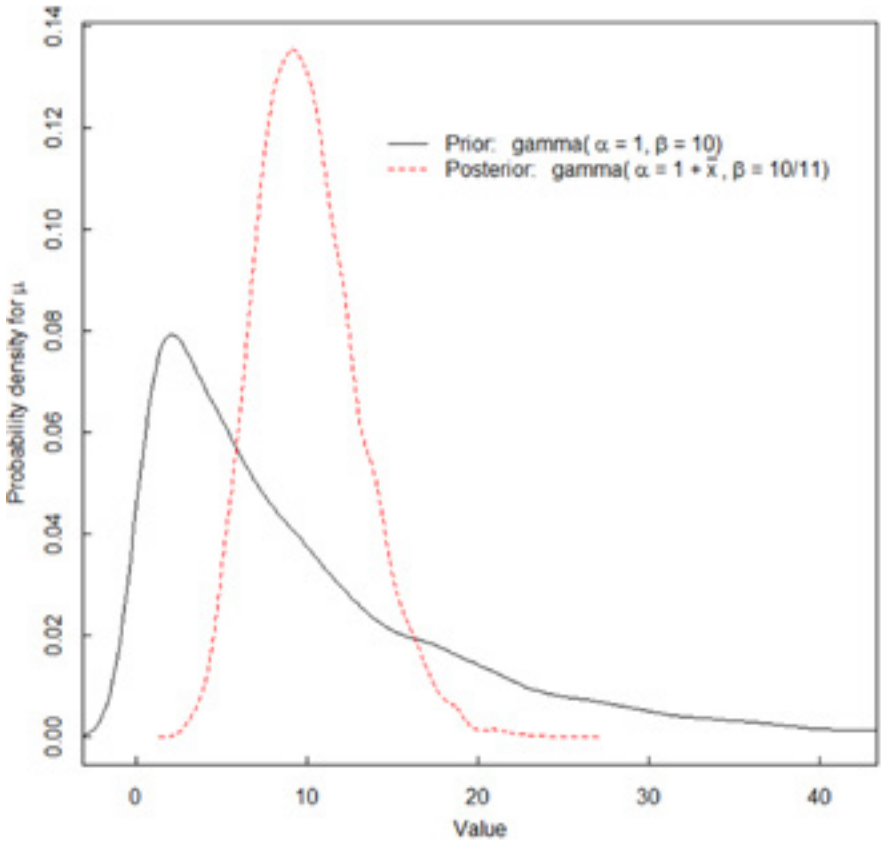

Fig. 4: The prior and posterior distribution for λ for n = 5, $\mu=10$, and $\bar{x}=10$.

mean 10.05 and standard deviation 1.41; see Fig. 4. Note that the Gamma parameters, conventionally denoted as α_{prior} and β_{prior} are not related to the FAP α or the nondetection probability β.

3.3 Simulation for Poisson data for frequentist and Bayesian approaches

3.3.1 Frequentist approach

1. Specify λ and *n.*
2. For each of many (10^5 or more) simulations, generate $X_i \sim Poisson(\lambda)$, $i = 1,2,...,n$.
3. Compute $\hat{\lambda} + k\sqrt{\hat{\lambda}/n}$ for a grid of trial values for *k* using $\hat{\lambda} = x$.
4. Select the trial value of *k* that includes at least 95% of the population (of future *X* values) with probability $\gamma = 0.99$; that is, $P(\hat{T}_{0.95} \geq T_{0.95}) = 0.99$, where $\hat{T}_{0.95} = \hat{\lambda} + k\sqrt{\hat{\lambda}/n}$.

With $n = 5$, λ =10, the Currie approximation is $\hat{T}_{.95}$ =12.5 and the exact value using simulation (to within negligible simulation error) is $\hat{T}_{.95}$ = 21.5. The probability that the FAP is 0.05 or less is only 0.07 with the Currie value and is, by design, 0.99 with the simulation approach. Unlike with Gaussian data, for Poisson data, the value of *k* depends on λ, so λ must be replaced with $\hat{\lambda}$.

3.3.2 Bayesian approach

1. Specify *n and the parameters of the Gamma prior* α_{prior} *and* β_{prior}*. In this example* α_{prior} *=1 and* β_{prior} *= 0.075 (a very wide prior with mean and standard deviation of 13.3.*
2. For each of many (typically 10^5 or more) simulations, generate $\lambda \sim Gamma(\alpha_{prior}, \beta_{prior})$ and $X_i \sim Poisson(\lambda)$, $i = 1,2,...,n$.
3. Compute $\alpha_{post} = \sum_{i=1}^{n} x_i + \alpha_{prior}$ and $\beta_{post} = n + \beta_{prior}$.
4. Choose the quantile of the posterior $\lambda_{post} \sim Gamma(\alpha_{post}, \beta_{post})$ such that $P(\hat{T}_{0.95} \geq T_{0.95}) = p = 0.99$. This is the count value that is greater than 95% of the distribution of *X* for 99% of the λ values generated in the simulations.

The Bayesian result is $\hat{T}_{0.95}$ = 23.4 for the same Poisson example. Recall that Currie's value of $\hat{T}_{0.95}$ is 13, the frequentist $\hat{T}_{0.95}$ given above is 21.5, and all values of $\hat{T}_{0.95}$ are approximations. The Bayesian estimate $\hat{T}_{0.95}$ is approximate because there is always mismatch between the true and assumed prior. The frequentist estimate $\hat{T}_{0.95}$ is approximate because it depends on the true value of λ so in practice, one uses $\lambda = \hat{\lambda}$. Currie's $\hat{T}_{0.95}$ is approximate for the reasons given. Recall that the accuracy of these approximate methods can be assessed using simulation and/or by analysis of historical data.

3.4 Example with two Poisson counts in each assay

Detection of *g* counts often requires measurement of both the nearby-in-energy "background" counts and the peak region "gross" counts (Section 5.1). The gross mean count rate is $\lambda_G = \lambda_B + \lambda_N$ [2,13,14]. The Bayesian approach is effective in this context for two main reasons: a conjugate prior (Gamma) can be specified for λ_G and λ_B, so the measured G and B counts each lead to $f_{posterior}(\lambda) = Gamma(\alpha_{prior} + \sum_{i=1}^{n} x_i, \beta_{prior} + n)$, and it is simple to enforce $\lambda_N \geq 0$. Although the choice of prior parameters α and β for both λ_G and λ_B is subjective, the user often can bound the range for both λ_G and λ_B from prior data, so α_{prior} and β_{prior} can each be within some modest range. If the Bayesian approach is applied repeatedly, its long-run behavior can be evaluated to check, for example, whether the nominal FAP is close to the actual FAP.

To illustrate, choose $\alpha_{prior} = 1$ and $\beta_{prior} = 0.075$ for λ_G and λ_B as in the previous Bayesian example for Poisson data. Generate $G \sim$ Poisson(λ_G) and $B \sim$ Poisson(λ_B). For each of many (10^5 or more) simulations, generate λ_G from its posterior $Gamma(1+G, 0.075+1)$ and generate λ_B from its posterior $Gamma(1+B, 0.075+1)$ and for those simulations for which $\lambda_G \geq \lambda_B$ (because $\lambda_N \geq 0$), compute $G - B$. Determine the threshold T for $G - B$ such that with probability at least $p = 0.99$, $P(G - B \geq T) \leq 0.05$. The result for G = 30 and B = 10 is T = 34 (Currie) and T = 45 (Bayesian tolerance, using the Skellam distribution, which is the distribution of the difference in two Poisson random variables). Then L_D is an estimate of the smallest net signal count rate λ_N that can be detected with high probability and low FAP in the presence of nonzero background count rate λ_B that has been previously estimated. Ignoring errors in the calibration factor ν (assuming $\nu = \nu_{True}$ and for simplicity here also assuming $\nu_{True} = 1$), the Currie-based MDA is 39 and the tolerance interval-based MDA is 77. Allowing for 5% RSD in the total error as in the previous example and assuming that $\nu_{Meas} = \nu_{True}(1+S+R)$ has a Gaussian distribution (any distribution is simple to accommodate here), then the Currie–based MDA, which corresponds to the net count rate assuming zero external background (see Section 5.1), increases from 39 to 45 and the tolerance interval–based MDA increases from 77 to 87.

4. Implications for the MDA

Recall he Poisson example in Section 3.3 for which Currie's $\hat{T}_{0.95} = \hat{\mu}_B + k_{1-\alpha}\hat{\sigma}_B$ =12.5 (which is rounded up to 13), and the one-sided tolerance limit is $\hat{T}_{0.95}$ = 22 for 99% confidence that the FAP is 0.05 or smaller. Therefore, the

estimated MDA based on the tolerance interval limit will be larger than the estimated MDA based on the Currie limit. Specifically, if the mean count rate shifts from $\mu = 10$ to $\mu = 19.5$ any future observation $X \sim Poisson(\lambda = 19.5)$ satisfies $P(X \geq 13) \geq 0.95$ for the Currie mean shift and $X \sim Poisson(\lambda = 34.4)$ satisfies $P(X \geq 22) \geq 0.95$ for the tolerance interval mean shift. The mean shift values $\lambda = 19.5$ and $\lambda = 34.4$ are easily computed by numerical search. The MDA is then calculated by converting the mean shift to an activity, which requires calibration.

Recall that the MDA is defined as $MDA = \frac{L_D}{\nu}$, where in this example $L_D = 19.5$ (Currie) or $L_D = 34.4$ (tolerance) and the calibration factor ν (a product of γ-*ray* yield, detector and geometric efficiency, counting time, and other factors) has measurement error that can introduce systematic error in the estimate of the MDA. References [2,13,14] account for systematic uncertainties in the estimate of the MDA using a modified version of the Currie estimator [2,3].

To allow for random and/or systematic errors in ν, $\nu_{Meas} = \nu_{True}(1 + S + R)$, implies that the mean shift when the signal is present has uncertainty. To illustrate, assume that it is desired to have at least 99% confidence that the mean shift is above some limit. Assuming Gaussian calibration errors, then, for example, assuming 5% relative standard deviation (which is assumed here to include both random and systematic components) in converting the mean shift to activity using $MDA = \frac{L_D}{\nu}$ increases the estimated mean shift that can be detected with high probability from 19.5 to 22.1 (Currie approximation) and from 34.4 to 38. (tolerance interval approximation).

5. Discussion

This section describes three additional topics related to MDA calculations.

5.1 Definition of the background

In some γ-based NDA applications, the challenge to define and measure the relevant background is important. For example, in attribute measurements of fresh fuel assemblies, one task is to assess whether a given assembly is a dummy (not containing ^{235}U). In this case, the background is defined as the response of the detector to γ emissions from neighboring assemblies if the assembly being measured were a dummy. That is, measurement behavior needs to be characterized if γ emissions could be measured from only the neighboring assemblies at the location of the assembly being measured. The measurement seeks to provide evidence that a signature from the item was detected (thereby verifying presence of ^{235}U) and that the measured signature originated from the item, not from radiation outside the item.

The minimum detectable quantity is not usually defined for attribute testing; however, it is sometimes desired (beyond the scope of this example) to estimate the probability that the test alarms for large mean shifts, such as a mean shift associated with 50% or more nuclear material missing.

Gamma-ray detectors detect distinct γ-rays energies. Sodium Iodide (NaI) and Cadmium-Zinc-Telluride (CZT) are common detector types. The presence of ^{235}U is verified in fresh fuel by estimating the area in the peak region of interest (ROI) associated with the 185.7 keV γ-ray. If the estimated peak area exceeds 3 times its estimated standard deviation, then based on the acceptance criteria established by the IAEA corresponding to a 99.7% confidence level (assuming no estimation error in the estimated standard deviation, so tolerance interval concepts are not being used; see the final paragraph in section 5.1) in the presence of the peak, the peak is considered to be present in the spectrum and the presence of ^{235}U is verified within the fuel. Because γ-*rays* at such energies interact with materials primarily through both the photoelectric effect (in which the γ-ray transfers all its energy to the detector medium) and Compton scattering (in which the γ-ray scatters off an electron in the medium or surrounding mediums causing a partial transfer of its energy to the detector medium), each measured peak in a γ-ray spectrum lies on top of a background caused by higher energy γ-rays that underwent Compton scattering within the detector. An example of this can be seen in Fig. 5 in which a γ-ray spectrum of a fresh fuel assembly as measured by a CZT detector is shown for γ-ray energies ranging from 20 keV to 305 keV. Because a fresh fuel assembly contains both ^{235}U and ^{238}U, and because the γ-rays that are associated with the decay of ^{238}U exist at energies between 700 and 1001 keV, the 186 keV γ-ray photo peak from ^{235}U will always be present on top of a Compton background associated with the scattering of γ-rays from ^{238}U within the CZT detector.

In fresh fuel verification scenarios where shielding and collimation can be used to detect γ-rays only from the selected assembly, the peak area is estimated as the difference between the total counts in the ROI that includes the peak and the counts associated with the Compton background in that region (recall Example 3.3). To assist in determining whether the attribute test condition has been satisfied, most software programs automatically notify the inspector when the net area of the peak ROI above the Compton background is larger than 3 times its estimated standard deviation.

In cases where attribute measurements are performed near other items containing the same type of nuclear material, a background measurement is needed to estimate the peak's count rate as detected from the surrounding environment. The background-only measurement corresponding to the item-plus-background measurement in Fig. 5 had a similar spectrum shape as that in Fig. 5, but the peak ROI counts

were approximately 60% lower. For this background-only measurement, the same CZT detector that was used for item-plus-background was put in an empty slot of a storage rack containing fresh fuel assemblies. The background spectrum was measured during the same training exercise and for the same count time as the spectrum in Fig. 5, which was from an attribute test measurement of a fresh fuel assembly within that same storage rack. Assuming zero room background, applying the attribute test to the background spectrum would yield a positive (and incorrect) verification because the estimated peak area was approximately 13 times its estimated standard deviation. Therefore, to ensure proper verification of items using the attribute test, careful consideration must be given regarding how the room background is measured in order to reject the possibility that the measured spectrum was the result of room background and not from the item to be verified.

When the background spectrum shows evidence that the peak of interest is present from measuring the surrounding environment, the verification of an item using the attribute test is executed using

$$\text{(Measured rate)} - \text{(background rate)} > 3\sqrt{\left(\frac{\hat{\sigma}_B}{T_B}\right)^2 + \left(\frac{\hat{\sigma}_M}{T_M}\right)^2}$$

where $\hat{\sigma}_B$ is the estimated standard deviation in the estimated peak area in the background measurement, $\hat{\sigma}_M$ is the estimated standard deviation in the area of the peak in the measured spectrum from the item, and T_B and T_M are the count times corresponding to the background and item measurement, respectively. Both the measured and background rates are corrected for the background caused by Compton scattering by estimating the count rate of the net peak, which involves a difference of two quantities as in Example 3.3. In cases where the attribute test software is unable to account for room background in automatically calculating whether the attribute test has been passed, the inspector performs the attribute test calculation for each item. The attribute test aims to answer the question 'Does the item contain the material as declared?', and an inspector's time is quite limited, so inspectors sometimes apply more stringent statistical tests to help confirm the attribute test result. One example of such a stringent test is

$$\textit{Measured rate} - 3\cdot\frac{\sigma_M}{T_M} > \textit{Background rate} + 3\cdot\frac{\sigma_B}{T_B}.$$

Inspectors typically perform the background measurement before performing the verification measurements, and the quantity on the right side of the stringent inequality is a single calculated value, which makes the evaluation simple to do while performing verification measurements. Measurements that do not pass the stringent test can be tested against the more formal method.

Recall that the Gaussian approximation to the Poisson is adequate for tolerance interval estimation if the Poisson mean $\lambda \geq 100$ (Fig. 3), so the factor of 3 used above is justified because for the data in Fig. 5, the quantiles of the Gaussian provide an adequate approximation to the true FAP, assuming $\hat{\lambda} = \lambda$ (but one should be aware of the need for the factor $\sqrt{1+1/n} = \sqrt{2} = 1.41$ as in Fig 3a versus Fig 3b). A more complicated method than a sum of Poisson counts below and above the peak ROI is often used to estimate the background under the blue line in Fig. 5; so $\hat{\sigma}_B$ and $\hat{\sigma}_M$ can involve more than the Poisson distribution (beyond this paper's scope).

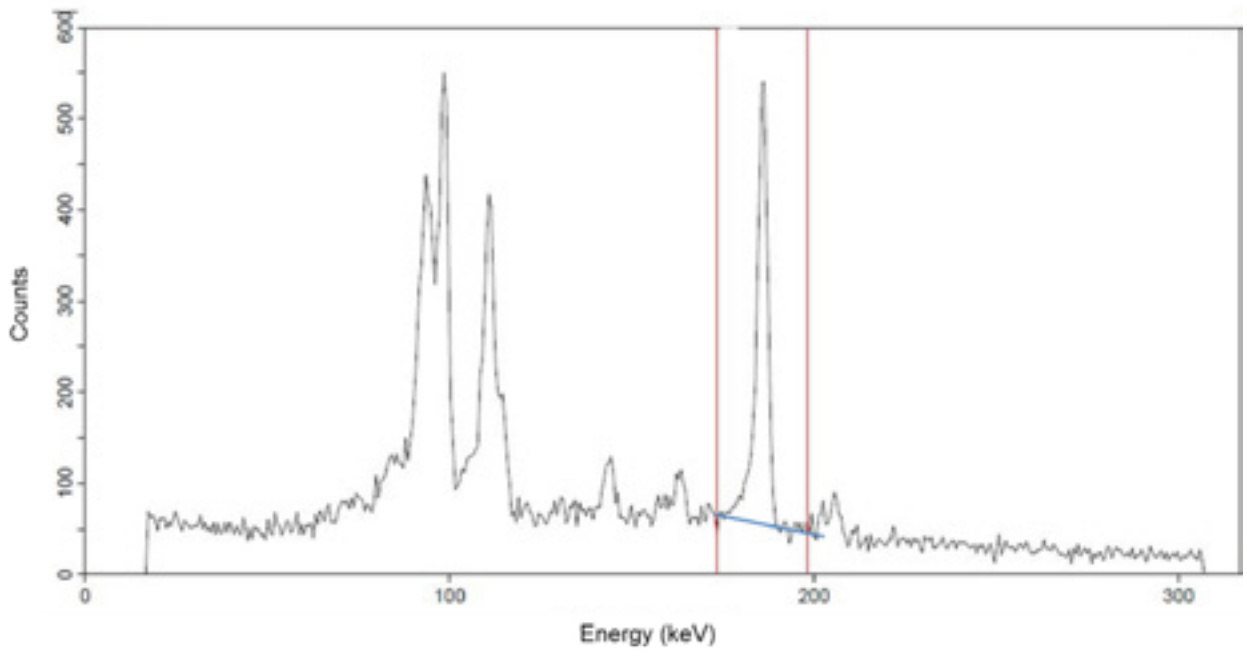

Fig. 5: γ-ray spectrum of a fresh fuel assembly from a CZT detector. The red lines indicate the ROI used to estimate 186 keV peak area while the blue line is an estimate of the Compton background beneath the 186 keV peak based on a linear interpolation of the background at γ-ray energies that are just above and below the ROI.

5.2 Tolerance interval versus prediction interval

A prediction interval is another approach to the MDA that leads to larger MDA values than the Currie-based MDAs and to smaller MDAs than the tolerance interval-based MDAs. The prediction interval approach averages over the parameter(s) θ so there is no probability statement regarding confidence in coverage [5].

5.3 Impact of analyzing predicted counts rather than estimated activity

Zykov [15] describes a pass-fail criterion for verification measurements (operator declarations compared to inspector measurements, as in Section 3.1) regarding the minimum detectable defect size (the minimum amount of missing radioactive material) if analysis of the inspector measurements is based on measurements that are predicted using modeling and the operator declarations. Such an approach would avoid explicit inversion of measurements to activity or nuclear material mass, and simulations to be presented elsewhere suggest that the minimum detectable defect size would be smaller. The minimum detectable defect size would be based on a tolerance interval approach, because that is more conservative than the Currie approach, as this paper has shown. This methodology could lead to more efficient verification sampling plans. Regarding testing for patterns, recall that the overall test for a pattern is based on the average difference statistic, $D = \frac{1}{n}\sum_{j=1}^{n}\frac{o_j - i_j}{o_j}$ [14], which could be defined on the basis of measured masses or on the basis of predicted and observed measurements. However, whenever an estimate of the D statistic (at the stratum, material balance component, or material balance area level) is needed, e.g. for the detection of diversion into D through material balance evaluation, it would be necessary for the inspector to estimate item mass, so explicit inversion of inspector measurements to item mass would be required.

6. Summary

This paper revisited Currie's MDA with attention to the FAP in Poisson and Gaussian data in NDA by *γ-ray* detection. It was shown that the actual FAP can be significantly larger than the nominal FAP if the nominal FAP is not calculated based on a tolerance interval; and, if the nominal FAP is calculated based on a tolerance interval, then the MDA is increased compared to the Currie approximation. Implications for safeguards have not yet been evaluated. A simple way to accommodate random and/or systematic errors in converting from a mean shift to an activity shift was illustrated.

7. References

[1] Currie, L., Limits for qualitative detection and quantitative determination: application to radiochemistry, Analytical Chemistry 40, 58-5936, 1968.

[2] Kirkpatrick, J., Venkataraman, R., Young, B., Minimum detectable activity, systematic uncertainties, and the ISO 11929 standard, Journal of Radioanalytical and Nuclear Chemistry 296, 1005-1010, 2013.

[3] International Organization for Standardization ISO 11929 determination of the characteristic limits (decision threshold, detection limit, and limits of the confidence interval) for measurements of ionizing radiation-fundamentals and application, Geneva, 2010.

[4] Young, D., Tolerance: an R package for estimating tolerance intervals, Journal of Statistical Software 36(5),1-39 2010.

[5] Hamada, M., Johnson, V., Moore, L., Wendelberger, J. Bayesian prediction intervals and their relation to tolerance intervals, Technometrics 46(4), 452-459, 2004.

[6] Janiga, I., Garaj, I., Two-sided tolerance limits of normal distributions with unknown means and unknown common variability , Measurement Science Review (3) (1), 75-78, 2003.

[7] Eberhardt, K., Mee, R., Reeve, C., Computing factors for exact two-sided tolerance limits for a normal distribution, Communication in Statistics- Simulation and Computation, 18(1), 397-413,1989

[8] *R Core Team. R: A language and environment for statistical computing. R Foundation for Statistical Computing, Vienna, Austria. ISBN 3-900051-07-0,* http://www.R-project.org/, 2012.

[9] Bonner, E., Burr, T., Martin, K., Norman, C., Santi, P., Uncertainty quantification as presented in training courses for safeguards inspectors, ESARDA 2017.

[10] Miller, R., Beyond ANOVA: Basics of Applied Statistics, Chapman & Hall, 1998.

[11] Liao, C., Lin, T., Iyer, H., One- and two-sided tolerance intervals for general balanced mixed models and unbalanced one-way random models, Technometrics 47(3), 323-335, 2005.

[12] Burr, T., Krieger, T., Krzysztoszek, K., Norman, C., Tolerance intervals for measurements with systematic and random errors, IAEA report 2017.

[13] Kirkpatrick, J., Young, B., Poisson statistical methods for the analysis of low-count gamma spectra, IEEE Transactions on Nuclear Science 56(3), 1278-1282, 2009.

[14] Kirkpatrick, J., Venkataraman, R., Young, B., Calculation of the detection limit in radiation measurements with systematic uncertainties, Nuclear Instruments and Methods in Physics Research A 784, 306-310, 2015.

[15] Zykov, S. Technical challenges and technological gaps in IAEA safeguards, Proceedings of the Institute of Nuclear Materials Management, 2015.

Micro Particle Suspensions for Preparation of Reference Materials for Particle Analysis Methods in Safeguards

R. Middendorp, M. Dürr, I. Niemeyer, D. Bosbach

Forschungszentrum Jülich GmbH
IEK-6: Nuclear Waste Management and Reactor Safety
52428 Jülich, Germany
E-mail: middendorp.r@outlook.com

Abstract:

In order to produce micro particle reference materials for nuclear safeguards particle analysis, a dedicated facility has been established at Forschungszentrum Jülich. This includes an aerosol-based particle production setup which is capable of producing uranium micro particles with consistent isotopic compositions and uranium contents. While the produced particles could be used as reference materials as obtained after production, further options for packaging the particles are being considered to simplify handling of the particles and to open new possibilities, such as the preparation of particle mixtures.

The transfer of the collected particles into a suspension has several advantages. For example, particles in suspension stored in a bottle would be amenable to extraction of an aliquot, which could be dried on a substrate of interest, such as silicon wafers, glass-like carbon disks or cotton-swipes, to obtain test samples. Also, various suspensions could be mixed in different ratios followed by drying on the desired substrates to obtained particle mixtures of two or more different particle types. However, while the particles are dispersed in suspension, various reactions could have an influence on the stability of the micro particle property values. In order to assess the stability of uranium micro particles in a suspension, experiments have been conducted using synthetic powders and uranium micro particles. Our results from dissolution and uranium isotope exchange studies show that ethanol is a suitable medium for the storage of particles over a period of a few months. Using particles produced with the particle production setup at Forschungszentrum Jülich, particle suspensions have been produced by transfer of collected particles into ethanol and distribution on silicon wafers and cotton-swipes produced consistent results. It was demonstrated that the production of particle mixtures is feasible. It was also shown that particles in suspension could represent a suitable packaging for a particle reference material which permits a quick and flexible preparation of various types of test samples.

Keywords: Particle Analysis; Environmental Sampling; Reference Material; NWAL; Suspensions

1. Introduction

The destructive analysis of samples collected during inspections of nuclear facilities is one of the verification measures applied by the International Atomic Energy Agency (IAEA) to derive safeguards conclusions. One of the employed methods is particle analysis, which is based on the release of small amounts of microparticulate matter during all material handling processes. Such particles are collected via swipe samples taken during inspections of the nuclear facilities. The collected samples are sent to the IAEA Network of Analytical Laboratories (NWAL) for analysis, which is typically performed using high accuracy micro-analytical tools, such as large geometry – secondary ion mass spectrometry (LG-SIMS). These methods are capable of measuring the isotopic composition of single microparticles. The measured isotopic composition of individual microparticles could act as a tool to detect undeclared activities in the inspected facility.

Over recent years, great progress was achieved in the improvement of the measurement accuracy of the isotopic composition of fissile nuclides within micrometer sized particles [1]. The analysis of individual particles has progressed beyond the analysis of the major isotopes (e.g. ^{235}U and ^{238}U) towards the minor isotopes (e.g. ^{234}U and ^{236}U) which provide additional information, e.g. on the facility operations history.

Due to the improved measurement accuracy, quality assurance (QA) has become more stringent and members of the IAEA's NWAL need to fulfill a set of criteria set by the IAEA. Generally, the QA require various quality control (QC) measurements to be performed for the analytical method [2]:

1) Calibration;
2) Validation;
3) Quality control;
4) Proficiency testing.

Each of these measures requires a dedicated test material of high homogeneity and stability, which are generally described as reference materials (RMs) [3]. For calibration and validation, not only the stability and homogeneity of

the material is of importance, the material is also characterized with respect to one or more property values to quantify the *true* value; i.e. the absolute value of the property with given uncertainty and traceability. Such materials are classified as certified reference materials (CRMs) and have strict requirements, as described in ISO 17034 [4].

Various attempts were undertaken to produce micrometer sized particles containing uranium and/or plutonium with well-defined isotopic compositions [5-10]. Over recent years, a setup has been established at Forschungszentrum Jülich [11-13] to produce micrometer sized uranium oxide microspheres, which are intended to be used for the various quality control measurements and are to be certified as CRM (in cooperation with EC-JRC) with respect to the uranium isotopic composition and uranium elemental content. The setup consists of an aerosol generator, after which the aerosol droplets are carried through an aerosol heater in which spherical particles are formed with a homogeneous size and shape. The obtained particles have been investigated in detail [13] and were shown to consist of triuranium octoxide (U_3O_8).

At present, the produced microparticles are collected using single-stage inertial impactors, which allow for the production of ca. 50 samples within a single run. The usage of such impactors does, however, have a number of limitations; the number of particles collected may differ between various production runs, the particles are deposited unevenly over the substrate and the production of particles mixtures under controlled conditions is not easily possible. Also, some applications require the production of more than 50 samples, which would require production of particles over multiple batches/days, which could lead to an expanded between-sample inhomogeneity.

This paper describes a method to transfer collected particles into particle suspensions. Such particle suspensions could then be mixed with similar suspensions containing different types of particles, for example different isotopic composition, which could then be distributed and dried over various substrates to prepare the final test samples. However, while in suspension, interaction of the particles with the solution could alter the properties of the particles. Therefore, a number of investigations were performed to determine whether and to what extend such interactions occur.

2. Particle Production at Forschungszentrum Jülich

The production of monodisperse uranium oxide microspheres with a nominal diameter around 1 µm at Forschungszentrum Jülich has been described elsewhere in detail [13]. The production is based on the formation of an aerosol from a dilute uranyl nitrate solution with the desired isotopic composition. The usage of uranyl nitrate was found to yield particles with minimal preparation [13], which would minimize the risk of cross-contamination. The diluted solution is fed using a syringe pump through a vibrating orifice aerosol generator, where a monodisperse aerosol is formed. The volume of a single droplet can be calculated by dividing the volume flow rate Q by the oscillating frequency f applied to the generator. When the uranium content w and the density ρ of the feed solution are known, the amount of uranium contained in a single droplet m can be calculated by multiplication of the droplet volume with the content and density.

The formed droplets are then guided with an air flow through an aerosol heater set to 500 °C; at 500 °C particles were found to be fully decomposed into uranium oxide whereas a further increase of the temperature causes the particles to deform, and a lower degree of monodispersity was obtained [13]. After cooling, the particles are collected using single-stage inertial impactors [14] onto glass-like carbon substrates. The collected particles were investigated by µ-X-ray diffraction (µ-XRD), µ-X-ray absorption near-edge structure (µ-XANES) and µ-Raman spectroscopy to identify the obtained chemical phase, all of these techniques resulted in an orthorhombic triuranium octoxide (U_3O_8) phase [13].

By using the single-stage inertial impactor, the produced particles can be collected on glass-like carbon substrates which, in turn, can be analyzed by SIMS without further handling, minimizing the risk of introducing any cross-contaminations. The usage of the inertial impactor does, however, cause a non-uniform deposition pattern of the particles on the substrate. An area with a diameter of 12 mm is deposited with particles where the particle loading density increases towards the outer rim of this deposition area and only few particles can be found at the center of the substrate (Figure 1).

The number of particles collected can be controlled in a limited manner by varying the particle collection time; with an increasing collection time, the total number of particles increases. However, due to the intricacies of aerosol transport, the particle concentration of the air flow through the impactors may vary between different production runs and even between collections within a single production run.

3. Particle Suspensions

The previously described problems with a single-stage inertial impactor can be overcome by using a suspension. When particles are dispersed in a solution, aliquots of this suspension can be distributed for analysis, where each aliquot contains approximately the same number of particles. Such suspensions also increase the maximum number of samples which can be produced during a single batch. During normal operation, the number of samples which can be collected is limited by the liquid feed input reservoir, and is sufficient for approximately 50 samples. Once the reservoir is empty, the system needs to be

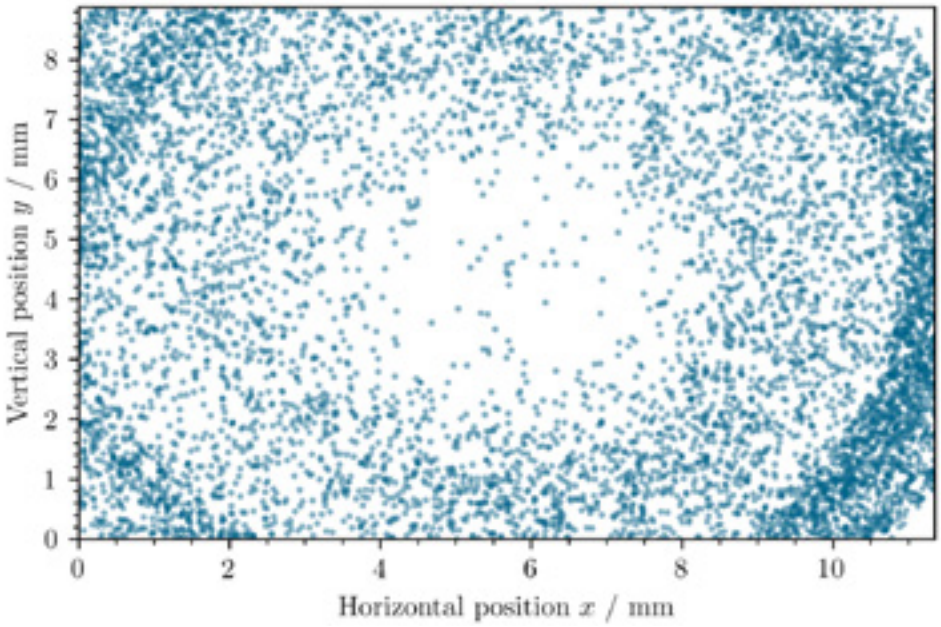

Figure 1: Spatial particle distribution of microparticles collected on a glass-like carbon disk using a single-stage inertial impactor, obtained from low-magnification SEM scans.

interrupted to refill the reservoir before continuing. The particles properties between two such runs could therefore be different. Although similar limitations would be present when using suspensions, particles collected during multiple production runs could be homogenized, eliminating the between-sample inhomogeneity.

Particle suspensions could be produced by two methods; either the particles can be collected in a suspension directly or particles are collected using an inertial impactor and are subsequently transferred into a suspension. The former method has proven to be unsuccessful as the air flow causes evaporation of the solvent during longer operation. Therefore, particles are collected using the single-stage impactors, typically onto silicon wafers due to the high degree of cleanliness and affordability. The silicon wafers can then be placed into a vessel filled with the selected medium and placed in an ultrasonic bath for a few minutes. The ultrasonic bath causes the detachment of particles from the surface into the medium, after which the silicon wafer can be removed.

The selection of the liquid medium has proven to be a critical factor in the production of particle suspensions. The medium should:

1. Be of high purity to prevent significant cross-contaminations,
2. Not cause dissolution of particles within the required processing time,
3. Be suitable to detach the particles from the substrate and,
4. Not cause agglomeration of particles.

Previous investigations [15] have shown that ethanol is most suitable as liquid medium, as water and dimethyl formamide cause dissolution of the particles, n-hexane and n-decane prevent the detachment of particles from the substrate and 2-propanol causes increased agglomeration of particles.

In order to demonstrate the suitability of particle suspensions using ethanol as liquid medium, particles produced during the same run as the particles shown in Figure 1 were transferred into ethanol and were subsequently dried onto a glass-like carbon substrate. The temperature at which the samples were dried proven to be a critical parameter, as with an increasing temperature agglomeration of particles was observed. The prepared samples were therefore placed in a glass Petri dish onto a heating plate set to 50 °C, the actual temperature at the surface of the substrate is, however, unknown. The prepared substrate was investigated by scanning electron microscopy (SEM), the obtained particle distribution is shown in Figure 2. The figure shows a much higher uniformity compared to Figure 1 and shows the value of homogenizing the particles using a suspension. Although not yet quantified, the homogeneity between samples is also expected to be much higher compared to the direct collection.

The prepared suspension also opens a number of new possibilities, such as the production of mixtures containing various types of particles. In order to demonstrate the possibility to produce particle mixtures, cerium particles were produced, which were subsequently transferred into an ethanol suspension. Cerium particles were generated as surrogate for uranium particles, due to the relative comparable chemistry of both elements and the simplified

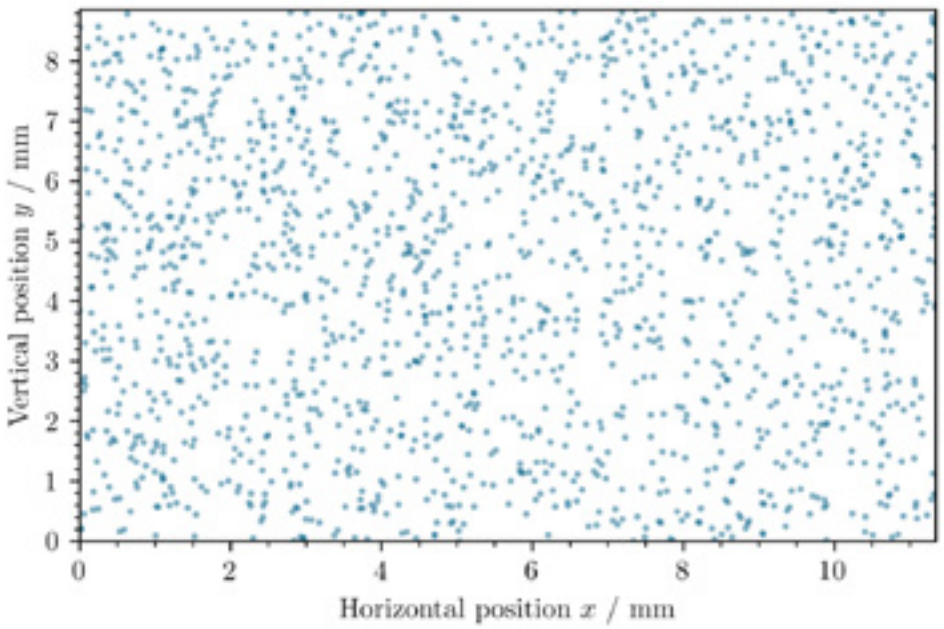

Figure 2: Spatial particle distribution of microparticles deposited on a glass-like carbon disk using an ethanol suspension, obtained from low-magnification SEM micrographs.

distinction between uranium and cerium (e.g. by SEM/EDX) compared to the distinction of uranium particles with different isotopic compositions. The cerium particle suspension was mixed with a uranium suspension, where the produced mixture was dried on a silicon wafer. The obtained wafer was then investigated by SEM/energy-dispersive X-ray spectroscopic (EDX) analysis where EDX spot measurements were performed on each identified particle to distinguish between uranium and cerium. Figure 3 shows collected EDX spectra of 12 randomly selected particles. The spectra show clear lines for either cerium (between 4.5 and 6 keV) or uranium (between 3.0 and 3.5 keV), no spectra containing both uranium and cerium were found. Of the 533 particles, 21 were identified as uranium particles and 509 were identified as cerium particles. A second sample prepared, to which less cerium suspension was added, showed a decrease of the relative amount of cerium particles in line with the first suspension, demonstrating that specific mixtures of particles could be produced, although the particle count of the initial suspensions need to be quantified before mixing.

The prepared suspensions also expand the possibilities to prepare different substrates. When using the inertial impactor, only solid, flat substrates can be used, whereas the suspensions could be distributed over any type of substrate as long

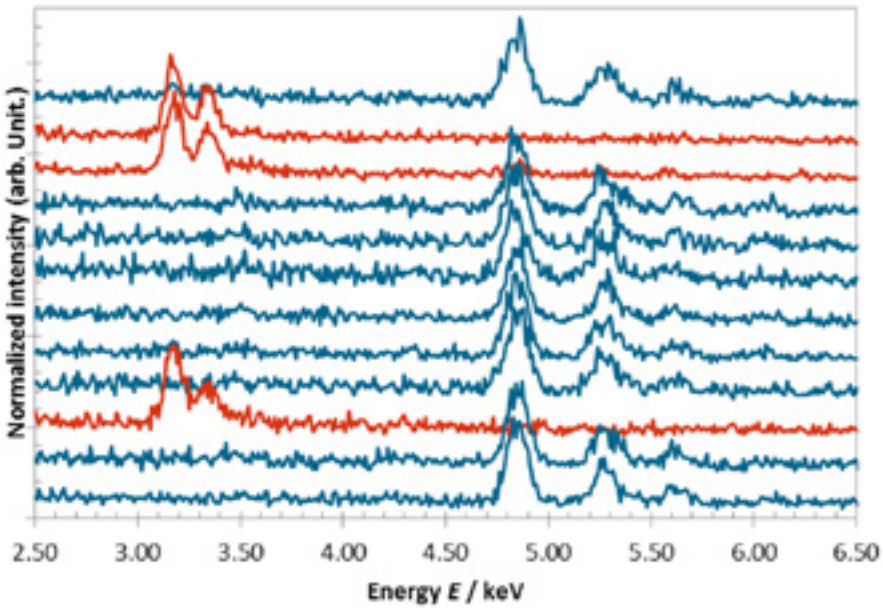

Figure 3: Measured EDX spectra of 12 randomly selected particles in a uranium/cerium mixture.

as the medium (ethanol) does not interact with the substrate. One such substrate would be cotton swipes, which are normally used to collect particles during inspections. To demonstrate the suitability of particle suspensions to prepare particle samples on such cotton swipes, an aliquot of the uranium/cerium mixture was dried on a small piece of cotton swipe. SEM/EDX analysis was complicated by the degradation of the swipe by the electron beam, though both uranium and cerium particles could be identified. One of the collected SEM micrographs is shown in Figure 4, in which uranium particles are marked by a yellow circle and cerium particles with a red circle. The SEM/EDX studies show the possibility to deposit microparticles onto substrates which could not be used with the inertial impactors, and open new possibilities for method optimization and quality control measurements in nuclear safeguards particle analysis.

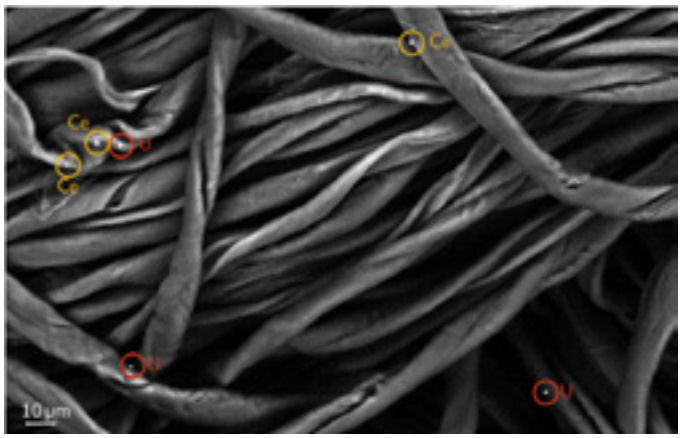

Figure 4: SEM micrographs of uranium (red) and cerium (yellow) particles transferred onto a cotton swipe from an ethanol particle suspension.

4. Stability of Particles in Suspensions

Although the previous section has shown the suitability of using particle suspensions as processing step and has shown some new possibilities with such suspensions, the suspensions could also have a negative impact on particle property values. The produced particles are intended to be certified as a reference material for both uranium isotopic composition and uranium content. Such certification does, however, not only require the property values to be quantified, but also required the determination of the expanded uncertainty, including contributions to the combined uncertainty of the assigned reference value stemming from the assessment of homogeneity and stability. During the storage of particles in a suspension, a number of effects could have an influence on the property values and/or the uncertainty of these values. For example, dissolution would decrease the uranium content, and exchange of uranium isotopes between particles and traces of natural uranium in the liquid medium would alter the composition. In order to assess these effects, various studies were undertaken.

The dissolution of particles was studied by storage of particles in an ethanol suspension for 365 days. After storage, an aliquot of the suspension was dried on a silicon wafer which was investigated by SEM. Figure 5 shows a collected micrograph of a particle compared with a micrograph collected of the sample before transfer into the suspension. Although the brightness/contrast differs slightly due to different SEM settings, no alteration of the particle could be observed. In contrast, strong signs of dissolution were observed for particles stored in water for only 16 days [15].

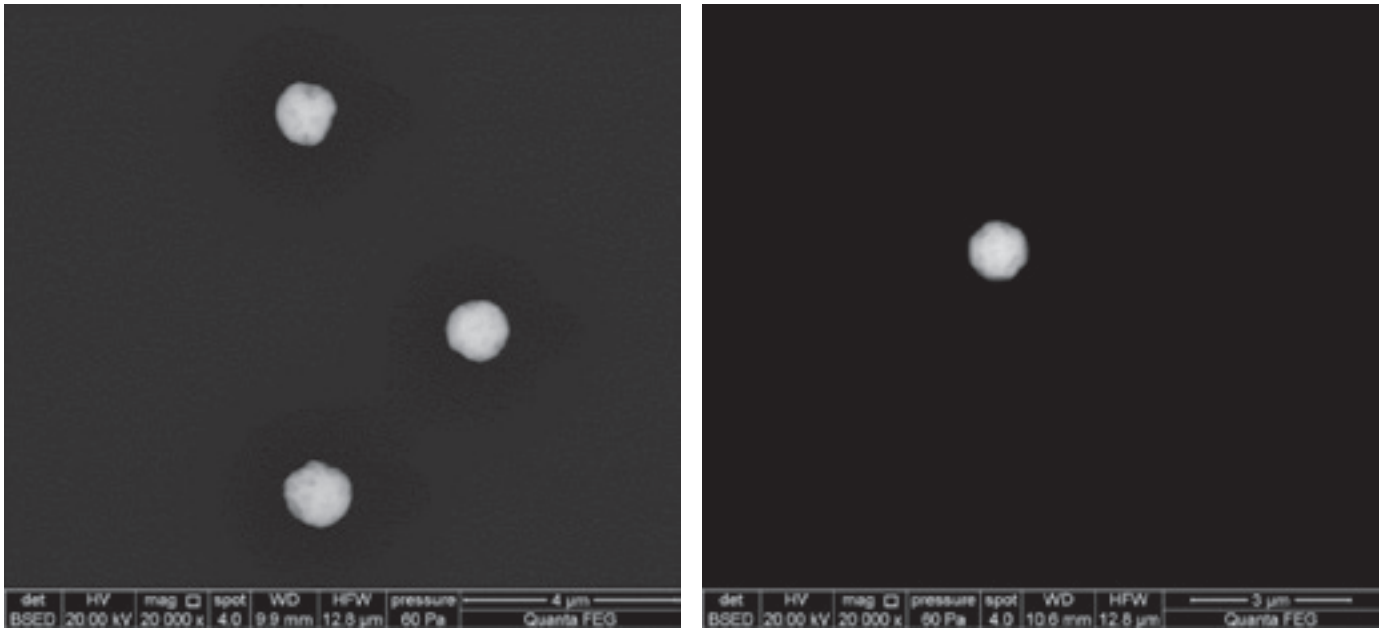

Figure 5: Microparticles (a) before and (b) after storage in ethanol for 365 days.

A second effect which might be of significance to the produced particle property values is isotope exchange. When a particle suspension is prepared consisting of two or more particle populations with different isotopic compositions, exchange of uranium between particles could alter the isotopic composition of the particles. Although no information on such exchange is currently available, Johnston et al. [16] measured the exchange of oxygen between water and various uranium oxides, including U_3O_8. In order to assess whether such exchange occurs between particles, particles consisting of depleted uranium (DU) and low-enriched uranium (LEU) were produced and subsequently transferred into suspensions. The suspensions were distributed over a number of clean silicon wafers. One wafer containing DU particles and a wafer containing LEU particles were transferred into a vial to which ethanol was added. The sample was stored for a given time, after which both wafers were removed and the uranium oxide particles separately dissolved in HNO_3 for quadruple–inductively coupled plasma–mass spectrometric (Q-ICP-MS) analysis. The particles were not suspended and remained separately attached to the respective silicon wafers during the extent of the studies. A schematic overview of the experimental setup is shown in Figure 6.

The experiment aims to investigate the stability of the isotopic composition of particle mixtures stored in ethanol. Two distinct effects could occur; exchange between particles and traces of natural uranium (NU) in the medium or exchange of uranium between particles. Figure 7 shows the measured isotope ratio of both the DU and LEU particles after storage for up to 202 days, neither of which show any significant change of the isotopic composition. Therefore, it can be concluded that no exchange occurs within the investigated timeframe.

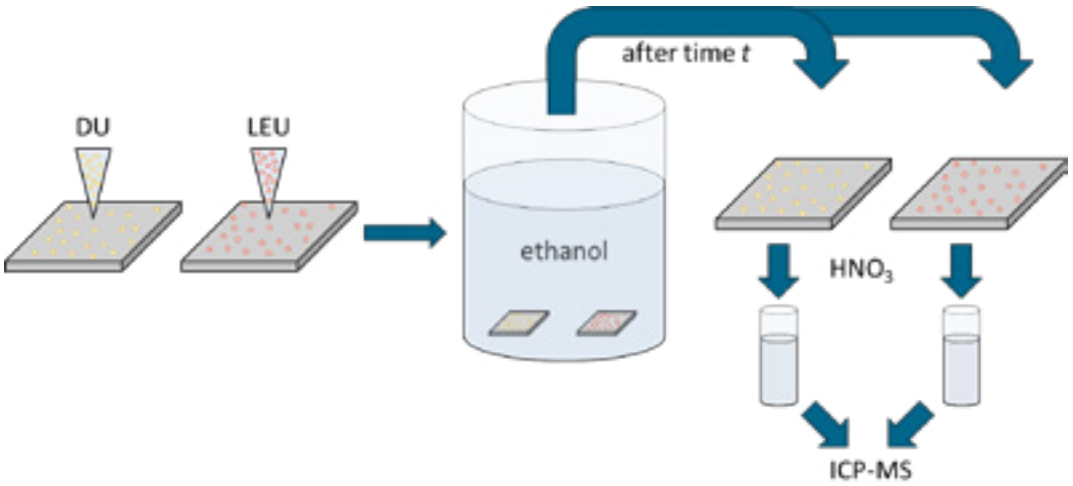

Figure 6: Schematic procedure to investigate the exchange of uranium between particles stored in an ethanol suspension.

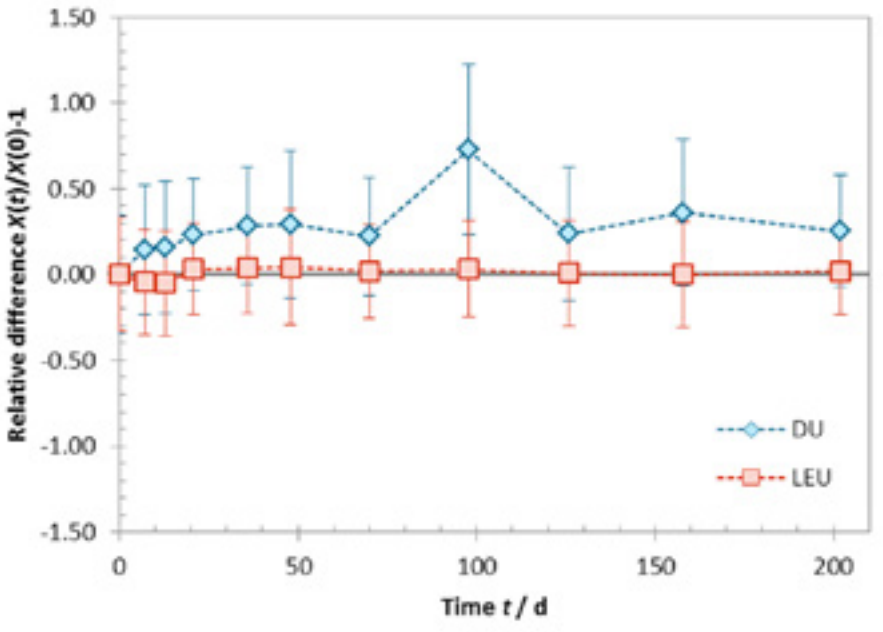

Figure 7: Measured change of the $m(^{235}U)/m(^{238}U)$ (X) isotope ratio after storage in ethanol.

5. Summary and Outlook

This paper proposes a method to transfer produced uranium microparticles into an ethanol suspension, which could then be divided into multiple samples. The proposed method greatly increases the uniformity of the particle distribution over the substrate. Also, the method reduces the spread of the total number of particles on different samples and allows the preparation of a larger number of samples, either from a single batch or combining multiple production runs. The particle suspensions also open new possibilities towards quality control materials for nuclear safeguards particle analysis. Mixtures of different particles could be prepared, as demonstrated with uranium and cerium particles, and mixtures of particles with different uranium isotopic compositions would also be feasible. The suspensions also allow for a wider choice of substrates, such as cotton swipes, or a multitude of substrates with a single batch of particles.

In order to verify the stability of particles in ethanol, particles were stored for 365 days in a suspension, during which no alteration of the particle morphology was observed. Also, no exchange of uranium isotopes between different particles was measured after a period of 202 days. These studies show that even over multiple months' storage in suspension, the particles remain unaltered. As the transfer of particles into suspensions, possible mixing of different suspensions and distribution over a large number of substrates can be performed within a few days, particle suspensions offer a wide range of new possibilities to enhance the quality control measurements without affecting the property values.

6. Acknowledgements

We thank F. Sadowski and D. Schneider from Forschungszentrum Jülich for Q-ICP-MS analyses.

This work was supported by the Federal Ministry for Economic Affairs and Energy, Germany, through the German Safeguards Support Programme to the IAEA under task C.45/A1961 and through the Programme "Neu- und Weiterentwicklung von Safeguardstechniken und -methoden" (FKZ 02W6263).

References

[1] Boulyga, S., Konegger-Kappel, S., Richter, S., Sangely, L., *Mass spectrometric analysis for nuclear safeguards*, J. Anal. At. Spectrom., **30**, 1469, 2015.

[2] ISO 17025:2005 *General requirements for the competence of testing and calibration laboratories*, 2005.

[3] BIPM, IEC, IFCC, ILAC, ISO, IUPAC, IUPAP, and OIML. *International vocabulary of metrology - Basic and general concepts and associated terms*, volume 3. 2012.

[4] ISO 17034:2016 *General requirements for the competence of reference material producers*, 2016.

[5] Stoffels, J.J., Cannon, W.C., Robertson, D.M., *A particulate isotopic standard of plutonium in an aluminosilicate matrix*. Journal of the American Society for Mass Spectrometry, **2**, 81-8, 1991.

[6] Raptis, K., Ingelbrecht, C., Wellum, R., Alonso, A., Bolle, W., Perrin, R., *The preparation of uranium-doped glass reference materials for environmental measurements*. Nucl. Instrum. Meth. A **480**, 40-43, 2002.

[7] Park, Y., Lee, M., Pyo, H., Kim, H., Sohn, S., Jee, K., Kim, W., *The preparation of uranium-adsorbed silica particles as a reference material for the fission track analysis*. Nucl. Instrum. Meth. A. **545**, 493, 2005.

[8] Kips, R., Leenaers, A., Tamborini, G., Betti, M., Van den Berghe, S., Wellum, R., Taylor, P., *Characterization of Uranium Particles Produced by Hydrolysis of UF_6 Using SEM and SIMS.* Microscopy and Microanalysis, **13**, 156-164, 2007.

[9] Ranebo, Y., Niagolova, N., Erdmann, N., Eriksson, M., Tamborini, G., Betti, M., *Production and Characterization of Monodisperse Plutonium, Uranium, and Mixed Uranium-Plutonium Particles for Nuclear Safeguard Applications.* Analytical Chemistry, **82**, 4055, 2010.

[10] Shinonaga, T., Donohue, D., Aigner, H., Bürger, S., Klose, D., Kärkelä, T., Zilliacus, R., Auvinen, A., Marie, O., Pointurier, F., *Production and Characterization of Plutonium Dioxide Particles as a Quality Control Material for Safeguards Purposes*. Analytical Chemistry, **84**, 2638, 2012.

[11] Knott, A., Dürr, M., *Production of monodisperse uranium particles for nuclear safeguards applications*. ESARDA Bulletin, **49,** 40, 2013.

[12] Middendorp, R., Knott, A., Dürr, M., *Preparation of Uranium Micro-Particles as Reference Material for Nuclear Safeguards*. ESARDA 37th Annual Meeting Proceedings, 448-497, 2015.

[13] Middendorp, R., Dürr, M., Knott, A., Pointurier, F., Ferreira Sanchez, D., Samson, V., Grolimund, D., *Characterization of the Aerosol-Based Synthesis of Uranium Particles as a Potential Reference Material for Microanalytical Methods*, Analytical Chemistry **89**, 4721, 2017.

[14] Esaka, F., Watanabe, K., Fukuyama, H., Onodera, T., Esaka, K. T., Magara, M., Sakurai, S., Usuda, S., *Efficient Isotope Ratio Analysis of Uranium Particles in Swipe Samples by Total-Reflection X-ray Fluorescence Spectrometry and Secondary Ion Mass Spectrometry*, Journal of Nuclear Science and Technology, **41**, 1027, 2014.

[15] Middendorp, R., Dürr, M., Bosbach, D., *The stability of uranium microspheres for future application as reference standard in analytical measurements*, Procedia Chemistry, **21**, 285, 2016.

[16] Johnston, F., Hutchison, D., Katz, J., *Oxygen exchange between uranium oxides and water*, J. Inorg. Nucl. Chem., 7, 392, 1958.

Towards novel field-deployable instrumentation for UF_6 enrichment assay – an overview of existing and emerging technologies

G. C.-Y. Chan, J. D. Valentine, and R. E. Russo
Lawrence Berkeley National Laboratory, 1 Cyclotron Road, Berkeley, CA 94720, USA

Abstract:

Uranium hexafluoride (UF_6) is the uranium compound typically involved in uranium enrichment processes. As the first line of defense against proliferation, accurate determinations of the uranium isotopic ratio (or enrichment) in UF_6 are critical for materials verification, accounting and safeguards. Currently, mass spectrometry (MS) is the most sensitive measurement technique for analysis of stable and long-lived isotopes. However, current MS techniques require too much infrastructure and operator expertise for field deployment and operation. In-field isotopic analysis of UF_6 has the potential to substantially reduce the time, logistics and expense of bulk sample handling by allowing for an 'informed' choice of samples to be sent to a central laboratory for further definitive analysis by standard techniques.

It is common that the next generation of analytical instruments is driven by technologies that are either currently available or just now emerging. Therefore, a comprehensive and in-depth review is conducted on state-of-the-art and emerging technologies for field enrichment analysis of UF_6. These technologies are evaluated based on their competitive advantages and current limitations for in-field UF_6 enrichment assay. The objective of the study is to identity the most promising technologies that can be used for development of the next-generation, field-deployable instrument for providing rapid, accurate, and precise UF_6 enrichment assay. In this paper, we provide an overview of instrument options, discuss their limitations, and examine the main gaps between needs and capabilities for their field use.

Keywords: uranium hexafluoride; enrichment assay; mass spectrometry; optical spectrometry

1. Introduction

Uranium hexafluoride (UF_6) is arguably the most important uranium compound in the nuclear fuel cycle, particularly for uranium isotope enrichment. The enrichment of the ^{235}U isotope in UF_6 is a necessary major step in the production of fuel for most nuclear power plants. As nuclear fuel cycle technology becomes more prevalent around the world, international nuclear safeguards and interest in UF_6 enrichment assay has been growing. As the first line of defense against proliferation, accurate analytical techniques to determine the uranium isotopic distribution in UF_6 are critical for materials verification, accounting, and safeguards at enrichment plants.

Currently, the International Atomic Energy Agency (IAEA) monitors the production of enriched UF_6 at declared facilities by collecting between 1–10 g of gaseous UF_6 into a sample bottle, which is then transferred and tamper-sealed in an approved shipping container. The sample is shipped under chain of custody to a central laboratory [e.g., IAEA's Nuclear Materials Analysis Laboratory (NMAL) in Seibersdorf] for high-precision isotopic assay by mass spectrometry (MS) [1, 2]. The logistics are cumbersome and the analysis is costly, and results are not available for some time after sample collection. In addition, new shipping regulations are making it more difficult to transport UF_6 [2]. The IAEA is challenged to develop effective safeguards approaches at enrichment plants while working within budgetary constraints [3].

There is one on-site enrichment-assay technique, termed COMbined Procedure for Uranium Concentration and Enrichment Assay (COMPUCEA), which offers exceptional analytical capabilities with typical combined (systematic and random) measurement uncertainty around 0.25% relative [4, 5]. COMPUCEA combines energy-dispersive X-ray absorption edge spectrometry and gamma-ray spectrometry to measure uranium elemental content and ^{235}U enrichment, respectively. The method is already in use in inventory verification campaigns at European LEU fuel fabrication plants [4]. Currently, the method is utilized only for solid samples and is not yet applied to UF_6 enrichment assay. IAEA is exploring extending the COMPUCEA system to in-field UF_6 enrichment determination [6]. Major shortcomings of the method are its comparatively complicated sample preparations, and its hours-long measurement time for each sample.

For off-site U-enrichment measurements, MS is currently the most sensitive analytical technique; however, current MS techniques require too much infrastructure and operator expertise for field deployment and operation. In-field UF_6 enrichment assay has the potential to substantially reduce the time, logistics and expense of bulk sample

handling by allowing for an 'informed' choice of samples to be sent to a central laboratory for definitive analysis by standard laboratory techniques.

The objective of the present study is to identify the potential, viable technologies that are likely to culminate in an expedited development of the next generation of field deployable instrumentation for rapidly determining UF_6 enrichment. One common approach to project the next generation of chemical instrumentation is to track the current trends and to extrapolate them [7]. This approach, albeit somewhat conservative, has been demonstrated with a fair degree of reliability in the fields of analytical science and chemical instrumentation [7]. Therefore, an extensive literature review on existing and emerging technologies for UF_6 enrichment assay is performed, and the competitive advantages and current limitations of different analytical techniques are compared. Based on the results of the review, requirements and recommendations for development of the next-generation field-deployable instrument for UF_6 enrichment assay are addressed.

2. Methodology

Current analytical techniques for UF_6 enrichment assay are based on one of three scientific principles: radiometry, mass spectrometry, and optical spectrometry. In this study, a comprehensive list of UF_6 enrichment-assay methods is reviewed and evaluated. COMPUCEA [4, 5] is a radiometric technique and serves as a benchmark for on-site U enrichment assay. Evaluated mass spectrometric techniques include: gas source mass spectrometry (GSMS) [8], thermal ionization mass spectrometry (TIMS) [9], inductively coupled plasma mass spectrometry (ICP-MS) [9, 10], multi-photon ionization mass spectrometry [11, 12], UF_6 molecular mass spectrometry with portable mass spectrometer [13], laser ionization mass spectrometry [14], surface-enhanced laser desorption and ionization (SELDI) [2], liquid sampling-atmospheric pressure glow discharge mass spectrometry (LS-APGD-MS) [15-18], and atmospheric-pressure solution-cathode glow-discharge mass spectrometry (AP-SCGD-MS) [19]. Techniques based on optical spectrometric principles include: optical atomic emission with argon afterglow discharge or ICP [20-22], glow discharge optogalvanic spectroscopy [23], laser-ablation laser induced fluorescence [24], laser ablation absorbance ratio spectrometry (LAARS) [25, 26], atomic beam tunable diode laser absorption [27], tunable laser infrared (IR) absorption [28, 29] and its high performance version with quantum cascade laser [30], and laser induced spectrochemical assay for uranium enrichment (LISA-UE).

GSMS, TIMS and ICP-MS are included to enable comparison with laboratory techniques. Otherwise, all other techniques should be directly compared with COMPUCEA for their potential to serve as an alternative field-based enrichment assay technique. Each technique is compared against seven assessment criteria; estimated technological maturity and instrument costs are also provided. Because of page limit, it is not feasible to describe, even briefly, all the reviewed techniques in great detail. Therefore, only those analytical techniques, according to published literature results, that so far show the highest potentials for UF_6 enrichment assay as alternatives for TIMS or multi-collector (MC)-ICP-MS will be emphasized.

2.1 Assessment criteria

The seven assessment criteria are: meeting predefined target of analytical accuracy and precision (two separate criteria), meeting relaxed target of accuracy and precision (two criteria), simultaneous ^{235}U and ^{238}U measurement, measurement time, and overall ease of operation. The IAEA published international target values (ITVs) [31] for a wide variety of measurement techniques for nuclear material accountancy and safeguards verification. The ITVs are considered to be achievable values in routine measurements and are uncertainties to be considered in judging the reliability of analytical techniques applied to the analyses of nuclear materials [31]. GSMS, TIMS and MC-ICP-MS are the only three MS systems listed under destructive analysis (DA) techniques [31]. Although more techniques (five) are listed under the category of non-destructive analysis (NDA), it is notable that measurement uncertainties from NDA techniques are much larger – typically more than an order of magnitude larger – than the three MS-based DA techniques [31].

To evaluate the analytical accuracy and precision of a candidate analytical technique, reported analytical figures of merit are compared to the ITVs of TIMS and MC-ICP-MS [31], which serve as comparison references. For these MS systems, the *u(r)* and *u(s)* (i.e., random and systematic uncertainties, respectively) ITVs are the same, and they are 0.5% (relative) for depleted U (^{235}U < 0.3% abundance), 0.2% (relative) for uranium with ^{235}U abundance between 0.3% and 1%, 0.1% (relative) for LEU (1% < ^{235}U < 20%), and 0.05% (relative) for HEU (^{235}U > 20%) [31]. The IAEA ITVs define the strict target for analytical accuracy and precision for all analytical techniques under evaluation. Because the IAEA ITVs are intended for more established techniques, to better gauge the potential of emerging techniques that are still under active development, an additional set of performance criteria is set by relaxing the target values by 10× (i.e., 5% relative for depleted U, 2% relative for samples with ^{235}U between 0.3% and 1%, and so on). In case the emerging technique is so new that experimental data are not yet available specifically for uranium, projected or extrapolated values from very similar techniques sharing the same scientific principle are used.

2.2 Importance of simultaneous measurement and signal correlation in isotope-ratio determination

Signal correlation is crucial in defining the accuracy and precision of isotope-ratio measurements, and thus, its importance needs to be stressed. So far, none of the analytical techniques ***directly*** measure the $^{235}U/^{238}U$ ratio. Instead, all available techniques indirectly gauge the $^{235}U/^{238}U$ ratio through separate measurements of the signals from ^{235}U and ^{238}U. All measurements unavoidably contain noise [32]. Noise can be further categorized as uncorrelated and correlated. Examples of uncorrelated noise include shot (also known as Poisson) noise and thermal (also known as Johnson) noise [32, 33]. Shot noise is the result of random arrival of particles [e.g., radioactive decay particles, photons for emission source, or ions for ionization source] onto the detector [33]. Thermal noise is the consequence of random movement of electrons in resistors in electronic devices [32, 33]. Correlated noise is due to flickering of the system, and examples include: variations in the sample introduction system, fluctuations in atomization, ionization or excitation efficiencies for optical and mass spectrometry, and interference noise from power supply [32, 33].

The relative error in the ratio of two signals, *x* and *y*, could be larger or smaller than those in the individual signals (i.e., a further degradation or an improvement in measurement precision); the outcome is heavily dependent on the correlation of noise in the two signals. To illustrate the importance of signal correlation, computer simulated signals with both correlated and uncorrelated noise components have been generated and are shown in Figure 1 below. Individually, the precisions of the two signals, *x* and *y* [relative standard deviations (RSD) ~ 20%] are rather unacceptable for many situations. However, because the two signals are highly correlated – that is signal dips and peaks occur at the same time for the two signals, the noise is greatly reduced in the ratio *x/y* (RSD ~ 1.5%). These highly correlated signals are usually achievable only when the two signals are acquired simultaneously, as repeatedly proven in the literature [34-36]. Signal correlation typically greatly degrades for sequential measurements (i.e., when signals *x* and *y* are measured one by one, sequentially in time).

From the foregoing discussion, not all noise sources are correlated in nature. The uncorrelated noise source that is particularly relevant to isotopic analysis is the counting statistics of shot noise. In an ideal case in which all other noise sources are eliminated, precision of isotopic analysis is then governed by counting statistics. Because radiometric techniques usually do not have other noise sources, their precisions are largely limited by counting statistics. For a truly simultaneous ICP mass spectrometer, it has been shown that isotopic-ratio precision close to counting-statistics limit is achievable [37]. Accordingly, one criterion on evaluation of a candidate analytical technique is on its capability to perform truly simultaneous measurement for ^{235}U and ^{238}U.

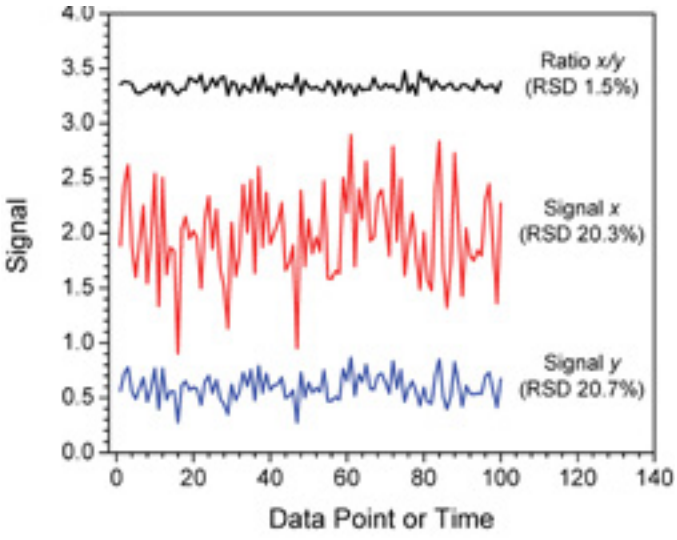

Figure 1: Two simulated signals, x and y, and the resultant signal ratios (x/y), demonstrating the importance of correlated noise and simultaneous measurement in improving the signal (isotopic) ratios.

3. Results and Discussion

3.1 Results of performance assessment

Table 1 summarizes the performance of the benchmark laboratory-based techniques (GSMS, TIMS, and MC-ICP-MS), the benchmark field technique (COMPUCEA), and the four emerging techniques that show promising potential for in-field UF_6 enrichment assay. There are three grades for each assessment metric. For metrics under the categories analytical performance and operation, the three grades are equivalent to pass (marked with a symbol "+"), marginal (symbol "○") and fail (symbol "–").

For analytical accuracy and precision, a "+" rating indicates meeting the stated criteria, a "○" rating represents not meeting the criteria but is within 3× the target (i.e., marginally fail), and a "–" rating denotes not meeting the criteria even if the target is relaxed by a factor of 3. The metric "simultaneous ^{235}U and ^{238}U measurements" summarizes if the ^{235}U and ^{238}U measurements are performed in truly simultaneous ("+"), quasi-simultaneous ("○") or sequential ("–") fashions. The metric "measurement time" refers to typical measurement time. Techniques rated "+" typically require less than 10 minutes for one measurement. Techniques that typically require more than 10 minutes but less than one hour are rated "○", and those requiring more than one hour are rated "–". The metric "overall ease of operation" reflects the overall complexity of the measurement procedures (including sample-preparation procedures) and instrument operation (e.g., turn-key *versus* complicated systems), as well as general robustness of the instrument and the technique.

All techniques are also compared on their "technology maturity" and "instrument cost". Unlike metrics on

analytical performance and operation, which can be readily quantified and most results are available in open literature, assessments and estimations on "technology maturity" and, in particular, "instrument cost" are difficult because they depend on so many other factors (e.g., technology breakthrough or bottleneck that have not yet been recognized, research support and effort) that in general are unforeseeable. Therefore, the assessments on these two metrics reflect only our best estimation. For technology maturity, techniques rated "+" indicate that they are currently in use on routine basis for UF_6 enrichment assay. Techniques rated "○" indicate that they are not yet used routinely for UF_6 enrichment assay but should be very close to or are already available for field testing, whereas techniques rated "–" indicate further development is needed before field testing can be materialized. "Instrument cost" is compared on a relative basis with three grades of descending capital equipment cost: "$$$", "$$" and "$".

It should be noted that the evaluations are based solely on results that can be found in the open literature, for example: journal articles, conference proceedings, publicly accessible reports, traceable presentations in scientific meetings or conferences, and IAEA or NNSA factsheets. Although we have included the latest open literature results to the best of our knowledge, because active research is still on-going on many emerging techniques, the most updated performance of a technique could be better than what was published in the open literature. Furthermore, it is appropriate to stress that each technique is evaluated solely for its suitability to provide on-site enrichment assay specifically for UF_6. Accordingly, a technique evaluated but not listed in Table 1 should not be viewed negative as a whole because it is possible that the candidate technique could be promising for other applications (e.g., for other types of U samples, as an in-laboratory analytical method, or its ability to perform quick screening measurement that does not require the stated high accuracy or precision).

	Analytical Performance					Operation			
	Accuracy meets target	Precision meets target	Accuracy within 10× target	Precision within 10× target	Simultaneous ^{235}U & ^{238}U measurements	Measurement time	Overall ease of operation	Technology maturity	Instrument cost
GSMS	+	+	+	+	+	–	–	+	$$$
TIMS	+	+	+	+	+	–	–	+	$$$
MC-ICP-MS	+	+	+	+	+	○	–	+	$$$
COMPUCEA	○	○	+	+	+[Note1]	–	–	○	$$
LS-APGD-MS (with Orbitrap MS)	?	+	?	+	+	+	○	–	$$
AP-SCGD-MS (with Orbitrap MS)	?	+[Est]	?	+[Est]	+	+	○	–	$$
LAARS	○	○	+	+	+	+	○	○	$
LISA-UE	–[Est]	–[Est]	?	○[Est]	+	+	+	–	$

Note 1: Signal correlation for measurement-noise reduction through simultaneous ^{235}U and ^{238}U measurement does not apply in COMPUCEA because the isotopic assay is performed through radiometric counting (gamma ray), in which the dominated noise source is counting statistics.

Table 1: Assessment summaries of benchmark and promising techniques for UF_6 enrichment assay. A superscript "Est" indicates estimation from scientific principle. A question mark indicates that information either is not yet available or is insufficient for estimation.

3.2 Benchmark techniques – GSMS, TIMS, MC-ICP-MS and COMPUCEA

The benchmark techniques will be briefly discussed in this section, whereas the details of each promising emerging technique will be individually discussed in the following sections. Overall, all the three benchmark, MS-based techniques offer outstanding analytical performance but demanding operation in terms of measurement time as well as expertise in instrument operation. All MS-techniques comprise two essential components – an ionization source and a mass analyzer. The mass analyzer responds only to ions (charged particles) but not neutrals; thus, an ionization source is required to convert the neutral (uncharged) sample to charged ions. The mass analyzer separates and measures the charged ^{235}U and ^{238}U atoms/molecules according to their different mass-to-charge ratios.

Gas source mass spectrometry (GSMS) accepts gaseous UF_6 samples directly for enrichment-assay measurements. Because of the homogeneity of gaseous samples, it is currently the most sensitive and precise measurement technique [38]. However, its drawback for UF_6 analyses is its long measurement time. The long measurement cycle is related to memory effects due to the corrosive and reactive nature of gaseous UF_6, which can be compensated only by multiple measurements alternating between the sample and two calibration standards. As a result, the duration for one measurement cycle is about 5 hours [38]. For TIMS measurements, samples are usually presented as a solution and deposited onto the TIMS filament for electrothermal vaporization as well as ionization. Measurement precision for TIMS is slightly lower than GSMS because the sample on a TIMS filament becomes isotopically inhomogeneous due to fractionation during the measurement process [38]. MC-ICP-MS employs a high temperature (>6000 K) inductively coupled plasma – requiring high power (~1.5 kW) – as the atomization and ionization source. The MC-designation refers to the specific type of mass analyzer, a multi-collector. The MC-mass spectrometer is a double-focusing system consisting of an electrostatic sector and a magnetic sector in which ions are separated according to their mass-to-charge ratio and focused onto a focal plane. The MC-system allows the operator to position several detectors at different positions along the focal plane of the mass spectrometer [39] for simultaneous collection and measurement of several masses.

A joint-laboratory study [40] compared U-isotopic ratio measurements by GSMS, TIMS and MC-ICP-MS. For a UF_6 sample with ^{235}U at natural abundance, the RSDs were 0.012%, 0.025% and 0.060%, respectively [40]. Sample throughput is about 1-2 samples/day for GSMS, increases to 5-10 samples/day for TIMS and further increases to around 20 samples/day for MC-ICP-MS [40].

The COMPUCEA technique, developed at the Institute for Transuranium Elements (ITU), is a transportable analytical system for on-site uranium concentration and enrichments assays [5]. Its application specifically for UF_6 enrichment assay is still under development by the IAEA [6], although its use on LEU-oxide samples is considered routine. In fact, IAEA has published an ITV for COMPUCEA – 0.4% *u(r)* and 0.2% *u(s)* for ^{235}U enrichment in LEU oxides [31]. ITVs for other enrichment levels (i.e., DU, NU and HEU oxides) are not published [31].

The COMPUCEA technique is based on energy-dispersive X-ray absorption edge spectrometry and gamma-ray spectrometry. Before presented to X-ray and gamma-ray measurements, the solid sample needs to undergo some laborious preparation steps. Briefly, the solid sample is quantitatively transformed into a uranyl nitrate solution, which involves sample digestion in 8 M nitric acid and subsequent dilution to 3 M acidity with a target U concentration about 190 g/L [5]. The solution is first characterized for its density and temperature [5]. During the process, standard laboratory tools (e.g., portable density meter, glass-ware, chemicals, hot plate, weighing balance) and operators' facilities (e.g., fume hood) are used [5].

The solution sample is then measured by X-ray and gamma-ray spectroscopy. Typically, for an LEU sample, three replicates of each measurement type are performed; acquisition of each X-ray and gamma-ray spectrum takes about 1000 s and 2000 s, respectively [5]. For a natural U sample, the time is increased to 5000 s for each gamma-ray counting [41]. Data treatment is not very straightforward because the two measurements are interdependent. Specifically, the X-ray measurement needs the knowledge of the enrichment to accurately convert the measured uranium concentration into mass fraction, whereas the gamma measurement needs the uranium concentration as input to correct for self-attenuation effect [41]. Therefore, data evaluation is made in an iterative manner. Furthermore, the sample parameters (including solution density, sample volume, and bottom thickness of sample container) need to be taken in account [4]. Software has been developed for automatic data acquisition and analysis for the in-field COMPUCEA measurement system [5].

The analytical performance is impressive for an on-site measurement. For LEU samples, the achievable combined uncertainty (*u(r)* and *u(s)*) is typically around 0.25% relative [4, 5] (published ITV for combined uncertainty is 0.45% [31]). According to a recent IAEA report [6], the adaptation of the chemical preparation steps for COMPUCEA determination of UF_6 enrichment is currently being studied by IAEA and with the European Commission. As chemical transformation of UF_6 to uranyl nitrate solution is comparatively simple compared with its oxide counterpart, it is anticipated that the COMPUCEA method will be available for on-site UF_6 enrichment assay in the very near future. The drawback of the method is the relatively long counting time, especially for natural (3×5000 s) and depleted uranium, and its labor intensive sample preparation process.

3.3 Emerging mass-spectrometric techniques

3.3.1 Liquid sampling-atmospheric pressure glow discharge mass spectrometry

Liquid sampling-atmospheric pressure glow discharge mass spectrometry (LS-APGD-MS), under joint development from Clemson University and Pacific Northwest National Laboratory (PNNL) [15-18], is the most well characterized emerging mass-spectrometric technique, especially for the determination of uranium isotopic ratio. Figure 2 shows a schematic diagram of the LS-APGD-MS setup. The glow discharge is a microplasma (volume ~ 1 mm^3) formed by imposing a low direct-current potential (typically several hundred volts) between the surface of

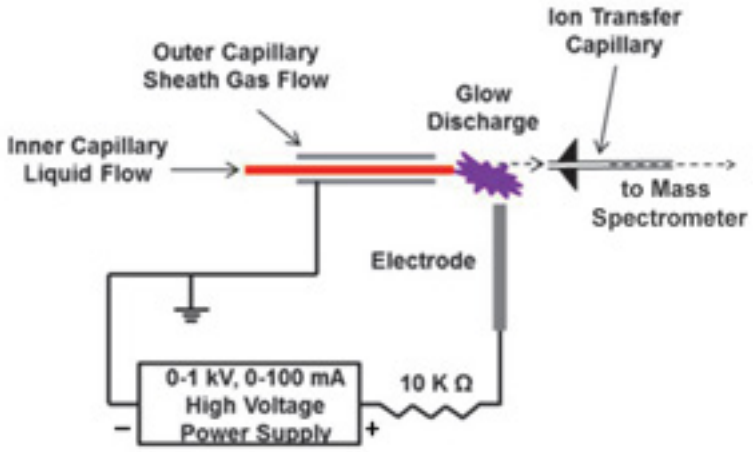

Figure 2: Schematic diagram of LS-APGD-MS. Adapted with permission from reference [2], published by Pacific Northwest National Laboratory, US Department of Energy.

an electrolyte solution (e.g., 2% nitric acid) and a metallic counter electrode [42, 43]. The supporting electrolyte solution flows at atmospheric pressure out of a small (~ 100 μm) glass capillary housed within a slightly larger metal capillary, between which cooling gas is passed [43]. The normal operating parameters include liquid electrolyte flow rates of 5–100 μL/min, cooling gas (typically helium or argon) flow rate of < 1 L/min, and power consumption of < 40 W [16].

Currently, the researchers coupled this LS-APGD ionization source to a high-resolution mass spectrometer (the Orbitrap). Hoegg *et al.* [15, 16] recently discussed various aspects of the LS-APGD and Orbitrap combination for uranium isotopic analyses, including optimization of various operating parameters (both for the discharge and the Orbitrap), preliminary analytical figures of merit, and known limitations. U-containing sample was introduced in a solution form and mixed with the supporting electrolyte. The researchers reported that the dominant U-species in the mass spectra was UO_2^+, and little U^+ or UO^+ were detected [15].

Based on published results [16, 18], the reported analytical precision is encouraging, and is, so far, the best in all the emerging techniques reviewed. In a recent published work [18], which the effort was primarily focused on factors affecting the precision of isotope ratio measurements, reported precisions (in terms of RSD of measured $^{235}U/^{238}U$ ratios from 1 μg/mL natural-U solutions, before correction of scaling factor) were in the range of 0.05% to 0.13% and met the ITV target for precision (i.e., 0.2% RSD for ^{235}U at natural abundance).

At present, the researchers evaluated the analytical accuracy through a correction scaling factor [15, 18]. In their latest report [18], the researchers determined this scaling factor through a certified reference material of natural U, and measured the $^{235}U/^{238}U$ ratios of three unknown natural-U samples. However, it has been stated that this correction scaling factor depends on the $^{235}U/^{238}U$ ratio, as well as a change every time that the system is restarted [18]. At this point, it would be difficult to estimate or project the accuracy of the LS-APGD-MS technique in the field for a sample with unknown ^{235}U abundance.

Although the LS-APGD, in its present form, would not directly accept gaseous UF_6 for analysis, a two-step reaction to transform UF_6 to a uranium solution is well established and regarded as a somewhat standard procedure [8]. The two-step reaction involves hydrolysis of UF_6 to UO_2F_2 ($UF_6 + 2\ H_2O \rightarrow UO_2F_2 + 4\ HF$), followed by conversion to nitrate salt with nitric acid ($UO_2F_2 + 2\ HNO_3 \rightarrow UO_2(NO_3)_2 + 2\ HF$).

One potential drawback of the LS-APGD-MS technique for UF_6 enrichment assay is memory effect, which has been documented in several reports [2, 16, 44]. The cause(s) for the memory effect is not well characterized, but it was suggested that material deposited on the capillary counter-electrode and/or the mass spectrometer capillary interface could be the source [2, 44].

3.3.2 Atmospheric-pressure solution-cathode glow-discharge mass spectrometry

Atmospheric-pressure solution-cathode glow-discharge mass spectrometry (AP-SCGD-MS), currently under development jointly at Rensselaer Polytechnic Institute and Indiana University [19], is identical in scientific principle to the LS-APGD-MS reviewed in the last section but different in design for the generation of the microplasma discharge (cf. Figure 3). The AP-SCGD is a direct-current plasma sustained directly on the surface of a flowing liquid electrode (typically at a rate of 1–2 mL/min), supported in ambient air without the need for a cooling gas or other gas flows [19]. Power of AP-SCGD is ~ 70 W (normally < 100 W) [45], and is generally slightly higher than that of the LS-APGD. A distinct difference between AP-SCGD and LS-APGD is that AP-SCGD sustains on a flowing liquid cathode, with the liquid in excess, whereas LS-APGD operates in a total

consumption mode in which all the electrolyte solution is consumed [15]. An advantage of the total consumption in LS-APGD is that no chemical waste solution is generated. Although the excessive flow of electrolyte generates chemical waste for AP-SCGD, the continuously self-renewing liquid surface of the flowing solution cathode potentially minimizes memory effects. In terms of instrument setup, footprint and operation requirements, AP-SCGD shares many similarities with LS-APGD.

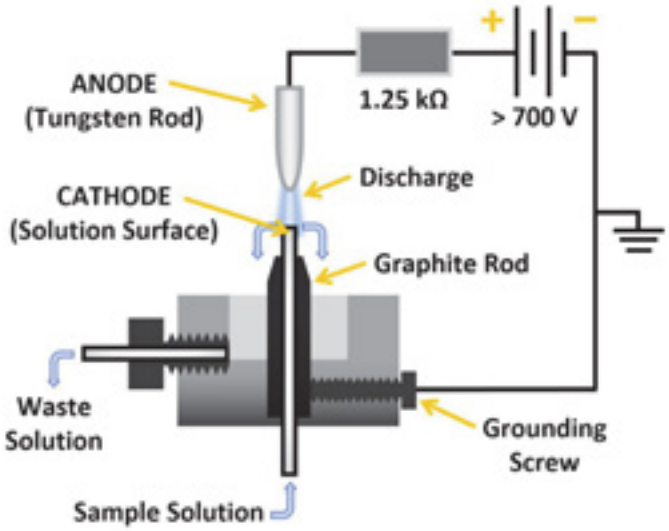

Figure 3: Schematic diagram of AP-SCGD cell utilized for mass spectrometry. Adapted with permission from reference [46], published by The Royal Society of Chemistry. Original figure is published under a Creative Commons Attribution-NonCommercial 3.0 Unported Licence.

Although not yet characterized for its performance on isotopic analysis, the AP-SCGD demonstrated a notably better detection limit than the LS-APGD as an ionization source for atomic mass spectrometry [19]. The latest work on AP-SCGD [19], reported the analytical performance of this source coupled to an Orbitrap mass spectrometer for atomic and molecular mass spectrometry. Specific for uranium solution samples, the reported detection limit in AP-SCGD was 0.8 ng/mL (parts per billion, ppb) with UO_2^+ as the measuring ion [19]. As detection limit is related directly to sensitivity and/or background noise, a better (lower) detection limit for the AP-SCGD implies that it offers higher sensitivity and/or lower background noise. As both factors are important for isotopic ratio measurements, the AP-SCGD should be considered as a candidate emerging technology meriting further evaluation of its full potential for uranium isotopic assay.

3.3.3 Is Orbitrap suitable as field-deployable mass spectrometer?

In the two emerging mass-spectrometric techniques covered above, both research teams employed Orbitrap mass spectrometer. Given the impressive isotopic-ratio precisions and detection limits achievable by the two techniques, one might think that the problem of looking for the next generation of field-deployable instrument for UF_6 enrichment assay is solved. Unfortunately, the current technology of the Orbitrap mass spectrometer makes it inappropriate to serve as a field-deployable instrument [2]. A comment from the LS-APGD-MS research team [2] is that *"Although a conveniently available instrument for this work* (the LS-APGD-MS)*, it* (the Orbitrap) *is not one that would be appropriate for the type of in-field work envisioned by the potential user."* To elaborate, although the Orbitrap is a benchtop instrument, it is rather large and heavy (490 pounds [47]). Also, the requirement for environmental conditions for the Orbitrap mass spectrometer is quite demanding. For instance, according to the pre-installation manual of the Orbitrap [47], the optimum operation temperature is between 18°C to 21°C and temperature fluctuations of 1°C or more over a 10 minute period can affect performance. There are also rather strict requirements for humidity and vibration controls [47].

It should also be noted that the high resolution offered by the Orbitrap likely contributes to the impressive analytical figures of merit reported for the LS-APGD-MS, as it is documented that several low-intensity, non-uranium ions remain after collision-induced dissociation (CID, a process to dissociate and reduce background ions in the mass spectrometer) and require the high-resolution capability of the Orbitrap to resolve them [17]. If the Orbitrap is replaced by a more fieldable (and very likely lower resolution) mass spectrometer, it is currently unknown how such replacement would affect the analytical accuracy and precision. Clearly, there is a need to couple, characterize and evaluate the LS-APGD and AP-SCGD (and possibly other similar glow-discharge variants) to a mass spectrometer that is more field-deployable and preferably capable of performing truly simultaneous measurements.

3.4 Emerging optical-spectrometric techniques

3.4.1 Laser ablation absorbance ratio spectrometry

Laser ablation absorbance ratio spectrometry (LAARS), developed at PNNL, is an all-optical technique for uranium isotopic assay. Its working principle is based on the isotopic shifts in atomic transitions between ^{235}U and ^{238}U atoms, and employs atomic absorption as the measurement means. The technique employs three lasers at a minimum – one for ablation sampling and two for simultaneous measurements of the relative abundances of ^{235}U and ^{238}U [25], as depicted in Figure 4. Laser ablation creates free uranium atoms from a solid sample, and these atoms are then probed by diode laser through atomic absorption. Measurements are conducted in a reduced-pressure environment to reduce spectral-line broadening. The current LAARS setup employs four lasers for better wavelength stability.

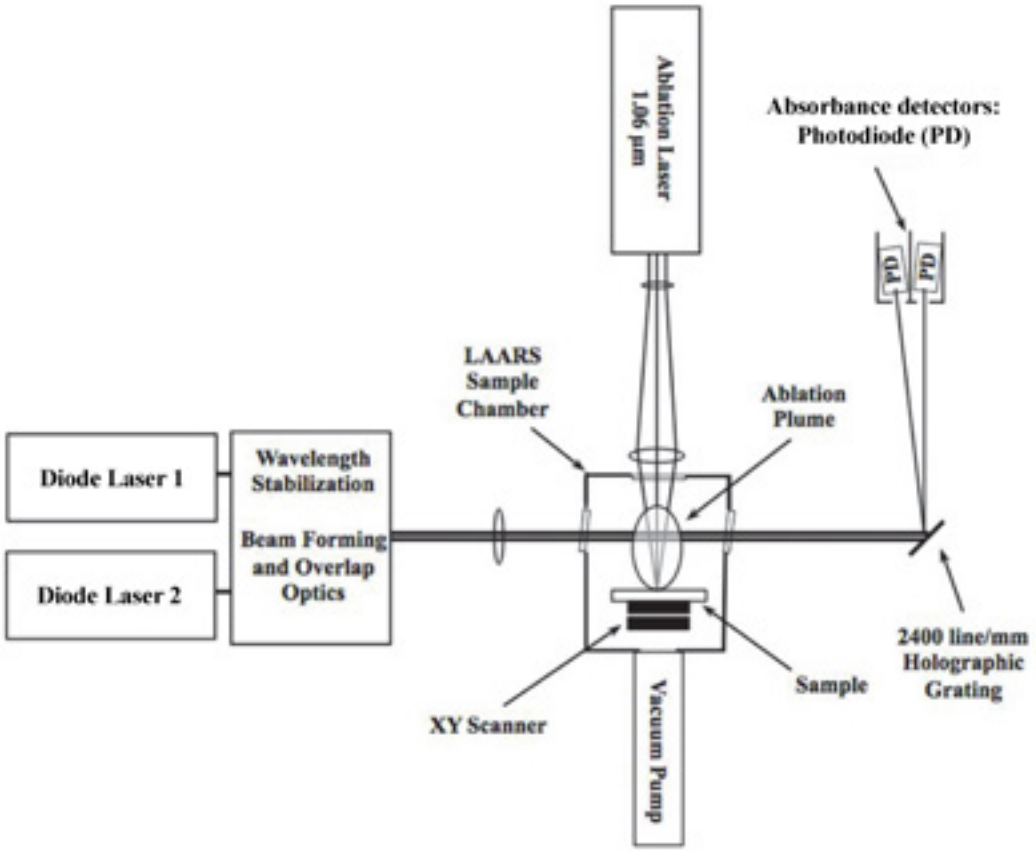

Figure 4: Schematic diagram of LAARS. Adapted with permission from reference [25], published by Los Alamos National Laboratory, US Department of Energy.

The Niemax research group in 2002 [48] is probably the first to report measurements of uranium isotope ratios in solid samples through combination of laser-ablation sampling and diode-laser atomic absorption (before the technique was coined as LAARS). With a two-diode-lasers approach, which allows *simultaneous* measurements of the two U isotopes, Liu *et al.* [48] reported a measurement precision of 1.1% RSD for a pure uranium-oxide sample with ^{235}U at natural abundance [48]. Reported accuracy for the $^{235}U/^{238}U$ ratio was within 5% (relative) for a uranium mineral sample (i.e., an impure sample) at natural isotopic abundance. In this predecessor to LAARS, the two diode lasers need to be tightly aligned with each other so that the two laser beams are probing identical volumes of the laser plume generated by the ablation laser. The absorption of the two beams is directly related to the number density of ^{235}U and ^{238}U atoms along their optical path, which directly translates to $^{235}U/^{238}U$ ratio of the sample if an identical plasma volume is probed. Because the number densities of atoms inside laser induced plasma are spatially dependent, a slight misalignment of the two measurement beams (which then probe different volumes of the plasma) could lead to analytical bias on the measured $^{235}U/^{238}U$ ratios.

The initial LAARS setup [25, 26] was somewhat similar to that reported by Liu *et al.* [48]. The LAARS system was evolved in the last few years and several sophisticated advancements are in place in the current version [49]. For instance, the two probe laser beams are directed into a single-mode optical fiber, in which the two beams overlap and are directed to the laser plume with a single achromatic focusing lens. This single optical fiber approach largely reduces the difficulty of optical alignment and warrants that identical laser-plume volumes are probed by the

two lasers. Wavelength stability of the ^{235}U probe beam was also improved through Zeeman splitting method and offset locking [49], although at the expenses of an additional diode laser.

Specific for UF_6 enrichment assay, LAARS employs a tailored solid thin-film sorbent to convert gaseous UF_6 to uranyl fluoride through a hydrolysis reaction [49]. Data from a presentation dated October 2014 [49] showed that accuracy and precision can achieve 0.1% in ^{235}U enrichment levels for natural U and LEU. Specifically, for three UF_6 samples with ^{235}U abundances at 0.725%, 3.982% and 5.119%, the reported *relative* bias with frequency-locked probe lasers were 10%, 0.8% and 0.3%, respectively [49]. Reported relative precisions for these three UF_6 samples were 8.3%, 1.5% and 1.5%, respectively [49]. The latest result [50, 51] demonstrated significant improvements in both accuracy and precision, especially for natural-U samples. For a sample with ^{235}U abundance at 5.119%, the relative bias and precision were about 0.1% and 0.6%, respectively. For a natural-U sample, the relative bias and precision were about 0.3% and 0.5%, respectively. Because the ITVs for relative random and systematic uncertainties [i.e., *u(r)* and *u(s)*] are both 0.1% for LEU and 0.2% for natural-U samples [31], the precision of LAARS is currently within 3× to 6× from the target as a replacement for laboratory-based mass spectrometry. Accuracies are close (within a factor of 2) to the target.

Measurement time for LAARS is fast and is typically around 10 minutes [25]. The overhead for sample preparation is also minimal; the reaction time for the conversion of gaseous UF_6 onto the solid thin-film sorbent is several minutes [25]. Because wavelength selectivity for the two isotopes comes from the narrow-bandwidth diode laser, a small optical spectrometer/grating is sufficient to separate the two signals [in this case, different atomic transitions (i.e., wavelengths) can be used for ^{235}U and ^{238}U], which further reduces the footprint of the instrument.

3.4.2 Laser induced spectrochemical assay for uranium enrichment

Laser induced spectrochemical assay for uranium enrichment (LISA-UE) is in a very early stage of development (starting October 2016), and is a joint effort between Lawrence Berkeley National Laboratory (LBNL) and Oak Ridge National Laboratory (ORNL). It is an all-optical technique for uranium isotopic assay and, in fact, is an extension of the well-known laser induced breakdown spectroscopy (LIBS) technique to low-pressure gaseous UF_6 samples. Like LAARS, its principle is based on the isotopic shifts in ^{235}U and ^{238}U atomic transitions. Instead of utilizing atomic absorption, LISA-UE employs atomic emission as the measurement means. It is known that isotopic shifts for some uranium atomic emission lines can reach tens of picometers and are large enough to be readily measured with an optical spectrometer even under ambient pressure and comparatively high temperature (e.g., 5000 K) [52]. In fact, atomic emission spectrometry has a long history of being utilized for uranium isotopic analysis [53, 54]. Recently, Krachler *et al.* [20, 21] validated isotopic analysis of ^{235}U and ^{238}U in depleted, natural and enriched uranium with ICP-atomic emission spectrometry, and further extended the analysis to other U-isotopes like ^{233}U.

The LISA-UE system is targeted for direct analysis of gaseous UF_6 samples, although a solid sample (e.g., UF_6 absorbed on a solid substrate) also can be used. Specifically for gaseous UF_6 samples, a small gas chamber with optical access couples directly to a UF_6 cylinder/pipeline valve for sampling (cf. Figure 5). Through the optical port, a

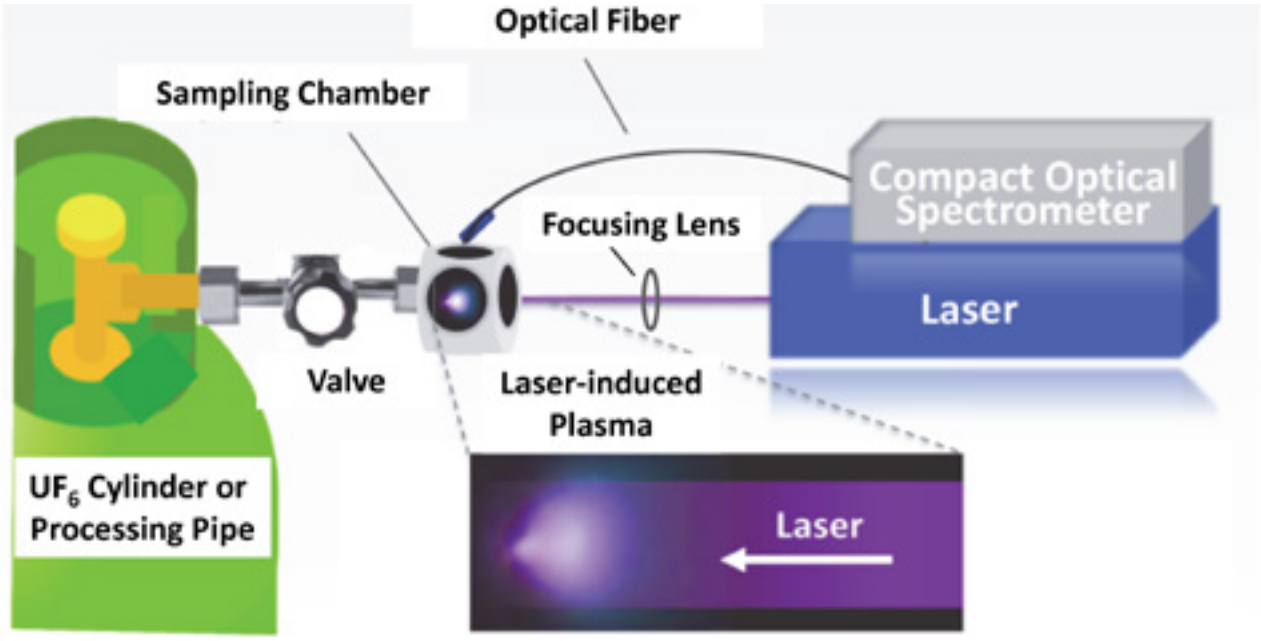

Figure 5: Schematic diagram of LISA-UE.

pulsed laser beam is focused into the UF_6 gas sample and the laser–gas interaction then creates a transient high temperature plasma excitation source. This high-temperature plasma is capable of breaking down the chemical bonds in the sample, converts it into its constituent atoms, and promotes a portion of these atoms into their excited states. These excited states, through radiative decay, emit photons that are characteristic of its elemental and isotopic identities. When this transient plasma starts to cool (typically after several microseconds), molecules form through recombination. It has recently been reported that resulting molecular emissions also carry isotopic information [55]. The technique is potentially applicable to both off-line and on-line measurements.

There are some marked contrasts between LAARS and LISA-UE. Only one ablation laser is required in LISA-UE whereas LAARS needs three/four lasers [25]. Similar to the LAARS ablation laser, there are no constraints on the LISA-UE laser wavelength, and a laser with nanosecond (or shorter) pulse width is required in both cases. Plasma emissions in LISA-UE are collected by single set of light-collection optics for simultaneous ^{235}U and ^{238}U measurement, which also inherently guarantee that an identical plasma emission volume is probed. Furthermore, one potential advantage of employing emission over laser absorption is that a large collection of spectral lines (atomic) and bands (molecular) are emitted from the laser induced plasma, which can be simultaneously measured with a multichannel optical spectrometer. As many of these spectral features carry the isotopic information of the sample, multiple emission-line/band measurement has been shown through simulations to improve analytical precision [55].

As LISA-UE is in a very early stage of development, its analytical capabilities are not yet known. However, it is anticipated that emission measurements on a collection of spectral features likely offers advantage over single line-pairs commonly employed in absorption measurements. For example, it has been shown through computer simulation that the use of a chemometric algorithm from a collection of spectral features provides several times improvement in the precision of ^{235}U abundance compared to those measurements utilizing only a single pair of emission lines [56]. In simulation, the ultimate precision was about 0.11% in absolute ^{235}U abundance for multiple line analysis [56], with signals accumulated from 10 laser pulses. Clearly, further improvement in precision can be achieved through more signal accumulation (i.e., accumulating signal from more than 10 laser pulses), although it is also anticipated that computer simulation probably offers the best-case scenario. The anticipated measurement time is a few minutes for each UF_6 sample. Commercial, field-deployable LIBS instruments for direct solid-sample analysis are readily available. Although these commercial systems are not specifically designed for gaseous samples, modification for handling gaseous samples is feasible. The size, as well as power requirements, of the components can be readily fit into a field-deployable instrument. While it is extremely early in the development cycle, the LISA-UE instrumentation set up – with a single laser excitation source and a single set of light-collection optics – is likely to be the simplest among all the techniques discussed above, which is advantageous as an in-field instrument.

4. Outlook

To summarize, a comprehensive and in-depth review was conducted on state-of-the-art and emerging technologies for field enrichment analysis of UF_6. All techniques were assessed for their potential to serve as an alternative for laboratory-based mass spectrometry. The evaluation was comprised of seven criteria, broadly defined: measurement characteristics and analytical capability, measurement time, and overall ease of operation and system complexity.

In terms of both analytical performance and sample throughput, the LS-APGD-MS is currently the best in all the emerging techniques reviewed, and is already shown to offer analytical precisions meeting the ITVs of TIMS and MC-ICP-MS. The AP-SCGD-MS, although currently utilized only for elemental analysis and not yet for isotopic measurements, already exhibits its pronounced sensitivity advantage for uranium detection. Unlike the ICP, these glow-discharge ion sources use microplasmas which allow operation under low power and low gas flow (if a plasma gas is ever needed) — and, thus, are highly field deployable. The technical challenge to transform them into the next generation field-deployable UF_6 enrichment-assay instrument, perhaps, relates to identifying and coupling to a multi-channel field-deployable mass spectrometer that, through simultaneous measurement, can maintain the current achievable analytical figures of merit.

Some emerging techniques based on optical spectrometric techniques are also promising. LAARS shows its promise with demonstrated precisions within 3× to 6× and accuracies within a factor of 2 [50, 51] from the target as a replacement for laboratory-based mass spectrometry for natural-U and LEU samples. LISA-UE is a new development and is based on well-established atomic emissions (LIBS). All of these emerging technologies show potential to be the next generation of rapid, field deployable instrumentation for UF_6 enrichment assay.

5. Acknowledgements

This work was performed under the auspices of the U.S. Department of Energy by Lawrence Berkeley National Laboratory under Contract DE-AC02-05CH11231. The project was funded by the U.S. Department of Energy/National Nuclear Security Administration's (DOE/NNSA's) Office of Nonproliferation and Arms Control (NPAC) in the Safeguards Technology Development Program.

6. References

[1] Anheier N., Cannon B., Martinez A., Barrett C., Taubman M., Anderson K., and Smith L.E.; *A new approach to enrichment plant UF_6 destructive assay sample collection and analysis;* PNNL-SA-112353, Pacific Northwest National Laboratory, 2015.

[2] Barinaga C.J., Hager G.J., Hoegg E.D., Carman A.J., and Hart G.L.; *Feasibility of a fieldable mass spectrometer FY 2015 year-end report;* PNNL-24842, Pacific Northwest National Laboratory, 2015.

[3] Smith L.E., and Lebrun A.R.; *Design, modeling and viability analysis of an online uranium enrichment monitor; in 2011 IEEE Nuclear Science Symposium Conference Record;* 2011; Paper 1030-1037

[4] Erdmann N., Amador P., Arboré P., Eberle H., Lutzenkirchen K., Ottmar H., Schorlé H., van Belle P., Lipcsei F., and Schwalbach P.; *COMPUCEA: A high performance analysis procedure for timely on-site uranium accountancy verification in leu fuel fabrication plants; ESARDA Bulletin;* 43; 2009; 30-39

[5] Berlizov A., Schachinger A., Roetsch K., Erdmann N., Schorlé H., Vargas M., Zsigrai J., Kulko A., Keselica M., Caillou F., Unsal V., and Walczak-Typke A.; *Feedback from operational experience of on-site deployment of bias defect analysis with COMPUCEA; J. Radioanal. Nucl. Chem.;* 307; 2016; 1901-1909

[6] International Atomic Energy Agency; *Development and implementation support programme for nuclear verification 2016-2017;* STR-382, International Atomic Energy Agency (IAEA), 2016.

[7] Hieftje G.M.; *The future of plasma spectrochemical instrumentation. Plenary lecture; J. Anal. At. Spectrom.;* 11; 1996; 613-621

[8] Mialle S., Richter S., Hennessy C., Truyens J., Jacobsson U., and Aregbe Y.; *Certification of uranium hexafluoride reference materials for isotopic composition; J. Radioanal. Nucl. Chem.;* 305; 2015; 255-266

[9] Boulyga S., Konegger-Kappel S., Richter S., and Sangely L.; *Mass spectrometric analysis for nuclear safeguards; J. Anal. At. Spectrom.;* 30; 2015; 1469-1489

[10] Ardelt D., Polatajko A., Primm O., and Reijnen M.; *Isotope ratio measurements with a fully simultaneous Mattauch-Herzog ICP-MS; Anal. Bioanal. Chem.;* 405; 2013; 2987-2994

[11] Okada Y., Kato S., Satooka S., and Takeuchi K.; *Measurements of U-235/U-238 isotopic ratio in the photoproduct UF_5 by multiphoton ionization and time-of-flight mass spectrometry; Appl. Phys. B;* 62; 1996; 515-519

[12] Armstrong D.P., Harkins D.A., Compton R.N., and Ding D.; *Multiphoton ionization of uranium hexafluoride; J. Chem. Phys.;* 100; 1994; 28-43

[13] Whitten W.B., Reilly P.T.A., Verbeck G., and Ramsey J.M.; *Mass spectrometry of UF_6 in a micro ion trap; in 7th International Conference on Facility Operations: Safeguards Interface;* Charleston, SC; 2004; Paper 345-349

[14] NNSA Office of Nonproliferation and Arm Control; *Safeguards technology factsheet - portable mass spectrometry working group (MSWG);* 2016.

[15] Hoegg E.D., Barinaga C.J., Hager G.J., Hart G.L., Koppenaal D.W., and Marcus R.K.; *Preliminary figures of merit for isotope ratio measurements: The liquid sampling-atmospheric pressure glow discharge microplasma ionization source coupled to an Orbitrap mass analyzer; J. Am. Soc. Mass Spectrom.;* 27; 2016; 1393-1403

[16] Hoegg E.D., Barinaga C.J., Hager G.J., Hart G.L., Koppenaal D.W., and Marcus R.K.; *Isotope ratio characteristics and sensitivity for uranium determinations using a liquid sampling-atmospheric pressure glow discharge ion source coupled to an Orbitrap mass analyzer; J. Anal. At. Spectrom.;* 31; 2016; 2355-2362

[17] Barinaga C.J., Hager G.J., Hart G.L., Koppenaal D.W., Marcus R.K., Jones S.M., and Manard B.T.; *Toward a fieldable atomic mass spectrometer for safeguards applications: Sample preparation and ionization; in 12th Symposium on International Safeguards: Linking Strategy, Implementation and People (IAEA-CN-220);* Vienna, Austria; 2014; Paper S08-08

[18] Hoegg E.D., Marcus R.K., Koppenaal D.W., Irvahn J., Hager G.J., and Hart G.L.; *Determination of uranium isotope ratios using a liquid sampling-atmospheric pressure glow discharge - Orbitrap mass spectrometer system; Rapid Commun. Mass Spectrom.;* 31; 2017; 1534-1540

[19] Schwartz A.J., Williams K.L., Hieftje G.M., and Shelley J.T.; *Atmospheric-pressure solution-cathode glow discharge: A versatile ion source for atomic and molecular mass spectrometry; Anal. Chim. Acta;* 950; 2017; 119-128

[20] Krachler M., and Carbol P.; *Validation of isotopic analysis of depleted, natural and enriched uranium using high resolution ICP-OES; J. Anal. At. Spectrom.;* 26; 2011; 293-299

[21] Krachler M., and Wegen D.H.; *Promises and pitfalls in the reliable determination of U-233 using high resolution ICP-OES; J. Anal. At. Spectrom.;* 27; 2012; 335-339

[22] Zamzow D., Murray G.M., Dsilva A.P., and Edelson M.C.; *High-resolution optical-emission spectroscopy of uranium hexafluoride in the argon afterglow discharge; Appl. Spectrosc.;* 45; 1991; 1318-1321

[23] Barshick C.M., Shaw R.W., Young J.P., and Ramsey J.M.; *Evaluation of the precision and accuracy of a uranium isotopic analysis using glow-discharge optogalvanic spectroscopy; Anal. Chem.;* 67; 1995; 3814-3818

[24] Smith B.W., Quentmeier A., Bolshov M., and Niemax K.; *Measurement of uranium isotope ratios in solid samples using laser ablation and diode laser-excited atomic fluorescence spectrometry; Spectrochim. Acta Part B;* 54; 1999; 943-958

[25] Boyer B.D., Anheier N., Cable-Dunlop P., and Sexton L.; *Incorporation of new, automated environmental sampling systems into safeguards approaches;* LA-UR-13-28412, Los Alamos National Laboratory, 2013.

[26] Bushaw B.A., and Anheier Jr N.C.; *Isotope ratio analysis on micron-sized particles in complex matrices by laser ablation-absorption ratio spectrometry; Spectrochim. Acta Part B;* 64; 2009; 1259-1265

[27] NNSA Fact Sheet; *Fieldable atomic beam laser spectrometer for isotopic analysis;* 2016.

[28] Berezin A.G., Malyugin S.L., Nadezhdinskii A.I., Namestnikov D.Y., Ponurovskii Y.Y., Stavrovskii D.B., Shapovalov Y.P., Vyazov I.E., Zaslavskii V.Y., Selivanov Y.G., Gorshunov N.M., Grigoriev G.Y., and Nabiev S.S.; *UF_6 enrichment measurements using TDLS techniques; Spectrochim. Acta Part A;* 66; 2007; 796-802

[29] Grigor'ev G.Y., Lebedeva A.S., Malyugin S.L., Nabiev S.S., Nadezhdinskii A.I., and Ponurovskii Y.Y.; *Investigation of $^{235}UF_6$ and $^{238}UF_6$ spectra in the mid-IR range; Atomic Energy;* 104; 2008; 398-403

[30] NNSA Fact Sheet; *Spectroscopic methods for ultra-low isotopic analysis of proliferant material;* SRNL-STI-2016-00217, 2016.

[31] Zhao K., Penkin M., Norman C., Balsley S., Mayer K., Peerani P., Pietri C., Tapodi S., Tsutaki Y., Boella M., Renha Jr. G., and Kuhn E.; *International target values 2010 for measurement uncertainties in safeguarding nuclear materials;* STR-368, International Atomic Energy Agency (IAEA), 2010.

[32] Hieftje G.M.; *Signal-to-noise enhancement through instrumental techniques. 1. Signals, noise, and S/N enhancement in the frequency domain; Anal. Chem.;* 44; 1972; 81A-88A

[33] Derks E.P.P.A., Pauly B.A., Jonkers J., Timmermans E.A.H., and Buydens L.M.C.; *Adaptive noise cancellation on inductively coupled plasma spectroscopy; Chemometrics and Intelligent Laboratory Systems;* 39; 1997; 143-159

[34] Hieftje G.M.; *Emergence and impact of alternative sources and mass analyzers in plasma source mass spectrometry; J. Anal. At. Spectrom.;* 23; 2008; 661-672

[35] Meija J., and Mester Z.; *Signal correlation in isotope ratio measurements with mass spectrometry: Effects on uncertainty propagation; Spectrochim. Acta Part B;* 62; 2007; 1278-1284

[36] Grotti M., Todoli J.L., and Mermet J.M.; *Influence of the operating parameters and of the sample introduction system on time correlation of line intensities using an axially viewed CCD-based ICP-AES system; Spectrochim. Acta Part B;* 65; 2010; 137-146

[37] Schilling G.D., Ray S.J., Sperline R.P., Denton M.B., Barinaga C.J., Koppenaal D.W., and Hieftje G.M.; *Optimization of Ag isotope-ratio precision with a 128-channel array detector coupled to a Mattauch-Herzog mass spectrograph; J. Anal. At. Spectrom.;* 25; 2010; 322-327

[38] Richter S., Kuhn H., Truyens J., Kraiem M., and Aregbe Y.; *Uranium hexafluoride (UF_6) gas source mass spectrometry for certification of reference materials and nuclear safeguard measurements at IRMM; J. Anal. At. Spectrom.;* 28; 2013; 536-548

[39] Wieser M., Schwieters J., and Douthitt C.; Multi-collector inductively coupled plasma mass spectrometry, in Isotopic analysis - fundamentals and applications using ICP-MS, 1st ed., Wiley-VCH Verlag, (2012) p 77-91

[40] de Oliveira O.P., de Bolle W., Alonso A., Richter S., Wellum R., Ponzevera E., Sarkis J.E.S., and Kessel R.; *Demonstrating the metrological compatibility of uranium isotope amount ratio measurement results obtained by GSMS, TIMS and MC-ICPMS techniques; Int. J. Mass Spectrom.;* 291; 2010; 48-54

[41] Erdmann N., Albert N., Amador P., Arboré P., Eberle H., Lutzenkirchen K., Ottmar H., Schorlé H., van Belle P., Lipcsei F., Schwalbach P., Jung S., and Lafolie R.; *COMPUCEA 2nd generation performance evaluation;* IAEA-CN-184/316, International Atomic Energy Agency, 2010.

[42] Quarles C.D., Carado A.J., Barinaga C.J., Koppenaal D.W., and Marcus R.K.; *Liquid sampling-atmospheric*

pressure glow discharge (LS-APGD) ionization source for elemental mass spectrometry: Preliminary parametric evaluation and figures of merit; Anal. Bioanal. Chem.; 402; 2012; 261-268

[43] Marcus R.K., Quarles C.D., Barinaga C.J., Carado A.J., and Koppenaal D.W.; *Liquid sampling-atmospheric pressure glow discharge ionization source for elemental mass spectrometry; Anal. Chem.;* 83; 2011; 2425-2429

[44] Carado A.J., Quarles C.D., Duffin A.M., Barinaga C.J., Russo R.E., Marcus R.K., Eiden G.C., and Koppenaal D.W.; *Femtosecond laser ablation particle introduction to a liquid sampling-atmospheric pressure glow discharge ionization source; J. Anal. At. Spectrom.;* 27; 2012; 385-389

[45] Schwartz A.J., Ray S.J., and Hieftje G.M.; *Evaluation of interference filters for spectral discrimination in solution-cathode glow discharge optical emission spectrometry; J. Anal. At. Spectrom.;* 31; 2016; 1278-1286

[46] Schwartz A.J., Shelley J.T., Walton C.L., Williams K.L., and Hieftje G.M.; *Atmospheric-pressure ionization and fragmentation of peptides by solution-cathode glow discharge; Chemical Science;* 7; 2016; 6440-6449

[47] Thermo Fisher Scientific; *Exactive™ series: Exactive™ and Q Exactive™ preinstallation requirements guide;* Revision A - 1288110, 2011.

[48] Liu H., Quentmeier A., and Niemax K.; *Diode laser absorption measurement of uranium isotope ratios in solid samples using laser ablation; Spectrochim. Acta Part B;* 57; 2002; 1611-1623

[49] Anheier N., Cannon B., Martinez A., Barrett C., Taubman M., Anderson K., and Smith L.E.; *A laser-based method for onsite analysis of UF_6 at enrichment plant;* PNNL-SA-105776, Pacific Northwest National Laboratory, 2014.

[50] NNSA Safeguards Technology Factsheet; *Laser ablation absorption ratio spectroscopy (LAARS);* PNNL-SA-123926, 2017.

[51] Barrett C.A., Cannon B.D., Martinez A., Chen C.S., Guerrero R., and Anheier Jr N.C.; *Destructive assay safeguards technology for sample collection and assay (presentation); in STM Workshop on Analytical Developments, Reference Materials, and Statistical Applications in the Nuclear Fuel Cycle;* Vienna, Austria 2016; Paper PNNL-SA-118821

[52] Chan G.C.Y., Choi I., Mao X., Zorba V., Lam O.P., Shuh D.K., and Russo R.E.; *Isotopic determination of uranium in soil by laser induced breakdown spectroscopy; Spectrochim. Acta Part B;* 122; 2016; 31-39

[53] Burkhart L.E., Stukenbroeker G., and Adams S.; *Isotope shifts in uranium spectra; Phys. Rev.;* 75; 1949; 83-85

[54] Edelson M.C., and Fassel V.A.; *Isotopic abundance determinations by inductively coupled plasma atomic emission spectroscopy; Anal. Chem.;* 53; 1981; 2345-2347

[55] Mao X., Chan G.C.-Y., Choi I., Zorba V., and Russo R.E.; *Combination of atomic lines and molecular bands for uranium optical isotopic analysis in laser induced plasma spectrometry; J. Radioanal. Nucl. Chem.;* 312; 2017; 121-131

[56] Chan G.C.Y., Mao X., Choi I., Sarkar A., Lam O.P., Shuh D.K., and Russo R.E.; *Multiple emission line analysis for improved isotopic determination of uranium – a computer simulation study; Spectrochim. Acta Part B;* 89; 2013; 40-49

Changes to the ^{252}Cf neutron spectrum caused by source encapsulation

R. Weinmann-Smith[1,2], S. Croft[3], M.T. Swinhoe[1], A. Enqvist[2]

[1] Safeguards Science and Technology Group (NEN-1), Nuclear Nonproliferation Division, Los Alamos National Laboratory, NM 87545, USA
E-mail: swinhoe@lanl.gov , rweinmann@lanl.gov

[2] Nuclear Engineering Department, University of Florida, Gainesville, FL 32611, USA
E-mail: enqvist@mse.ufl.edu

[3] Safeguards and Security Technology, Nuclear Security & Isotope Division, Oak Ridge National Laboratory, One Bethel Valley road, Oak Ridge, TN 37831, USA
E-mail: crofts@ornl.gov
LA-UR-17-22582

Abstract:

Lightly encapsulated ^{252}Cf sources are commonly used to characterize and calibrate neutron detectors for safeguards applications without much attention being paid to what it means for the encapsulation to be neutronically "light". In this work we quantify the impact of encapsulation on both the neutron spectrum and neutron intensity. We find that a 1.3 mm shell of copper reduces the mean energy by about 1 %. Thus encapsulation can be used to deliberately adjust the mean energy to match, for example, that of the spontaneously fissile Pu nuclides. The spectrum cannot be matched perfectly however and so the influence of encapsulation on a particular system calibration is case specific. We demonstrate using encapsulation to match the Pu neutron detection efficiency for a common safeguards detector, the Active Well Coincidence Counter.

Keywords: NDA; Monte Carlo; Prompt Fission Neutron Spectrum, ^{252}Cf, encapsulation

1. Introduction

Monte Carlo modeling is a well established way to make performance estimates of neutron assay systems for safeguards [1]. The models may be benchmarked against experimental results obtained using sealed sources containing ^{252}Cf, which is a convenient source of spontaneous fission neutrons, as a surrogate for the materials of interest. Often a correction is needed to allow for the difference between the energy spectrum of the ^{252}Cf neutrons and the neutron emission spectrum of interest [2]. For a bare ^{252}Cf source the prompt fission neutron spectrum from ^{252}Cf may be approximated reasonably well by simple analytical shapes. For instance in ISO 8529 [3] a Maxwellian distribution with a temperature parameter of 1.42 MeV corresponding to a mean energy of 2.13 MeV is recommended. Fröhner [4] makes the case for the next simplest macroscopic representation, namely the Watt spectrum, with a temperature parameter equal to 1.175 MeV and the fragment kinetic energy per nucleon parameter of 0.359 MeV corresponding to a mean energy of approximately 2.122 MeV. These approximations are valid for lightly encapsulated ^{252}Cf sources, but the meaning of light encapsulation is not quantified in the literature. Presumably the Amersham X1 capsule [5] would qualify. This is a cylindrical assembly about 10 mm long and 7.8 mm in diameter with a combined wall thickness of roughly 1.6 mm of stainless steel. But it is well established that even such a modest capsule perturbs the angular distribution from what would otherwise be a near perfect isotropic pattern. The neutrons emitted isotropically by a small amount of ^{252}Cf source material exit the capsule in an anisotropic distribution with near cylindrical symmetry about the axis of the capsule [5,6]. When calibrating a fluence measuring device correction factors for the anisotropic emission of the source must be made [5-8]. Less well known is the impact on the neutron spectrum caused by neutron interactions in the source encapsulation. Whether the difference between a 1 mm and a 3 mm stainless steel container, or some other jacketing material, matters or not clearly depends on the detailed response function of the system. However, the lack of general guidance on what constitutes a lightly encapsulated source and the general neglect of the effect of encapsulation on the neutron spectrum in the scientific literature means it is difficult to make an informed judgment. In this work we take a step to resolving this dilemma by analyzing the effect of encapsulation on a specific system. In Section 2 we present a simple analysis justifying why encapsulation needs to be considered in neutron metrology and establishing that for common source types spectral indices might be expected to exhibit a linear behavior with wall thickness. In Section 3 we draw on published results taken from a report [9] in which the authors were deliberately trying to moderate the spectrum of ^{252}Cf and ^{241}Am/Be(α,n) sources as an alternative to using accelerator facilities to obtain a variety of spectra for calibration of neutron dosimetry instruments. In particular we show how the mean energy from ^{252}Cf surrounded by spherical shells scales roughly linearly with shell thickness. In real situations we are concerned with the full energy distribution, as modified by all reaction channels, and also with potential losses and gains to the number of neutrons emerging per initial source neutron. This was studied in Section 4 through a series of Monte Carlo simulations using the Los Alamos MCNP6 code [9, 10]. The effects of spheres of

common materials were simulated, along with some common commercial encapsulations. Finally the spectrum modification was coupled to the Active Well Multiplicity Counter (AWCC) [12 detection efficiency, and the source encapsulation was modified to match the detection efficiency of ^{240}Pu. Manufactured cylindrical encapsulation was measured for verification.

2. A simple analysis

We might intuitively expect that simple spectral indices of the emergent neutron spectrum will vary linearly with the thickness of the encapsulation when the thickness is small. Consider as an example how the mean energy for a point emitter located at the centre of a thin spherical shell of encapsulating material will shift as a function of shell thickness under the approximation that the only reaction of significance taking place is elastic scattering. Because of the assumption that the source is lightly encapsulated the probability, p_s, that a neutron will scatter on its way out is given, to first order, by

$$p_s = \Sigma_s t \ll 1$$

where Σ_s is the macroscopic scattering cross section of the shell material and t is its thickness.

Thus, a fraction $(1-p_s)$ of neutrons emerge without scattering and without suffering any energy loss. The neutrons that do scatter will lose on average an energy of half the amount of the maximum energy that can be transferred to the target nucleus as recoil kinetic energy under the additional assumption that the scattering is isotropic in the center of mass reference frame. Thus, we can write the mean fractional neutron energy loss, f, as

$$f = \frac{2A}{(1+A)^2}$$

where A is the ratio of the mass of the target nucleus to that of the rest mass of the neutron. For an element we may take, to a good approximation, A to be numerically equal to the molar mass in g.mol^{-1}.

The mean energy of the scattered neutrons, $\overline{E}_s$, is consequently lower than the mean energy, $\overline{E}$, of the emitting source and can be expressed as

$$\overline{E}_s = \overline{E}(1-f) = \overline{E}\left(1-\frac{2A}{(1+A)^2}\right)$$

The mean energy of the emerging spectrum of neutrons, $\overline{E}_{ext}$, is formed from the contributions of both the unscattered and scattered neutrons and becomes

$$\overline{E}_{ext} = (1-p_s)\overline{E} + p_s\overline{E}_s = (1-p_s)\overline{E} + p_s\overline{E}\left(1-\frac{2A}{(1+A)^2}\right)$$

which upon rearrangement and substitution yields

$$\overline{E}_{ext} = \overline{E}\left(1-\frac{2A}{(1+A)^2}\Sigma_s t\right)$$

This formula predicts that for an idealized scattering capsule the mean emergent energy will fall linearly with wall thickness. Real capsules can drop energies more effectively through inelastic processes and other channels such as (n,2n) interactions. The latter is also an example of a neutron gain process, in contrast (n,α) interactions are an example of a neutron loss process. Although we did not consider these kinds of interaction in the simple view presented, for a thin wall, the basic idea remains sound. Thus, we anticipate the ratio between the emergent mean energy and that of the ideal unencapsulated source to trend roughly as follows

$$R = \frac{\overline{E}_{ext}}{\overline{E}} = 1-bt$$

where b is a coefficient specific to the composition and density of the wall material.

3. Illustration using literature data

Hsu and Chen [9] performed a series of calculations in which ^{252}Cf was placed at the center of spheres of various radii and of various materials to see if they could create reference spectra that would be useful for calibrating health physics instruments. Spheres of radius 25.4, 50.8, 76.2, 101.6, 153.2 and 203.2 mm were selected. Twelve materials were studied Be, graphite, Al, Fe, Cu, Pb, LiD, H_2O, D_2O, polyethylene $(CH_2)_n$, glass and concrete. Neutron spectra at 500 mm from the center were computed. The results are presented graphically and are difficult to interpret. Gains and losses are not quantified. The mean energy as a function of wall thickness is given numerically only in the case of copper. With zero wall thickness the mean energy is given as 2.54 MeV. This is far higher than the generally accepted value of about 2.12 to 2.13 MeV [2,3]. However, by forming the ratio of the emergent spectrum to the initiating spectrum we expect that this apparent bias will be largely suppressed. The data was fit to the form

$$R = e^{-bt}$$

which reduces to the linear form ($R \approx 1-bt$) expected for thin shell walls when $bt \ll 1$.

In the present case the exponential fit produces an excellent fit across the whole range of spheres modeled with $b = 0.0079\,mm^{-1}$ and an R^2 value of 0.99992, as evident in Figure 1. The uncertainty in the b value is unknown because uncertainties were not reported in the original work. It is also apparent from Figure 1 that a copper sphere with a radius greater than about 10 or 20 mm cannot be considered thin in the context of our earlier simple theoretical development. A radius (wall thickness) of a few mm falls in the linear range and we see that to get a 1% shift in mean energy requires a wall thickness of about $0.01/0.0079 = 1.27$ mm of Cu; this equates to a shift of about 21 keV in the mean energy. For the HLNCC-II [13], a common thermal well counter with a single ring of ^{3}He filled proportional counters, the fractional change in detection efficiency in the vicinity of 2 MeV is about 17% per MeV [14]. Thus a 21 keV reduction in mean energy translates into a projected relative increase in efficiency of about 0.36% (from about 0.1750 counts per neutron to about 0.1756 counts per neutron. This is a change which is readily measureable.

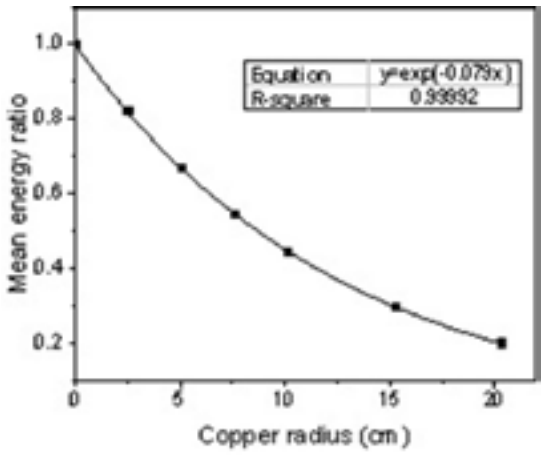

Figure 1: Plot of mean energy ratio, *R*, as a function of moderator radius, *t*, taken from [9] for the case of ^{252}Cf at the center of Cu spheres along with the fitted result.

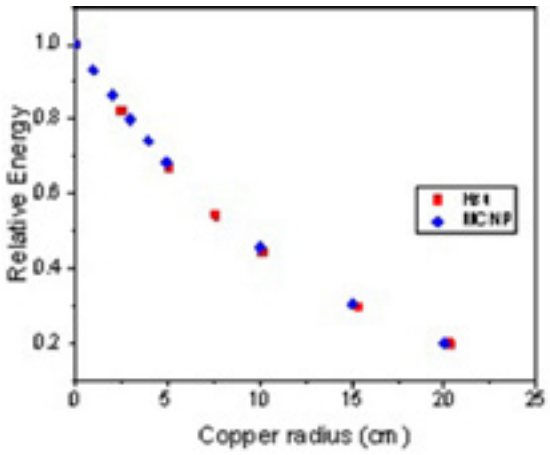

Figure 2: Comparison of our MCNP calculations and the results of Hsu et al [9] interpreted as a relative energy to remove the obvious mean energy discrepancy in that work.

4. Detailed modeling

Although instructive the results of Hsu and Chen do not cover the range of interest relevant to our present discussion – which is the use of lightly encapsulated sources typical of those obtained from a variety of vendors and used routinely in safeguards laboratories. For this reason we performed a series of focused Monte Carlo simulations. These calculations give not only the mean energy shift but the shape of the spectrum and also allow losses and gains to be tallied.

The model used the MCNP6.1.1b default energy spectrum of spontaneous fission of ^{252}Cf with a mean energy of 2.13 Mev, corresponding to Watt spectrum parameters of a=1.180 MeV and b=1.03419 MeV^{-1} . Coincidence counting was not simulated, so default physics options including non-analog transport were used. The neutrons were started at a point source at the origin. The energy was tallied over a sphere centered at the origin with a radius of 300 mm. Figure 2 shows the average energy of neutrons crossing this sphere as a function of thickness of copper. The results of Hsu are also included in the figure, and both show the same general trend. The mean energy of prompt fission neutrons from ^{240}Pu spontaneous fission, again using the default MCNP6.1.1b spontaneous fission energy spectrum is 1.93 MeV. Using the exponential relationship shown in Figure 2, we would require a sphere of 13.9mm copper thickness to produce an average energy equal to that of a notional bare ^{240}Pu source.

Table 1 shows the gains, losses, net neutrons, and average energy, for spheres of the materials calculated in MCNP for thicknesses between 1 and 20 cm. The gains, losses, and net values are per source neutron. Lead has the least effect on the average energy while polyethylene has the most. Beryllium's (n.2n) reaction causes a 6.5% increase in emitted neutrons at a thickness of 15 cm. Stainless steel has a negligible net intensity effect but a potentially significant energy effect at the thicknesses of common encapsulations.

Aluminum				
Spherical Radius (cm)	**Gains**	**Losses**	**Net**	**Average energy (MeV)**
1	$6.28*10^{-7}$	$3.82*10^{-4}$	$1.00*10^{0}$	$2.07*10^{0}$
2	$1.22*10^{-6}$	$7.50*10^{-4}$	$9.99*10^{-1}$	$2.02*10^{0}$
3	$1.73*10^{-6}$	$1.11*10^{-3}$	$9.99*10^{-1}$	$1.96*10^{0}$
4	$2.22*10^{-6}$	$1.45*10^{-3}$	$9.99*10^{-1}$	$1.91*10^{0}$
5	$2.64*10^{-6}$	$1.79*10^{-3}$	$9.98*10^{-1}$	$1.85*10^{0}$
10	$4.25*10^{-6}$	$3.33*10^{-3}$	$9.97*10^{-1}$	$1.58*10^{0}$
15	$5.71*10^{-6}$	$4.70*10^{-3}$	$9.95*10^{-1}$	$1.32*10^{0}$
20	$6.66*10^{-6}$	$6.00*10^{-3}$	$9.94*10^{-1}$	$1.08*10^{0}$

Beryllium				
Spherical Radius (cm)	**Gains**	**Losses**	**Net**	**Average energy (MeV)**
1	$3.07*10^{-2}$	$2.00*10^{-2}$	$1.01*10^{0}$	$2.00*10^{0}$
2	$5.87*10^{-2}$	$3.83*10^{-2}$	$1.02*10^{0}$	$1.87*10^{0}$
3	$8.41*10^{-2}$	$5.50*10^{-2}$	$1.03*10^{0}$	$1.74*10^{0}$
4	$1.07*10^{-1}$	$7.05*10^{-2}$	$1.04*10^{0}$	$1.60*10^{0}$
5	$1.28*10^{-1}$	$8.50*10^{-2}$	$1.04*10^{0}$	$1.47*10^{0}$
10	$2.02*10^{-1}$	$1.37*10^{-1}$	$1.06*10^{0}$	$8.78*10^{-1}$
15	$2.43*10^{-1}$	$1.78*10^{-1}$	$1.07*10^{0}$	$4.79*10^{-1}$
20	$2.65*10^{-1}$	$2.28*10^{-1}$	$1.04*10^{0}$	$2.48*10^{-1}$
Concrete				
Spherical Radius (cm)	**Gains**	**Losses**	**Net**	**Average energy (MeV)**
1	$8.84*10^{-7}$	$9.42*10^{-4}$	$9.99*10^{-1}$	$2.05*10^{0}$
2	$1.47*10^{-6}$	$1.85*10^{-3}$	$9.98*10^{-1}$	$1.97*10^{0}$
3	$2.06*10^{-6}$	$2.74*10^{-3}$	$9.97*10^{-1}$	$1.88*10^{0}$
4	$2.72*10^{-6}$	$3.61*10^{-3}$	$9.96*10^{-1}$	$1.80*10^{0}$
5	$3.21*10^{-6}$	$4.48*10^{-3}$	$9.96*10^{-1}$	$1.71*10^{0}$
10	$1.04*10^{-5}$	$1.27*10^{-2}$	$9.87*10^{-1}$	$1.29*10^{0}$
15	$6.38*10^{-4}$	$4.96*10^{-2}$	$9.50*10^{-1}$	$9.21*10^{-1}$
20	$5.81*10^{-3}$	$1.38*10^{-1}$	$8.62*10^{-1}$	$6.41*10^{-1}$
Copper				
Spherical Radius (cm)	**Gains**	**Losses**	**Net**	**Average energy (MeV)**
1	$5.19*10^{-5}$	$2.22*10^{-3}$	$9.98*10^{-1}$	$1.98*10^{0}$
2	$9.91*10^{-5}$	$4.61*10^{-3}$	$9.95*10^{-1}$	$1.84*10^{0}$
3	$1.42*10^{-4}$	$7.22*10^{-3}$	$9.93*10^{-1}$	$1.70*10^{0}$
4	$1.82*10^{-4}$	$1.01*10^{-2}$	$9.90*10^{-1}$	$1.58*10^{0}$
5	$2.14*10^{-4}$	$1.32*10^{-2}$	$9.87*10^{-1}$	$1.46*10^{0}$
10	$3.25*10^{-4}$	$3.48*10^{-2}$	$9.65*10^{-1}$	$9.75*10^{-1}$
15	$3.82*10^{-4}$	$7.05*10^{-2}$	$9.30*10^{-1}$	$6.47*10^{-1}$
20	$4.07*10^{-4}$	$1.25*10^{-1}$	$8.75*10^{-1}$	$4.26*10^{-1}$
Heavy water				
Spherical Radius (cm)	**Gains**	**Losses**	**Net**	**Average energy (MeV)**
1	$8.53*10^{-4}$	$7.43*10^{-4}$	$1.00*10^{0}$	$1.98*10^{0}$
2	$1.64*10^{-3}$	$1.44*10^{-3}$	$1.00*10^{0}$	$1.83*10^{0}$
3	$2.38*10^{-3}$	$2.16*10^{-3}$	$1.00*10^{0}$	$1.68*10^{0}$
4	$3.06*10^{-3}$	$2.69*10^{-3}$	$1.00*10^{0}$	$1.54*10^{0}$
5	$3.69*10^{-3}$	$3.24*10^{-3}$	$1.00*10^{0}$	$1.40*10^{0}$
10	$6.20*10^{-3}$	$5.46*10^{-3}$	$1.00*10^{0}$	$8.54*10^{-1}$
15	$7.85*10^{-3}$	$7.03*10^{-3}$	$1.00*10^{0}$	$5.02*10^{-1}$
20	$8.92*10^{-3}$	$8.39*10^{-3}$	$1.00*10^{0}$	$2.91*10^{-1}$
Iron				
Spherical Radius (cm)	**Gains**	**Losses**	**Net**	**Average energy (MeV)**
1	$3.25*10^{-5}$	$8.69*10^{-4}$	$9.99*10^{-1}$	$2.02*10^{0}$
2	$6.05*10^{-5}$	$1.70*10^{-3}$	$9.98*10^{-1}$	$1.91*10^{0}$
3	$8.59*10^{-5}$	$2.56*10^{-3}$	$9.97*10^{-1}$	$1.80*10^{0}$
4	$1.10*10^{-4}$	$3.41*10^{-3}$	$9.97*10^{-1}$	$1.70*10^{0}$
5	$1.31*10^{-4}$	$4.28*10^{-3}$	$9.96*10^{-1}$	$1.60*10^{0}$
10	$2.03*10^{-4}$	$8.90*10^{-3}$	$9.91*10^{-1}$	$1.18*10^{0}$
15	$2.43*10^{-4}$	$1.40*10^{-2}$	$9.86*10^{-1}$	$8.79*10^{-1}$
20	$2.61*10^{-4}$	$2.05*10^{-2}$	$9.80*10^{-1}$	$6.77*10^{-1}$

Glass				
Spherical Radius (cm)	**Gains**	**Losses**	**Net**	**Average energy (MeV)**
1	$7.80*10^{-7}$	$1.23*10^{-3}$	$9.99*10^{-1}$	$2.09*10^{0}$
2	$1.34*10^{-6}$	$2.43*10^{-3}$	$9.98*10^{-1}$	$2.04*10^{0}$
3	$2.14*10^{-6}$	$3.62*10^{-3}$	$9.96*10^{-1}$	$1.99*10^{0}$
4	$2.84*10^{-6}$	$4.78*10^{-3}$	$9.95*10^{-1}$	$1.95*10^{0}$
5	$3.53*10^{-6}$	$5.92*10^{-3}$	$9.94*10^{-1}$	$1.90*10^{0}$
10	$6.15*10^{-6}$	$1.12*10^{-2}$	$9.89*10^{-1}$	$1.65*10^{0}$
15	$8.30*10^{-6}$	$1.59*10^{-2}$	$9.84*10^{-1}$	$1.39*10^{0}$
20	$9.46*10^{-6}$	$2.00*10^{-2}$	$9.80*10^{-1}$	$1.14*10^{0}$
Graphite				
Spherical Radius (cm)	**Gains**	**Losses**	**Net**	**Average energy (MeV)**
1	$0.00*10^{0}$	$1.37*10^{-4}$	$1.00*10^{0}$	$2.08*10^{0}$
2	$0.00*10^{0}$	$2.66*10^{-4}$	$1.00*10^{0}$	$2.02*10^{0}$
3	$0.00*10^{0}$	$3.87*10^{-4}$	$1.00*10^{0}$	$1.96*10^{0}$
4	$0.00*10^{0}$	$5.01*10^{-4}$	$9.99*10^{-1}$	$1.90*10^{0}$
5	$0.00*10^{0}$	$6.09*10^{-4}$	$9.99*10^{-1}$	$1.84*10^{0}$
10	$0.00*10^{0}$	$1.06*10^{-3}$	$9.99*10^{-1}$	$1.50*10^{0}$
15	$0.00*10^{0}$	$1.42*10^{-3}$	$9.99*10^{-1}$	$1.17*10^{0}$
20	$0.00*10^{0}$	$1.92*10^{-3}$	$9.98*10^{-1}$	$8.67*10^{-1}$
Water				
Spherical Radius (cm)	**Gains**	**Losses**	**Net**	**Average energy (MeV)**
1	$0.00*10^{0}$	$3.28*10^{-4}$	$1.00*10^{0}$	$1.94*10^{0}$
2	$0.00*10^{0}$	$8.30*10^{-4}$	$9.99*10^{-1}$	$1.75*10^{0}$
3	$0.00*10^{0}$	$3.11*10^{-3}$	$9.97*10^{-1}$	$1.57*10^{0}$
4	$0.00*10^{0}$	$1.14*10^{-2}$	$9.89*10^{-1}$	$1.41*10^{0}$
5	$0.00*10^{0}$	$3.06*10^{-2}$	$9.69*10^{-1}$	$1.25*10^{0}$
10	$6.62*10^{-8}$	$3.06*10^{-1}$	$6.94*10^{-1}$	$6.93*10^{-1}$
15	$1.99*10^{-8}$	$6.25*10^{-1}$	$3.75*10^{-1}$	$3.79*10^{-1}$
20	$1.99*10^{-8}$	$8.17*10^{-1}$	$1.83*10^{-1}$	$2.08*10^{-1}$
Lead				
Spherical Radius (cm)	**Gains**	**Losses**	**Net**	**Average energy (MeV)**
1	$5.24*10^{-4}$	$2.62*10^{-4}$	$1.00*10^{0}$	$2.07*10^{0}$
2	$1.01*10^{-3}$	$6.06*10^{-4}$	$1.00*10^{0}$	$2.00*10^{0}$
3	$1.46*10^{-3}$	$9.46*10^{-4}$	$1.00*10^{0}$	$1.94*10^{0}$
4	$1.88*10^{-3}$	$1.25*10^{-3}$	$1.00*10^{0}$	$1.88*10^{0}$
5	$2.27*10^{-3}$	$1.13*10^{-3}$	$1.00*10^{0}$	$1.83*10^{0}$
10	$3.80*10^{-3}$	$2.98*10^{-2}$	$1.00*10^{0}$	$1.56*10^{0}$
15	$4.81*10^{-3}$	$4.51*10^{-3}$	$1.00*10^{0}$	$1.33*10^{0}$
20	$5.45*10^{-3}$	$6.31*10^{-2}$	$9.99*10^{-1}$	$1.14*10^{0}$
Lithium deuteride				
Spherical Radius (cm)	**Gains**	**Losses**	**Net**	**Average energy (MeV)**
1	$7.71*10^{-4}$	$1.89*10^{-3}$	$9.98*10^{-1}$	$1.95*10^{0}$
2	$1.45*10^{-3}$	$4.65*10^{-3}$	$9.96*10^{-1}$	$1.77*10^{0}$
3	$2.07*10^{-3}$	$9.46*10^{-3}$	$9.93*10^{-1}$	$1.61*10^{0}$
4	$2.62*10^{-3}$	$1.35*10^{-2}$	$9.88*10^{-1}$	$1.44*10^{0}$
5	$3.11*10^{-3}$	$2.03*10^{-2}$	$9.81*10^{-1}$	$1.29*10^{0}$
10	$4.84*10^{-3}$	$1.00*10^{-1}$	$9.02*10^{-1}$	$7.06*10^{-1}$
15	$5.82*10^{-3}$	$2.71*10^{-1}$	$7.32*10^{-1}$	$3.62*10^{-1}$
20	$6.35*10^{-3}$	$4.78*10^{-1}$	$5.25*10^{-1}$	$1.79*10^{-1}$

Polyethylene				
Spherical Radius (cm)	**Gains**	**Losses**	**Net**	**Average energy (MeV)**
1	$0.00*10^{0}$	$8.30*10^{-5}$	$1.00*10^{0}$	$1.89*10^{0}$
2	$0.00*10^{0}$	$9.10*10^{-4}$	$9.99*10^{-1}$	$1.66*10^{0}$
3	$0.00*10^{0}$	$7.62*10^{-3}$	$9.92*10^{-1}$	$1.44*10^{0}$
4	$0.00*10^{0}$	$2.98*10^{-2}$	$9.70*10^{-1}$	$1.25*10^{0}$
5	$0.00*10^{0}$	$7.39*10^{-2}$	$9.26*10^{-1}$	$1.08*10^{0}$
10	$0.00*10^{0}$	$4.81*10^{-1}$	$5.19*10^{-1}$	$5.02*10^{-1}$
15	$0.00*10^{0}$	$7.83*10^{-1}$	$2.17*10^{-1}$	$2.34*10^{-1}$
20	$0.00*10^{0}$	$9.14*10^{-1}$	$8.59*10^{-2}$	$1.12*10^{-1}$
Stainless Steel				
Spherical Radius (cm)	**Gains**	**Losses**	**Net**	**Average energy (MeV)**
1	$3.28*10^{-5}$	$1.47*10^{-3}$	$9.99*10^{-1}$	$2.01*10^{0}$
2	$6.29*10^{-5}$	$2.91*10^{-3}$	$9.97*10^{-1}$	$1.89*10^{0}$
3	$8.88*10^{-5}$	$4.34*10^{-3}$	$9.96*10^{-1}$	$1.78*10^{0}$
4	$1.12*10^{-4}$	$5.77*10^{-3}$	$9.94*10^{-1}$	$1.67*10^{0}$
5	$1.32*10^{-4}$	$7.18*10^{-3}$	$9.93*10^{-1}$	$1.57*10^{0}$
10	$2.06*10^{-4}$	$1.45*10^{-2}$	$9.86*10^{-1}$	$1.13*10^{0}$
15	$2.43*10^{-4}$	$2.39*10^{-2}$	$9.76*10^{-1}$	$8.23*10^{-1}$
20	$2.64*10^{-4}$	$3.87*10^{-2}$	$9.61*10^{-1}$	$6.10*10^{-1}$

Table 1: Effects of spherical encapsulation of various materials on a Cf-252 source.

4.1 Commercial encapsulation

While the previous information is interesting academically, most source encapsulation encountered is standard manufactured capsules from source vendors. Variations in the capsules are introduced through spacers in the source cavity void, inner and outer capsules of different materials, and the inclusion of threaded studs or other modifications. 304L Stainless steel is the most common capsule material in our experience, but Zircalloy-2 is also used.

Physical information about the capsules as simulated is described in Table 2. The A3026 capsule is provided by Eckert & Ziegler [15]. The FTC capsules are provided by Frontier Technology Corporation [16], where s denotes a shorter version of the capsule. The FTC 10 capsules are single encapsulation. The FTC 100 capsule is the second encapsulation that surrounds a FTC 10 capsule and both were included in the simulations. FTC 10 and FTC 100 are the equivalent of Savannah River National Laboratory's SR-Cf-1X and SR-CF-100 capsules respectively. X1 capsules are provided by Amersham, now known as QSA [17]. Table 2 shows the physical characteristics and Table 3 shows the gains, losses, net, and average energy of the spectrum. Simulations demonstrated a negligible difference between 304 and 304L SS, which is to be expected as only the concentration of carbon atoms (less than 1% overall) change.

Capsule	Material	Mass (g)	Outer diameter (cm)	Outer length (cm)
A3026	304 SS	18.4	0.942	3.6
FTC 10s	304L SS	1.7	0.551	1.19
FTC 10	304L SS	2.9	0.551	2.46
FTC 100	304L SS	15.9	0.942	3.76
Amersham X1	SS	3.1	0.782	0.98

Table 2: Common encapsulation's physical characteristics.

Capsule	Gains	Losses	Net	Average energy (MeV)
A3026	$1.816*10^{-5}$	$7.563*10^{-4}$	$9.993*10^{-1}$	2.067
FTC 10s	$5.643*10^{-6}$	$2.221*10^{-4}$	$9.998*10^{-1}$	2.112
FTC 10	$5.111*10^{-6}$	$2.072*10^{-4}$	$9.998*10^{-1}$	2.113
FTC 100	$1.411*10^{-5}$	$5.760*10^{-4}$	$9.994*10^{-1}$	2.083
Amersham X1	$1.012*10^{-5}$	$4.476*10^{-4}$	$9.996*10^{-1}$	2.100

Table 3: Common encapsulation's effects on the emergent neutrons.

Figure 3 shows the emission spectra of bare ^{240}Pu and bare ^{252}Cf together with the calculated spectrum from a point ^{252}Cf source inside a 13.9 mm radius sphere of copper. Although the mean energy can be easily matched, the spectra show that the shape of the tailored spectrum is non-the-less significantly different from that of ^{240}Pu. Whether this is important depends on the nature of the measurement configuration and the objectives of the experiment. For detectors with non-linear response functions matching the average energy is insufficient to match the measurement efficiency. For example a detector with a peak detection efficiency at 1 MeV will have a different efficiency for neutrons at only 1 MeV compared to neutrons half at 0.5 MeV and half at 1.5 MeV.

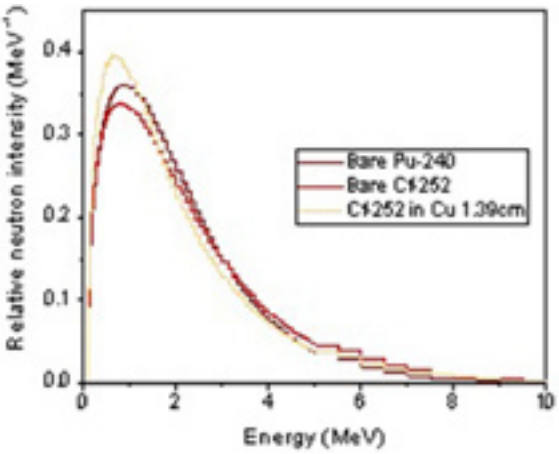

Figure 3: Normalized Spectra from bare ^{240}Pu, bare ^{252}Cf and ^{252}Cf within a 13.9 mm copper sphere

4.2 Effects in the AWCC

A complete analysis of the effects of encapsulation is detector specific. The Active Well Coincidence Counter (AWCC) was simulated to find the encapsulation of ^{252}Cf necessary to match the ^{240}Pu efficiency and measurements were made to verify the simulations. A plot of the simulation with one polyethylene shell is shown in Figure 4. A series of measurements were taken with cylindrical encapsulation of varying wall thicknesses of stainless steel, copper, and polyethylene. The encapsulations are shown in Figure 5. The ^{252}Cf source was Isotope Product Laboratories' A7-869 in the A3026 capsule. First, the exit spectra of the capsules were simulated. Then the measured and simulated ring ratios of the total neutron counts in the AWCC were compared. The AWCC non-linear detection efficiency as a function of neutron energy was simulated. Finally the AWCC measured and simulated efficiencies are compared, and an estimation of the encapsulation to match ^{240}Pu efficiency is given.

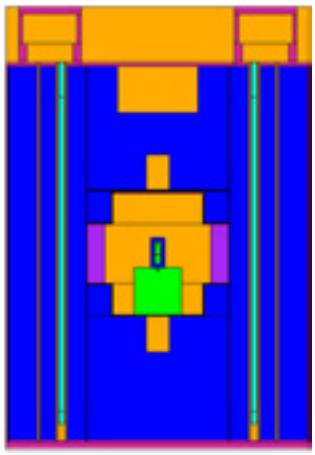

Figure 4: MCNP6 simulation of the AWCC in fast mode with one polyethylene shell.

Figure 5: Encapsulations with wall thicknesses of 0.5 cm.

The AWCC can operate in thermal mode without thermal neutron absorbers or in fast mode with cadmium liners and a nickel reflection ring. In fast mode the sample cavity cadmium liner reduces the count rate in high mass samples and the cadmium liners of the interrogation source ensure a high energy interrogation flux for better penetration of large samples. In this study the fast mode was used. The cadmium liners of 1.6 mm thickness absorb neutrons below about 0.7 eV.

The exit ^{252}Cf spectra from the capsules are shown in Figure 6. The results show that increasing encapsulation amplifies the change in spectrum. The strong thermalization efficiency of polyethylene is demonstrated by the increasing flux at lower energies, indicating a relatively bimodal distribution compared to the other materials. The absorption resonances in copper at 0.002 MeV and other energies can be seen.

The AWCC has two rings of ^{3}He detectors at different depths of polyethylene as shown in Figure 7, so as neutrons in a specific energy range are moderated their detection efficiency by one ring goes up while the other goes down, dampening the change in overall detector efficiency. This effect is more pronounced in neutron detectors with more rings, while single ringed neutron detectors such as the HLNCC-II [13] are more susceptible to changes in the source energy spectrum.

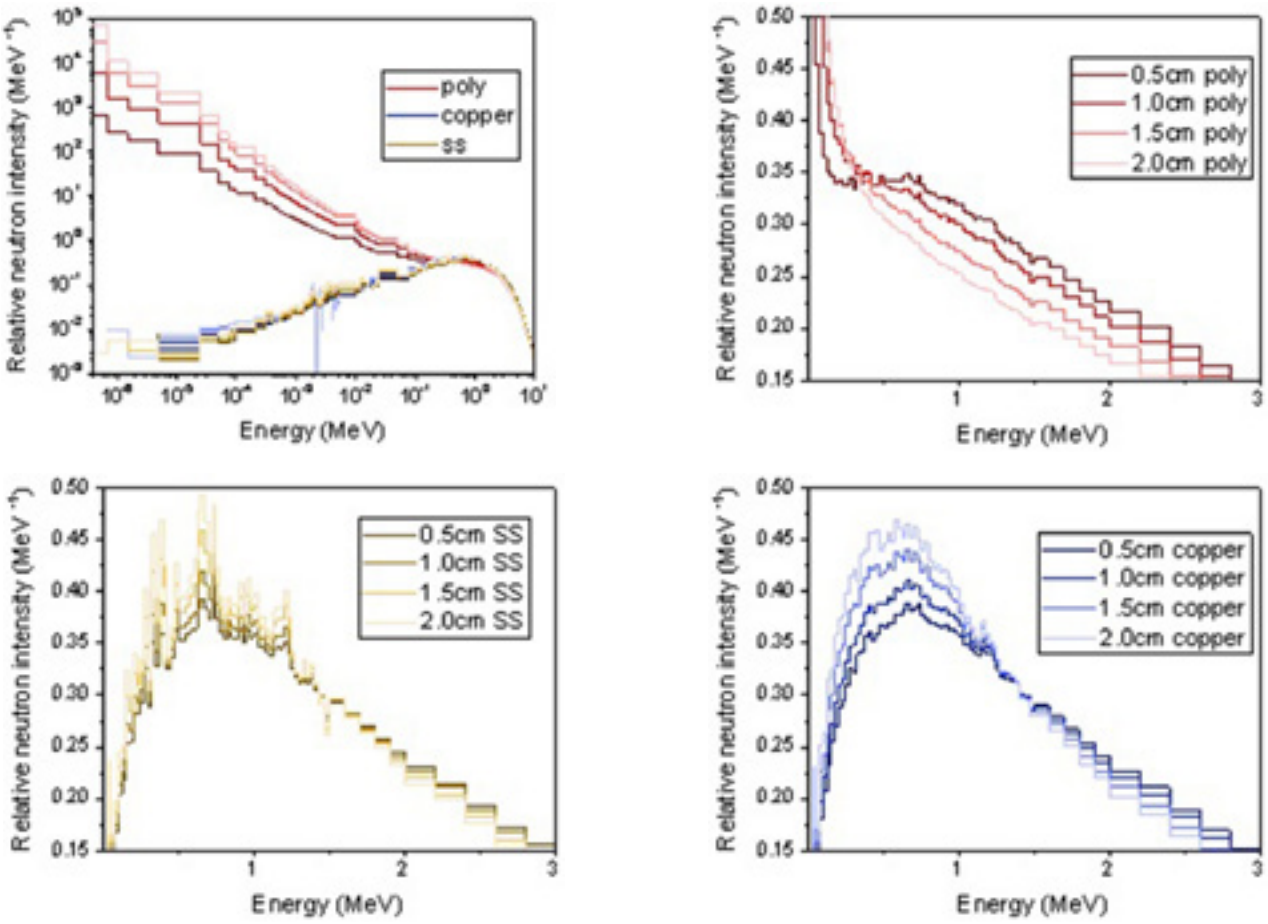

Figure 6: Exit spectra of encapsulation. Note the log-log scale in the first figure. Individual materials are shown in a range of 0-3 MeV on a linear scale.

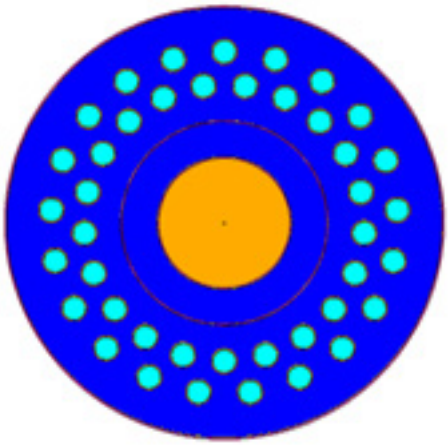

Figure 7: Top down view of the AWCC design.

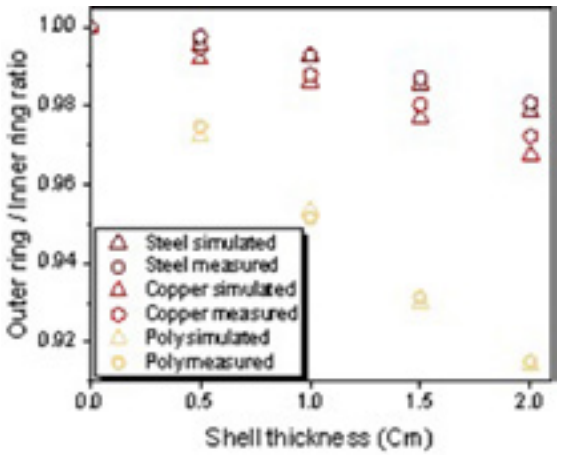

Figure 8: Measured and simulated AWCC ring ratios relative to the bare A7-869 source for various encapsulations.

The measurements and simulations of the ring ratio were compared to verify the accuracy of the simulations. Generally, the ratio of the neutron counts of the two AWCC rings indicates the detected neutron energy. Higher energy neutrons are more likely to reach the outer ring before being absorbed in the inner ring, and so the ratio of counts detected depends on the energy spectrum emitted by the source. The ratio is independent of the source strength, which is a major source of uncertainty in comparing measurements to MCNP simulations. The values were normalized to the ratio of only the standard A3026 source encapsulation to remove bias in the simulation of the detector. The results are shown in Figure 8. The relative statistical uncertainty was too small to clearly plot and was less than

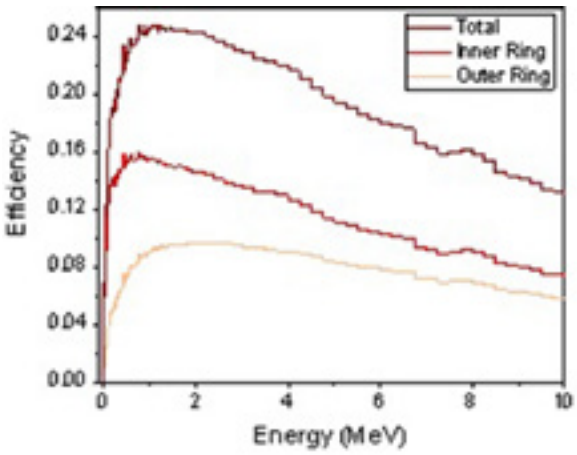

Figure 9: AWCC response function.

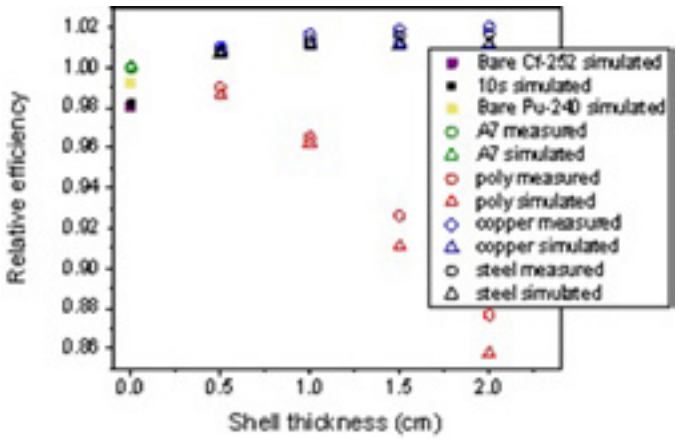

Figure 10: Simulated and measured efficiencies normalized to the A7-869 source in A3026 encapsulation.

0.02% for measurements and 0.09% for simulations. The measurements and simulations agree within 2 standard deviations for all cases except the 2 cm shell thickness of copper. The strong agreement demonstrates that the simulation accurately simulates the measurement.

The AWCC response function, the efficiency as a function of neutron energy emitted by the source, was simulated and is shown in Figure 9. The AWCC response function demonstrates how a neutron spectrum's mean energy does not directly correspond to the efficiency. A spectrum of neutrons half at 0.5 MeV and half at 2.5 MeV will have a lower efficiency than neutrons at their average of 1.5 MeV. The simulation shows that the peak efficiency is around 1.2 MeV. The inner ring has a higher efficiency due to moderation and geometric considerations and its peak efficiency occurs at a neutron energy of about 0.6 MeV while the outer ring peak efficiency occurs at about 2.1 MeV.

Finally, measurements and simulations of the AWCC detection efficiency can be compared to demonstrate the encapsulation's effect on the detector response. Agreement of measurements and simulations indicates the accuracy of the simulations. The simulations can then be used to model measurements that were unavailable to perform physically, like a bare ^{252}Cf source with no encapsulation. It is important to compare encapsulation's effects on detection efficiency, not on average energy. The result of the comparison is shown in Figure 10 and is normalized to the efficiency of the A7-869 source in the A3026 capsule. The relative uncertainties were 0.07% for the simulations and 0.02% for the measurements, which are too small to appear in the figure.

The ^{252}Cf encapsulation required to match the detection efficiency of ^{240}Pu was calculated. The simulations of a bare ^{240}Pu source and a bare ^{252}Cf source give relative efficiencies of 0.992 and 0.980, compared to ^{252}Cf in an A3026 capsule. The difference between the absolute detection efficiency of ^{252}Cf and ^{240}Pu is 0.23%, but the values of absolute detection efficiency are not reported because of uncertainties in the source strength and bias in the simulations. Adding the A3026 capsule increases the relative efficiency to 1, and an additional 0.5cm of polyethylene around the A3026 capsule reduces the relative efficiency to 0.986, which differs from the ^{240}Pu relative efficiency by -0.006 and differs by a ^{240}Pu absolute efficiency of -0.13%. A polyethylene shell thickness of 0.35cm gives a relative efficiency of 0.992 compared to A3026 encapsulation. The absolute efficiency differs from that of ^{240}Pu by 0.004% which is within one sigma uncertainty. In other words, 0.35cm of polyethylene around a ^{252}Cf source in an A3026 capsule will match the AWCC detection efficiency of ^{240}Pu.

5. Conclusion

A few mm of metallic encapsulation influences the energy spectrum emerging from ^{252}Cf to a degree that is measurable in safeguards systems. This also means that the average energy of a point ^{252}Cf spontaneous fission neutron source can be tailored to match any lower value. This is a useful feature to exploit when using ^{252}Cf to measure the neutron detector efficiency as a surrogate for Pu sources in cases where the detector response is a simple function of energy. The modified spectrum however shows significant differences from a Pu spectrum with the same average energy and thus is unlikely to be adequate for detectors with strongly non-linear energy efficiency profiles. In non-linear response detectors such as the Active Well Coincidence Counter, Monte Carlo simulations can be used to calculate the encapsulation needed. In the AWCC a cylindrical encapsulation of polyethylene around an A7-series source with a wall thickness of 0.35cm will match the efficiency of a bare ^{240}Pu pure fission source. Conversely, this information shows the effects of unwanted encapsulation and guides the user towards a decision about an encapsulation being 'neutronically light'.

Acknowledgements

This work was sponsored in part by the U.S. Department of Energy (DOE), National Nuclear Security Administration (NNSA), Office of Nonproliferation and Verification Research and Development (NA-22). This work was funded in part by the Consortium for Verification Technology under Department of Energy National Nuclear Security Administration award number DE-NA0002534.

References

[1] Menlove, H. O, Swinhoe, M. T., Rinard, P. M., Calibration of Pu and Cm Detectors using 252Cf. Los Alamos Report LA-13961-MS. (2002)

[2] Croft, S., Favalli, A., Swinhoe, M.T. and Rael, C.D., State of the art Monte Carlo modeling of active collar measurements and comparison with experiment, Proc. 52nd Annual INMM Meeting, Palm Desert, CA, USA, July 2011

[3] International Organization for Standardization, Reference neutron radiations -- Part 1: Characteristics and Methods of Production, ISO 8529-1:2001-02-01(E), see also ISO 8529-1:2001/Cor 1:2008(F) which provide a typographical correction to Table A.4 the ^{241}Am-Be(α,n) spectrum. (2001)

[4] Fröhner, F.H., Evaluation of ^{252}Cf prompt fission neutron data from 0 to 20 MeV by Watt spectrum fit, Nuclear Science and Engineering 106 (1990) 345-352.

[5] Bardell, A.G., Burke, M., Hunt, J.B., Tagziria H., and Thomas, D.J., Anisotropy of emission from radionuclide neutron sources, National Physical Laboratory report CIRM 24, ISSN 1369-6793. Dec. 1998.

[6] Tsujimura, N., Yoshida, T., and Momose, T., Calculations of anisotropy factors for radionuclide neutron sources due to scattering from encapsulation and support structures, Radiat. Prot. Dosim. 126(1-4) (2007) 168-173.

[7] Hawkes N.P., Freedman R., Tagziria, H., and Thomas D.J., Measurement and calculation of the emission anisotropy of an X1 ^{252}Cf neutron source, Radiat. Prot. Dosim. 126(1-4) (2007) 78-82.

[8] Roberts N.J., Jones L.N., Wang Z., Liu Y., Wang Q., Chen X., Luo H., Rong C., Králik M., Park H., Choi K.O., Pereira W.W., da Fonseca E.S., Cassette P., Dewey M.S., Moiseev N.N., and Kharitonov I.A., International key comparison of measurements of neutron source emission rate (1999-2005) – CCRI(III)-K9. AmBe, Metrologia Tech. Suppl. 06018, 48 (2011) 35pp.

[9] Hsu, H.-H. and Chen, J., Moderation of neutron spectra, Los Alamos National Laboratory report LA-UR-97-0749.

[10] Pelowitz, D.B.(Editor), MCNPX User's Manual, Version 2.7.0 Los Alamos National Laboratory report, LA-CP-11-00438 (2011).

[11] Pelowitz, D.B.(Editor), MCNPX 2.7.0 Extensions, Los Alamos National Laboratory report, LA-UR-11-02295 (2011).

[12] HO Menlove, Description and operation manual for the active well coincidence counter, Los Alamos Scientific Laboratory report LA-7823-M, (1979).

[13] HO Menlove and JE Swansen, A high-performance neutron time correlation counter, Nucl. Technol . 71(1985)498-505

[14] Croft, S. and Chard, P.M.J., Neutronic characterization of plutonium oxide reference samples at Harwell, Proc. 15th Annual ESARDA Symp. on Safeguards and Nuclear Material Management, Rome, Italy, 11-13 May 1993. Report ESARDA 26 EUR 15214 EN CEC, Luxembourg, (1993)511-519.

[15] Eckert & Ziegler, available at http://www.ezag.com (accessed on April 4th, 2017).

[16] Frontier Technology Corporation, available at http://www.frontier-cf252.com (accessed on April 4th, 2017).

[17] QSA Global Inc., available at http://www.qsa-global.com/californium-252/ (accessed on April 4th, 2017).

Detection of fuel pins diversion with the self-indication neutron resonance densitometry technique

R. Rossa1, A. Borella1, P.-E. Labeau2, N. Pauly2, K. van der Meer1

[1] SCK•CEN, Belgian Nuclear Research Centre, Boeretang, 200, B2400 Mol, Belgium
[2] Université libre de Bruxelles, Avenue F.D. Roosevelt, 50, B1050 Brussels, Belgium
Email: rrossa@sckcen.be

Abstract

The verification of spent fuel assemblies is among the activities conducted during a safeguards inspection, and several non-destructive assay techniques are being developed to improve the accuracy of existing methods. Among other techniques, the self-indication neutron resonance densitometry (SINRD) relies on the passive neutron emission from the spent fuel assemblies. Previous research conducted at SCK•CEN found that the optimal configuration was obtained with the fuel kept in air and surrounded by a polyethylene slab.

The SINRD technique was proposed mainly for the direct quantification of the ^{239}Pu mass in spent fuel, whereas this contribution is focused on the potential to detect the diversion of fuel pins from a spent fuel assembly. First, the detector responses of several fission chambers placed in the guide tubes of a PWR 17x17 fuel assembly were calculated with the Monte Carlo code MCNPX. Different fissile material coatings (e.g. ^{239}Pu, ^{238}U) were taken into account to consider detectors mostly sensitive to thermal and fast neutrons. In addition, the response to ionization chambers was modelled for the detection of gamma-rays. Fuel assemblies with material compositions corresponding to different initial enrichment, burnup, and cooling time were modelled to evaluate the sensitivity of the detector responses to the fuel irradiation history.

The detector responses were calculated also for several diversion scenarios where fuel pins from a complete fuel assembly were replaced with dummies made of stainless steel. The diversions ranged from 15% to 50% of the total pins. The detector responses obtained from the diversion cases were compared to the values for the complete fuel assemblies to determine the capability of SINRD to detect the diversion of fuel pins. Promising results were obtained by combining the responses of the different detector types.

Keywords: SINRD, spent fuel, NDA, partial defect, Monte Carlo

1. Introduction

A technical objective of nuclear safeguards is to ensure the detection of the diversion of nuclear material from peaceful applications to the manufacture of nuclear weapons (IAEA, 1972).

Safeguards inspections are carried out by the International Atomic Energy Agency (IAEA) in the countries signatories of the Non-Proliferation Treaty (NPT) (IAEA, 1970). Since most of nuclear material placed under safeguards is in the form of spent fuel, the verification of this material is of major interest for the IAEA (IAEA, 2013).

However, the measurement of spent fuel presents many challenges due to its very high radiation emission and decay heat. Currently the spent fuel verification is performed with non-destructive assay (NDA) techniques such as the digital Cherenkov viewing device (DCVD) (Chen et al., 2003), (Chen et al., 2009), (Branger et al., 2014), the spent fuel attribute tester (SFAT) (Arit et al., 1995), (Honkamaa et al., 2003), and the Fork detector (Rinard et al., 1988), (Borella et al., 2011). In addition, many other NDA techniques are under development to improve the accuracy of the verification (Tobin et al., 2011).

This contribution is focused on the capabilities of the self-indication neutron resonance densitometry (SINRD) (Menlove et al., 1969) for the detection of diversion from a spent fuel assembly. The basic principle of SINRD is described with the Monte Carlo models used in the study. Then the overview of the simulations is given, considering both complete fuel assemblies and diversion scenarios, and the capabilities of SINRD for this application are discussed. Finally the conclusions are presented with an outlook on future research.

2. Description of the SINRD technique

The self-indication neutron resonance densitometry is a non-destructive assay technique that relies on the spontaneous neutron emission of spent nuclear fuel (LaFleur, 2011), (LaFleur et al., 2015), (Rossa et al., 2015), (Rossa, 2016).

The basic principle of SINRD is described in Figure 1. The total cross-section for neutron-induced reaction of ^{239}Pu is plotted with the transmission of a neutron flux through samples containing different percentages of ^{239}Pu. The transmission values were calculated with Monte Carlo simulations considering a sample of ^{239}Pu with density and dimensions equal to a PWR fuel pin. It is evident from the figure that the attenuation of the neutron flux is related to the amount of ^{239}Pu in the sample. The SINRD technique aims at measuring the attenuation of the neutron flux around the 0.3 eV region due to the presence of ^{239}Pu in the fuel assembly. The neutron detection

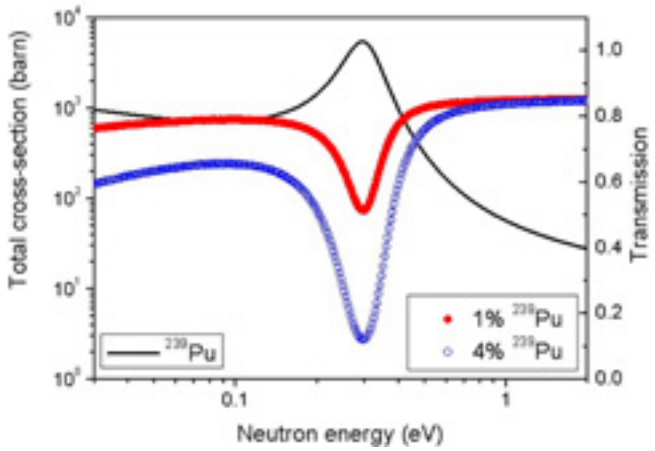

Figure 1: Total cross-section of ^{239}Pu and transmission of a neutron flux through samples containing ^{239}Pu. The cross-section values were obtained from the ENDF/B-VII.0 data library, whereas the transmission was calculated with Monte Carlo simulations.

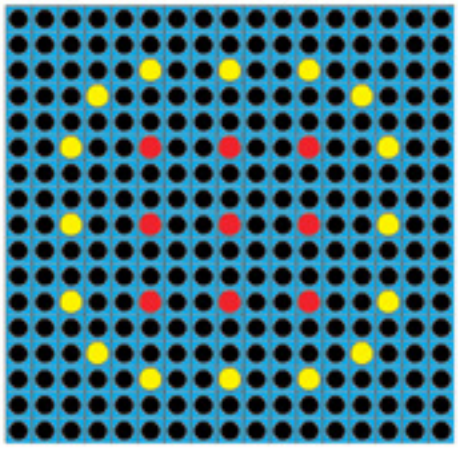

Figure 2: MCNPX model of the fuel assembly used for the study. The fuel pins are depicted in black, the peripheral guide tubes in yellow, and the central guide tubes in red.

in the 0.3 eV region is enhanced by using a fission chamber with ^{239}Pu as fissile material, according to the self-indication principle (Fröhner et al., 1966).

The neutron flux in the 0.3 eV energy region is estimated with SINRD by taking the difference between the neutron counts of two ^{239}Pu fission chambers. One detector is covered by a thin Gd filter, whereas the other detector is covered by a Cd filter. These materials were chosen because they have a cutoff in the neutron absorption below and above 0.3 eV, respectively.

In addition, the thermal neutron flux and fast neutron flux were estimated in this work by calculating the response of a bare ^{239}Pu fission chamber and ^{238}U fission chamber, respectively.

The approach for the study of the SINRD technique was extended in this paper by calculating the response of ionization chambers for the detection of gamma-rays. The multiple insertion of neutron and gamma-ray detectors in a fuel assembly was proposed for the PDET detector (Ham et al., 2009), (Ham et al., 2015), and can be beneficial also for the SINRD technique.

3. Model developed for the study

3.1 Monte Carlo model

The capability of SINRD for the detection of partial defects was investigated in this article with Monte Carlo simulations. The Monte Carlo code MCNPX v.2.7.0 (Pelowitz, 2011) was used to simulate a PWR 17x17 fuel assembly stored in air and surrounded by a 12-cm slab of polyethylene to ensure neutron moderation. The model of the fuel assembly is shown in Figure 1. The fuel geometry chosen for the simulation contains 264 fuel pins and 25 guide tubes. These are used for the insertion of control rods during the reactor operation and provide enough room for neutron or gamma-ray detectors once the fuel is discharged.

The measurement setup chosen for this study can be representative of an encapsulation plant where spent fuel with long cooling time is verified before the final disposal (Park et al., 2014).

3.2 Calculation of the neutron detectors counts

The total counts of the neutron detectors (N_{bare}) were calculated with Formula (1) as the product between the coefficient C_N, the incoming neutron flux (φ_N) and the microscopic cross-section (σ_{DET}) of the active material in the detector itself. The coefficient C_N was calculated with Formula (2) as the product between the amount of fissile material in the detector (n_{fiss}), the total neutron emission from the spent fuel assembly (N_E), and the measurement time (t). The Photonis CFUE43 fission chamber (Photonis, 2017) was taken as reference design, but the active length was increased to 2 m to obtain a fissile material mass of 263.89 mg (Rossa, 2016). This choice was made to maximize the count rate, whereas the technical feasibility of such detector will be included in future work. The total neutron emission was taken from the reference spent fuel library (Rossa et al., 2013), whereas the measurement time was set to one hour.

The neutron flux (φ_N) and the microscopic cross-section (σ_{DET}) included in Formula (1) are a function of the incoming neutron energy E_N. The neutron flux was obtained from the MCNPX simulations and accounts also for the multiplication effect. The cross-section values were taken from the ENDF/B-VII.0 nuclear data library (Chadwick, 2006) and averaged over 600 logarithmically-interpolated energy bins between 10^{-9} and 20 MeV. The fission cross-sections of ^{239}Pu and ^{238}U were used to model detectors sensitive mainly to thermal and fast neutrons, respectively.

$$N_{bare} = C_N \int_{E_N} \varphi_N(E_N)\, \sigma_{DET}(E_N)\, dE_N \quad (1)$$

$$C_N = n_{fiss}\, N_E\, t \quad (2)$$

The presence of a thin Gd or Cd filter around the ^{239}Pu fission chamber was accounted for with Formula (3), where n_{fil} and σ_{fil} are the atom density and cross-section of the filter.

$$N_{fil} = C_N \int_{E_N} \varphi_N(E_N)\ \sigma_{DET}(E_N)\ e^{-n_{fil}\sigma_{fil}(E_N)}\ dE_N \qquad (3)$$

The neutron counts in the energy region close to 0.3 eV were calculated as the difference between the counts of two fission chambers, one covered by a Gd filter and one covered by a Cd filter.

The uncertainty of the neutron counts for the different detectors was estimated as the square root of the corresponding neutron count.

3.3 Calculation of the gamma-ray detectors response

The gamma-ray detector response (P) was calculated with Formula (4) as the product between the coefficient C_P, the gamma-ray flux (φ_P) and the response function of the detector (f_{DET}). The coefficient C_P is the product between the total photon emission from the spent fuel assembly and the measurement time. The total photon emission was taken from (Rossa et al., 2013) and the measurement time was set to one hour as for the neutron measurements.

The photon flux (φ_P) and response function (f_{DET}) were obtained from MCNPX simulations and are function of the incoming gamma-ray energy E_γ. The photon flux was calculated in the guide tubes with the model of the spent fuel described in Section 3.1, whereas the response function was obtained by modelling the detector alone as an aluminum cylinder filled with nitrogen. The transport of both photons and electrons was simulated to obtain the response function (f_{DET}), which was calculated as the energy deposition tally (F6 type) in the gas-filled cavity. The energy range of the source term was divided into 23 bins from 50 keV to 5 MeV, and separate simulations were performed defining the source with a uniform histogram distribution over a single energy bin.

$$P = C_P \int_{E_\gamma} \varphi_P(E_\gamma)\ f_{DET}(E_\gamma)\ dE_\gamma \qquad (4)$$

The statistical uncertainty of the gamma-ray detector response was neglected since ionization chambers are normally operated in current mode and reach a stable signal well within the considered measurement time.

4. Overview of the performed simulations

4.1 Complete fuel assemblies

The simulations performed for this study considered both complete fuel assemblies and assemblies with diverted pins. In the case of a complete fuel assembly the fuel pins are identical in material composition and source strength, and these characteristics were taken from the reference spent fuel library (Rossa et al., 2013), (Borella et al., 2015). The sensitivity of the detector responses to the fuel irradiation history was evaluated by considering fuel assemblies with material composition and source strength corresponding to:

- initial enrichments: 2.0, 2.5, 3.0, 3.5, 4.0, 4.5, and 5.0%;
- burnup: 5, 10, 15, 20, 30, 40, and 60 GWd/$t_{HM.}$

The range of initial enrichment and burnup was chosen to represent the majority of operating conditions of current PWR reactors and it is in line with previous research (Trellue et al., 2010), (Borella et al., 2015).

4.2 Diversion scenarios

In the diversion cases the fuel pins were replaced by dummies made of stainless steel with the same dimensions of a fuel pin. The diversion scenarios are shown in Figure 3 and the replaced pins were between 50% and 15% of the fuel pins in a fuel assembly. The diversion scenarios were symmetrical since it resulted from previous work as the most challenging pattern to detect (Sitaraman et al., 2009), (Rossa, 2016). Nevertheless, it is worth noting that dummy pins placed in the outer section of the assembly may be easy to detect by visual inspection due to the optical alteration of the spent fuel pins through irradiation.

For the simulations with the diversion scenarios the fuel pins had a material composition and source strength corresponding to fuel with the following:

- 2% initial enrichment and 30 GWd/t_{HM} burnup;
- 3.5% initial enrichment and 10, 30, or 60 GWd/t_{HM} burnup;
- 5% initial enrichment and 30 GWd/t_{HM} burnup.

In all simulations included in this contribution the fuel pins had a cooling time of 5 years.

5. Results

5.1 Complete fuel assemblies

For each simulation in this study the detectors responses calculated according to the approach described in Sections 3.2 and 3.3 were normalized to the value obtained in the central guide tube. In addition, the guide tubes were divided for this study into 16 peripheral and 9 central guide tubes depending on the geometrical location in the fuel assembly. The two groups are identified in Figure 1 by different colors. The average detector responses were calculated in the two guide tubes groups.

The average detector responses obtained in the cases with complete fuel assemblies were used to establish a reference band associated to each type of detector response (i.e. thermal neutrons, resonance region neutrons,

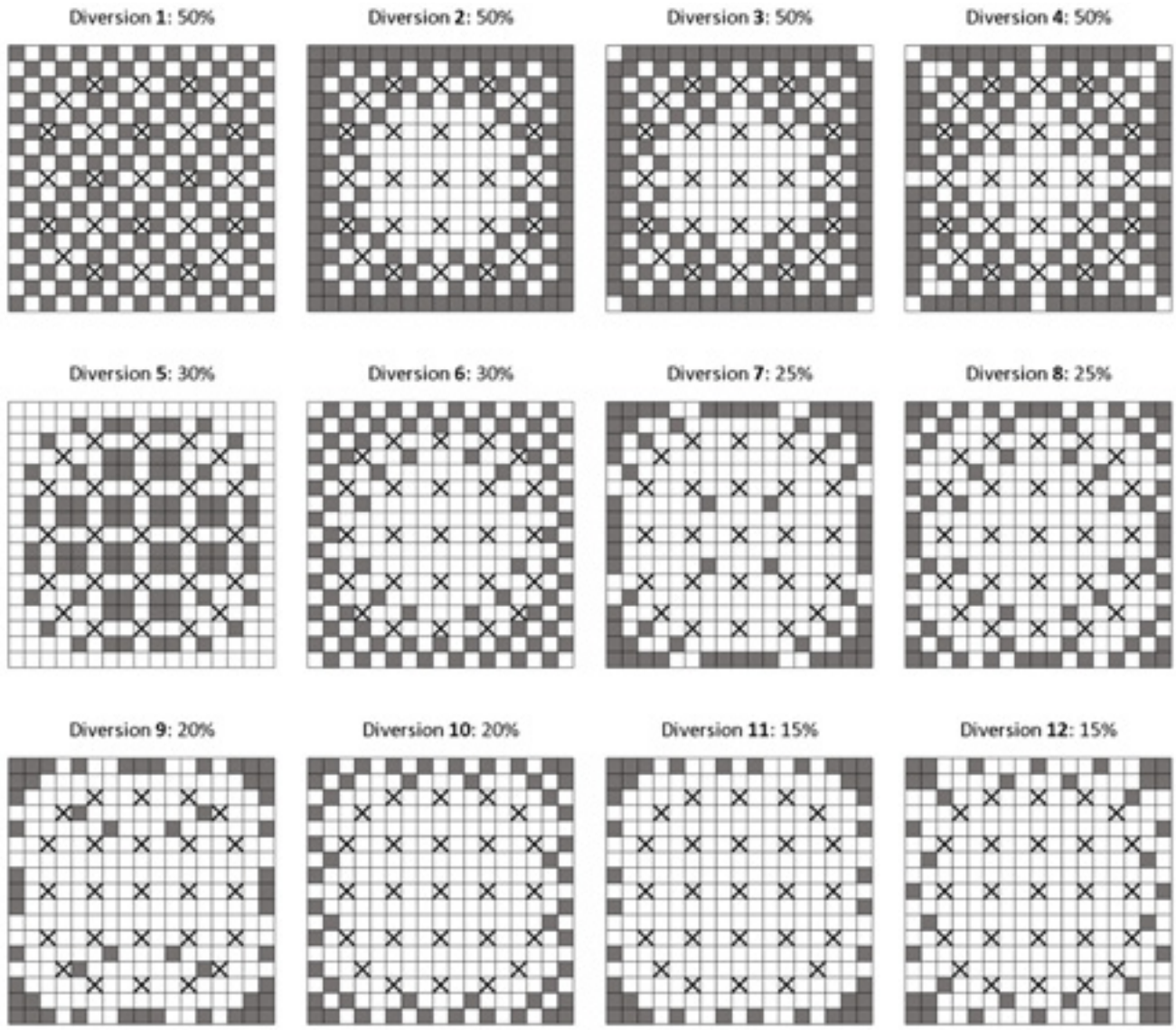

Figure 3: Overview of the diversion scenarios. The fuel pins are depicted in white, the dummy pins in grey, and the guide tubes with crosses.

fast neutrons, gamma-rays). The low and high boundaries are reported in Table 1 for the nine central guide tubes and for the sixteen peripheral guide tubes. In order to obtain the low boundaries for the neutron detectors in Table 1, the minimum detector responses obtained in the whole set of complete fuel assemblies were further decreased by the 1-σ value to account for uncertainty. Similarly the high boundaries were obtained by increasing by 1-σ the maximum values obtained for each detector type. The boundaries for the gamma-ray detector were taken as the minimum and maximum detector responses obtained in the whole set of complete fuel assemblies.

Both boundaries for thermal and resonance region neutrons are lower for the central guide tubes compared to the peripheral guide tubes, whereas the opposite occurs for fast neutrons and gamma-rays. In general the width of the reference band is larger for peripheral guide tubes compared to central guide tubes, and it is significantly larger for neutron than for gamma-ray detectors.

	Central guide tubes		Peripheral guide tubes	
	Low boundary	**High boundary**	**Low boundary**	**High boundary**
Thermal neutrons	1.153	1.263	1.695	2.298
Resonance region neutrons	1.122	1.271	1.576	2.290
Fast neutrons	0.862	1.090	0.802	0.977
Gamma-rays	0.985	0.987	0.904	0.912

Table 1: Normalized detector responses calculated for the complete fuel assemblies for thermal neutrons, neutrons around the 0.3 eV region, fast neutrons, and gamma-rays. The low and high boundaries are given for the nine central guide tubes and the sixteen peripheral guide tubes.

5.2 Diversion scenarios

The average detector responses obtained for the diversion scenarios were compared to the reference bands shown in Table 1, and the values that fell outside these bands signaled possible diversion cases. Figures 4-7 show the normalized detector responses calculated for the diversion scenarios for the different detector types. The results are the average values for the nine central guide tubes and for the sixteen peripheral guide tubes.

The results for the thermal neutron detectors show that most of the diversion cases fall within the reference band of the complete fuel assemblies. Only for diversion with fuel with 5% initial enrichment the detector responses are above the high boundaries both for central and peripheral guide tubes.

Considering the detectors measuring neutrons around the 0.3 eV resonance region (Figure 5), most of the diversions with fuel assemblies with initial enrichment of 5% fall outside the reference band. In addition, also some scenarios with 50% of replaced pins from fuel with 3.5% initial enrichment and burnup larger than 30 GWd/t have values above the reference band.

The results for the fast neutron detectors show that for all diversion scenarios the average values for the central guide tubes are within the reference band. The average detector responses for the peripheral guide tubes are lower than the reference band for some scenarios with 50% and 30% of replaced pins. In all cases there is not a significant difference due to the fuel irradiation history.

Figure 7 shows that for all diversion scenarios the average responses of the gamma-ray detectors are outside the reference band of the complete fuel assemblies. The peripheral guide tubes are the most affected by the replacement of fuel pins. As in the case of fast neutron detectors, the irradiation history of the fuel assembly does not influence significantly the results. By comparing the different detector types, the gamma-ray detectors show a larger variation due to the fuel pins diversion compared to the neutron detectors.

The reference bands reported in the figures in this section were calculated for fuel assemblies with uniform composition. Variation of burnup among pins due to core loading strategies might have a noticeable impact on the bands and needs to be investigated.

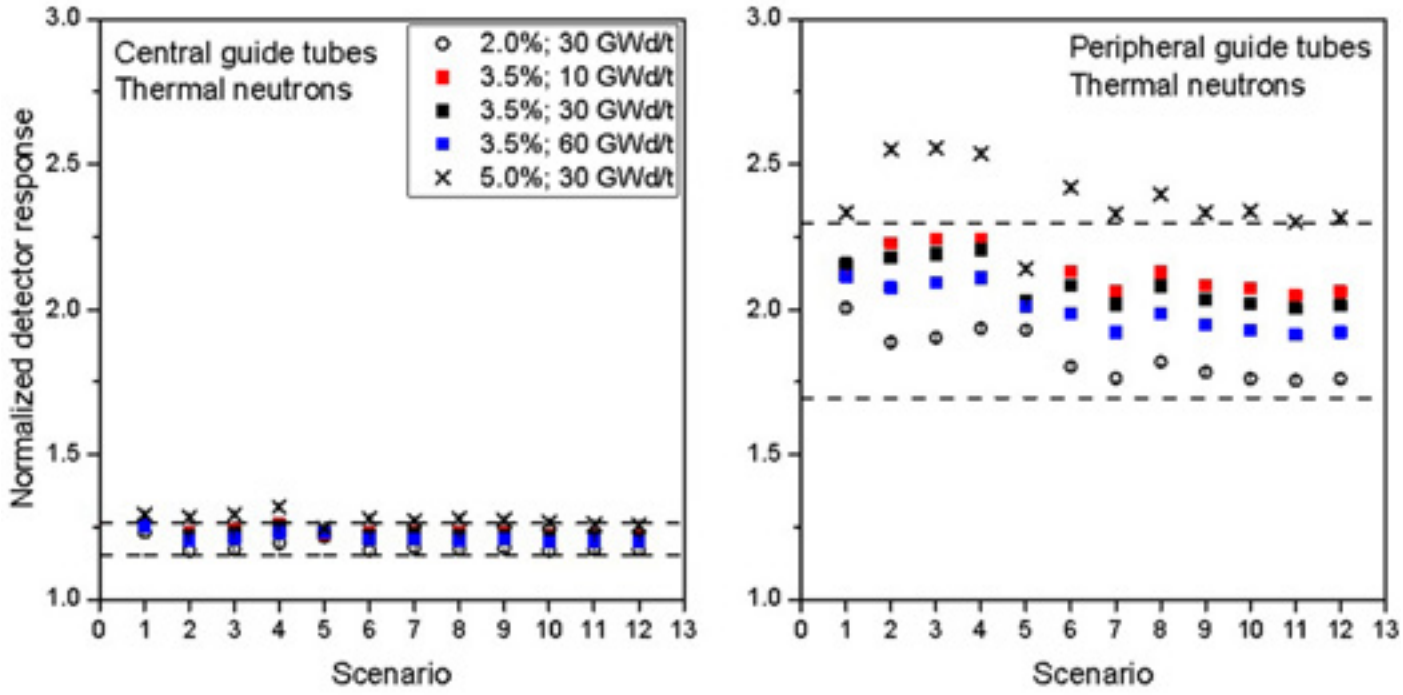

Figure 4: Normalized detector responses for thermal neutrons in the different diversion scenarios. The average value for central guide tubes (left), and peripheral guide tubes (right) are shown. The lower and upper boundaries for the cases with complete fuel assemblies are also reported.

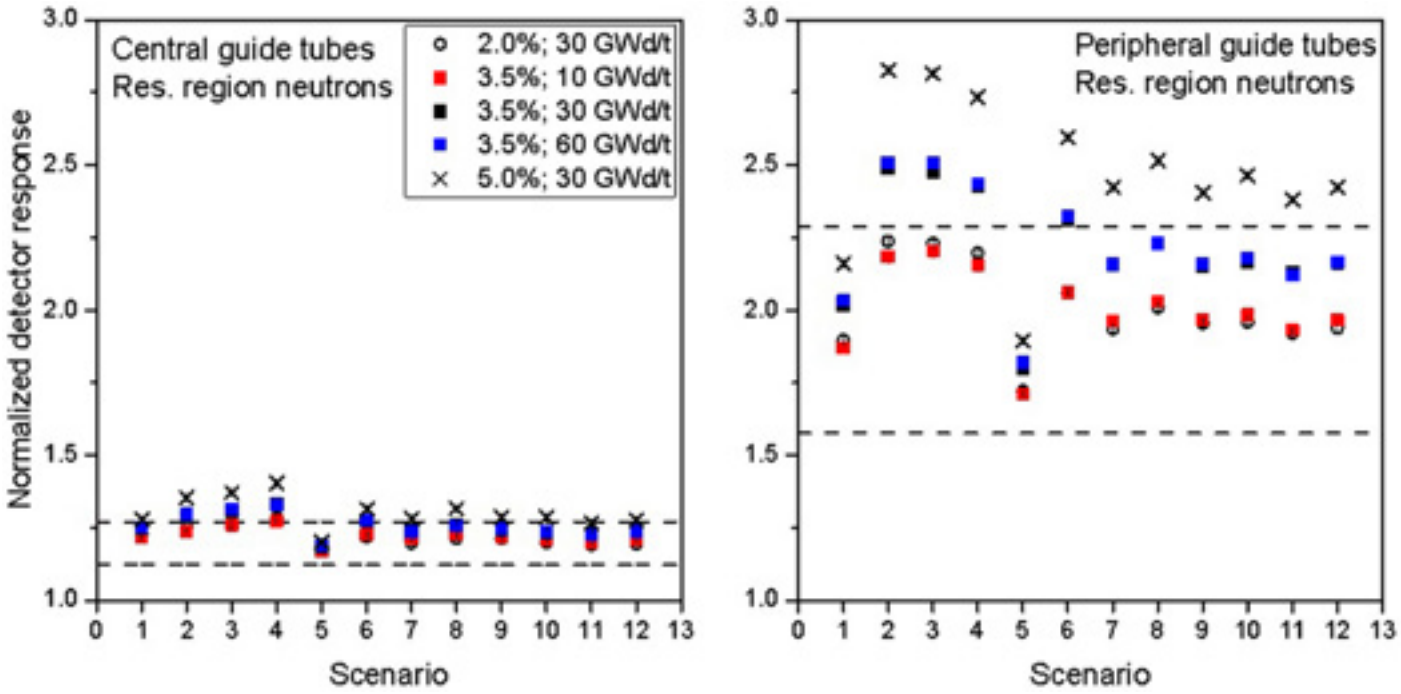

Figure 5: Normalized detector responses for neutrons around the 0.3 eV resonance region in the different diversion scenarios. The average value for central guide tubes (left), and peripheral guide tubes (right) are shown. The lower and upper boundaries for the cases with complete fuel assemblies are also reported.

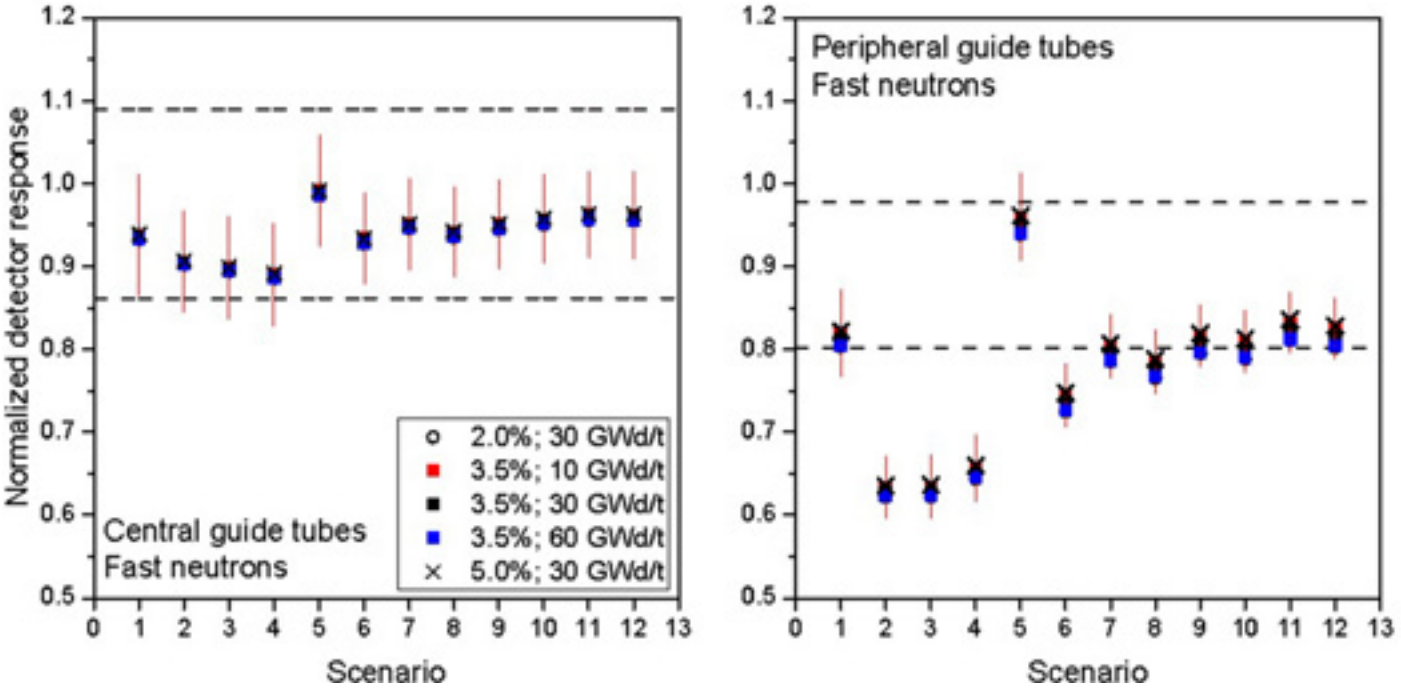

Figure 6: Normalized detector responses for fast neutrons in the different diversion scenarios. The average value for central guide tubes (left), and peripheral guide tubes (right) are shown. The lower and upper boundaries for the cases with complete fuel assemblies are also reported.

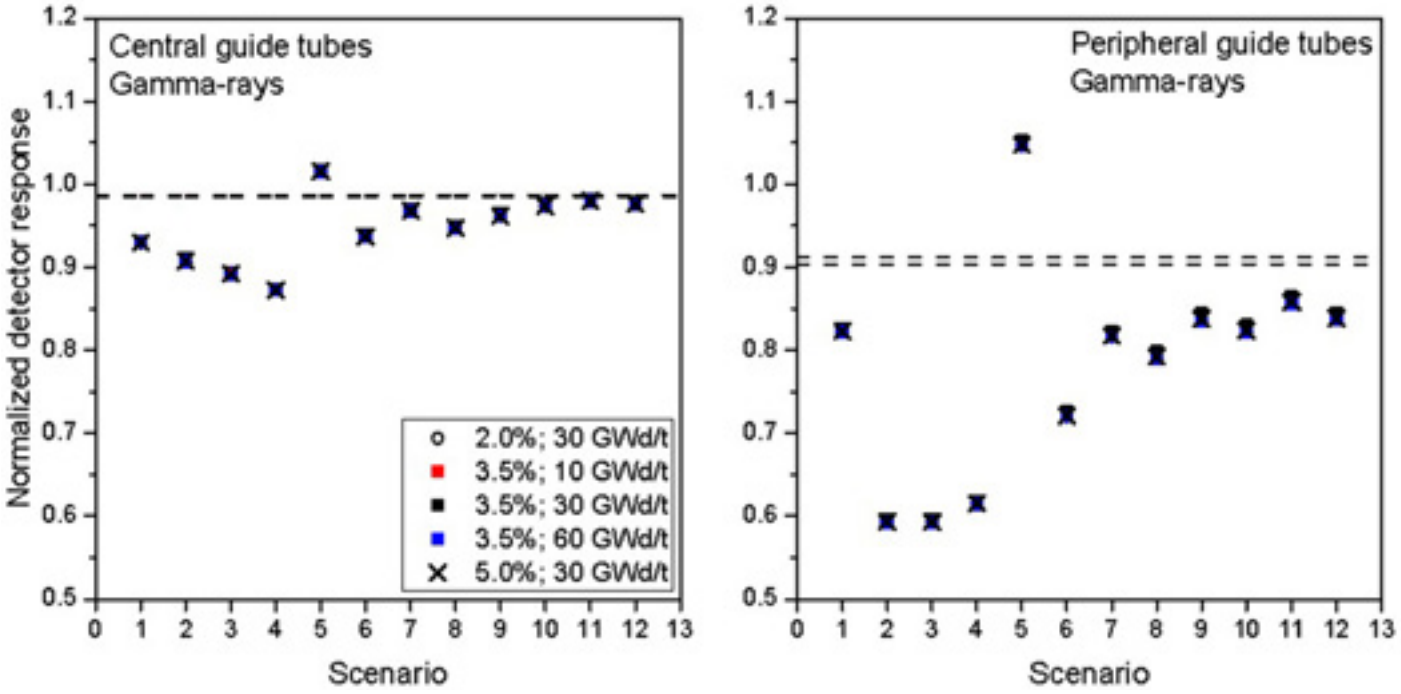

Figure 7: Normalized detector responses for gamma-rays in the different diversion scenarios. The average value for central guide tubes (left), and peripheral guide tubes (right) are shown. The lower and upper boundaries for the cases with complete fuel assemblies are also reported.

6. Conclusions

The capabilities of SINRD to detect the substitution of metal pins for fuel pins from a complete assembly were investigated in this paper. The neutron and gamma-ray fluxes were estimated in the guide tubes of a PWR fuel assembly to mimic the use of multiple detectors during the measurements. The response of detectors sensitive mainly to thermal neutrons, neutrons with energy around 0.3 eV, fast neutrons, and gamma-rays were considered.

A first series of simulations concerned complete fuel assemblies with different irradiation histories to estimate the influence of initial enrichment, burnup, and cooling time on the detector responses. The results from the complete fuel assemblies were used to identify a reference band of values obtained for complete fuel assemblies. The values calculated for the diversion scenarios were then compared with the reference bands of each detector type, and the values that fell outside the reference bands were an indication of diversion.

The peripheral guide tubes in almost all scenarios were the most affected by the fuel pins diversion and were outside the reference bands for multiple detector types. For all diversion scenarios the average gamma-ray detector response for the guide tubes was outside the reference band, whereas for some diversion cases with 50% and 30% of replaced pins also the values for neutron detectors were outside the reference bands. Overall the gamma-ray detectors showed a larger change due to the diversion of pins compared to the neutron detectors.

Future work will continue the assessment of the SINRD technique for the detection of fuel pins diversion by considering additional diversion scenarios and other approaches to the data analysis. The comparison among different NDA techniques for the same diversion scenarios is also foreseen.

7. Legal matters

7.1 Privacy regulations and protection of personal data

"I agree that ESARDA may print my name/contact data/photograph/article in the ESARDA Bulletin/Symposium proceedings or any other ESARDA publications and when necessary for any other purposes connected with ESARDA activities."

7.2 Copyright

The authors agree that submission of an article automatically authorises ESARDA to publish the work/article in whole or in part in all ESARDA publications – the bulletin, meeting proceedings, and on the website. The authors declare that their work/article is original and not a violation or infringement of any existing copyright.

8. References

Arit R., et al., 1995. "SFAT in physical inventory verification of spent LWR fuel". Proceedings of the 17th ESARDA annual meeting.

Borella A., et al., 2011. “Spent fuel measurements with the Fork detector at the nuclear power plant of Doel”. Proceedings of the 33rd ESARDA annual meeting.

Borella A., et al., 2015. “Extension of the SCK•CEN reference spent fuel inventory library”. Proceedings of the 37th ESARDA annual meeting.

Branger E., et al., 2014. “Improved DCVD assessments of irradiated nuclear fuel using image analysis techniques”. Proceedings of the 2014 IAEA safeguards symposium.

Chadwick M. B., et al., 2006. “ENDF/B-VII.0 next generation evaluated nuclear data library for science and technology”. Nuclear data sheets, volume 107, issue 12.

Chen J. D., et al., 2003. “Cherenkov characterization of BWR assemblies using a prototype DCVD with a back-illuminated CCD”. Report prepared for the Canadian safeguards support program and the Swedish support program (CSSP Report 2004-01-01, SKI Report ISRN SKI-R-03/45).

Chen J. D., et al., 2009. “Partial defect detection in LWR spent fuel using a digital Cerenkov viewing device”. Proceedings of the 50th INMM annual meeting.

Fröhner F. H., et al., 1966. “Accuracy of Neutron Resonance Parameters from Combined Area and Self-Indication Ratio Measurements”. Proceedings of the Conference on Neutron Cross Section Technology, P. Hemmig (ed.), CONF-660 303, Washington D.C. (1966) Book 1, pp. 55-66.

Ham Y. S., et al., 2009. “Development of a safeguards verification method and instrument to detect pin diversion from pressurized water reactor (PWR) spent fuel assemblies phase I study”. Lawrence Livermore National Laboratory technical report LLNL-TR-409660.

Ham Y. S., et al., 2015. “Partial defect verification of spent fuel assemblies by PDET: principle and field testing in interim spent fuel storage facility (CLAB) in Sweden”. Proceedings of the 2015 ANIMMA conference.

Honkamaa T., et al., 2003. “How STUK verifies spent nuclear fuel - and why?” Proceedings of the 25th ESARDA annual meeting.

International Atomic Energy Agency (IAEA), 1972. “The structure and content of agreements between the Agency and States required in connection with the treaty on the nonproliferation of nuclear weapons”. INFCIRC/153 (corrected).

International Atomic Energy Agency (IAEA), 1970. “Treaty on the non-proliferation of nuclear weapons”. INFCIRC/140.

International Atomic Energy Agency (IAEA), 2013. “IAEA department of safeguards long term R&D plan, 2012-2023”. STR-375.

LaFleur A. M., 2011. “Development of self-interrogation neutron resonance densitometry (SINRD) to measure the fissile content in nuclear fuel”. Ph.D. dissertation at Texas A&M University.

LaFleur A. M., et al., 2015. “Analysis of experimental measurements of PWR fresh and spent fuel assemblies using self-interrogation neutron resonance densitometry”. Nuclear Instruments and Methods Section A, 781 (2015) 86-95.

Menlove H. O., et al., 1969. “A resonance self-indication technique for isotopic assay of fissile material”. Nuclear applications, volume 6, 401-408.

Park W. S., et al., 2014. “Safeguards by design at the encapsulation plant in Finland”. Proceedings of the 2014 IAEA safeguards symposium.

Pelowitz D., editor, 2011. “MCNPX user’s manual version 2.7.0”. Los Alamos National Laboratory LA CP 11-00438.

Photonis, 2017. http://www.photonis.com/nuclear/products/fission-chambers-for-in-core-use/.

Rinard P. M., et al., 1988. “Safeguarding LWR spent fuel with the FORK detector”. Los Alamos National Laboratory report LA-11096-MS.

Rossa R., et al., 2013. “Development of a reference spent fuel library of 17x17 PWR fuel assemblies”. ESARDA Bulletin n. 50.

Rossa R., et al., 2015. “Investigation of the self-interrogation neutron resonance densitometry applied to spent fuel using Monte Carlo simulations”. Annals of Nuclear Energy 75 (2015) 176-183.

Rossa R., 2016. “Advanced non-destructive methods for criticality safety and safeguards of used nuclear fuel”. Ph.D. dissertation at Université libre de Bruxelles ULB.

Sitaraman S., et al., 2009. “Symmetric pin diversion detection using a partial defect detector (PDET)”. Proceedings of the 50th INMM annual meeting.

Tobin S. J., et al., 2011. “Next generation safeguards initiative research to determine the Pu mass in spent fuel assemblies: purpose, approach, constraints, implementation, and calibration”. Nuclear Instruments and Methods in Physics Research A 652 (2011) 73-75.

Trellue H. R., et al., 2010. “Description of the Spent Nuclear Fuel Used in the Next Generation Safeguards Initiative to Determine Plutonium Mass in Spent Fuel”. LA-UR-11-00300.

Brain Science and International Nuclear Safeguards: Implications from Cognitive Science and Human Factors Research on the Provision and Use of Safeguards-Relevant Information in the Field

Z. N. Gastelum, L. E. Matzen, H. A. Smartt, K. E. Horak, E. M. Moyer, M. E. St. Pierre
Sandia National Laboratories
Albuquerque, New Mexico, USA

Abstract:

Today's international nuclear safeguards inspectors have access to an increasing volume of supplemental information about the facilities under their purview, including commercial satellite imagery, nuclear trade data, open source information, and results from previous safeguards activities. In addition to completing traditional in-field safeguards activities, inspectors are now responsible for being able to act upon this growing corpus of supplemental safeguards-relevant data and for maintaining situational awareness of unusual activities taking place in their environment. However, cognitive science research suggests that maintaining too much information can be detrimental to a user's understanding, and externalizing information (for example, to a mobile device) to reduce cognitive burden can decrease cognitive function related to memory, navigation, and attention.

Given this dichotomy, how can international nuclear safeguards inspectors better synthesize information to enhance situational awareness, decision making, and performance in the field? This paper examines literature from the fields of cognitive science and human factors in the areas of wayfinding, situational awareness, equipment and technical assistance, and knowledge transfer, and describes the implications for the provision of, and interaction with, safeguards-relevant information for international nuclear safeguards inspectors working in the field.

Keywords: safeguards; inspection; cognition; information

1. Introduction

In today's information age, more safeguards-relevant data is available for International Atomic Energy Agency (IAEA) nuclear safeguards inspectors than ever before. Inspectors are not only responsible for an increasing number of nuclear facilities as the number of safeguarded facilities continues to grow around the world, but more information about those facilities is available. This increased information availability is in part due to enhanced reporting requirements under the Additional Protocol, but also due to the unprecedented growth in availability and diversity of open source information. Providing this information alone is unlikely to support more effective safeguards inspections. More important, for both the traditional and emerging sources of information that can be used to support IAEA safeguards inspections, is the actionable provision of that information – providing the right information, in the right format, at the right time.

Since at least the 1990s, proposals have been brought forward to provide advanced information technology platforms for IAEA safeguards inspectors. Some of these proposals, such as deploying Agency laptops with inspectors, have become a reality and now a norm. Other proposals such as the integration of mobile touch screen devices like tablet computers or smart phones into inspection information collection or documentation, or the use of 3D holographic displays, have been more futuristic and less likely to be deployed near-term [for example, references 1, 2, 3]. Meanwhile, new software products have been developed or commercially procured by the Department of Safeguards to support information collection, analysis, and processing both at Headquarters and in the field [4, 5, 6, 7, 8]. While these tools appear to have preliminary positive results, there has been little evidence of formal assessments of how these tools impact a safeguards inspector's or analyst's cognition of the safeguards information being presented.

In this paper, we will explore unique insights from the cognitive science and human factors communities as they apply to international safeguards inspector use of, and interaction with, information during in-field activities. We focus on traditional in-field safeguards activities related to nuclear material accounting and design information verification with the understanding that findings might also be highly applicable to safeguards activities conducted under complementary access. To identify the cognitive science and human factors principles most relevant for international nuclear safeguards activities, we first catalogued the most common safeguards activities conducted in the field. We then documented procedures for commonly used equipment or activities, and the information available to inspectors while conducting those activities. General categories of safeguards activities included, for example, destructive sampling, visual observation, and the use of safeguards equipment for non-destructive measurements of radioactive materials. From the catalogue of in-field safeguards activities and their relevant information environments, a list of relevant cognitive

science and human factors concepts was assembled which included the following areas of study:

- Wayfinding;
- Inattentional blindness;
- Situational awareness;
- Equipment troubleshooting; and
- Knowledge transfer.

In addition to these cognitive science and human factors concepts relevant for safeguards tasks, a few common themes were identified that span across safeguards activities, including operation in one's non-native language, exhaustion, stress due to time constraints, and operation in industrial environments. While these factors were also considered relevant to effective execution of international safeguards activities in the field, their pervasiveness and the difficulty to ameliorate them within international safeguards inspection scenarios led to removal from consideration in this aspect of our research.

In this paper, we will describe each of the selected cognitive science and human factors areas of study in turn, including a discussion of their relevance to safeguards activities and the current understanding of best principles or practices that may influence how to interpret their findings for international nuclear safeguards.

2. Application of Cognitive Science and Human Factors Literature to International Nuclear Safeguards

Cognitive science and human factors are scientific fields that study human behavior, activity, and learning from two distinct perspectives. For the purposes of this research, cognitive science studies human thought, learning, and mental organization related to how individuals interact with and understand information related to international nuclear safeguards inspection activities. Human factors, on the other hand, studies human interactions with a system (such as a safeguards procedure or piece of equipment) and can impact how individuals act in their physical environment based upon information they are provided. Thus, both disciplines can provide unique insight into effective and efficient means to provide information to international nuclear safeguards inspectors working in the field.

2.1 Wayfinding

Wayfinding is a form of spatial cognition in which people determine where they are in an environment and how to navigate to where they want to go [9]. Wayfinding can include navigation by map, landmarks, or verbal/written directions outdoors or indoors.

2.1.1 Wayfinding for International Safeguards

When safeguards inspectors move from one part of a facility to another, they must rely on their wayfinding skills to effectively navigate a nuclear site or facility. This includes both indoor and outdoor navigation. For outdoor navigation, inspectors can have access to the global positioning system (GPS), maps with landmarks, or other aids. Indoors, inspectors rely on a facility map or their own mental map of the facility based on previous experience. Even if they are being escorted by an operator, inspectors should be aware of where they are so that they can efficiently go from one area to another within a facility and ensure that they are being taken to the correct location. They should also be able to note if routes taken at a site or facility appear circuitous or seem to avoid areas that were previously on the regular route (which may be cause for follow-up questions).

2.1.2 Theoretical Background of Wayfinding Research

Some prior studies have potential relevance for international nuclear safeguards inspections. Several studies [10, 11, 12] have attempted to compare wayfinding using paper maps to wayfinding using mobile maps or GPS devices. These studies have had mixed results, with some finding that users took longer to reach their destinations when using a paper map [11] and others finding that participants took longer when using GPS [12]. The generalizability of the results of these studies is limited by factors such as small sample sizes [10], small screen sizes on the electronic devices [12], and inexperience with mobile maps on the part of the participants [12]. In the years since these studies took place, increasing familiarity with mobile maps and GPS among the general population could lead to very different results. However, one finding that is likely to hold true is that mobile map users tend to have a poorer understanding of the overall layout of the area in which they are navigating [10]. A paper map provides participants with an overview of the area, an aspect of navigation that is often absent when people navigate using point-to-point directions provided by a navigation app. This finding indicates that safeguards inspectors may have very different mental models of a facility if they learn its layout by walking through it as opposed to studying blueprints or diagrams. This in turn may influence how they navigate through a site or facility and how they notice changes or discrepancies.

Another area of wayfinding research that applies directly to the safeguards domain addresses indoor navigation. This is an area of interest for researchers who are trying to understand how to help people navigate through complex buildings, such as hospitals, transportation hubs, or large shopping centers. While navigation apps and mobile maps have been widely adopted for outdoor use, these tools typically fail for indoor environments, where GPS does not work (due to signal weakness) and navigation landmarks

such as street names and numbers are absent. Researchers have attempted to address these problems by developing indoor navigation systems that use waypoints rather than continuous information about a person's location. For example, Mulloni, Seichter and Schmalstieg [13] demonstrated a system that provides turn-by-turn directions from one waypoint to another. In another study, Mulloni et al [14] used a similar system in which localization markers were used to help attendees navigate during a conference. Trilateralization from Wi-Fi transmitters is also a possible solution [see 15].

These navigation techniques might be applicable within the safeguards domain to help inspectors navigate a complex facility. However, in any application of navigation aids, it is important to note that there are substantial individual differences in terms of how people navigate [16]. Indoor navigation systems must be designed so that they are robust to individual differences in the users' spatial abilities and navigation preferences. Furthermore, indoor navigational aid deployment would require approval and cooperation from the facility operator regarding placement of such markers, maintenance of their integrity, and the use of mobile technologies to engage or interpret them.

2.2 Inattentional Blindness

Inattentional blindness, also known as "change blindness" or "perceptual blindness", is the concept that the changing of certain stimuli, considered to be in plain sight, is missed by an observer. Studied to a relatively large extent within the academic psychological research community, it has sometimes been relegated to a status of marginal importance due to the historical difficultly of drawing practical inferences from the research results [17]. However, human observers' tendency to miss changes that occur right in front of them has been demonstrated repeatedly [18, 19].

2.2.1 Inattentional Blindness and International Safeguards

The discovery of Iraq's nuclear weapons program the early 1990's led to a shift in international nuclear safeguards from the verification of solely the correctness of a state's declaration, to verification of both the correctness and *completeness* (i.e., no undeclared nuclear activities) of the declaration. This led to a change in expectation that safeguards inspectors would become more investigative, and the incorporation of multiple visual observation and detection of anomaly tasks required as part of safeguards inspection activities. However, inattentional blindness research indicates that even highly focused safeguards inspectors may miss key information from their environment. For example, one of the most well-known examples of inattentional blindness is from an experiment conducted by Daniel Simons and Christopher Chabris [20], in which the researchers documented a sustained period in which test subjects asked to count the number of ball passes between a select group of individuals failed to notice the presence of someone dancing in a gorilla suit in the scene. The experiment calls into question whether international safeguards inspectors focused on one type of data collection in the field might inadvertently miss critical information that could indicate anomalous or undeclared activities.

2.2.2 Theoretical Background of Inattentional Blindness Research

Recent research in the field of inattentional blindness has focused on humans in real-world contexts rather than laboratory studies. This research is showing that change blindness occurs often and in many circumstances. One such study demonstrated that many observers failed to notice when a conversation partner was replaced in the middle of a real-life interaction [21, 22]. These research efforts have established that attention is needed to see change, and that we possess a finite ability to focus our attention on our environment. Therefore, changes to semantically central items in a scene are detected faster than changes elsewhere [18] which suggests that we assign preferential attention to certain objects based on context [23]. While attention is required for conscious change perception, the focus of our attention can change frequently while viewing a scene. If a change occurs in the scene, we may miss it despite actively viewing the scene [24, 25].

Various studies in change detection have shown that only about four items can be monitored at a time. This supports other research which implies we possess only one mechanism for the formation and maintenance of coherent visual attention, primarily concerned with the perception of objects [26]. This research may have implications on how safeguards inspectors divide tasking within an area of a nuclear facility in order to limit over-burdening the brain's visual observation capacity.

Additionally, scene representation plays a large part in our ability to visually attend to objects, and we only attend to what we need from the scene for the task at hand [25], reinforced by our experience with the stimuli being viewed. We usually do not need to mentally represent all the objects around us at any given time in order to make sense of our environment. Rather, we need only to represent the objects, and properties of those objects, involved in a task at hand. Thus it is possible that we operate with a dynamic representation of a scene that is highly sensitive to the demands of the current task and the expectations of the observer [27]. For safeguards inspectors working in the field, therefore, their mental models will appropriately shift between broad site-level understanding and smaller, more detailed visual representations needed to complete specific safeguards verification tasks.

Other studies in inattentional blindness indicate that the amount of knowledge or familiarity an individual possesses about the objects in any given scene influences their ability to detect changes to that object [28]. For example,

social drug users are more likely to detect changes to drug paraphernalia in photographs than are non-drug users [29] and American football experts are better able to spot changes to football scenes than are novices [30]. This has also been demonstrated regarding change detection with people [21], for objects described to individuals about scenes they view afterwards [18], and objects of interest to the observer [31]. This means we detect changes much more easily for objects we are familiar with or are told are of importance in a particular scene. In this context, international nuclear safeguards inspectors would be expected to have higher than average change detection capabilities in nuclear facilities they are familiar with, but may still suffer from inattentional blindness to changes in a facility when focusing on a specific task or area not associated with the change.

2.3 Situational Awareness

Situational awareness is the term used to describe a person's understanding of "what is going on" [32, 33]. This topic has received considerable research attention over the past three decades because it is a crucial component of human performance in any dynamic situation. According to the most widely-used model of situational awareness, to perform efficiently humans must be able to 1) perceive the important things in their environment, 2) understand them, and 3) be able to predict what will happen next [32].

2.3.1 Situational Awareness for International Safeguards

The highly investigative and observational nature of international nuclear safeguards activities, combined with a potentially hazardous working environment, makes inspector situational awareness crucial for their ability to safely and effectively observe anomalous or unusual activities during the course of their on-site activities. Inspectors must be aware not only of their current task at hand, but the operation of a nuclear facility or site that provides broader context to their safeguards verification activities.

2.3.2 Situational Awareness Theory

A variety of methods have been employed for improving situational awareness. Experience is a key component of situational awareness, with more experienced individuals generally exhibiting higher levels of situational awareness [34]. Thus, training and knowledge transfer can directly influence situational awareness. The way in which information is presented to an individual also has significant impact on situational awareness, which has led to a great deal of research on how to visualize information for rapid consumption by the user [35, 36, 37, 38].

In general, the design of a system has a substantial impact on situational awareness. A well-designed system or tool should present the user with the right information at the right time and in the right format to support the components of situational awareness: perception, comprehension, and projection. The details of these tasks are often domain-specific, so many researchers have focused on developing methodologies for understanding situational awareness within a specific operational context such as cyber defense [35], emergency medicine [39] and law enforcement [40].

Though situational awareness has not been explicitly studied in relation to international safeguards inspections, the techniques outlined above could be applied to understanding the components of situational awareness for different types of inspection activities. Once these components have been identified, new technologies such as data visualizations or enhanced training techniques could be developed to improve inspectors' situational awareness.

2.4 Equipment Troubleshooting

Humans interact with systems such as technical equipment on a regular basis, most commonly via intuitive action/reaction modes. This is especially true for people who are frequent users of the equipment. However, when equipment malfunctions or breaks, use of that equipment can quickly become frustrating. User guides are not always straightforward or available, and often require the user to know the specific problem with the equipment in order to troubleshoot it effectively. Troubleshooting is a form of problem solving in which users "diagnose faulty systems and take direct, corrective action to eliminate any faults in order to return the systems to their normal states" [41].

2.4.1 Equipment Troubleshooting for International Safeguards Equipment

IAEA safeguards inspectors use a large variety of safeguards equipment depending on the activity they will be carrying out in the field and facility-specific requirements. Some equipment is brought with the inspector or shipped from IAEA headquarters, while other safeguards equipment is stored on-site. While an inspector might only use a limited number of pieces of equipment for a specific safeguards inspection, there are many types of equipment that they might use over the course of their safeguards activities at different facilities or for different inspection types. In cases where maintenance is scheduled or an especially challenging piece of equipment will be used, a technician may accompany the inspector. However, inspectors often encounter equipment failure or malfunction during the course of routine use of equipment that they are required to resolve in the field.

2.4.2 Theoretical Foundations of Equipment Troubleshooting

Research in novice troubleshooting strategies tends to focus on structured representations of the system in

which large parts of the problem space can be discounted early on [42]. This "pruning of the search tree" is much like the selective search carried out by expert chess players. The representation of the system as a functional hierarchy can be used to facilitate their troubleshooting in some cases [43, 44, 45].

Kurland and Tenney posit that documentation provided for troubleshooting can be too difficult for a novice to extract, leading to information overload. In other cases, documentation might not be available. According to research conducted by Schaafstal [42] and Kurland and Tenney [46], challenges facing novice troubleshooters can come from one of two areas: 1) their limited experience with and understanding of the system, or 2) lack of a systematic approach in which robust and flexible troubleshooting strategies are applied for goal-oriented problem solving. Both Shaafstal et al [42] and Jonassen and Hung [41] stress the importance of a training regimen for troubleshooting that includes both a systematic understanding of the equipment at hand as well as a system-independent strategy for troubleshooting that prevents information overload and ensures a consistent troubleshooting approach across systems. For international safeguards inspectors, this will require training both on the safeguards equipment the inspectors will use in the field and equipment troubleshooting strategies that are equipment-agnostic.

2.5 Knowledge Transfer

Knowledge transfer refers to sharing information and experience across different teams or parts of an organization [47]. This includes knowledge that individuals or teams have gained through experience, as well as routines and procedures that have been developed over time [48]. Institutional knowledge resides in many places, including individuals, organizational structures, operating procedures, institutional culture, tools and technologies, and in the interrelationships created by combining individuals, tasks, and tools [47]. When one team hands off work to another, or when people move in or out of an organization, transferring knowledge is crucially important for maintaining continuity. Similarly, as new forms of institutional knowledge are acquired, they must be disseminated through the organization in order to improve the performance of the organization as a whole.

2.5.1 Knowledge Transfer for International Safeguards

Knowledge transfer is a critical component of international safeguards inspection activities, to ensure that facility subject matter expertise is passed from experienced to newer inspectors, as well as the transfer of information learned from in-field inspection activities from one inspector (or inspection team) to another. While most of the research regarding knowledge transfer has related to shift workers who have brief periods of overlap, IAEA safeguards inspector knowledge transfer poses a new challenge due to the amount of time between inspector visits to a facility. In this case, knowledge is being transferred mostly through paper or electronic documentation (though some may occur via in-person briefs before an inspection). Due to travel time and the potential for multiple inspections at different facilities or countries to occur in a single trip, an in-person brief may take place days or weeks before visiting the facility. Further, some information may be left at IAEA headquarters with only notes taken into the field to avoid potential loss or exposure of sensitive information (significantly increasing reliance on memory).

2.5.2 Theoretical Background of Knowledge Transfer

Knowledge transfer has been studied in shift work environments, such as manufacturing environments [48], hospitals [49], and nuclear power plants [50]. Handoffs between shifts are crucial for maintaining continuity and preventing duplication of effort in which different teams are independently trying to solve the same problems [48]. Failures of knowledge transfer between shifts have been identified as key components in industrial accidents [51, 52] and medical errors [53]. Research on knowledge transfer in these domains has identified key strategies that are used to facilitate the handoff of information (Patterson et al., 2004) and handoff checklists that could be applied to a variety of domains [52].

Face-to-face meetings are often used to transfer knowledge from one shift to the next, but this transfer can also occur via *boundary objects*. Boundary objects are artifacts that support the translation of information from one group to another, allowing disparate groups to communicate and work toward common goals [54, 55]. Bosua and Venkitachalam [48] explored the use of boundary objects in shift handovers. Of the three shift environments studied, only one had a system for codifying knowledge and making it easily available to all shifts. The culture of codifying and transferring knowledge facilitated handoffs from one team to the next.

The safeguards domain shares some features with shift work environments, such as the need to transfer knowledge from one inspection team to the next. However, it also differs from shift work environments in several key ways. For example, shifts in a hospital setting occur back-to-back, allowing different teams to overlap and share information during the transition between shifts. In contrast, there may be weeks or months between facility inspections and different teams of inspectors may not meet face-to-face. This introduces additional challenges, such as the need for robust boundary objects that can adequately transmit knowledge from one team to the next, as well as the need to account for changes that may occur between inspections. While international safeguards inspectors do complete extensive documentation regarding their in-field inspection activities, the format of this information may or may not support effective knowledge transfer between

teams. The question remains as to how safeguards-relevant knowledge from inspections at a specific site is best transferred from one team to the next.

3. Conclusions

Some of the cognitive science and human factors disciplines related to mechanisms by which international safeguards inspectors interact with information in the field are well studied, such as interior and outdoor wayfinding using various navigational aids. Others, such as knowledge transfer, are well studied in specific situations but do not currently capture significant nuances for international safeguards application space. Over the next three years, researchers at Sandia National Laboratories will develop and execute human performance experiments on mechanisms for the effective provision of information for safeguards inspection-like scenarios. We will seek to measure accuracy, timeliness, and situational awareness of test subjects performing safeguards-relevant activities and suitable proxies dependent upon the type, quantity, and provision mechanism of information to which test subjects have access. In this way, the project team seeks to have both an impact on the state of understanding in the cognitive science and human factors fields, as well as provide meaningful and actionable results that can be implemented to support international safeguards inspectors working in the field.

4. Acknowledgements

The work described in this paper is funded by Sandia National Laboratories' Laboratory Directed Research & Development office.

5. References

[1] DeLand, S, Blair, D and Horak, K; *Mobile Computing for On-Site Inspection; Proceedings of the Annual Meeting of the Institute of Nuclear Materials Management*; Indian Wells, CA, USA; 2015.

[2] Gastelum, ZN, Henry, MJ, Burtner, ER, Doehle, JR, Zarzhitsky, DV, Hampton, SD, LaMothe, RR, Nordquist, PL; *The Development of an Example Precision Information Environment for International Safeguards Use Cases; Proceedings of the Annual Meeting of the Institute of Nuclear Materials Management*; Indian Wells, CA, USA; 2015.

[3] Gastelum, ZN, Brotz, JK, Le, TD, Whalen, RT, Bolles, JC; *Proposed Use Cases for Augmented Reality for Nuclear Nonproliferation Verification and Training; Proceedings of the Institute of Nuclear Materials Management;* Atlanta, GA, USA; 2016.

[4] Steinmaus, K, Norman, C, Ferguson, M, Rialhe, A, Baute, J; *The Role of the Geospatial Exploitation System in Integrating All-Source Analysis; Proceedings of the Annual Meeting of the Institute of Nuclear Materials Management*; Palm Desert, CA, USA; 2013.

[5] Vilece, K, Norman, C, Baute, J, Giaveri,cG, Kiryu, M, Pellechi, M; *Visualization of Environmental Sampling Results at Inspected Facilities; Proceedings of the Annual Meeting of the Institute of Nuclear Materials Management*; Orlando, FL, USA; 2012.

[6] Norman, C, Baute, J, Binner, R, Walczak-Typke, AI, Aillou, F, Zhao, K, Bonner, E; *Dynamic Exploratory Visualization of Nuclear Fuel Cycle Verification Data in Support of the State Evaluation Process; Proceedings of the Annual Meeting of the Institute of Nuclear Materials Management*; Indian Wells, CA, USA; 2015,.

[7] Crowley, J, Gagne, D, Calle, D, Murray, J, Kirkgoeze, R, Moser, F; *Computational Methods for Physical Model Information Management: Opening the Aperture; Proceedings of the 2014 Symposium on International Safeguards: Linking Strategy, Implementation and People;* Vienna, Austria; 2014.

[8] IAEA; *The Modernization of Safeguards Information Technology: Completing the Picture;* 2017. https://www.iaea.org/sites/default/files/17/01/mosaic.pdf

[9] Raubal, M, Egenhofer, M; *Comparing the complexity of wayfinding tasks in built environments; Environment & Planning B*; 25; 1998; 895-913.

[10] Willis, KS, Hölscher, C, Wilbertz, G, Li, C; *A comparison of spatial knowledge acquisition with maps and mobile maps*; *Computers, Environment and Urban Systems; 33*; 2009; 100-110.

[11] Lee, W, Cheng, B; *Effects of using a portable navigation system and paper map in real driving; Accident Analysis and Prevention;* 40; 2008; 303-308.

[12] Ishikawa, T, Fujiwara, H, Imai, O, Okabe, A; *Wayfinding with a GPS-based mobile navigation system: A comparison with maps and direct experience; Journal of Environmental Psychology; 28;* 2008; 74-82.

[13] Mulloni, A, Seichter, H, Schmalstieg, D; *Handheld augmented reality indoor navigation with activity-based instructions; Proceedings of MobileHCI*; 2011.

[14] Mulloni, A, Wagner, D, Schmalstieg, D, Barakonyi, I; *Indoor positioning and navigation with camera phones; Pervasive Computing*; 2008; pp. 22-31.

[15] Shchekotov, M; *Indoor Localization Method Based on Wi-Fi Trilateralization Technique*; *Proceedings of the 16th Conference of Fruct Association*; Oulu, Finland; 2014.

[16] Lawton, CA; *Strategies for indoor wayfinding: The role of orientation*; *Journal of Environmental Psychology;16;* 1996; 137-145.

[17] Simons, DJ, Rensink, RA; *Change blindness: past, present, and future; TRENDS in Cognitive Science;* Vol. 9; No. 1; 2005.

[18] Rensink, RA, O'Regan, JK, Clark, JJ; *To see or not to see: The need for attention to perceive changes in scenes*; *Psychological Science*; Vol. 8; Issue 5; 368–373.

[19] Simons, DJ, Levin, DT; *Change blindness*; *Trends in Cognitive Sciences;* Vol 1; Issue 7; 1997; 261–67.

[20] Simons, DJ, Chabris, CF; Gorillas in our Midst: *Sustained Inattentional Blindness for Dynamic Events; Perception*; Vol 28; Issue 9; 1999.

[21] Simons DJ, Levin DT. *Failure to Detect Changes to People during a Real-World Interaction;*

Psychonomic Bulletin & Review; Vol 5; Issue 4; 1998; 644–49.

[22] Levin, DT; Simons, DJ, Angelone, BL, Chabris, CF; *Memory for Centrally Attended Changing Objects in an Incidental Real-World Change Detection Paradigm; British Journal of Psychology;* Vol 93; Issue 3; 2002; 289–302.

[23] Kelley, TA, Chun, MM, Chua, K-P; *Effects of scene inversion on change detection of targets matched for visual salience; Journal of Vision*; Vol 3, Issue 1; 2003; 1–5.

[24] Williams, P, Simons DJ*; Detecting changes in novel, complex three-dimensional objects; Visual Cognition*; Vol 7; Issue 1-3; 2000; 297–322.

[26] Rensick, RA; *Seeing, sensing, and scrutinizing; Vision Research;* Vol 40; 2000; 1469 – 1487.

[27] Rensick, RA; *Change Detection*; *Annual review of Psychology*; Vol 53; 2002; 245 -77.

[28] Archambault, A, O'Donnell, C, Schyns, PG; *Blind to Object Changes: When Learning the Same Object at Different Levels of Categorization Modifies its Perception; Psychological Science*; Vol 10; 1999; 249–255.

[29] Jones, BT, Jones, BC, Smith, H, Copley, N; *A Flicker Paradigm for Inducing Change Blindness Reveals Alcohol and Cannabis Information Processing Biases in Social Users; Addiction;* Vol 98; 2003; 235–244.

[30] Werner, S, Thies, B; *Is 'Cange Blindness' Attenuated by Domain-Specific Expertise? An Expert-Novices Comparison of Change Detection in Football Images; Visual Cognition*; Vol 6; 2000; 163–173.

[31] Shore DI, Klein, RM. The Effects of Scene Inversion on Change-Blindness. *Journal of General Psychology;* Vol 127; Issue 1; 2000; 27-43.

[32] Endsley, M R; *Toward a Theory of Situation Awareness in Dynamic Systems; Human Factors;* Vol 37; 1995; 32-64.

[33] Endsley, M; *Theoretical Underpinnings of Situation Awareness: A Critical Review; Situation Awareness: Analysis and Measurement* (Eds. Endsley, M, Garland, D); Erlbaum; Mahwah, NJ, USA; 2000; 3-32.

[34] Underwood, G, Ngai, A, Underwood, J; *Driving Experience and Situation Awareness in Hazard Detection; Safety Science*; Vol 56; 2013; 29-35.

35 D'Amico, A, Kocka, M; *Information Assurance Visualizations for Specific Stages of Situational Awareness and Intended Uses: Lessons Learned; IEEE Workshop on Visualization for Computer Security*; 2005; 107-112.

[36] Feibush, E, Gagvani, N, Williams, D; V*isualization for Situational Awareness; IEEE Computer Graphics and Applications*; Vol 20; Issue 5; 2000; 38-45.

[37] Kim, YJ, Hoffmann, CM; *Enhanced Battlefield Visualization for Situation Awareness; Computers & Graphics;* Vol 27; Issue 6; 2003; 873-885.

[38] Toet, Al, Jspreert, JK, Waxman, AM, Aguilar, M; *Fusion of Visible and Thermal Imagery Improves Situational Awareness; Displays;* Vol 18; 1997; 85-95.

[39] Sapateiro, C, Antunes, P; *An Emergency Response Model toward Situational Awareness Improvement; Proceedings of the 6th International ISCRAM Conference;* Gothenburg, Sweden; 2009.

[40] Datcu, D, Lukosch, S, Lukosch, H, Cidota, M; *Using Augmented Reality for Supporting Information Exchange in Teams from the Security Domain; Security Informatics;* Vol 4; 2015.

[41] Jonassen, DH, and Woei H; *Learning to Troubleshoot: A New Theory-Based Design Architecture*; *Educational Psychology Review;* Vol. 18; No. 1; 2006; 77-115.

[42] Schaafstal, A, Maarten, J, van Berlo, M; *Cognitive Task Analysis and Innovation of Training: The Case of Structured Troubleshooting*; *Human Factors*; Vol 42; No. 1; 2000 75-86.

[43] Bereiter, SR, Miller, SM; *A Field-Based Study of Troubleshooting in Computer-Controlled Manufacturing*

Systems; IEEE Transactions on Systems, Man, and Cybernetics; Vol 19, 1989; 205–219.

[44] Egan, DE, Schwartz, BJ; *Chunking in Recall of Symbolic Drawings; Memory and Cognition*; Vol 7; 1979; 149–158.

[45] Rasmussen, J; *Information Processing and Human-Machine Interaction: An Approach to Cognitive Engineering*; Elsevier; Amsterdam; 1986.

[46] Kurland, LC, Tenney, YJ*; Issues in Developing an Intelligent Tutor for a Real-World Domain: Training in Radar Mechanics; Intelligent Tutoring Systems: Lessons Learned* (Eds Psotka, J, Massey, LD, Mutter, SA); Psychology Press; Hove, UK; 1988; 119–180.

[47] Argote, L, Ingram, P; *Knowledge Transfer: A Basis for Competitive Advantage in Firms*; *Organizational Behavior and Human Decision Processes;* Vol. *82;* 2000; 150-169.

[48] Bosua, R, Venkitachalam, K; *Fostering Knowledge Transfer and Learning in Shift Work Environments; Knowledge and Process Management;* Vol. 22; 2015; 22-33.

[49] Kerr, MP; *A Qualitative Study of Shift Handover Practice and Function from a Socio-Technical Perspective; Journal of Advanced Nursing*; Vol. 37; 2002; 125-145.

[50] Patterson, ES, Roth, EM, Woods, DD, Chow, R, Gomes, JO; *Handoff Strategies in Settings with High Consequences for Failure: Lessons for Health Care Operations*; *International Journal for Quality in Health Care;* Vol. 16; 2004; 125-132.

[51] Lardner, R; *Effective Shift Handover: A Literature Review; Offshore Technology Report - Health and Safety Executive OTO*; 1996.

[52] Wilkinson, J, Lardner, R; *Pass it on! Revisiting Shift Handover after Buncefield; Loss Prevention Bulletin;* Vol 229; 2012; 25-32.

[53] Cook, RI, Woods, DD, Miller, C; *A Tale of Two Stories: Contrasting Views of Patient Safety; National Health Care Safety Council of the National Patient Safety Foundation at the AMA*; 1998.

[54] Star, SL, Griesemer, JR; *Institutional Ecology, 'Translations' and Boundary Objects: Amateurs and Professionals in Berkeley's Museum of Vertebrate Zoology; Social Studies of Science;* Vol 19; Number 3; Issue 1907-39; 1989; 387-420.

[55] Trompette, P, Vinck, D; *Revisiting the Notion of Boundary Object; Revue d'Anthropologie des Connaissances;* Vol 3; 2009; 3-25.

The forward-problem approach in Safeguards verification: directly comparing simulated and measured observables

S.Vaccaro[1], I. Gauld[2], M. Vescovi[3], H. Tagziria[4], A. Smejkal[1], P. Schwalbach[1]

[1] European Commission, Directorate General Energy, Directorate Euratom Safeguards, Luxembourg
[2] Oak Ridge National Laboratory, Oak Ridge, TN, USA
[3] iScience, Milan, Italy
[4] European Commission, Directorate Joint Research Centre, Directorate Nuclear Safety & Security, Ispra, Italy

Abstract:

Physical verification by NDA in nuclear safeguards implies typically the adoption of an inverse-problem approach. This is, indeed, the definition of a problem, in which we use physical observables to deduct other physical quantities, which in our case are contained in the operator's declaration. A typical example is the Plutonium mass, measured using Pu isotopics and neutron coincidence doubles counts, linked to the Pu 240 effective mass by a calibration.

An alternative approach has been recently proposed and is now close to the in-field deployment by the Euratom Safeguards Directorate of European Commission's DG ENER. In fact, the detailed knowledge of the physical processes that are taking place in the sample and within the detector allows computing the amount of the measured observable, by modelling the physical system as it results from the operator's declaration, in a forward-problem approach.

The present paper describes the first two examples of the forward-problem approach's application to actual real-life safeguards verification. The first example deals with a Monte-Carlo-based modelling tool that has been developed to enable the inspectors to perform an improved verification of fresh fuel assemblies by neutron coincidence collar (NCC), taking into account the growing complexity of the fuel's design. The second example shows how the verification of spent fuel is improved regarding the false alarm rate and the partial defect detection capability, by the integration of the automated review package iRAP and the modelling by the Oak Ridge transmutation code (ORIGEN).

The potential applications of the new approach are not limited to the two described in this article, which, however, represent relevant proofs of concept of the potential that a change of perspective in verification by NDA may generate.

Keywords: NDA, Forward problem, Spent Fuel, Fresh Fuel, ORIGEN, Neutron Coincidence Collar

1. Introduction

In 2017, Euratom Safeguards celebrates its 60th anniversary – the legal being the Euratom Treaty, signed in Rome on March 25, 1957. During this long history, a number of field practices, approaches and methods have been developed, consolidating Euratom inspectorate position as one of the reference institutions in the international Safeguards community.

An essential component of the conformity controls, which allow the inspectors to draw independent conclusions, is the Credibility Control, linking the declarations by the nuclear operators to the physical reality, as observed by the inspectors. The physical verifications, that the inspectors carry out in order to perform a credibility control, often consist in the measurement of physical quantities, related to the declared nuclear material properties, by Non-Destructive Assay (NDA).

The advantage of NDA measurements is the possibility to perform the necessary verification, without excessive interference with the operator's industrial process and without alteration of the nuclear material under assay, its physical form or its container. However, one drawback of NDA methods is the not always obvious interpretation of discrepancies, because of an imperfect estimate of measurement uncertainty, especially caused by the difficult quantification of uncertainty in the instrument calibration. Moreover, for the measurement methods used in NDA verification, an appropriate metrological traceability is made impossible by the non-existence of reference materials of the same type, quantity range and physical form of the samples to be measured.

The growing availability of technologies allowing high performance calculations, since the late 1990s, has allowed tackling these limitations of the NDA methods, by using physical-model-based simulation to define the instruments' calibration, starting from a detailed knowledge of the physical system defined by the instrument, the sample and by their mutual interactions. In this perspective, although modeling was used to overcome some of its limitations, simulation did not change the traditional calibration approach, relating an observable physical quantity (for instance, a neutron or gamma count rate) to the values of the quantity of interest (for instance, the quantity of nuclear material).

More recently, a further step has been taken, by using real-time simulation to predict directly the observable physical quantities (corresponding to declarations from the operator), which are then compared with the measurement results [1][2]. This different forward-problem approach, has allowed overcoming some limitations of the traditional calibration approach in particularly complex cases. The

following paragraphs will describe its consequent practical and conceptual implications.

2. Inverse and Direct problems: definition and application to Nuclear Safeguards Measurements

During verification, as in every measurement operation, we establish a relation between two different abstract spaces. One, which we define as Model Space ($\mathcal{M}$), contains all the knowledge we have from the physical system, defined by a set of parameters including the information contained in the operator declaration. The other abstract space, which we define as Data Space ($\mathcal{D}$), consists of the data from the observable quantities.

The general measurement problem is defined by the following relationship:

$$d = \boldsymbol{G}(m)$$

where $d \in \mathcal{D}$, $m \in \mathcal{M}$ and $\boldsymbol{G}$ is a generic operator linking explicitly the observed data and the model parameter.

In other terms, the general measurement problem is about establishing a relationship linking the causes (the physical theory leading to the model parameters) and the effect (the observed data). As shown in Figure 1, the direction we choose interpreting this link determines whether we are dealing with a direct (forward) or with an inverse problem.

The inverse problem approach will be, then, the one starting from the measured data (e.g. correlated neutron flux) to determine one or more *unknown* parameters (e.g. fissile material mass and/or isotopic composition) defining the physical system under observation. Those parameters subject to verification are thus not measured directly, but they are rather the result of inversion algorithms solving complex equations, deriving the unknowns from the measured observables.

Figure 2 schematically represents the inverse problem in the specific case of nuclear safeguards verification: the measured data go through a model, in order to deduct the unknowns, which are eventually compared to the declared values in the verification phase. One of the implications of this process is that measurement uncertainties on the initial observables need to be propagated throughout the inversion model, which is not trivial from the mathematical point of view.

Sometimes, to simplify the model, assumptions like “infinite thickness” of the samples need to be taken or the model is replaced by empirical calibration curves. These latter suffer from a critical drawback: the Certified Reference Materials of the same type (i.e. in size, weight, matrix, fissile mass, package form) do not exist; therefore, selected samples from the operator’s facility are used for calibration. In this way, a measurement’s metrological traceability not directly possible; sometimes, indirect traceability can be established, e.g. by help of destructive assay of samples. Interpreting discrepancies in the verification results is then only possible with the intervention of experts in the specific measurement technique, who are able to assess uncertainties including knowledge from additional information sources.

Moreover, the inverse problem can represent a case of *ill-posed* problem in the sense of Hadamard [3], where the *well-posedness* conditions are that

a. A solution exists;

b. The solution is unique;

c. The solution’s behavior changes continuously with the initial conditions.

In particular, we can immediately understand why the condition b. is not met in a simple practical case: two fuel assemblies with different ^{235}U masses, but different location of burnable poison rods, may give the same (i.e. statistically comparable) double neutrons count rate, if measured in a thermal-mode neutron collar. In this case, thus, the solution of the observed data inversion is not unique.

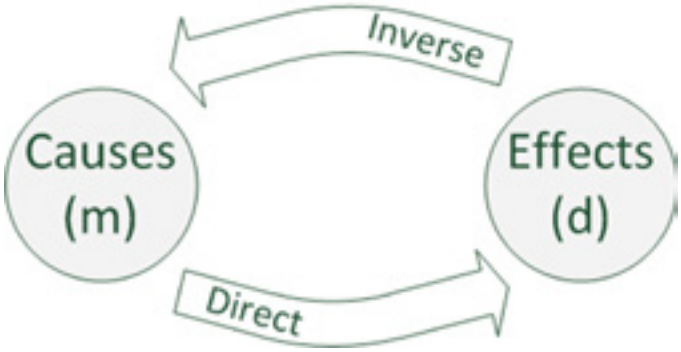

Figure 1: Schematic representation of direct and inverse problems

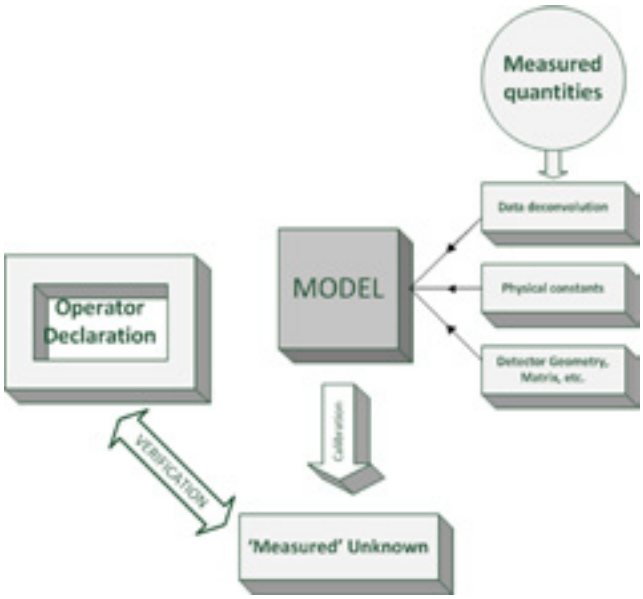

Figure 2: Schematic representation of the inverse problem as applied to nuclear safeguards verification.

On the other hand, the choice of a forward problem approach would start from the modeling of the physical system involved in the measurement, where the quantities of interest (e.g. fissile material mass/isotopic composition) become parameters of the model. As shown in Figure 3, the operator's declaration will then identify specific values of the mentioned parameters, while the model will predict the observable's quantities under these specific conditions. The verification phase will then consist in the direct comparison of the measured versus the predicted observables. The whole verification task becomes, in this way, a typical *hypothesis testing* exercise, in which a predicted quantity undergoes a direct comparison with its experimental value, under the hypothesis defined by the operator declaration.

We can then observe that a forward problem approach avoids the most difficult aspects of the mathematical inversion (deconvolution algorithms, non-unique solution, experimental error propagation), which are no longer needed in the verification task. At the same time, using the same set of information available and the same set of data, the credibility of the verification conclusion is not affected. Even in a forward-problem approach, though, one can still postulate other operator declarations that could result in the same or similar predicted quantities (within measurements and model uncertainties). However, we have to keep in mind that the primary task of the inspectorate is to verify the declarations provided by operator and not necessarily to develop the declared parameters independently.

It is also worth pointing out that measurement uncertainties are not eliminated by modelling: rather, a clear distinction is made between the uncertainty components arising from the calculation and those originating from the measurement itself (e.g. sample positioning, homogeneity, counting statistics).

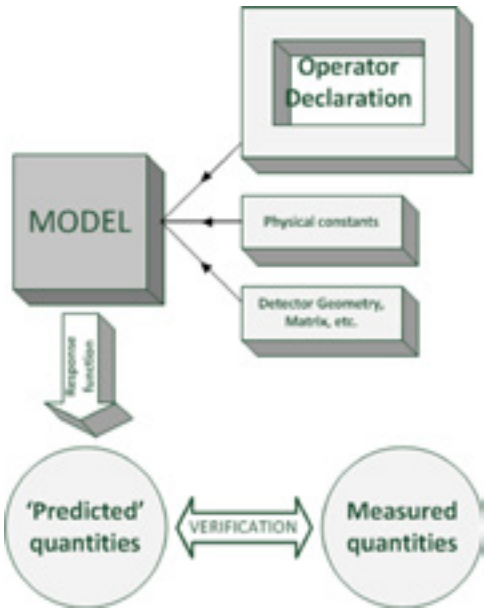

Figure 3: Schematic representation of the forward problem as applied to nuclear safeguards verification.

3. Euratom field-ready inspection tools using a forward-problem approach

Euratom Safeguards directorate makes use of Monte Carlo modeling in several deployed instruments, thus overcoming the issues with lack of reference materials and metrologically traceable calibration standards [4][5]. The improved computing capabilities and some specific verification issues have recently suggested that a forward problem approach with real-time simulation can improve the current verification practices. Clearly, every model needs to be appropriately benchmarked against well-characterised reference materials.

3.1 XFuelBuilder tool for Fresh LWR Fuel verification

Fresh fuel verification by Neutron Coincidence Collar (NCC) poses difficulties, in particular due to the increasing optimization of fuel performance, resulting in greater complexity of fuel design. In particular, fuel producers optimize the fuel assemblies by the use of strategically located burnable poison-enriched rods and by pins that have a variation in ^{235}U enrichment both axially and radially in the assembly.

In order to allow the inspectors to cope with this complexity, European Commission's Joint Research Centre and iScience have developed for Euratom Safeguards inspectorate *XFuelbuilder*, a tool based on the Monte Carlo simulation of NCC measurements. *XFuelbuilder* is in fact a software package, with a user friendly graphical interface, that allows the inspector to prepare a MCNP input file in a simple visual way and then run the simulation of the fuel + collar physical system. The modelling has been done using the MCNP-PTA code, developed at the Joint Research Centre of the European Commission in Ispra, in order to simulate the electronics pulse train analysis (PTA), including a shift register logic for coincidence counting. A benchmark of the modelling has been done at the PERLA laboratory at the Joint Research Centre in Ispra and is reported in past articles [4][5][6].

XFuelbuilder includes already the built-in models of the NCCs used by Safeguards inspectorates, both in thermal and fast mode configuration. The inspector can retrieve a stored assembly model or add a new pin or assembly design. Once chosen the collar type, the fuel design and the collar position along the fuel's active length, the inspector can run the simulation, thus obtaining the Reals, the Accidentals and the Totals as he or she would do in any neutron measurement. These values are then easily compared with the measured data, acquired by NCC assay of the assembly. Figure 4 describes the data flow of the whole verification task.

XFuelbuilder, choosing a forward-problem approach, is not affected by the already mentioned ill-posedness of the NCC verification problem, being at the same time a user friendly tool for the inspector. Moreover, it is capable to integrate many of the declared fuel details in the verification

itself. This approach is also going to improve practical aspects of NCC verification, usually needing a passive measurement before the active one, in order to take into account for the correlated neutrons from ^{238}U spontaneous fission. While this two-phase process obliges the inspector to deploy and remove the source and is a practical limit to the possibility to make such measurements as unattended, in *XFuelbuilder* both induced and spontaneous fission are taken into account. Then, in principle, only the active measurement needs to be done, thus giving the inspectorate the possibility of unattended measurements. After a refinement phase, aimed at maching the inspectors' needs, Euratom Safeguards is starting to deploy *XFuelbuilder* as of 2018, starting from facilities where unattended NCC verification is needed.

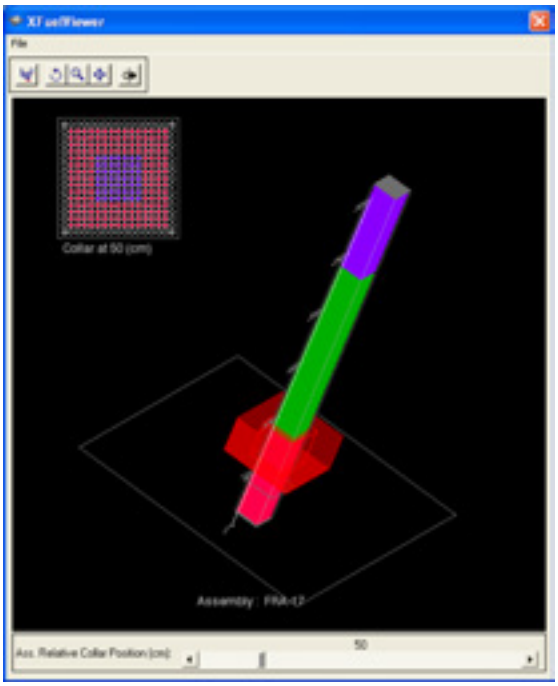

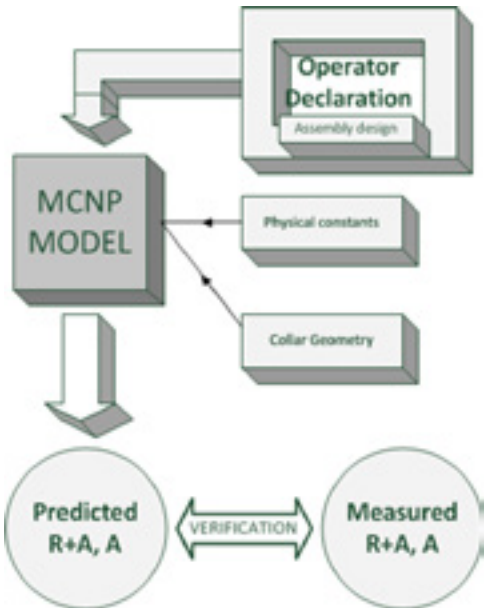

Figure 4: Screenshot and data flow of XFuel Builder

3.2 iRAP-ORIGEN method for improved Fork detector measurement results evaluation

Spent-fuel is one of the big challenges for NDA. In fact the high neutron and gamma activity from irradiated assemblies make it extremely difficult to measure and quantify fissile material in a simple and direct way. Although some promising methods may address this issue in the future [8], the Fork detector is at present the workhorse for the verification of fuel in preparation of intermediate/long term or final, geological storage, where recovery (and re-measurement) is practically not possible. In Fork detector verifications, safeguards inspectors measure the neutron and total gamma fluxes from an irradiated fuel assembly to check its consistency with the declared burn up, initial enrichment and cooling time of the assembly itself.

Euratom Safeguards is presently field testing a data evaluation tool [9][10], based on the integration of the review code iRAP (joint development of Euratom and IAEA) and the ORIGEN code (Oak Ridge Isotope GENeration), which is part of the package SCALE developed by Oak Ridge National Laboratory [11]. The iRAP-ORIGEN integration has been developed and improved under various Action Sheets on the EC-US DOE agreement in the field of nuclear material safeguards R&D. This cooperation has submitted a paper (now under review) summarising the work performed and including a more detailed uncertainty analysis of the calculations that are the basis of the method and of the assumptions made in the modelling of the fuel assemblies that are calculated [12].

The iRAP-ORIGEN tool allows, on the one hand, to process unattended Fork measurements, and extract the assembly neutron and gamma signature. On the other hand, a simulation combining an ORIGEN irradiation and depletion calculation, using the operator's declarations as input data, and a Monte Carlo computed detector response function compute the expected values of the same signature. The data flow of the complete process is explained in Figure 5.

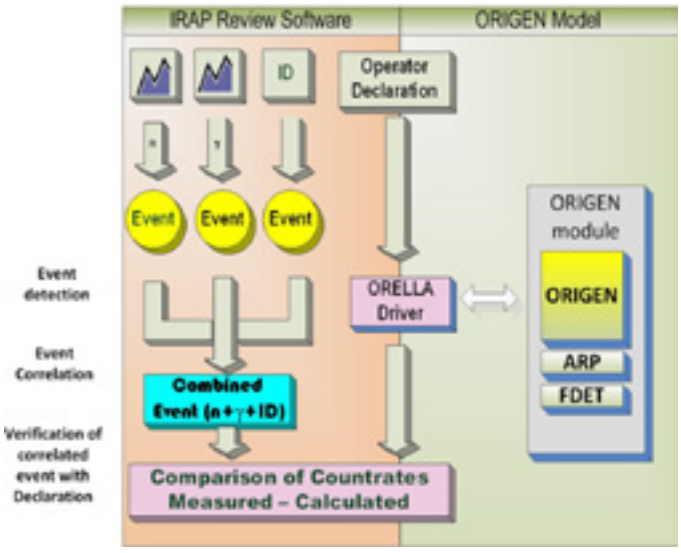

Figure 5: Data flow of an iRAP-ORIGEN Verification

This tool has already proven to be accurate in in taking into account the factors, which may influence the neutron and gamma signatures of spent fuel (e.g. cooling between irradiation cycles, within-assembly neutron multiplication). iRAP-ORIGEN is also ready for unattended measurements evaluation and is proving particularly inspector-friendly in installations where remote data transmission is available. The tool assists both the Inspectors and the Facility Operators: by providing a convenient mechanism for rapidly comparing operator declarations with measurement results. Alarms that are due to simple clerical or transcription errors may be resolved quickly, without need for further re-verification activities at a later date.

Finally, still remaining a rather simple and limited technique, this improved version of Fork measurements is complementary to other techniques, aimed at the assembly integrity verification, like tomography [13], or aimed at other types of fuel characterization, like Passive Neutron Albedo Reactivity (PNAR) [8].

4. Conclusions

A forward-problem approach, consisting in real-time simulations using declaration data as parameters in a model that predicts directly measured observables, may be helpful in nuclear safeguards NDA verification, especially in cases where calibration can hardly take into account the complexities of the specific sample.

Euratom Safeguards Directorate, in partnership with research institutions such as the European Commission's Joint Research Centre and the Oak Ridge National Laboratory, has already developed tools, which are ready to bring this *hypothesis testing* approach into every day's inspection activities. The first two application fields are the verification of fresh LWR fuel by Neutron Coincidence Collar and the verification of irradiated fuel assemblies by Fork detector.

The forward-problem approach is also an opportunity for resource optimization, as it can be very well integrated in a remote data infrastructure, which allows performing the computational part of the verification at the headquarters.

Finally, it is worth mentioning that the use of a forward-problem approach is going to require a corresponding reflection of such physical verifications in the safeguards approaches, especially regarding the meaning of anomalies in terms of diversion scenarios and Material Balance Evaluation.

References

[1] Zykov, *Technical Challenges and Technological Gaps in IAEA Safeguards*, in: Proceedings of the 56th annual meeting of the Institute for Nuclear Material Management, July 12-16th 2015, Indian Wells, USA;

[2] Peerani *et al.*, *Real-time simulation of neutron counters*, Radiation Measurements 43 (2008) p 1506–1510;

[3] Hadamard, J., *Sur les problèmes aux dérivés partielles et leur signification physique*, Princeton University Bulletin, Vol. 13 (1902), p. 49-52;

[4] Looman, M., Peerani, P., Schwalbach, P., *Calibration with Monte Carlo calculations of a neutron collar for the verification of FRM-II fuel elements*, in: Proceedings of the 25th Annual Symposium on Safeguards and Nuclear Material Management, 13–15 May 2003, Stockholm, Sweden;

[5] Peerani, P., Looman, M, *Computational modelling of NDA instruments for nuclear safeguards* in: Proceedings of the 24th Annual Symposium on Safeguards and Nuclear Material Management, 28–30 May 2002, Luxembourg, p. 131–137;

[6] Peerani et al., *A user-friendly tool for easy and fast in-field Monte Carlo simulation of neutron collars*, in: Proceedings of 37th ESARDA Symposium on Safeguards and Nuclear Non-Proliferation, Manchester, UK, 19-21 May 2015

[7] Tagziria et al., *XfuelBuilder for the Analysis of Simulations and Measurements of fresh fuel assemblies using neutron coincidence collars by nuclear inspectors*, current conference.

[8] S.J. Tobin *et al.* , *Technical Cross-Cutting Issues for the Next Generation Safeguards Initiative's Spent Fuel Nondestructive Assay Project*, Journal of Nuclear Materials Management 40(3), p.18-24, 2012.

[9] S. Vaccaro, J. Hu, J. Svedkauskaite, A. Smejkal, P. Schwalbach, P. De Baere and I. C. Gauld, *A New Approach to Fork Measurements Data Analysis by RADAR-CRISP and ORIGEN Integration*, IEEE Transactions on Nuclear Science 61, 4, 2014.

[10] I. Gauld, J. Hu, P. DeBaere, S. Vaccaro, P. Schwalbach, H. Liljenfeldt, and S. Tobin, *In-Field Performance Testing of the Fork Detector for Quantitative Spent Fuel Verification*, Proceedings of the 37th Annual Meeting ESARDA Symposium 2015, Manchester.

[11] S. M. Bowman, *SCALE 6: Comprehensive Nuclear Safety Analysis Code System*, Nuclear Technology 174(2), p 126–148, May 2011.

[12] S. Vaccaro, I. C. Gauld, J. Hu, P. De Baere, P. Schwalbach, A. Smejkal, A. Tomanin, C. Demartini, A. Sjöland, S. Tobin, D. Wiarda, *Advancing the Fork Detector for Quantitative Spent Nuclear Fuel Verification*, submitted to *Nuclear instruments and Method part A*.

[13] T. Honkamaa, F. Levai, A. Turunen, R. Berndt, S. Vaccaro, and P. Schwalbach, *A Prototype for Passive Gamma Emission Tomograph, IAEA Symposium on International Safeguards*, IAEA CN-220/129, 2014.

Ultrasonic Identification Methods of Copper Canisters for Final Geological Repository

C. Clementi[1,2], F. Littmann[2], L. Capineri[1], C. Andersson[3], U. Ronneteg[4]

1 Dept. Information Engineering – University of Florence, Florence, Italy
2 European Commission, Joint Research Centre, Nuclear Security Unit, Ispra, Italy
3 Swedish Radiation Safety Authority,
4 Swedish Nuclear Fuel and Waste Management Co

Abstract:

The Swedish system for taking care of the spent nuclear fuel includes long term geological disposal of the fuel encapsulated into copper canisters. For such Safeguards applications, it is of utmost importance to be able to trace canisters once closed in order to keep the Continuity of Knowledge from the Encapsulation Plant to the Geological Repository. One possibility is to use a tagging of the canister. This work introduces an innovative system for tagging copper canisters based on the ultrasonic reading of cavities machined on copper lids. The realization of a new identification method for copper canisters is the aim of the research. For corrosion reasons it is better to not engrave any code on the external parts of copper canisters. According to the copper lid geometry, the proposed solution envisages the machining from the inside of several inclined Flat Bottom Holes or chamfers around the circumference of the lid, while still keeping the required thickness of the copper for safety reasons. They represent a unique identification code for each canister, easily readable by an ultrasonic immersion probe on a 360° scan. A laboratory prototype for the identification system has been manufactured and successfully tested.

The copper lid is reproduced on a scaled version and a series of chamfers 50° inclined are drilled around the bottom of the lid. The reading system hosted a probe placed 14° inclined according to the Snell's law. The received ultrasonic signal represents the binary code realized by the chamfers [1].

The paper will describe the optimization studies made on the transducers, the angle and width of chamfers, the binary identification codes, preliminary design and testing of a reading system.

Keywords: ultrasound; identification; copper canister, geological repository.

1. Introduction

The spent fuel coming from operations of Swedish nuclear power plants will be inserted into copper canisters and then stored in deep geological repositories. The Swedish Nuclear Fuel and Waste Management Company's (SKB) developed the method for final disposal of fuel in copper canisters surrounded by bentonite clay about 500 metres underground in Swedish bedrock. This solution will keep the fuel isolated from human beings and the environment for many years.

The new SKB's method for final disposal of fuel comprises a number of facilities that together provide a safe chain (Figure 1). The fuel coming from Swedish reactors is stored for one year minimum in the spent fuel ponds at the reactors before it is shipped to the interim storage facility. There

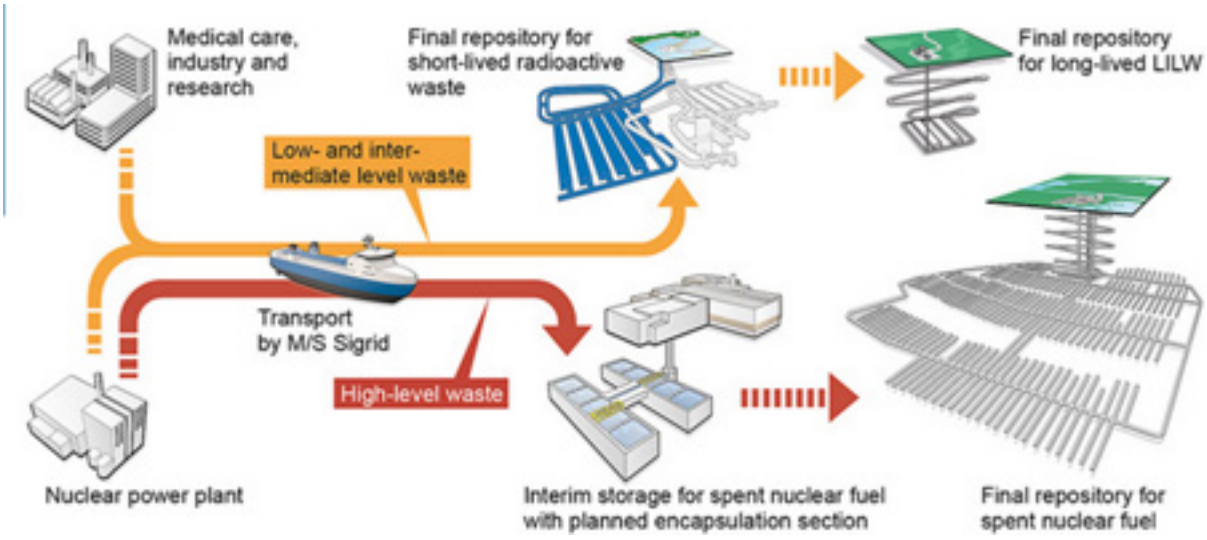

Figure 1: The SKB project for the management of spent nuclear fuel in Sweden.

the fuel is placed in storage baskets which are stored in ponds. Later storage canisters with spent fuel will be lifted from the pools and moved to the encapsulation plant where the fuel is inserted in copper canisters with iron inserts. After encapsulation, the canisters are transported to the final repository and then located in the deposition hole. About 6000 copper canisters will be deposited, with an average of one canister per day.

Repositories present several new challenges for international Safeguards. One of them is maintaining the Continuity of Knowledge (CoK) from the encapsulation plant to the final repository.

The International Atomic Energy Agency and EURATOM safeguards approaches propose to use canisters identification during transport and deposition from the encapsulation plant to the final repository [2]. Convectional tagging techniques are various but SKB has to date not presented any method for labelling the copper canisters [3], [4], [5], [6]. An engraving or marking of the canister may impede the long term safety and integrity of the canister since it may reduce the corrosion barrier [2]. Therefore alternative solutions should be developed. Next paragraphs illustrate a possible identification method based on ultrasounds developed by the SILab, Seals and Identification Laboratory, of the Joint Research Centre of the European Commission in Ispra (VA). The first part of the research deals with studies oriented to identify the best positioning of holes or chamfers to be read by a specific transducer. Afterwards a series of simulations and experimental tests have been implemented on copper samples and slices of the copper canister (copper flanges) with the aim to demonstrate the possibility of identification of canisters by ultrasounds. In the end, the identification method is validated on a small-scaled copper lid with chamfers investigated by an ultrasonic reading system prototype.

2. The identification method

Since many years, SILab develops ultrasonic identification techniques on bolt seals with artificial cavities made on stainless steel washers, giving a fingerprint from the reflection of unique patterns. In the case of copper canisters, the geometry (Figure 2.) and dimension of the lid are much bigger than seals, therefore an adaption of the ultrasonic method is required. In particular, the solution proposed in this paper deals with the identification of copper canisters by the ultrasonic investigation of a series of Flat Bottom Holes (FBHs) or chamfers milled on the inner surface of the lid where the copper thickness is higher than 50 mm, as shown in Figure 3. Because of corrosion reasons, in fact, the minimum copper thickness must not be less than 50 mm and the machining of holes or chamfers must not affect the integrity and the stability of canisters.

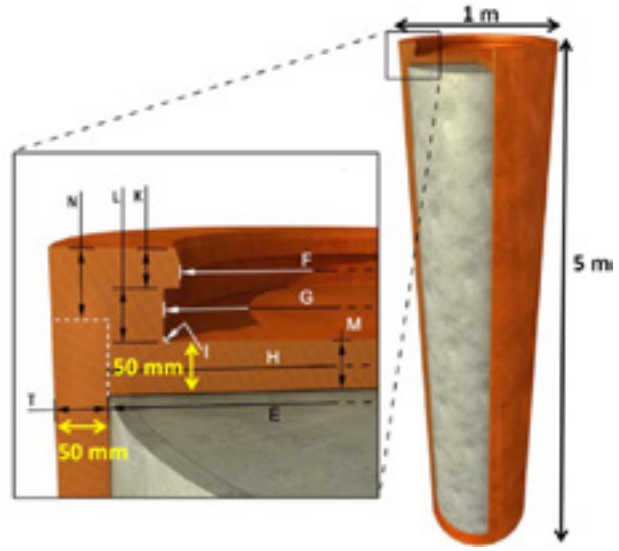

Figure 2: Copper canister geometry.

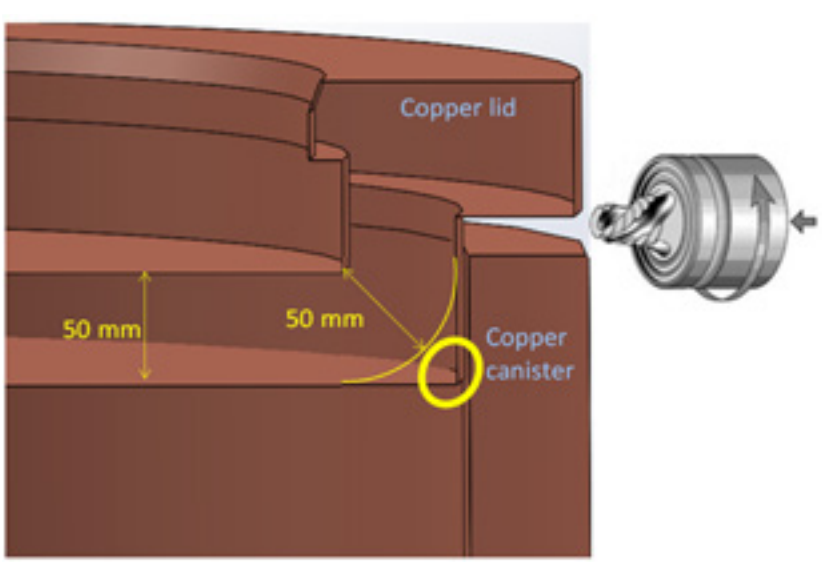

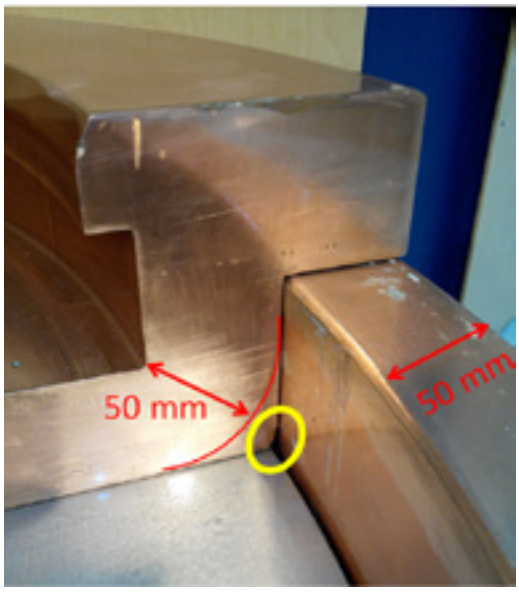

Figure 3: Area (circled in yellow) where the thickness of the lid is higher than 50 mm.

The study of the best dimension and position of holes is realized by 3D simulations and experimental measurements carried out on copper flanges that are part of a lid already been welded to the canister. The first idea was to drill configurations of FBHs with different positions and dimensions on the bottom surface of copper lids as shown in Figure 4, on the left. The ultrasonic reading of these cavities was designed to be accomplished by a single probe located on the top of the lid, rotating 360° along with the lid circumference. Before machining FBHs in copper flanges, ultrasonic tests were carried out on cylindrical copper samples with different FBHs. The analysis of results revealed the possibility to acquire echoes, however, depending on the inspection frequency, the attenuation of ultrasound in copper could affect measurements negatively and then a different configuration of holes was studied [7]. In order to decrease the distance between cavities and probe, FBHs are replaced by inclined flat holes or chamfers arranged as illustrated in Figure 4, on the right. Cavities

This new disposition of holes involves the repositioning of the transducer as shown in Figure 5. The probe must be inclined according to the Snell's Law in order to guarantee the perpendicularity between the ultrasonic beam and reflectors. Considering the velocities of sound in water (V1=1500 m/s) and in copper (V2=4651 m/s), the probe angle should be around 14° assuming that the inclination of the chamfer is 50°.

$$\sin(\alpha 1)/V1=\sin(\alpha 2)/V2 \rightarrow \alpha 1=\sin^{-1}(1500/4651)\cdot\sin(50)=14.3° \quad (1)$$

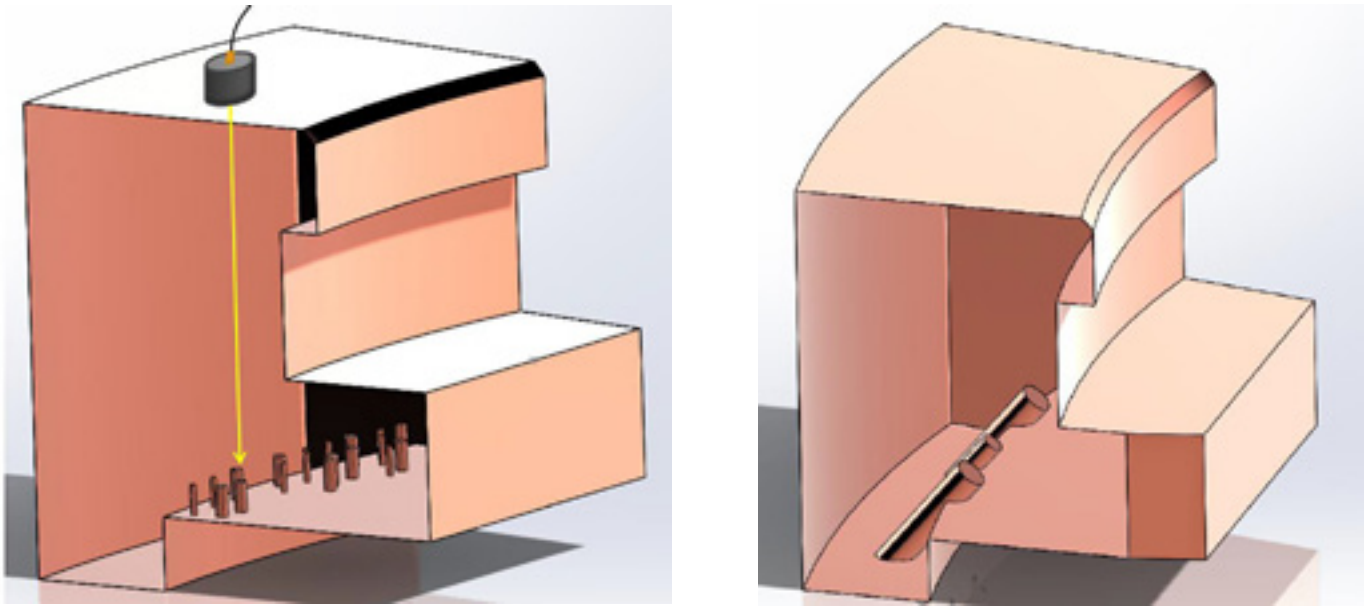

Figure 4: Two possible types of identification cavities: FBHs on the left, inclined flat holes on the right.

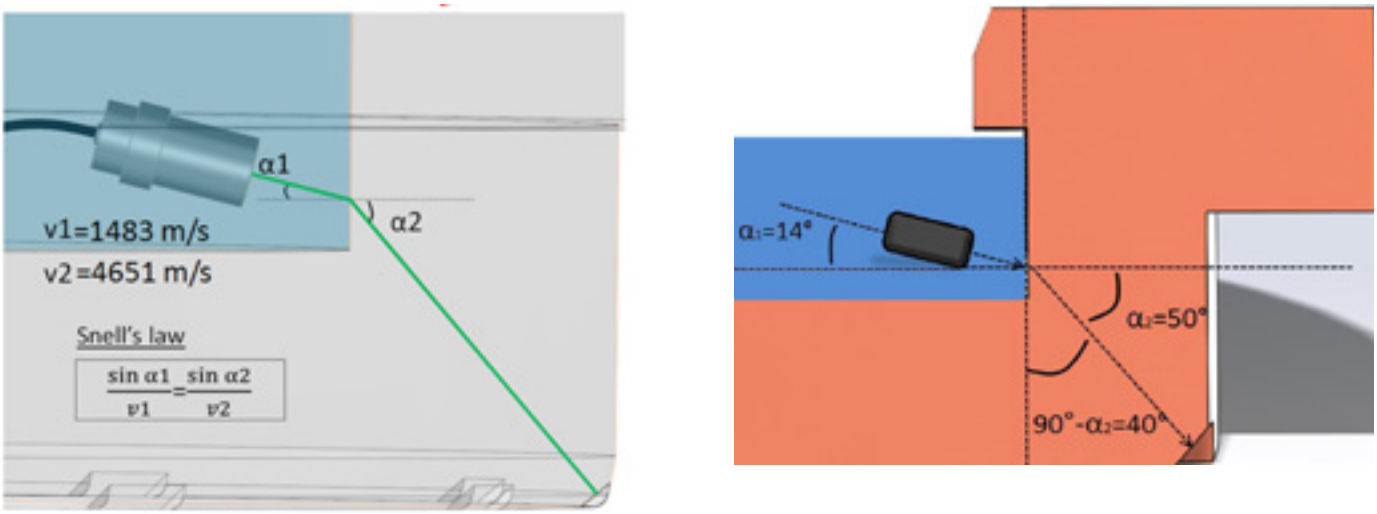

Figure 5: Position of the transducer according to the Snell's law.

Depending on the configuration of chamfers around the lid circumference, the transducer will receive different ultrasonic amplitude responses. Therefore, each canister can be identified by a unique code of chamfers readable by ultrasounds.

3. Simulations and experimental tests

Several experimental tests were carried out on copper flanges with the aim to verify the possibility of detection of flat bottom holes 50° inclined [8]. The inclination of holes has been chosen at 50° by authors for tests but it could be changed in case of necessity. The following Figure 6 shows the set-up of measurement for the investigation of an inclined hole (on the left) and the corresponding A-scan signal (on the right).

Considering that the Time of Flight (TOF) of the echo received is 31.3 μs, the corresponding measured distance is 65.88 mm, value in accordance with the geometrical distance d_h.

The analysis of measurements pointed out that ultrasonic echoes reflected by inclined holes can be detected with a good signal to noise ratio.

Before validating the method on a laboratory prototype, simulations on the CIVA software [9] were implemented to study the best dimensions and positions of chamfers to be machined on the copper lid circumference. The CIVA Ultrasonic Testing (UT) module is specific for ultrasonic NDT and offers two different types of evaluations: the beam computation and the inspection simulation, both useful for our purpose. The set-up simulated (Figure 7) is a 2D profile of the copper lid with a 50° inclined chamfer.

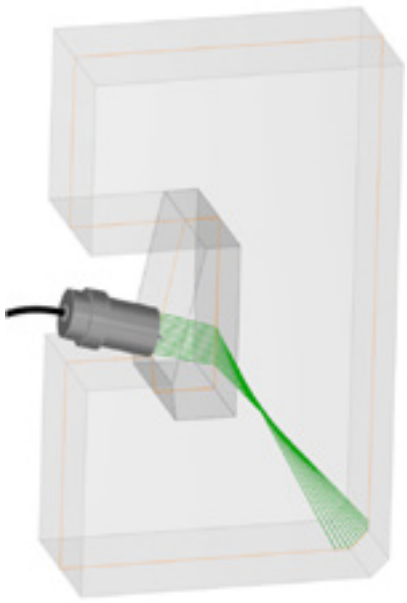

Figure 7: Simulated set-up.

The setting of transducer parameters and position is made in accordance with the testing piece geometry. Before simulating the ultrasonic response of the chamfer, the beam computation is realized to appreciate how ultrasounds propagate in the test piece. As illustrated in Figure 8 the probe is not exactly focused in correspondence of the chamfer but the focal spot is located at a depth of about 25 mm from the impact point. However the beam divergence angle is approximately 7° and the focal spot diameter at the chamfer depth is 13.2 mm. As a result, if the chamfer width is too small compared to the focal spot diameter, the echo reflected back will be not revealed by the probe.

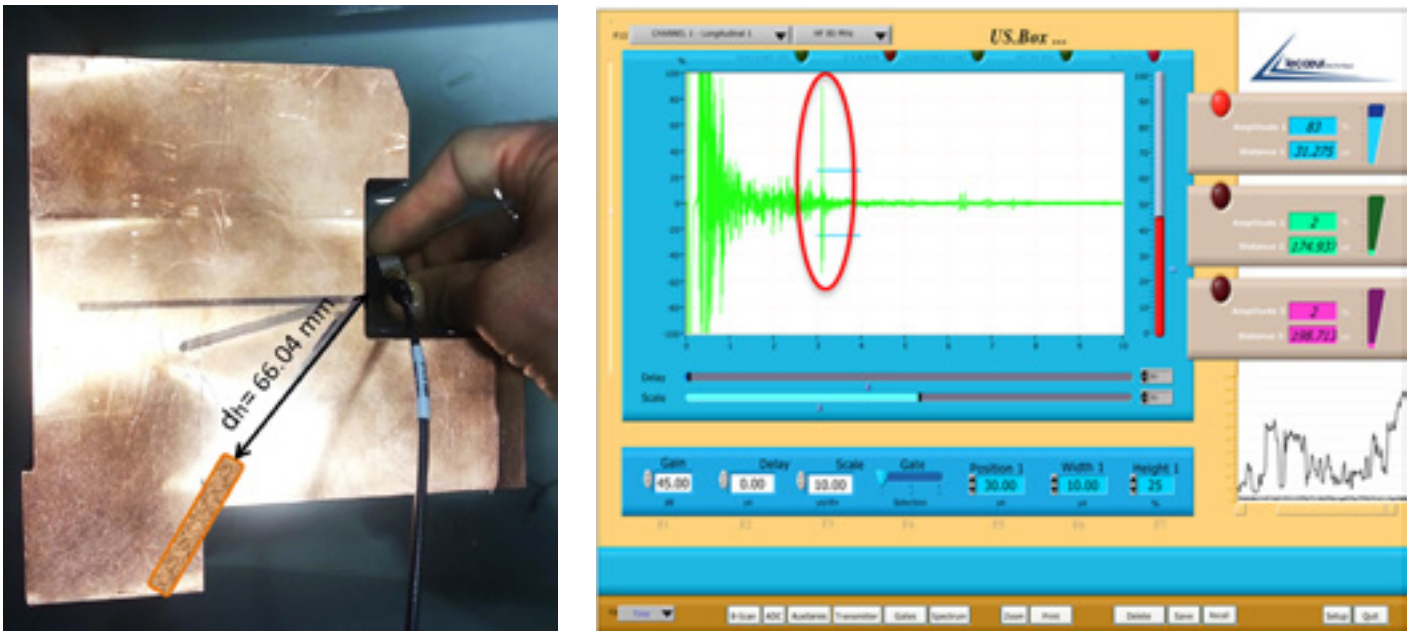

Figure 6: Set-up of the ultrasonic investigation and corresponding A-scan acquisition.

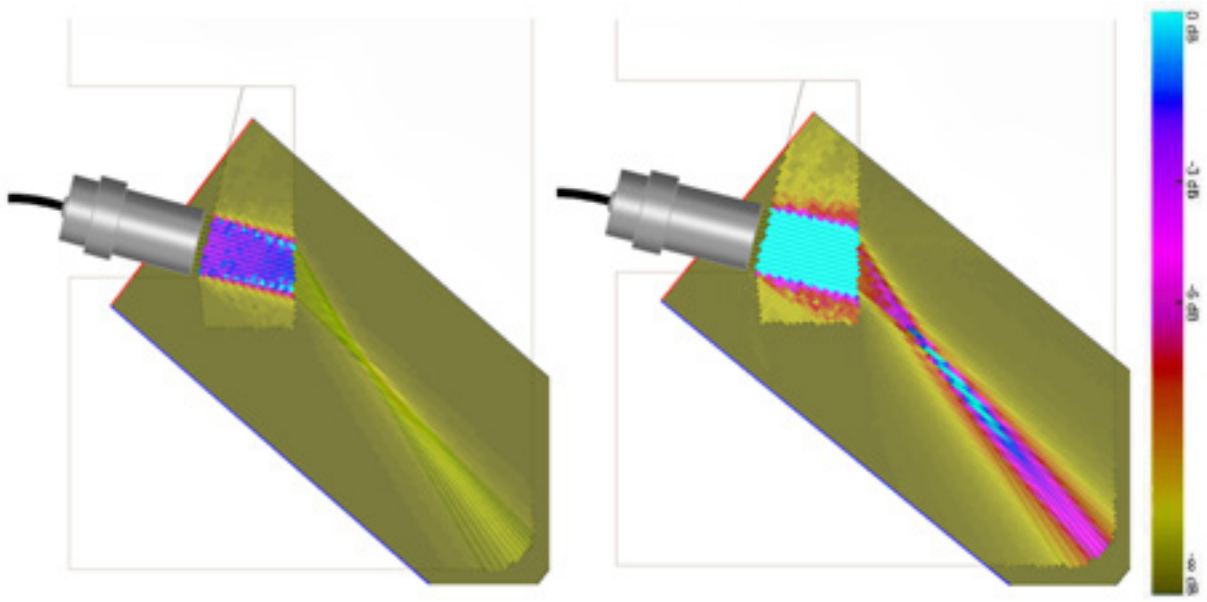

Figure 8: Beam computations for the first simulation set-up. On the left the default beam with 0dB of dynamic, on the right the post processed beam with 15dB of dynamic. Sky blue stands for the highest intensity, yellow for the lowest.

The simulation of the interactions between ultrasonic field and chamfers is implemented by the inspection simulation module. The aim of this study is identifying the best chamfers dimensions in order to do not engrave too much copper. Figure 9 illustrates four chamfers with different widths: 5, 10, 15 and 20 mm respectively. The yellow arc represents the minimum copper thickness of 50 mm to be always kept. As shown, the dimensions of all the chamfers agree with the thickness requirements but smaller they are better it is from the canister integrity point of view.

The results of simulations pointed out the chance to receive good ultrasonic echoes from each one of the chamfers. However the larger the chamfer is, the better signal quality is received. By consequence, a good compromise could be a chamfer around 10 mm wide.

4. Validation on a laboratory prototype

Following the ultrasonic tests on copper samples and CIVA simulations, an identification reading system prototype has been developed. In particular, the validation of the identification method is carried out on a scaled version (¼) of the copper lid where a barcode of cavities and chamfers is realized (Figure 10). The scale is reduced but the geometry of the ultrasonic reading zone is scale 1 compared to the real one meter diameter copper lid.

The chamfers, 50° inclined and 12 mm wide, are arranged around the small lid circumference 22.5° angle spaced (Figure 11). The binary code is created by an alternation of chamfers and cavities, which reflect the ultrasonic beam in different ways. The presence of cavities made easier the production of chamfers in the prototype. However, in the real case, only chamfers will be realized on the lid and ultrasounds will be deflected by unmodified areas. The transducer, rotating around the circumference of the lid, will receive an echo in correspondence of chamfers only.

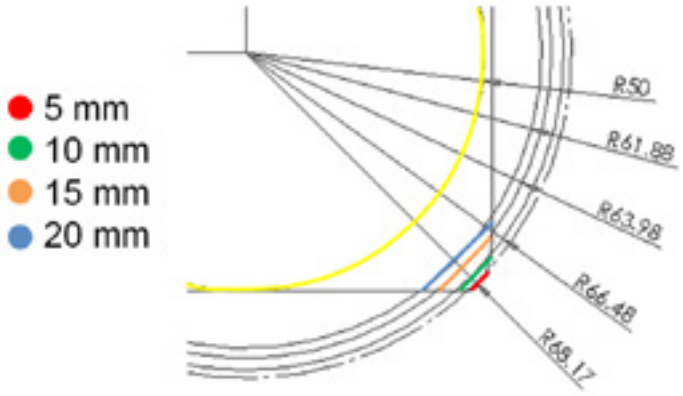

Figure 9: Study of best chamfer dimensions.

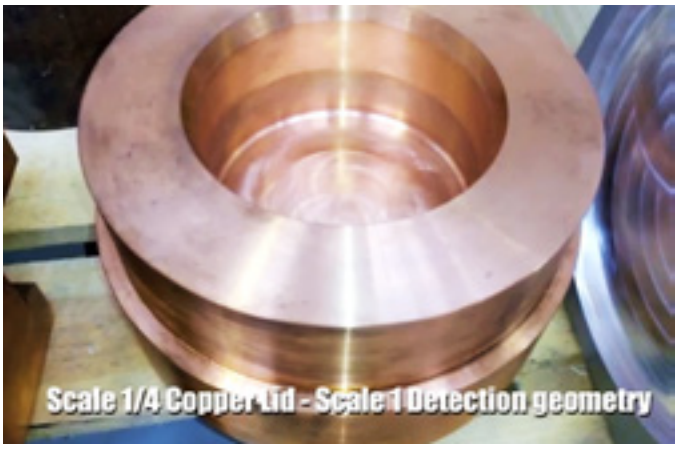

Figure 10: Picture of the small scaled copper lid (¼).

The reading system prototype that hosts the probe is realized by a modified version of reading head used for seals verification (Figure 12). The transducer is installed 14° inclined in order to receive the signal reflected by chamfers according to the Snell's law. The ultrasonic reading of chamfers is realized by an immersion testing in that a bit of water is poured inside the lid. The signal acquired by a 360° rotation of the transducer represents the code realized by chamfers and cavities.

5. Conclusions

Afterwards the result of the experimental testing is compared to a CIVA simulation, reproducing the same set-up of measurement (Figure 13). The simulated echo is evident in both A-scan and B-scan modes and the simulated amplitude ultrasonic response agrees with the experiments. As a result, we can state that the identification method is validated on this small-scaled copper lid, which means that each future copper canister could have a different binary code made of chamfers.

As a result, from simulations and measurements on scaled copper lid, we can state that the identification method proposed is validated and then each future copper canister could have a different binary code made of chamfers. This positive result paves the way for a future identification of all copper canisters, which will be easy, cheap and reliable. When manufacturing the lid, it will be enough to mill or turn a few additional chamfers to deliver on each lid a different binary code, This code will be read at the Encapsulation Plant when the canisters is welded and then on arrival in the Geological Repository.

The implementation of this identification method will contribute to support the CoK of copper canisters with nuclear spent fuel. However identification might not be sufficient to prevent attempts of falsification or duplication of canisters then another approach is necessary to ensure the originality of each container. For this purpose, an authentication method is developed by authors [10].

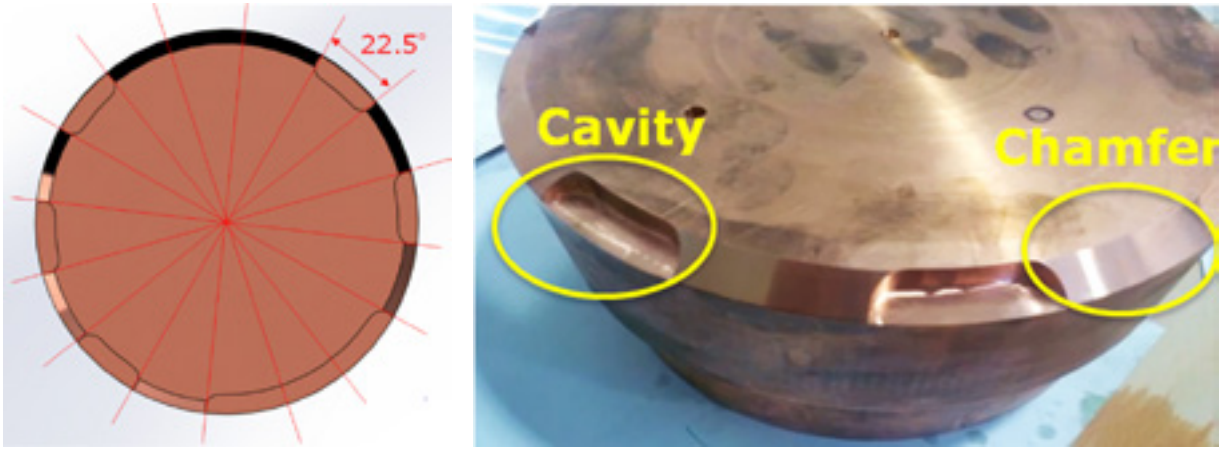

Figure 11: Chamfers arranged around the circumference of the prototype lid 22.5° angle spaced.

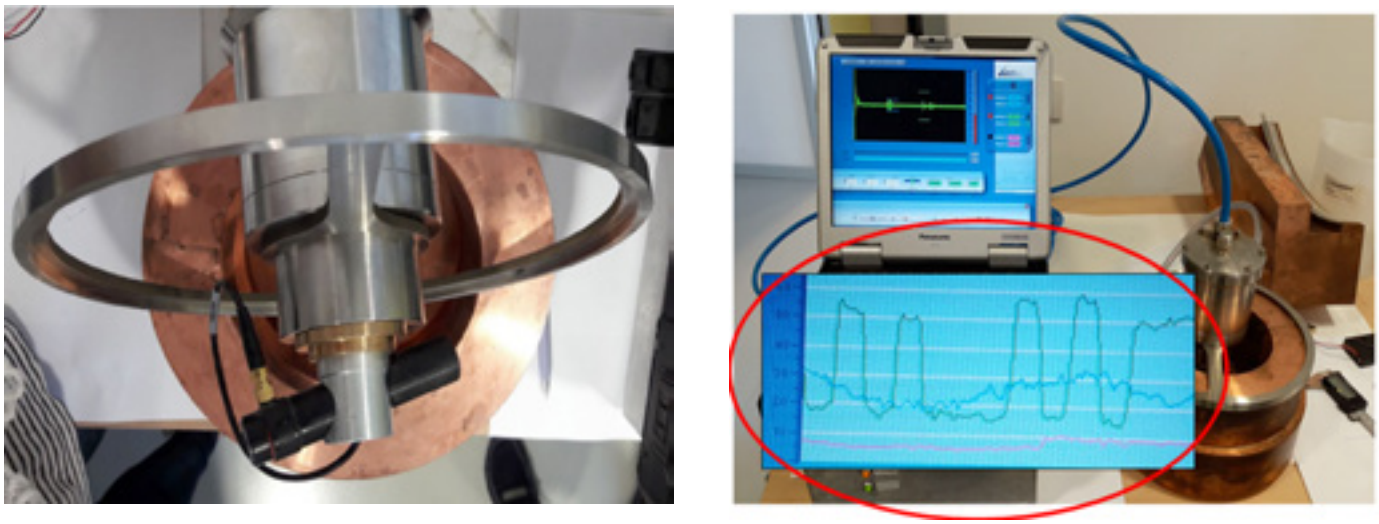

Figure 12: Reading system prototype and binary code acquired by a 360° rotation of the transducer around the small scaled copper lid.

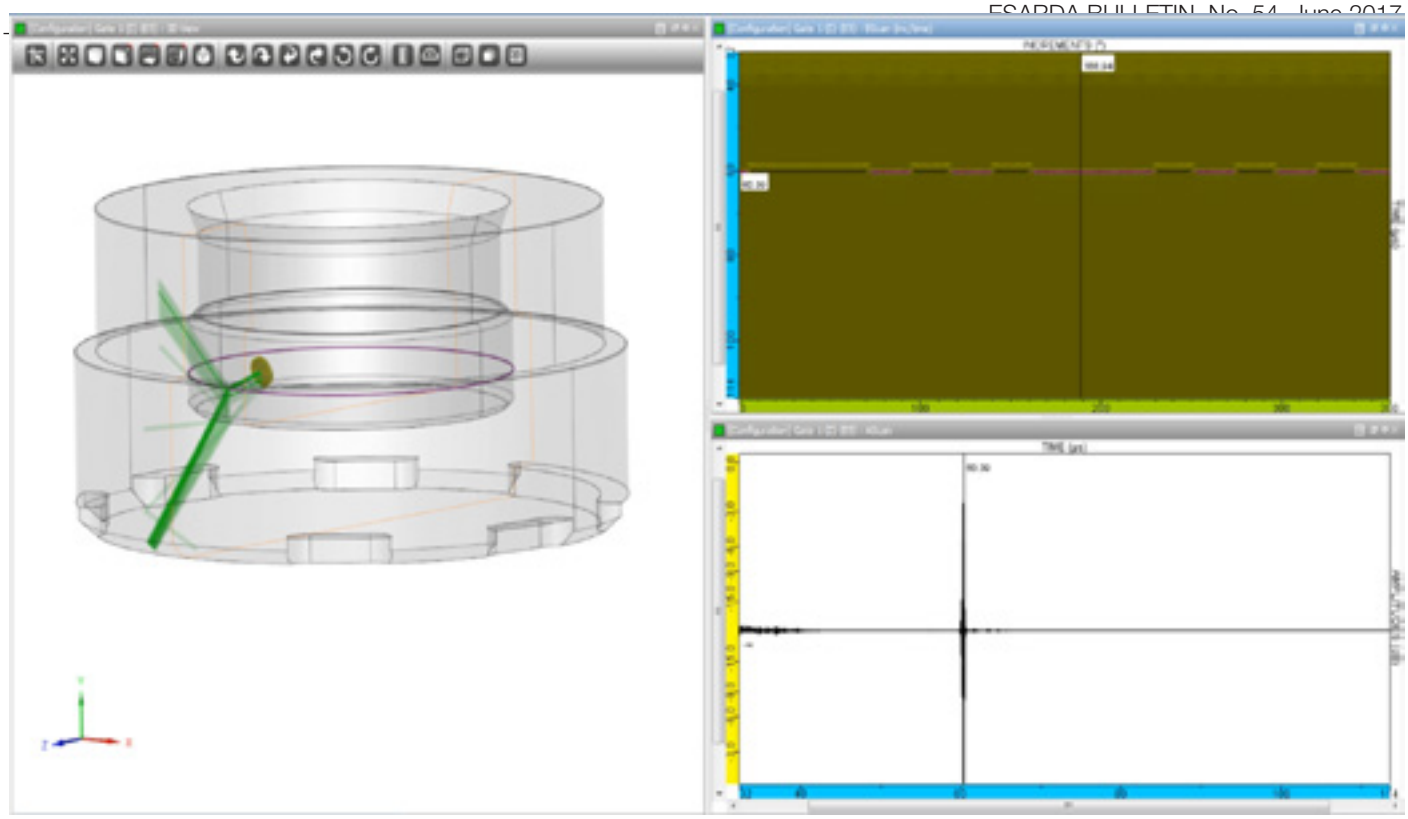

Figure 13: CIVA software simulation of the ultrasonic investigation of the copper lid prototype.

6. References

[1] Chernikova D., Axell K., Nordlund A., Wirdelius H., *Novel passive and active tungsten-based identifiers for maintaining the continuity of knowledge of spent nuclear fuel copper canisters*, journal of Annals of Nuclear Energy, 08/2014

[2] Hildingsson L., Andersson C., *Safeguards aspects Regarding a Geological Repository in Sweden*; Swedish Radiation Safety Authority; Stockholm, Sweden.

[3] Bennett J. C., Day D. M., and Mitchell S. A., *Summary of the CSRI workshop on combinatorial algebraic topology (CAT): Software, applications and algorithms*, Tech. Rep., 2009.

[4] L. O. Brown, S. K. Doorn, and P. B. Merkle, *SERS-active nanoparticles as a barcoding technology for tags and seals*, in Proc. INMM 51st Annual Meeting, Baltimore, MD, USA, 2010, p. 1.

[5] Chernikova D., Axell K., and Nordlund A., *A new approach to environmentally safe unique identification of long-term stored copper canisters,* in Proc. Symp. Int. Safeguards, Vienna, Austria, Oct. 2014, pp. 25, paper CN-220-104.

[6] Demyanuk D., Kroening M., Lider A., Chumak D., and Sednev D., *Intrinsic fingerprints inspection for identification of dry fuel storage casks*, ESARDA Bull., vol. 50, pp. 7986, Dec. 2013.

[7] Capineri L., *Seal fingerprint acquisition device*, Final Technical Report Task 1, Contract JRC/IPR/2015/E.8/0051/NC, February 2016.

[8] Clementi C., Calzolai M., Capineri L., Littmann F., *Ultrasonic identification of copper canisters to be used for long term geological repository*, IEEE International Ultrasonics Symposium 2016, DOI: 10.1109/ULTSYM.2016.7728561, Tours, France, September 2016.

[9] Available in: http://www.extende.com/ultrasonic-testing-with-civa.

[10] Clementi C., Capineri L., Littmann F., *Innovative Method to Authenticate Copper Canisters Used for Spent Nuclear Fuel Based on the Ultrasonic Investigation of the Friction Stir Weld*, IEEE Access, Volume 5, Issue 1, December 2017, DOI: 10.1109/ACCESS.2017.2694878.

International Engagement in Arms Control Verification Using a Systems Approach

M. Dreicer[1], I. Niemeyer[2], G. Stein[3]

[1] Lawrence Livermore National Laboratory, Livermore, USA
[2] Forschungszentrum Jülich, Jülich, Germany
[3] Consultant, Bonn, Germany

Abstract:

A series of exercises and targeted meetings held by the European Safeguards Research and Development Association (ESARDA) Verification Technologies and Methodologies Working Group and the Institute of Nuclear Materials Management (INMM) Nonproliferation and Arms Control Technical Division provided valuable insight into how a systems approach could help identify nonproliferation and arms control verification requirements. International experts from nuclear weapons states and non-nuclear weapons states, with a wide-range of expertise in nuclear safeguards, arms control verification, radiation detection, political science, and defense studies, participated in the discussions. It was demonstrated that with a systems approach, it is possible to design a transparent state-level systems framework to define arms control verification objectives, processes, and timescales for an effective verification regime based on the strategic goals of a treaty, while taking into account restrictions from different security environments. This approach was also shown to be an effective mechanisms for international and technical engagement on such complicated issues. Possible future research activities could include: (1) increased efforts to link the material and weapons sectors of the nuclear weapons complex; (2) further attention on how to satisfy the competing needs for effective verification and protection of national security; (3) greater consideration on how to define the treaty-controlled items so that declarations can be verified effectively; (4) continued testing of a systems approach to analyze the pros and cons of possible verification regimes, to conduct a form of sensitivity analysis and provide feedback and a better understanding of confidence levels that could be achieved; and (5) possible ideas of how to engage in substantive dialogue in a broad international environment, such as the on-going International Partnership for Nuclear Disarmament Verification (IPNDV), while taking into account the range of weapons and verification experience and the need to uphold NPT Article VI.

Keywords: verification, arms control, systems approach

1. Introduction

Establishing a method to systematically identify verification options for nuclear weapons control agreements could significantly contribute to future development of an effectively verifiable treaty [1]. A transparent presentation of a nation's nuclear defense complex would allow for the definition of potential cheating pathways and aid in the development the verification requirements for declarations/data exchanges and an inspection regime. The increased transparency could foster confidence and improve communication between potential stakeholders.

The application of a systems approach, such as the International Atomic Energy Agency's (IAEA) State Level Concept (SLC) used for safeguards implementation [2,3], to arms control agreements could help build a framework for a verification architecture that would be useful for structuring the analysis of options. A series of technical meetings, over the course of 2014 and 2015, were held to determine whether it was possible to design such a framework to achieve high-confidence arms control verification. The key challenges were to:

- leverage the more than 50 years of IAEA verification lessons-learned to build a high-confidence, coherent and comprehensive picture of a State's compliance;
- develop a systems framework that integrated the material and weapons enterprise – utilizing a broad range of information from cooperative technical monitoring data (declared), national technical means (undeclared), open source, and state & international trade controls; and
- facilitate cooperation between nuclear weapons states and non-nuclear weapons states.

International experts from nuclear weapons states (NWS) and non-nuclear weapons states (NNWS), with a wide-range of expertise in, *inter alia*, nuclear safeguards, arms control verification, radiation detection, political science, and defence studies, participated in exercises and discussions to test the feasibility for using a systems approach and identify knowledge gaps. In order to make the effort less abstract, two fictitious countries and a hypothetical treaty were devised and used during two exercises. An effort was made to represent some real-world complexity without making it too difficult, so relatively simple physical models of national nuclear weapons enterprises could be created. By formulating a scenario that incorporated more than the technical aspects of verification, it was possible to look at the state-as-a-whole and consider the additional factors that influence national security decision-making.

Two constraints that were NOT applied during the exercises: (1) the declaration of security-sensitive information was not restricted because a country could make a future decision that it was in its interest to declassify information or share it under conditions deemed advantageous; and (2) the verification requirements focused only on the country to be monitored/verified without consideration of the acceptability of the same requirements being imposed on the verifier. These conditions would not likely to be true in reality but significantly simplified the conditions for the purpose of an exercise.

2. Workshops and Exercises

The initial exercise objective was to determine whether acquisition pathway analysis (APA) could be used to help define the objectives for a future regime by analyzing potential diversion (cheating) pathways and potential treaty verification measures to be applied in a nuclear weapons state. This exercise was hosted by the European Safeguards Research and Development Association (ESARDA) at the Verification Technologies and Methodologies Working Group Meeting, held at the Joint Research Centre, Ispra, Italy, in autumn of 2014 [4]. The model bilateral treaty between the two fictitious nuclear weapons states in the exercise limited the total number of warheads deployed and stockpiled. It was determined that any undeclared warheads above the initially declared total of 1,970 (in the fictitious state that maintained six types of nuclear warheads, deployed across three types of delivery platforms) and any warheads deployed above the maximum of 500 would constitute cheating.

The participants worked to identify cheating pathways and potential verification mechanisms for only one of the states, with a nuclear weapons enterprise including all stages of a nuclear fuel cycle and weaponization facilities (including a stockpile of military fissile material; warhead components production facilities; warhead production, maintenance, and dismantlement facilities; different types of storage depots; military bases; and delivery vehicles).

The exercise allowed the group to explore the parallels between using an acquisition pathway analysis (APA) approach for arms control verification, as compared to IAEA safeguards applications. The general impressions from applying the APA methodology in this new context are outlined in Table 1.

During this first exercise, the group quickly discovered that national security concerns and a country's defence posture greatly influenced the identification of the likely cheating pathways and the type of cheating deemed the most important. To take this additional perspective into account, a second short exercise was held by the Institute of Nuclear Materials Management (INMM) at Lawrence Livermore National Laboratory, during the summer of 2015 [5]. At this

Acquisition Pathway Analysis (Components	IAEA Safeguards	Arms Control Verification
(Physical) Model	Many different facility types and potential pathways	More complex due to consideration of both civilian fuel cycle and military domain (material, production, warhead storage, deployed warheads), larger number of path families
Accountable items	Nuclear Material R&D (Additional Protocol) Well-defined (one Significant Quantity)	**Multiple**, depending on treaty limits – Overall number of warheads – Overall number of delivery systems – Dismantlement
Path attractiveness/path prioritization	Formalized (time, cost, difficulty) Different for each country Path Relevance is clearer	Formalized (time, cost, difficulty, **military significance**) **Non-technical factors** (strategic/ military considerations)
Verification measures	Defined in treaty/agreement	**Undefined unless treaty under consideration**
No of proliferators	Many but state-by-state evaluation	Bi- or multi-lateral – treaty dependent
Application	Establish and prioritize technical objectives	Help define verification measures need for a specific treaty or identify priorities to achieve confidence
Applicability	Formalized, mathematical modelling approach, State level	Basis for systematic, structured analysis, dialogue, State-level or sub-set

Table 1: Comparison of the use of Acquisition Pathway Analysis (APA) in the context of IAEA safeguards and arms control verification.

meeting, a simpler scenario was developed for the two fictitious neighbouring countries and an exercise was structured to take national security objectives into account, while developing a verification regime for each country. Representatives from political science and defence studies, as well as safeguards, arms control experts from nuclear and non-nuclear weapons states were invited to consider a scenario that encompassed the whole nuclear enterprise (e.g. materials, weapons and delivery vehicles). A formal exercise framework (Figure 1) was imposed to focus the participants on national objectives and priorities.

During this second exercise, the model treaty limited the total nuclear forces to the existing levels for 10 years, including strategic and tactical nuclear weapons. All types of delivery systems and the total number of warheads (including deployed and non-deployed) were capped. The development, testing, and deployment of new types of warheads and delivery systems was prohibited.

The same fictitious neighboring countries used in the first exercise were reconfigured to represent different levels of development, capabilities, and populations. The larger state, with a population of 200 million, was a moderately advanced industrialized state with regional military and economic dominance, and ambitions for broader global influence. It had a sophisticated nuclear weapons enterprise consisting of civilian and military nuclear fuel cycles and a total of 322 nuclear warheads. The smaller ascending power, with a population of 100 million, was newly industrialized with a modest conventional force. It recently developed its nuclear capability as a primitive nuclear deterrent. Its nuclear enterprise consisted of both civilian and military nuclear fuel cycle and had possession of a total of 110 warheads.

Detailed nuclear enterprise models were provided to the exercise participants, so that they would spend their time considering verification for key pathways rather than attempting an APA exercise in a short period of time. Figure 2 is the examples for the larger fictitious state (named “Trenzalia”).

The final discussion session was held at the 8th INMM–ESARDA Joint Workshop at Jackson Hole, Wyoming, in October 2015 [6], was not directed towards any specific scenario, but instead focused more on application of systems engineering approaches and the complications that protection of sensitive national security information introduces into the process.

3. Key insights

The group of experts participating in the workshops demonstrated that It is possible (although complicated) to create a state-level systems framework to define objectives, processes, and timescales for an effective verification regime based on the strategic goals of an arms control treaty, while still considering restrictions from different security environments. The use of exercises, with fictitious states and model treaties, effectively focused the discussion on the application of a systems approach beyond IAEA safeguards, and provided the specific security and verification objectives needed to carry out such an assessment. This context directly influenced the assessment of pathway attractiveness, timeliness, detection goals, and level of effective verification. Finding the balance between intrusiveness and transparency was a recurrent theme and the need for flexibility was stressed. The verification technology required to find solutions will have to be treaty-specific, but advance work can be done so that various technical options can be ready for consideration in the context of actual negotiations.

The range of viewpoints brought by nuclear weapons state and non-nuclear weapons state experts illustrated how a diversity can spur new research directions. By mixing safeguards, arms control, international relations and political science experts it was possible to challenge the group to adjust their usual focus and methods to a different domain.

During the first exercise, most the participants brought extensive international safeguards experience, which drove

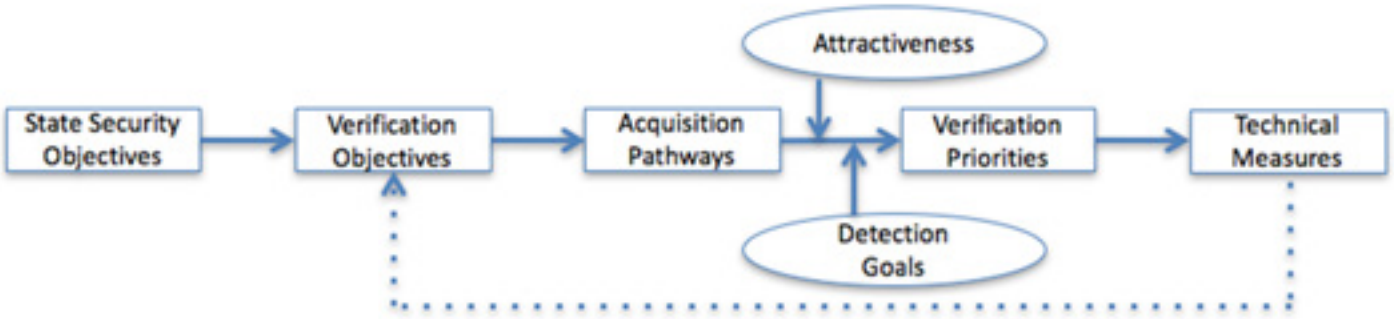

Figure 1: Framework used to explore the usefulness of a systems approach to development of a treaty verification regime.

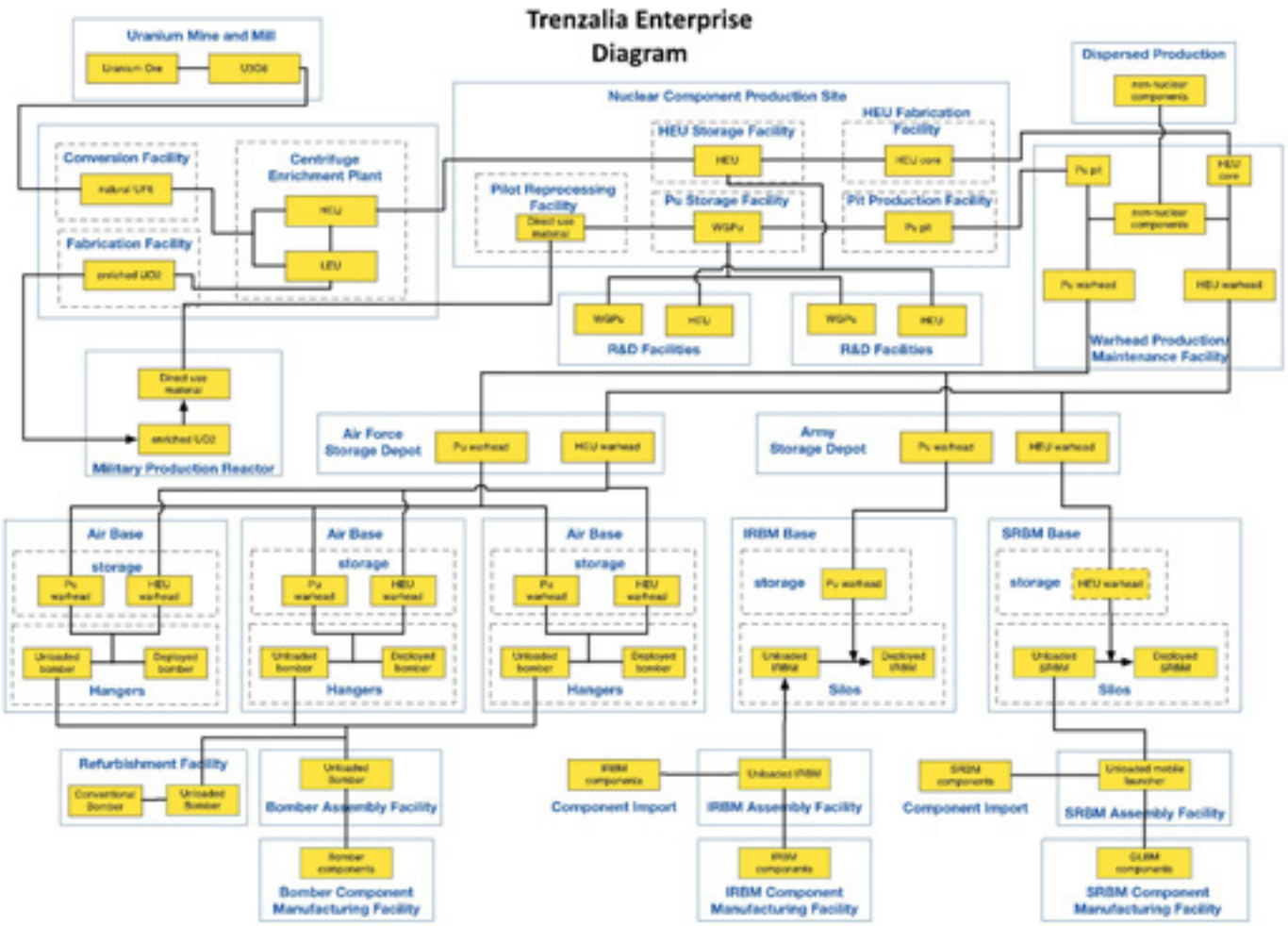

Figure 2: Nuclear enterprise model for the larger power with a moderately advanced industrialized state, with regional military and economic dominance.

the group into detailed of APA analysis with efforts to define attractive pathways and timeliness goals, as is currently done by the IAEA. As the effort bogged down, it was clear that the state-level approach would need to be modified to fit into this different arms control context. In applying safeguards in NNWSs, the goal is to prevent and detect the diversion of clearly defined materials for the whole state, however, in NWSs with a Voluntary Offer, safeguards are applied only in volunteered facilities in the complex, so the whole enterprise has not been considered. In the arms control context, depending on the definition of the treaty accountable items (TAI), the cheating pathways across the whole military and civilian complex must be taken into account, so, it will be necessary to link the materials and weapons sectors of that nation's nuclear weapons complex. So, when planning for the verification of items such as weapons or weapons components, the State's security and defense objectives will have a significant influence.

Defining clear metrics to evaluate pathway "attractiveness" and "timeliness of detection" for possible cheating must also be modified in this context. The metrics used by the IAEA provide a good basis for further work, but new or revised metrics would be dependent on the objectives of the treaty and the security situation of the countries involved. For example, the technical difficulty of cheating might not be the issue if a functioning facility exists but "stealth" or "denial and deception" to hide prohibited activities could be a credible cheating scenario. Maintenance and operational costs could be considered as obstacles to cheating for a particular pathway, however, if those costs were already included in the national budget, it might not have an influence on the attractiveness of exploiting the pathway.

The participants found that the detection goals for diversion or production of significant quantities of TAIs are greatly influenced by the perceived stability in a region. Increased transparency with lower-confidence verification of the exact numbers of TAIs might be acceptable between countries with a trusted stable relationship. However, if each state has only a low number of weapons, accurate verification of numbers and locations of TAIs is likely to be a very strong requirement for treaty ratification.

An effort was made during the second exercise to simulate an environment where national security was highlighted as part of the scenario. The two fictitious states were better defined (so there was no need to create this) and the

participants were split into two groups. Each side went through the process outlined in Figure 1 and determined its own national security and verification objectives. With this additional information, the analysis of the different cheating pathways would be considered in the context of strategic and/or defense advantage. For example, if deterrence were the objective, having an undeclared (and undetected) cache of weapons would not provide much benefit. However, if the objective was to gain a strategic advantage for a certain area of a disputed border, it would be important to detect cheating with respect to the number and locations of weapons.

The imbalance between the two-hypothetical nuclear capable states during the exercise illustrated how the security objectives would drive the focus of a verification regime. The more capable state was interested in maintaining its advantage and therefore required verification that no new capability could be achieved without detection in the smaller state. So, the pathway analysis focused on the material and weapons production sectors of the complex. The less capable state was less concerned about improvements in the neighbor's already powerful nuclear weapons capability than it was about the numbers and location of weapons near its borders, so its focus was on the verification of numbers and locations of the TAIs.

Ultimately, finding the balance between the degree of intrusiveness and allowable transparency must be achieved to provide confidence in treaty compliance. A nation's security requirements and the protection of sensitive information and facilities will constrain the final verification regime. Protection of nuclear weapons knowledge (including materials, facilities and processes) are crucial to national security and are governed by the Nuclear Non-proliferation Treaty (NPT) Article I (if nuclear and non-nuclear weapons states are involved). Using an iterative process, verification measures could be developed to provide sufficient confidence in compliance in a way that would couple existing technical capabilities with operational and security requirements. It could also help point the way for future technology R&D programs.

Greater details on the scenarios and results of the technical discussions can be found in an upcoming book [7].

4. Future Research

Further development is needed but the authors believe that a clear and transparent framework provides an effective mechanism for international and technical engagement on these complicated issues. In particular, continued research can be done to advance implementation of an acquisition pathway analysis methodology in nuclear weapons states. Increased efforts to link the material and weapons sectors of the nuclear weapons complex are essential. More consideration should be given on definition of treaty-controlled items and the "significant quantity" of these items. Further work to refine metrics for pathway attractiveness, detection probabilities, and detection goals will depend on the items to be verified, related pathways and the security objectives of a state.

Continued testing of a systems approach and validating the framework would help to analyze the pros and cons of possible verification regimes by allowing for sensitivity analysis, to better understand high priority pathways and the confidence levels that non-compliance would be detected. Further work would also help bound the potential for using modeling and simulation to evaluate effective verification options and the potential impacts on the design of future declarations.

A clear benefit from the series of ESARDA/INMM expert meetings was the development of a cadre of international technical experts gaining familiarity and experience with these issues. The majority of the activity was carried out during professional society meetings rather than directly-funded research programs. Based on the positive experience of working across a diverse community in an international environment, continuing substantive dialogue, in venues such as the on-going International Partnership for Nuclear Disarmament Verification (IPNDV), should be encouraged. The inclusion of broader international technical expertise (outside of the NWS) creates opportunities for innovation. The framework described in this paper, could provide a structure to guide complicated and sensitive discussions that facilitates engagement across a broad range of weapons and verification expertise in support Article VI of the NPT. It also has the potential for structuring regional dialogue on sensitive issues.

5. Acknowledgements

The authors would like to thank ESARDA and INMM for hosting the technical meetings and all those who participated and shared their expertise and idea. The authors would like to acknowledge Cliff Chen (Lawrence Livermore National Laboratory) and Keir Allen (Atomic Weapons Establishment) for their significant contributions to this effort.

6. Disclaimer

The views in this chapter do not represent the views of any governments, institutions or professional organizations. This work performed under the auspices of U.S. Department of Energy by Lawrence Livermore National Laboratory under contract DE-AC52-07NA27344. LLNL-CONF-731157, LLNL-PRES-731448.

7. References

[1] Dreicer M, Stein G; Applicability of Nonproliferation Tools and Concepts to Future Arms Control; ESARDA Bulletin No. 49:95-99; 2013.

[2] Cooley J; The State-level Approach to International Safeguards; Institute of Nuclear Materials Management Conference Proceedings; 2009.

[3] Renis T, de Villiers VZ, Radecki Z, Vela Espinoza EW; Development and updating of State-level safeguards approaches: Experience and lessons learned. Proceedings ESARDA Symposium 2017, Düsseldorf, Germany; 2017.

[4] Allen K, Dreicer M, Chen CD, Niemeyer I, Listner C, Stein G; Systems approach to arms control verification; ESARDA Bulletin No. 53:83-91; 2015.

[5] Chen CD, Dreicer M, Proznitz P, Benz J, Duckworth L; Systems Concept for Arms Control Verification; https://cgsr.llnl.gov/content/assets/docs/arms_control_verification_report.pdf; 2015.

[6] INMM/ESARDA Working Group 2 Report – Arms Control, Jackson Hole Wyoming; http://www.inmm.org/AM/Template.cfm?Section=8th_INMM_ESARDA_Workshop&Template=/CM/ContentDisplay.cfm&ContentID=6633; 2015.

[7] Niemeyer I, Dreicer M, Stein G, eds.; Nuclear Nonproliferation and Arms Control Verification. Innovative Systems Concepts; Springer (in publication) 2017.

Field Trial of the Enhanced Data Authentication System (EDAS)

M. Thomas, R. Hymel, G. Baldwin
Global Security Programs, Sandia National Laboratories
P.O. Box 5800
Albuquerque, NM 87185, USA
Email: mthomas@sandia.gov; gtbaldw@sandia.gov; rwhymel@sandia.gov
A. Smejkal, R. Linnebach
Nuclear Safeguards Directorate
European Commission Directorate-General for Energy
Luxembourg
andreas.smejkal@ec.europa.eu; ralf.linnebach@ec.europa.eu

Abstract:

The Enhanced Data Authentication System (EDAS) is a means to securely branch information from an existing measurement system or data stream to a secondary observer. In an international nuclear safeguards context, the EDAS connects to operator instrumentation, and provides a cryptographically secure copy of the information for a safeguards inspectorate. This novel capability could be a complement to inspector-owned safeguards instrumentation, offering context that is valuable for anomaly resolution and contingency.

Sandia National Laboratories gathered operator and inspector requirements, and designed, developed, and fabricated prototype EDAS software and hardware. In partnership with Euratom, we performed an extended EDAS field trial at the Westinghouse Springfields nuclear fuel manufacturing facility in the United Kingdom. We inserted EDAS prototypes in operator instrumentation lines for a barcode scanner and weight scale at a portal where UF_6 cylinders enter and exit the facility. The goal of the field trial was to demonstrate the utility of secure branching of operator instrumentation for nuclear safeguards, identify any unforeseen implementation and application issues, and confirm whether the approach is compatible with operator concerns and constraints.

During the field trial, the data streams were collected for nine months, and the EDASs branched 698 barcode and 663 weight scale events. Our analysis found that both EDAS units accurately branched 100% of the data that flowed through the instrumentation lines when we compared them to the recorded operator data. With multiple deployed EDASs we found that it is possible to correlate the branched data and create a more holistic narrative of facility activities. Euratom reported the field trial as a full success due to the continuous, correct, and secure branching of safeguards relevant data. At the same time, the operator is satisfied that EDAS did not interfere with plant operations in any way. The success of this field trial is an important step toward illustrating the potential and utility of EDAS as a safeguards tool.

Keywords: secure branching; data collection, field trial; operator instrumentation; unattended monitoring; minimally intrusive

1. Introduction

EDAS is a means to securely branch information from an existing measurement system or data stream to a secondary observer, as illustrated in Figure 1. An EDAS junction box creates a “branch” of the main communication path data and transmits the replicated data to the secondary observer from a tap-off point close to the measurement system sensor. In an international nuclear safeguards deployment, the primary observer represents the facility operator system while the secondary observer is the safeguards inspectorate system. The EDAS junction box connects to the output of existing operator instrumentation and sends a copy of the information to the safeguards inspectorate EDAS computer. The junction box cryptographically secures the branched data using encryption for confidentiality and authentication to provide data integrity. This branching capability could be a complement to inspector-owned safeguards instrumentation, offering context that is valuable for anomaly resolution and contingency.

The EDAS development project is a collaborative effort between the U.S. DOE Sandia National Laboratories in the United States, the European Commission Directorate General for Energy (DG-ENER) in Luxembourg, and the European Commission Joint Research Centre (JRC) in Italy. The original project began in May 2008 under the auspices of a DOE-Euratom agreement[1] as Action Sheet (AS) 32,

[1] “Agreement between the European Atomic Energy Community represented by the Commission of the European Communities and the United States Department of Energy in the field of Nuclear Material Safeguards Research and Development,” 6 Jan 1995. That agreement was superseded in November 2010 with one of expanded scope, “Agreement between the European Atomic Energy Community represented by the European Commission and the United States Department of Energy in the field of Nuclear Material Safeguards and Security Research and Development.”

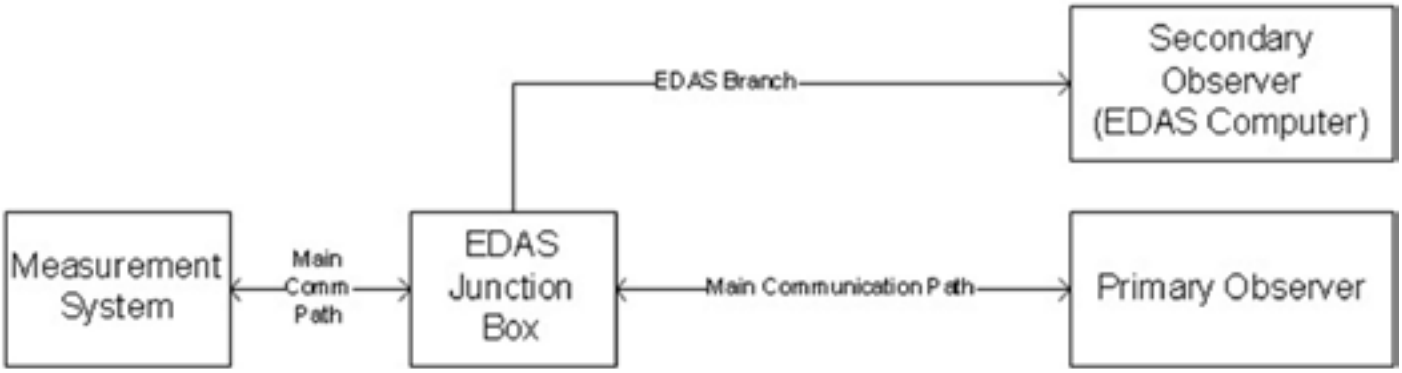

Figure 1: EDAS Branching Diagram

"Enhanced Data Authenticity via an Electronics Platform for the Secure Transmission and Recording of Sensors." That work focused on the inspector requirements for secure branching. The project team designed, built and demonstrated an initial prototype of EDAS to key stakeholders [1]. The project continued under AS 41, "Application of the Enhanced Data Authentication System to Operator Instrumentation." In this second phase, we adapted the concept to meet operator requirements as well; that is, to ensure that EDAS is non-interfering to facility operations, fail-safe, and conforms to instrumentation interface standards [2, 3]. Sandia incorporated the combined inspector and operator requirements into redesigned hardware and software for EDAS [4]. The new prototypes have been tested extensively, culminating in an extended field trial at an operational nuclear facility subject to Euratom safeguards [5].

The goal of the EDAS field trial was to demonstrate the utility of secure branching of operator instrumentation for nuclear safeguards, identify any unforeseen implementation and application issues, and confirm whether the approach is compatible with operator concerns and constraints. Euratom arranged to conduct the field trial at the Westinghouse Springfields nuclear fuel manufacturing facility in Lancashire, United Kingdom. We inserted EDAS junction boxes in two operator instrumentation lines, a barcode scanner and a weight scale, at a portal where Model 30B UF_6 cylinders enter (full) and exit (empty) the facility. Data collection occurred for approximately nine months, from March through November 2015. The branched data transmitted continuously to an inspector computer and was collected by the Euratom Remote Acquisition of Data and Review (RADAR) [6] data acquisition software for subsequent analysis by inspectors.

2. EDAS Prototypes

Sandia designed, developed, and manufactured prototype EDAS software and hardware to meet both operator and inspector requirements, incorporating commercial off-the-shelf (COTS) and custom hardware, as well as open source and custom software. The EDAS junction box features a modular design, which separates its general branching functionality from that which is specific to a particular instrumentation interface. The junction box prototypes interface to the operator main communication path via standard 9-pin RS232 serial, which matches the field trial barcode scanner and weight scale interfaces. The branched data is sent from the junction box to the inspector (EDAS computer) via a RJ45 Ethernet interface and, when employing network extenders, there is no practical distance limit, allowing for a variety of installation configurations. Figure 2 is a picture of the EDAS junction box, which is approximately 9.5 x 6.3 x 4.0 cm. Power is supplied either via a barrel adapter or USB.

The EDAS junction box employs a low-cost commercial BeagleBone™ Black embedded processor and a custom accessory board, called a "cape," that is mounted on top of the BeagleBone™ Black board. The Sandia-developed cape is interface-specific; it performs the branching function for both the "transmit" and "receive" signals in the RS-232 serial specification. Figure 3 is a picture of the EDAS cape inside the case. It links the primary instrumentation signal path between the in and out serial connectors, and includes sensing electronics to generate an isolated copy of the signal. The isolation acts as a diode and

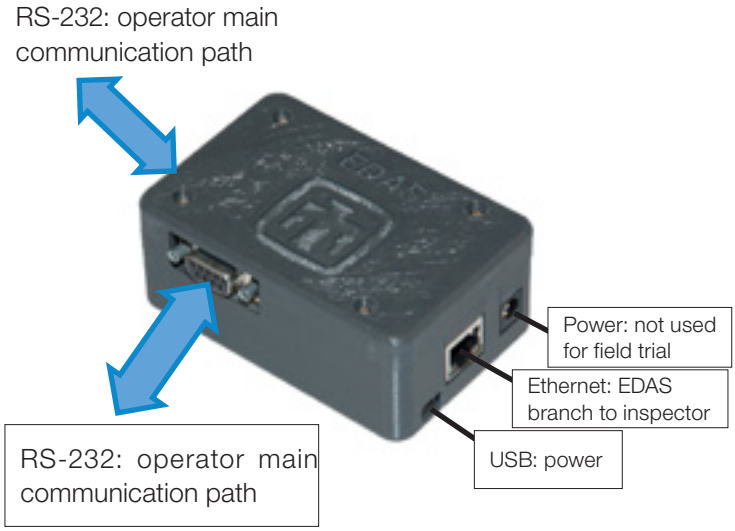

Figure 2: The EDAS Junction Box

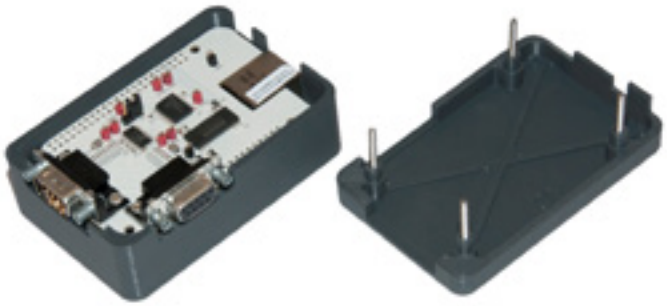

Figure 3: EDAS Cape (the white-colored board with mounted electronics)

prevents any information from the inspector being introduced onto the operator main communication path. DB-9 serial connectors on the cape use different genders, so that the primary instrumentation cables could be disconnected from the EDAS junction box and mated directly to each other, should the operator have a reason to bypass the EDAS entirely.

The EDAS uses a streamlined version of Linux, created for embedded systems, called Yocto. We eliminated any functionality from the operating system not needed by EDAS by removing software functions that may consume processor and memory resources. We also made the EDAS junction box more secure by disabling access to ports not used for normal operation (e.g., FTP).

The custom firmware directs the embedded processor to collect and buffer all branched data from the main instrumentation signal path. The data are then compiled into discrete packets; digitally signed using a public key cryptographic algorithm; encrypted; and finally pushed over an Ethernet connection to the inspector computer. The firmware also periodically creates and sends state of health "heartbeat" messages to confirm that EDAS is operating normally. The inspector computer runs custom software that receives and decrypts the EDAS packets, verifies their authenticity, and writes the data to an output file for post-processing and analysis.

3. RADAR Integration

The EDAS junction box has no *a priori* understanding of, or expectation for, the meaning of the data it branches. Rather, it forms data into packets based on preset configuration settings and sends each via TCP/IP over Ethernet to the inspector computer. The EDAS inspector computer software receives all EDAS packets from the EDAS branch and writes these to a log file. In order for these EDAS packets to be interpreted equivalently for the facility operator and inspector, we used the Remote Acquisition of Data and Review (RADAR) software package.

RADAR, developed by Euratom, is a modular and standardized software platform for data acquisition from different sensors. Typical sensors (e.g., shift registers or multi-channel analyzers) are configured and operated by RADAR Data Acquisition Modules (DAM). In order to use EDAS field trail data in the RADAR framework, EDAS DAMs were developed for both the field trial barcode scanner and weight scale. The EDAS DAMs are fully integrated into the RADAR system like other, already existing, DAMs.

Euratom configured and activated the EDAS modules to derive meaning from the barcode and weight scale branched bytes so that they are identically interpretable for the inspector and the facility operator. During the field trial, the inspector computer continually ran the EDAS RADAR software modules, which scanned the EDAS log files for new records. The modules converted the branched signals into event records containing a time stamp, the scanned barcode ID or weight measurement, and cryptographic authentication status.

The development of the RADAR EDAS modules represents an important phase of the collaboration between Euratom and Sandia. Sandia shipped several EDAS junction boxes and software to Euratom headquarters in Luxembourg where EDAS RADAR software modules were developed and tested in a test bed using representative field trial equipment and simulators. EDAS integration with RADAR greatly facilitated our ability to analyze data from the field trial because much of the analysis involved the comparison of operator records to the interpreted barcode and weight scale records in the RADAR files. With development of the field trial RADAR EDAS modules complete, it would be simple to develop new EDAS modules for RADAR to support branching signals from other types of instrumentation.

A further benefit is that RADAR converts EDAS data to a standard format that can be analyzed by an automated review and analysis tool, such as the integrated Review & Analysis Platform (iRAP). iRAP, originally developed by Euratom, has been made available to the International Atomic Energy Agency (IAEA), and is now the subject of a software collaboration between both organizations. Under a license agreement between the IAEA and EURATOM, iRAP will be developed jointly towards an "all-in-one review platform." [7]

4. Field Trial Setup

The field trial took place at a UF_6 cylinder portal at the Springfields nuclear fuel manufacturing facility. During operations, full Model 30B cylinders enter the portal staging area one at a time and are placed on a scale. Per the facility procedure, an operator must scan the cylinder identification number with a barcode scanner and measure its weight. These two operations can happen in either order. To measure a weight, an operator must enter a command into the operator system, which triggers three consecutive weight commands. The operator weight scale control unit

subsequently sends three successive weight measurements, in kilograms, to the operator system. The operator system then averages these three weights, which becomes the final weight measurement record. Both the barcode scan and weight scale measurements are recorded in an operator log file. The cylinder then enters the facility for processing. After processing, the cylinder reenters the portal and its identification number and weight measurement are recorded. The empty cylinder then leaves the facility. For the field trial, EDAS junction boxes formed branch points in the barcode scanner and weight scale communication lines.

In early March 2015, the Sandia EDAS developers, Euratom inspectors, and operator representatives met at the Springfields facility to install the EDAS system and commence the field trial. The Sandia team installed, configured, and initialized the EDAS prototypes. Euratom provided the inspector computer to acquire the field trial data, and configured and activated the EDAS inspector computer software and RADAR EDAS DAMs. The Springfields operator installed a lockable custom cabinet, pictured in Figure 4, to house both the EDAS junction boxes and the inspector computer. The cabinet was fitted with feedthrough connectors for both signal and power lines.

The EDAS was configured for a standard 9-pin RS-232 interface for the barcode scanner, but we discovered during the installation visit that the installed barcode scanner used a pen interface. The operator promptly replaced that barcode scanner with a new one that uses a 25-pin interface. To obtain the correct signal on the EDAS, the operator installed a Datalogic CBX800 adapter, shown in Figure 5, in the signal line between the barcode scanner and operator system. It is important to note that the Datalogic adapter split the barcode signal, with one portion going to the operator system and the other to the barcode EDAS. In other words, the EDAS received data that was already branched by the CBX800 adapter.

Figure 4: EDAS Cabinet provided by the Operator

The operator classified the continuous and direct output from the scale as part of the facility safety system; branching here would have required a prohibitively long and uncertain approval process. Therefore, the EDAS branch point for the weight scale was installed at the output of the control unit for the scale, not at the scale itself. The control unit was a Mettler Toledo model IND690 weighing terminal. EDAS, therefore, did not sense weight continuously. Both the operator and EDAS received weight data only when the facility instrumentation control system triggered the IND690 to send a reading.

Figure 6 shows the installed EDAS junction boxes and the Euratom inspector computer. The inspector computer was a ruggedized Windows computer with several redundant

Figure 5: Datalogic CBX800 adapter that split the barcode scanner communication path

Figure 6: EDAS System installed in operator cabinet, showing the Euratom computer (left), network switch (middle), and two EDAS branching units (right)

components for increased reliability. A switch directed EDAS network traffic between the EDAS junction boxes and inspector computer. We verified the successful branching of several facility barcode and weight events over several days before the system ran unattended for the duration of the field trial.

5. Field Trial Analysis

The field trial collected data for nine months, between March 5, 2015 and November 26, 2015. EDAS data were collected by RADAR on the installed inspector computer, and Euratom inspectors retrieved the complete datasets on November 26 when the field trial system was decommissioned. Euratom obtained a separate transcript from the Springfields operator of timestamped system logs of barcode and weight scale data over the same period. Sandia analyzed these data using custom analysis software to compare and correlate the data.

In order to gauge the success of the EDAS field trial against our original goals, we posed the following questions:

- Did each EDAS operate continuously for the field trial duration?
- Do the EDAS and operator barcode scanner and weight datasets match? Did the EDAS miss any events with respect to the operator? Did the EDAS capture any events not contained in the operator logs?
- For every barcode scan is there a corresponding weight measurement, and does every weight measurement have an associated barcode scan?
- Are all weight scale data preceded by associated “send weight” commands? Conversely, is any command missing a weight scale response?
- Were other anomalies discovered?

The field trial analysis specifically addresses these questions, and the following sections report the results of the analysis. Additional interpretation is deferred to the Discussion section.

5.1 Analysis Methodology

We wrote software to automate the analysis of the field trial data. The software was coded to apply several rules and assumptions that define the continuous operation of EDAS, correct format of a record, and tolerances for expected differences between the EDAS and operator system data. The following are the rules and assumptions we used for the field trial analysis:

- The barcode scanner EDAS junction box will hereafter be referred to as “EDAS-B.”
- The weight scale EDAS junction box will hereafter be referred to as “EDAS-W.”
- A barcode ID is an alphanumeric string.
- A weight sent by the Mettler-Toledo IND690 is measured in kilograms and has two digits of precision after the decimal point.
- A weight scale command is considered valid if it matches the Mettler-Toledo IND690 control sequence: S<CR><LF><ACK>. Note that any variations are flagged as anomalies.
- Packets sent from the EDAS junction box to the inspector computer are digitally signed and encrypted. For a received packet to be classified as authentic, the packet must correctly decrypt and authenticate.
- To prove that the EDAS junction boxes were continuously operating, we configured them to periodically send heartbeat messages, and expected to observe contiguous heartbeat messages at a rate of at least once every two minutes.
- For comparing the EDAS-B and operator barcode data, a match is recorded when the values are identical AND occur within four minutes of each other.
- For comparing the EDAS-W and operator weight scale data, a match is recorded if the values vary by less than 0.1 kg AND occur within four minutes of each other. Note that slight precision differences in measurement values are expected since three weight values are averaged independently by the operator and the RADAR EDAS weight scale module on the inspector computer.
- Per the operator’s cylinder entry/exit procedure, we expect the barcode scan and weight scale measurements for a cylinder to occur within one minute of each other.
- An operator weight command to the IND690 (weight scale terminal) immediately and automatically triggers a weight measurement. We create an association if a weight command precedes a weight measurement AND the timestamps are within two seconds of each other. Note that this analysis is only possible with EDAS data because the operator does not keep a record of commands in the operator system logs.

Note that all selected time thresholds to compare values are heuristics selected by the authors. These values were selected via analysis of the data as they afforded enough flexibility to identify all true matches. At the same time, the chosen thresholds had a tight enough tolerance to not conflate incorrect events. In the case of EDAS heartbeat messages, we selected a two-minute threshold as sufficiently frequent to prove the junction boxes were continuously operating. When comparing EDAS junction box and operator barcode or weight scale data, we selected a four-minute threshold to account for observed clock drift over the course of the field trial between the operator and EDAS systems. This value allowed our analysis to identify all true positives while eliminating the possibility of incorrect matches since containers are processed at the portal at a much slower rate.

5.2 Test for Continuous EDAS Operation

Both the EDAS-B and EDAS-W units operated continuously for the nine-month duration of the field trial. To assess continuous operation, we first checked that there were no interruptions in heartbeat messages from either EDAS junction box. There was no time during the field trial where more than two minutes passed between these messages. We also searched the inspector computer log files for evidence of a network disconnect between an EDAS junction box and the inspector computer. The only recorded instance of establishing a network connection was the initial connection at the beginning of the field trial.

5.3 Test for EDAS and Operator Dataset Equality

Our analysis software compared the EDAS measurements collected by RADAR with the operator system data files to check whether either of the EDAS junction boxes missed any records captured by the operator system. A match of a barcode or weight is determined according to rules set in the Analysis Methodology section. A discrepancy, or difference, is any deviation from the above conditions, or any missing or additional EDAS data with respect to the operator system. Table 1 illustrates the total number of barcode and weight data points analyzed for the field trial.

Measurement Type	Operator	Operator Manual Bypass	EDAS
Barcode Scanner	705	7	698
Weight Scale	664	1	663

Table 1: Total Barcode and Weight Events. Some operator barcode and weight data were manually entered into the system, effectively bypassing the EDAS.

EDAS-B did not branch seven events of the 705 found in the operator log files over the course of the field trial. These events transpired on four different occasions spread over the field trial duration. After speaking with the facility operator, we determined that these seven anomalous events were manually entered into the operator system because the cylinder label was damaged, and was unreadable by the barcode scanner. In other words, the operator bypassed EDAS-B since the barcode scanner was not used for these seven events. Of the 664 operator weight events, we identified one additional empty weight measurement of 0.0 kg in the operator log file that does not show up in the EDAS-W data. The operator determined that this anomalous weight entry is an artifact created by their control system when initially powering the IND690, and is not generated by the scale itself. Since this data did not derive from the scale or travel along the weight scale instrumentation line, it was not branched by EDAS-W. In summary, both EDAS-B and EDAS-W correctly branched 100% of events that passed through each instrumentation line from the measurement device.

We also compared the EDAS measurements collected by RADAR with the operator system data files to check whether either EDAS-B or EDAS-W observed any measurements not recorded by the operator system. Our analysis found that of the 698 and 663 events recorded by each junction box, there was a 100% match with the operator files, indicating that each EDAS junction box did not branch any extra events not reported by the operator.

5.4 Test for Barcode / Weight Correlation

Since each cylinder must have both its barcode scanned and weight measured when entering or exiting, we looked for correlation between these events captured by EDAS-B and EDAS-W. Of the 698 barcode and 663 weight events, 654 of them correlated. This leaves 44 bar code scans that did not have associated weight data. Further analysis discovered several reasons for these discrepancies: (1) operator scanning a test pattern rather than a cylinder barcode, (2) inadvertently scanning the same barcode identification number multiple times in rapid succession, or (3) accidentally scanning a barcode on a UF_6 cylinder intended for autoclave processing (i.e., not the portal). Note that for this last case, a second barcode scanner, connected to a different operator system, scans the cylinder identification number for subsequent processing in the autoclave. There were nine instances of weight data without corresponding barcode scans. As discussed earlier, many of these discrepancies are attributable to the seven barcode identification numbers that were manually entered by the operator, and not branched by EDAS-B. The remainder consist of weights that are outside the range expected for a UF_6 cylinder in that they are less than the typical tare weight. The operator confirmed that these extra weight events were for scale testing purposes.

We also analyzed the operator records for correlation between barcode and weight data events, and found the discrepancies to be the same as the EDAS data. There were 705 barcode and 664 weight events from the operator record. We would initially expect the discrepancies between the operator and EDAS records to match. However, when backing out the seven manual barcode scan entries, where EDAS-B was bypassed, and the single empty weight entry, where EDAS-W was bypassed, we measure 698 barcode and 663 weight events, and found that 654 of them correlated, identical to the EDAS data.

5.5 Test for Weight Command / Data Correlation

Of the 663 weight readings branched by EDAS-W, 100% were correlated to a weight command that immediately preceded the event. We did not perform this test on the operator data since commands are not included in their log files. Also note that this analysis does not apply to the barcode scanner data, since a human operator must squeeze the barcode scanner trigger to command the device; so, there is no command signal for EDAS-W to branch.

5.6 Test for Other Anomalies

During field trial setup, it became clear that the EDAS junction box electronics do not keep time well. The BeagleBone™ Black has an inaccurate system clock. For this reason, we relied instead on the inspector computer time: the inspector computer affixes its own timestamp to each EDAS message it receives. However, even using this timestamp in lieu of the EDAS timestamp was not without issues. We observed a dozen occasions when the inspector computer timestamps on successive EDAS heartbeat messages were spaced only a few seconds apart, rather than the configured separation of once per minute. We believe that these heartbeat messages, sent by the EDAS junction box, were queued while the inspector computer was otherwise busy and unable to process them, causing a backlog of messages. At a later point, the inspector computer processed them in rapid succession, resulting in a cluster of closely spaced timestamps for these messages. Analyzing the EDAS timestamps, even though incorrect in an absolute sense, revealed they were sufficiently accurate on smaller timescales to confirm that the heartbeat messages were generated at the expected frequency.

Another issue was the assignment of the local time zone to the timestamped EDAS data packets. Two daylight savings transitions occurred during the course of the field trial, causing timestamps to suddenly skip or move backwards an hour. An appropriate time correction factor was applied to the analysis software to rectify this issue for data analysis.

6. Discussion

The field trial analysis has shown that EDAS and the inspector computer operated continuously and correctly over the nine-month duration of the field trial, showing that EDAS can run unattended in an operational nuclear facility for long periods of time. There was never an interruption in heartbeat messages in either EDAS-B or EDAS-W, and no network connectivity issues or errors occurred in the log files. In addition, the data were secure in that they were free of decryption and authentication errors, which satisfies the inspector requirements for the data being both confidential and trustworthy, respectively, from the branch point forward. Further, it is noteworthy that the RADAR EDAS modules ran continually for the entire field trial without any data interpretation issues or interruption.

EDAS correctly branched 698 barcode scanner and 663 weight scale events over the course of the field trial without interfering with the operator system. It is notable that neither EDAS junction box recorded any events that were absent from the operator system. Also, neither EDAS missed any unexplained barcode or weight scale events when compared to the operator record. While the operator did manually bypass EDAS-B several times, both junction boxes branched 100% of the data that flowed through each for the entire field trial duration. The cases where the operator manually bypassed EDAS-B, due to damaged cylinder labels, highlights a tenet of the EDAS non-interference requirement and illustrates one reason a facility operator might bypass a junction box, without much affecting the overall safeguards narrative.

With multiple EDASs installed in a facility, there are other first-order analyses that can correlate data to look for consistency. When a UF_6 cylinder enters or exits the facility, one would expect the cylinder to be both barcode scanned and weighed at approximately the same time. Yet comparing barcode scans to weights between the EDAS junction boxes showed over 40 discrepancies. As discussed earlier, all of these differences can be explained by operator tests and errors in procedure. In other words, correlation between barcode and weight scale data is not possible for these artifacts since they are not attributable to an actual cylinder entry or exit measurement. The operator barcode and weight log file data were also compared, and the discrepancies matched those of the analysis between the EDASs, showing equivalency in narratives between both systems.

Another analysis found 100% correlation of EDAS weight commands and data, which proves that, in every case, a command immediately preceded a weight measurement. More generally, the installation of multiple EDASs independently observing various aspects of a process can increase context for the safeguards inspector to draw conclusions on declarations since they can correlate more data streams to confirm agreement in the data. The ability to check data consistency across multiple EDASs makes undeclared operations on a process more complex and difficult to perform without detection.

The decision to build a lockable custom cabinet to house the field trial equipment affected setup and installation. While such a cabinet is advantageous for an inspectorate to house the inspector computer, there are downsides to placing the EDAS junction boxes inside. For one, it makes it difficult for the small form-factor EDAS junction box to be installed as close to an instrumentation sensor as possible. In addition, the pass through connectors, built into the cabinet wall, add more capacitance to the instrumentation signal path, which will affect data transmission and integrity for both the operator and inspectorate. Another point is that the operator created an external bypass path at the connectors of the cabinet itself, foregoing the bypass option designed into the EDAS junction box.

The field trial exposed several issues with timing. The built-in EDAS clock, included with the BeagleBone™ processor, is not very accurate and resets to a default value if it loses power. A low-cost, high-accuracy, real-time clock with

battery backup can be added to future versions of the EDAS junction box to fix the problem. It is also essential to standardize the time zone used by the EDAS and inspector computer, irrespective of installation location. A universal time zone such as UTC (Coordinated Universal Time), which does not observe daylight savings transitions, is recommended. Clock drift between EDAS and the operator system is another important concern for the future since the inspector does not have the ability to regulate time on the operator system. The time drift between these systems is an issue that could impact event correlation and should be given further consideration.

More sophisticated field trial analyses could yield patterns of facility operations for the branched instrumentation by correlating multiple measurements over time. For this field trial, it may be possible to calculate the net weight difference of cylinders, get a sense of the residence time of each cylinder within the facility, and the direction of cylinder movement. Such data can yield an indication of uranium hexafluoride mass processed at the facility per unit time as well as how many and which cylinders are currently inside the facility, or were recently processed and shipped. The types of patterns extracted by an EDAS installation can be extrapolated to other areas of the nuclear fuel cycle.

7. Conclusions

Euratom reported the field trial as a full success due to the continuous, correct, and secure branching of safeguards-relevant data. More generally, it is advantageous that EDAS allows the use of existing operator instrumentation to collect operator-owned instrumentation data. The EDAS supports various installation configurations and could branch data from a wide array of instruments used for nuclear safeguards in different parts of the fuel cycle, such as monitoring material flow in nuclear facilities by branching operator-owned NDA instruments in material balance areas. An overview of nuclear safeguards instrumentation can be found here [8]. Another point is that EDAS could reduce cost by decreasing the installation of redundant safeguards instrumentation in facilities. Such duplicate equipment uses facility real estate and can decrease facility throughput (e.g., the extra time to weigh a UF_6 cylinder on both operator- and inspector-owned weight scales).

Any field trial at a facility can represent a challenge for an operator, due to potential interference with standard operations and additional work required to establish an acceptable solution that complies with the plant operational and safety systems. The installation of the EDAS junction boxes and the associated Euratom computer was completed relatively easily. The main observation from the operator is that the EDAS system was, in effect, invisible to plant operations. That is, there were no instances of interference with use or operation of the weight scale, barcode scanner, or associated operator systems.

There are several field trial takeaways that can be integrated into a future version of EDAS. These include incorporating better time keeping with a battery backup, and using a universal time zone to timestamp data. The junction box RS232 serial interface is compatible with a significant portion of legacy instrumentation. For broader interface compatibility we recommend that future EDAS hardware be compatible with 25-pin RS-232 (e.g., a standard 25- to 9-pin adapter), and potentially other instrumentation interfaces, such as USB or Ethernet. In addition, a tamper indicating enclosure is a recommended addition to protect the EDAS cryptographic keys.

The EDAS junction box should be installed as close to the sensor as possible as the data is cryptographically confidential and authentic starting from the tap-off point until it reaches the inspector computer. Since the data between the sensor and junction box are unsecured, it is important that EDAS is deployed as part of a comprehensive safeguards solution. For example, tamper indicating conduit could be installed to secure the sensor to junction box communication path and/or surveillance could be used to monitor the instrumentation. Looking forward, the safeguards community could work with manufacturers to integrate EDAS directly into the sensors of new instrumentation.

The success of the EDAS field trial is a critical step in addressing the IAEA Long Term R&D plan item 7.1, “Develop minimally intrusive techniques that are both secure and authenticated to enable the use of operator’s systems, instruments and process monitoring for cost effective safeguards implementation.” EDAS is a useful tool for the nuclear safeguards inspection community to securely monitor processes using operator instrumentation without undue burden on the facility operator — not to mention reducing the burden on IAEA’s budget for new unattended monitoring systems. More generally, EDAS could be a useful tool in other areas where a secondary observer has the need to monitor a measurement system or data stream.

8. Acknowledgments

This field trial represents work performed under Action Sheet 41 for the U.S. DOE – Euratom collaboration sponsored by the NNSA International Nuclear Safeguards Engagement Program (INSEP). The EDAS collaboration comprises Sandia National Laboratories in the United States, the European Commission Directorate General for Energy (DG-ENER) in Luxembourg, and the European Commission Joint Research Centre (JRC) in Italy. We wish to acknowledge the participation of the Westinghouse Springfields nuclear fuel manufacturing facility in Lancashire,

United Kingdom, for providing the operational facility for the EDAS field trial.

Sandia National Laboratories is a multi-mission laboratory managed and operated by National Technology and Engineering Solutions of Sandia LLC, a wholly owned subsidiary of Honeywell International Inc. for the U.S. Department of Energy's National Nuclear Security Administration under contract DE-NA0003525.

SAND2016-11899 J

9. References

[1] João G.M. Gonçalves, et al; *Enhanced Data Authentication System (EDAS): Concept, Demonstration and Applications,* proceedings of the Institute of Nuclear Materials Management 52nd Annual Meeting, Palm Desert CA, July 2011.

[2] George Baldwin, et al; *Secure Branching of Facility Instrumentation for Safeguards*; American Nuclear Society 9th International Conference on Facility Operations – Safeguards Interface, Savannah, Georgia, September 2012.

[3] Maikael Thomas, et al; *Enhanced Data Authentication System: Converting Requirements to a Functional Prototype*; proceedings of the European Safeguards Research & Development Association 35th Annual Meeting, Bruges, Belgium, May 2013.

[4] Maikael Thomas, et al; *Prototype Hardware and Software for the Secure Branching of Facility Instrumentation*; proceedings of the Institute of Nuclear Materials Management 55th Annual Meeting, Atlanta, Georgia, July 2014.

[5] Maikael Thomas, et al; *Testing the Enhanced Data Authentication System (EDAS)*; proceedings of the International Atomic Energy Agency Symposium on International Safeguards: Linking Strategy, Implementation, and People, Vienna, Austria, October 2014.

[6] P. Schwalbach, et al; *RADAR and CRISP - Standard tools of the European Commission for remote and unattended data acquisition and analysis for nuclear safeguards;* proceedings of the International Atomic Energy Agency Symposium on International Safeguards, Vienna, Austria, 2006.

[7] A. Smejkal, et al; *Automated processing of safeguards data: Perspectives on software requirements for a future "All-in-one Review Platform" based on iRAP*, 37th ESARDA Symposium, Manchester, England, 2015.

[8] *Safeguards Techniques and Equipment: 2011 Edition*, International Nuclear Verification Series No. 1 (Rev. 2), International Atomic Energy Agency, Vienna, Austria, 2011.

Restating the fundamental principle of nuclear security culture and the importance of cultural differences

I. Iarema

MA in International Peace and Security at King's College London, Chevening scholar, UK
for the 15th ESARDA 2016 course on Nuclear Safeguards and Non-Proliferation held by the Institute for Transuranium Elements, Nuclear Security Unit (Ispra)
Joint Research Centre, European Commission
Via E. Fermi, Ispra 21027 (VA) Italy
E-mail: iryna.iarema@kcl.ac.uk

Abstract

In 2008, the IAEA published Nuclear Security Culture guidelines to serve as a tool for countries on building an effective nuclear security culture. Although the guidelines provide an adequate apparatus to help establish nuclear security culture at facilities, some limitations to them need to be carefully addressed. Here, by using empirical data, possible pitfalls on the way to achieving strong nuclear security culture are examined. In particular, those identified deal with:

1) *Recognition of the credibility of the threat to nuclear facilities and nuclear materials in use, storage and in transport.*

2) *Appreciation of the influence of national cultural differences and subcultures when building nuclear security culture.*

It is believed that taking these factors into account and correcting shortcomings will not require substantial financial resources. Customising approaches to the application of nuclear security culture concept will help fill the gaps where they exist.

Keywords: nuclear security culture, terrorism, insider threat, organisational culture, national cultural influence, subcultures, design basis threat, integrated approach

1. Introduction

The past thirty years have seen increasingly rapid advances in appreciation of the role of the human factor in sustaining safety and security of nuclear operations. If the Chernobyl accident in 1986 gave birth to the concept of nuclear safety culture (IAEA, 1986, 1992), the term "nuclear security culture" emerged in the early 2000s following the June 2000 meeting of the IAEA Working Group Experts on the revision of the Convention on the Physical Protection of Nuclear Material (CPPNM) (IAEA, 2008, p. 1). At the political level, momentum to give due attention to nuclear security culture was gained with the endorsement of the nuclear security culture concept by the IAEA Board of Governors at its September 2001 meeting and subsequent recognition of its priority by the 2001 IAEA General Conference (IAEA, 2008).

In 2008, the IAEA introduced guidelines on building nuclear security culture based on Edgar Schein's model of organisational culture (Khripunov, 2012, p. 9). According to the guidelines, nuclear security culture is defined as '*the assembly of characteristics, attitudes and behaviour of individuals, organizations and institutions which serves as a means to support and enhance nuclear security*' (IAEA, 2008, p. 3). It is important to note that nuclear security culture should not be regarded as an element applicable only to the physical protection of power plants or other facilities that possess nuclear materials. The 2005 Amendment to the Convention on the Physical Protection of Nuclear Material (CPPNM) (IAEA, 2005) expanded the scope of protection of nuclear materials[1] (Fournier, 08.05.2016), so subsequently nuclear security culture should at the very least cover nuclear materials in use, storage as well as in transport. Taking a multilevel approach, it would be logical to regard nuclear security culture in all its complexity, including cyber-protection with its subsequent requirement of vigilant handling of electronic correspondence, proper organised records and attention to details in material accountancy and control. On the other hand, it is important not to overstretch the concept to the extent that it goes from being operational to becoming too broad or vague for formulation and implementation. Therefore, here I will stick to the IAEA definition of nuclear security culture, which reflects precautionary measures primarily applicable to nuclear power plants, and imply that the 2005 Amendment extended it to a necessity to safeguard nuclear materials in domestic use, storage and transport.

An effective nuclear security is based on the belief, shared by all personnel, that a credible threat from theft, sabotage, unauthorized access, illegal transfer, and other malicious acts exists (IAEA, 2008; Khripunov, 2005, p. 60). According to the findings of the Centre for Nuclear Non-Proliferation and Disarmament (refered in Zakariya & Kahn, 2015, p. 295), '*there are six groups of actors responsible for the proper development of security culture: countries, organizations, managers in organizations, personnel, the public and the international community*'. The tasks performed by them are by them are characterised by

[1] '*In July 2005, the Parties to the CPPNM adopted the Amendment to broaden the scope of the original Convention to cover the protection of nuclear facilities or nuclear material in domestic use, storage and transport*' (Fournier, 08.05.2016).

legal roles and resources they possess for the realization of nuclear security culture. With this regard, the important role of the IAEA is to provide support to states by issuance of guidelines and recommendations for establishment of a potent nuclear security culture and coordination of international efforts in that direction. Among recent IAEA undertakings is preparation of the technical guidance on *Self-assessment of nuclear security culture in facilities and activities that use nuclear and/or radioactive material* (IAEA, 2.07.2014 (draft)). Although the need for such assistance to the states is beyond all question, a concern is raised here on the recognition of important factors that can influence the application of the concept of nuclear security culture and ultimately may render null some of the efforts. These factors concern:

1. Recognition of the credibility of the threat to nuclear facilities and nuclear materials in use, storage and in transport. The risk that nuclear materials may fall into terrorist hands became most apparent with the fall of the Soviet Union; however, already in 1977 the U.S. Office of Technology Assessment (OTA, 1977, p. 17) identified that even without access to classified literature '*a small group of people could possibly design and build a crude nuclear explosive device ...*' The fact that the threat has not yet materialized does not mean that the nuclear sector is immune to extremism and terrorism, especially when recently, as some experts conclude (M. G. Bunn, Malin, Roth, & Tobey, 2016), there is a significant rise of interest in high casualty terrorism. A greater emphasis should be placed on the plausibility of malicious interest in the nuclear 'dimension' that can be materialised through outsider/insider activities. Moreover, new scenarios, including cyber-technologies, should be taken into account, tested and preparations to withstand the attack should be made. It may come as no surprise that many countries do not regard nuclear terrorism as a threat, which is reflected or rather not reflected in their design basis threat definitions. Some other countries diminish the risk and significance of insider threat even when acts of factual diversion of nuclear material have occurred. A too relaxed view of the threat is equal to risking that nuclear materials eventually could end up in the possession of terrorists. Thus, it is important to instil the underlying assumption that a threat exists and that it is quite plausible that a terrorist group could make a nuclear bomb if they acquire the material. This recognition is not to spread panic but rather to create a bedrock for a good nuclear security culture. Building and holding a strong view would require limited or even zero financial resources for facilities operators; however, it is something that might be difficult to change without dedication and applying significant efforts.

2. Appreciation of the influence of national cultural differences and subcultures when implementing nuclear security culture. Each professional community has attitudes distinct to itself, for example, individuals involved with safety may have different or sometimes conflicting views with security-related personnel (Winter, 2007, p. 73). Thus, sometimes we can observe divergence in various professional subcultures, which can exert influence on nuclear security culture. In addition, landmark studies by Hofstede et al. (G. Hofstede, 1983, 1984, 1985; G. Hofstede, Hofstede, & Minkov, 1991; G. Hofstede & McCrae, 2004; G. Hofstede, Neuijen, Ohayv, & Sanders, 1990) showed the relationships between societal-level variables, organisational practices and prevalent behaviours within the organisation. The GLOBE study (House, Hanges, Javidan, Dorfman, & Gupta, 2004) further discussed in more details the role of leadership in different cultures and its significance to organisational practices in 62 societies. Why is this important? Despite the process of globalisation, and the reduction or elimination of economic barriers, cultural differences remain, and can constitute barriers of their own (House et al., 2004, p. 1). The uniform approach to nuclear security culture followed the purpose to make it universal across the globe; however, neglecting cultural differences can cause collisions and bottlenecks in its implementation. Training programmes, if not customised by the headquarters and practitioners in the field, risk portraying nuclear security culture as an alien monster to some societies or cause for ridicule in others. Therefore, similar to the way the IAEA applies the state-level concept to safeguards (for more details on state-level approach see Cooley, 2011), it should also treat the nuclear security culture concept. For this, however, more knowledge of social sciences is needed, as well as sensitivity and tolerance, together with the skills of how to deal with some intrinsic difficulties, since culture is a very delicate thing and, as most experts agree, is difficult to change.

One may consider that these arguments are somehow interconnected, since a security narrative is often the result of the threat perception, which in its turn is influenced/mediated or created by national specifics. Despite the validity of this concern, giving rein to such an approach can create numerous ramifications with the risk of turning it into Aristotle's chicken or the egg causality dilemma. Thus, the logic to separate one argument from another was introduced simply with the purpose of emphasizing current difficulties and restraints with understanding nuclear security culture in order to streamline its implementation.

Appreciation of these restraining elements not only will help to mitigate possible divergence and inconsistency with concept application and eliminate impediments on the way to the achievement of strong security culture, it will also promote the adherence by states to relevant international instruments and commitments. This is especially relevant with the entry into force of the 2005 Amendment to

the CPPNM on 8 May 2016, where nuclear security culture, as Nilsson (Nilsson, 2007, p. 13) pointed out earlier, has elevated to a fundamental principle of nuclear security and become an obligation under international law. Ultimately, this study provides an opportunity to advance our knowledge of nuclear security culture in order to reduce scepticism, which unfortunately is often found around interdisciplinary constructed concepts, especially those dealing with human factors, jargoned as 'warm-ware' among the nuclear security community (Carroll, 2007, p. 24), and consequently to enhance its operability.

2. Recognition of the credibility of the threat to nuclear facilities and nuclear materials in use, storage and in transport

2.1 Nuclear security foundations and 9/11 events as a turning point

Although there has been a limited amount of research on nuclear security culture, it is prudent to name it among the fundamental principles of risk management in the nuclear security field (Zakariya & Kahn, 2015, p. 294). The IAEA regards nuclear security culture in the scope of an *integrated approach against nuclear terrorism* comprising a range of activities '*concerned with the physical protection of nuclear material and nuclear installations, nuclear material accountancy, detection of and response to trafficking in nuclear and other radioactive material, the security of radioactive sources, security in the transport of nuclear and other radioactive material, emergency response and emergency preparedness in Member State*' (Foreword to the Nuclear Security Culture Implementing Guide, IAEA, 2008). Thus, helping Member States establish a strong nuclear security culture is an important element of such an integrated approach.

When it comes to profiling the nuclear threat, the most typical categorisation involves four scenarios. These primarily include acquisition and usage for malicious purposes:

(a) nuclear explosive devices,

(b) nuclear material to build an improvised nuclear explosive device,

(c) radioactive material to construct a radiological dispersal device (RDD),

(d) the dispersal of radioactivity through sabotage of installations in which nuclear and other radioactive material can be found or of such material in transport (Findings of the President of the International Conference on Nuclear Security: Global Directions for the Future cited in the Appendix V of Khripunov, Ischenko, & Holmes, 2007, p. 152).

For the sake of justifying my argument on the credibility of the threat, a brief review of the evolution of risks to nuclear materials and facilities is presented first; there follow some cases of actual failures of security systems to illustrate how to marry this with the nuclear security culture concept.

The need to safeguard nuclear materials worldwide became acute after the dissolution of the Soviet Union, with a large number of nuclear materials, facilities and significant nuclear military arsenals falling out of central governmental control and being scattered around new states which were in the process of establishing their own controls over the 'nuclear heritage' as well as forming new administrative structures. In addition, the end of the Cold War era constituted by the bi-polar world order (the United States of America versus the Union of Soviet Socialist Republics) symbolised the beginning of a new international architecture. In the new world, the rise of new regional powers has been accompanied by the course of globalisation and an increase in the role of international actors in international politics. Among the negative trends associated with such processes were potential WMD proliferation activities of the states and the rise of international terrorism.

With regard to the latter, attention to protection against nuclear terrorism as one of the core issues of states' security peaked after the tragic 9/11 events. The Al-Qaeda terrorist attacks in 2001 in the USA revealed the ever-growing threat emanating from non-state actors and the daunting repercussions it can have due to the insecurity of critical and symbolic infrastructure. The magnitude of the consequences of such attacks for the entire world community was recognised by the United Nations Security Council, which unanimously adopted a series of anti-terrorism resolutions (1368, 1373, 1540) in the aftermath of the attacks and in subsequent years. The most important UN resolution in the field of nuclear security, Resolution 1540, actually sets requirements for the states, *inter alia*, to: '*to refrain from supporting by any means non-State actors from developing, acquiring, manufacturing, possessing, transporting, transferring or using nuclear, chemical or biological weapons and their delivery systems*'. Concerns that terrorist groups could acquire nuclear weapons have raised the question of security of nuclear weapons and materials as well as the availability of expertise to produce them.

The security of military nuclear technology was specifically called to attention, since the reports alluded to Al-Qaeda's interest in either obtaining an intact nuclear weapon from the territory of the former Soviet Union or in acquiring fissile material for manufacturing an improvised nuclear device through co-operation with rogue nuclear scientists (Daly, Parachini, & Rosenau, 2005, pp. 26, 31, 34-36). Some of those plots allegedly included transfer of nuclear materials even from the territories of Western European countries (Salama & Hansell, 2005, p. 621). Despite the secretive nature of states' guardianship over nuclear stocks (M. G. Bunn et al., 2016, p. vi), some of the concerns were dismissed as illegitimate due to the belief that none of the states would want their nuclear arsenals to fall into the hands of terrorists;

therefore, it was assumed that the control exercised by states over their nuclear weapons (since they form a crucial part of military security assets) would be quite stringent.

As highlighted in the 9/11 Report, the civil nuclear sector was under particular peril, especially in the light of evidence of jihadists plotting attacks against nuclear power plants (NPPs) in the West, namely in the USA (Kean & Hamilton, 2004, p. 154) or against Cap de la Hague NPP in Normandy, France (Salama & Hansell, 2005, p. 621). The data suggested that, at the time, Al-Qaeda leader Osama Bin Laden was refrained from exercising attacks on nuclear power plants only because of the fear that it could '*get out of control*' (cited in Ferguson & Potter, 2005, p. 195). However, counting on such reluctance by terrorist groups in the future and cultivating certitude for the improbability of such a scenario would amount to playing with fire while endangering many civilian lives and risking economic collapses. With 65 countries reportedly covered by a 'nuclear renaissance', '*the need to develop a variety of more efficient tools for achieving sustainable nuclear security culture*' (Khripunov, 2010, p. 95) becomes even more apparent due to the appearance of a larger amount of sensitive and symbolic infrastructure (Steinhäusler, 2007, p. 56). An attack on the scale of 9/11 in the nuclear field definitely would be more '*difficult to accomplish in an environment of heightened security and vigilance*' (Mowatt-Larssen & Allison, 2010); thus this should be promoted on a national and international scale.

Summarising the above, we have witnessed the dual nature of the threat: on the one hand, the availability and accessibility of a vast nuclear material stockpile as a result of the Soviet collapse, and on the other hand, materialization of attacks by terrorist groups, as showcased in the 9/11 events, who might be willing to take advantage of the nuclear materials supply in pursuit of their goals or plan attacks against nuclear installations, which is worrisome in the light of the projected expansion of nuclear power. All this warrants the need to enhance existing measures to protect, control, and account for nuclear materials (Nikonov, 2007, p. 75). However, very often the actual practice of states shows that the threat of nuclear terrorism is underappreciated or not taken seriously at all.

2.2 Security breaches in countries and evolving nature of threats

The report on the security breach in the Y-12 National Security Complex (U.S.DOE, 2012) in the U.S.A., where highly enriched uranium (HEU) was stored, described how a group of anti-nuclear protestors headed by an elderly nun overcame multiple security system layers and revealed the failures of several levels of defence. That incident happened to a large extent due to the absence of a vivid security culture. If the intruders had not been unarmed peaceful protesters, but a terrorist group, the outcome could have been strikingly more severe and gloomy. Basically, this showcases that a vigilant attitude to nuclear security should be promoted in all countries without exception.

At the same time in 2012, in the Seversk Chemical Combine — one of Russia's largest plutonium and HEU processing facilities, a case of high-level corruption, luckily not involving nuclear materials but definitely representing an insider threat, occurred (Roth, Bunn, Malin, & Tobey, 2014, p. 28). In this light, the changes in the last 16 years to the Criminal Code of the Russian Federation (namely, articles 215, 220, 225), where punitive measures were significantly relaxed, are alarming, especially taking into account its huge stockpile of nuclear materials. In particular, in Russia there has been liberalisation of the criminal offence for those who work in state positions and deal with nuclear/radioactive materials. In most cases, imprisonment was substituted or could potentially be substituted by compulsory labour. Such an environment cannot promote a security culture; moreover, keeping in mind shocking trends, which as reported by a Rosatom spokesman in 2011, *'in just two years, 208 directors of Rosatom enterprises had been disciplined and 68 top managers fired for corruption*' (cited in Roth et al., 2014, p. 28). The report on nuclear security culture in Russia (Khripunov, Holmes, Nikonov, & Katsva, 2004) masterly describes a number of incidents where facility workers and managers were complicit in the theft or diversion of sensitive materials. If in the 1990s the facts of materials diversion were implemented by disgruntled employees (i.e., Leonid Smirnov dreaming of a new refrigerator) many of whom were underpaid or on the verge of poverty, nowadays the profile of wrongdoers has changed. Now those who abuse their positon are usually dealing with millions of dollars.

The above examples featuring two countries were selected not to pinpoint malfunctions in each of them, but rather to represent different perspectives and 'profile' of the insider/outsider threat, which at first sight seem to be rather 'innocent' if compared to terrorism attacks with civilian casualties; however, they are shocking enough to demonstrate how imperfect a security system could be and how ignorant the security assumptions could be.

But what if we assume that Leonid Smirnov, who diverted 1.5 kilograms of 90 percent enriched HEU from the Luch Production Association in Podolsk, Russia, in 1992 (M. Bunn & Sagan, 2014, p. 5), had managed to sell it on the black market? What if that 1.5 kg of highly enriched uranium were used by a terrorist group, then the criminal offence for diversion of materials in Russia, perhaps, would be significantly higher? Since co-option cannot be excluded, higher security standards should be generated. However, not only the legislative and regulatory framework should be rigidly enforced, a greater emphasis should be placed on the threat of nuclear terrorism itself.

Chatham House, a leading UK-based think tank, commissioned a report in 2015 on *Cyber Security at Civil Nuclear*

Facilities, which pinpoints to a very common problem related to the downplay of the threat in the nuclear sector – a limited incident disclosure. National security sensitivity surrounding critical infrastructure has contributed to the fact that the nuclear industry became 'inward-looking and closed' (Baylon, Brunt, & Livingstone, 2015, p. 15). When incidents of cyber-attacks on the nuclear sector are not disclosed, due to various reasons, such as potential loss of public support for a nuclear power or loss of reputation for a country *per se*, this creates a false impression that there have been very few incidents and the nuclear sector is immune to the threat (Baylon et al., 2015).

Finally, the threat to nuclear and radiological materials has been evolving due to the ramification and proliferation of terrorist networks, especially separation of the Daesh, known as the Islamic State of Iraq and the Levant (ISIL), from Al-Qaeda and subsequent terrorist attacks in the Middle East and European cities. Events particularly related to the nuclear industry happened in 2015-2016 in Belgium. In November 2015, police in Belgium discovered that a senior nuclear worker at the MoI SCK-CEN research facility had been placed under surveillance by individuals linked to the Islamic State-sanctioned attacks in Paris in 2015 (M. Bunn, 2016). Reports in the press suggested that the terrorist cell may have planned to blackmail or co-opt the worker to gain access to either the facility or radiological materials (Malone & Smith, 2016). An expert in the field, Matthew Bunn, warns that the idea that the HEU at SCK-CEN might have been the terrorists' ultimate objective should not be dismissed; excluding it as a far-fetched or implausible scenario is wrongful (M. Bunn, 2016). In addition to that, one should not exclude cyber-attacks on nuclear facilities, especially on nuclear power plants. Keeping in mind the enormous capabilities of the ISIL to use social networks for their recruitment purposes, they could also develop more capabilities in ICT technologies to launch cyber-attacks to sabotage the plant or to remove nuclear material (Baylon et al., 2015, p. 4). The events in Belgium remind us of how close a terrorist could get to a nuclear target, which signifies that the threat remains as real as ever (Downes & Salisbury, 2016).

It is through the lens of the credibility of threat that nuclear security culture should be formed and it is the task of leadership not to forget about this fundamental principle for building nuclear security culture within its organization and around nuclear materials in transportation.

3. Influence of national cultural differences and subcultures

3.1 The concept of subcultures and their potential conflicting paradigms

Nuclear security is ultimately dependent on individuals working in the field (IAEA, 2008, p. 2). Individuals are raised in a particular cultural environment and trained within a particular field, where special rules and procedures exist and personal qualities are cultivated. Therefore, while there are certain qualities propagated for a strong nuclear security culture, they might be in discord with the national culture or professional assumptions held by an individual.

Within an organization, the culture can be broad and uniform (i.e., the same patterns of behaviour and attitudes are found throughout the organization at all levels), or it can be diverse and divided into 'subcultures' (i.e., when the behaviours and attitudes of certain parts or levels of the organization are substantially different from those of other parts or levels) (Packer, 2007, p. 45).

The nuclear industry needs people from a broad range of backgrounds, consisting of scientists and engineers as well as trainers, managers, human resources professionals, accountants, custodians, administrative staff, etc. (Pepper & Bachner, 2014, p. 2). Educational requirements, as well as work ethics, differ in different professions; however, individuals from all of the abovementioned fields need to increase awareness in the fields of nuclear security culture.

Winter (2007, p. 73) pointed to the differences in attitudes between safety and security specialists in nuclear industry. For safety culture, a transparent and broad communication of threats is required to prevent it from happening, while for security culture, such a disclosure might be counterproductive, and for precautionary measures the information, by contrast, should be communicated only to certain authorized people. Holmes (2007, p. 3) adds that '*safety specialists, for instance, typically advocate building redundancy into nuclear installations to guard against equipment failure, while security specialists are more sceptical because redundancy furnishes extra opportunities for theft or diversion of sensitive materials*'. Such divergence in attitudes can create tensions and could potentially have repercussions for the nuclear security, especially in the context of newly emergent threats where experience of interactions between subcultures is limited. For example, cyber security professionals and specialists in nuclear plant operation responsible for safety even often work in different buildings, often not communicating sufficiently one with another, which exacerbates the cultural divide between these occupational groups (Baylon et al., 2015). An important task with regard to this occupational divergence will be to foresee potential clashes between the subcultures, so that it does not compromise nuclear safety and security in the organisation.

3.2 National cultures' effects on nuclear security culture

The fact that national culture can exert its influence on organisational culture was already described by one of the most prominent researchers of culture, Geert Hofstede, in 1984 (G. Hofstede, 1984). He posited that there are national influences on work-related values in different societies.

Edgar Schein, in his seminal work *Organisational Culture and Leadership* (Schein, 2004, p. 55), acknowledges that, in addition to the interplay of subcultures which often reflects the primary occupational cultures of the organization members, to fully understand what goes on inside the organization, one should consider the organization's macro context as well, because much of what one observes inside simply reflects the national culture.

Although numerous definitions of (national) culture exist, culture is not a universally accepted notion, and there are still numerous problematic aspects about it (G. J. Hofstede, Pedersen, & Hofstede, 2002, p. 40). Therefore, it is imperative to postpone our interpretation of national culture until we know enough of it (G. J. Hofstede et al., 2002, p. 17), to avoid becoming pawns of stereotypes. However, there is something that different definitions of national culture have in common; this is '*the sense that culture pertains to the social world; it determines how groups of people structure their lives*' (G. J. Hofstede et al., 2002, p. 40). Hofstede, in his book *Culture's Consequences* (1984), provided some of the dimensions for analysing culture using a great deal of empirical data. Since then, more information has been added to the analysis and additional criteria for comparing cultures have been added; however the most typical are still based on the following five dimensions: identity, hierarchy, gender, truth and virtue (G. J. Hofstede et al., 2002, p. 40). Each dimension spans a continuum from one extreme position to the other: Collectivism – Individualism (identity), Large Power Distance – Small Power Distance (hierarchy), Femininity – Masculinity (gender), Strong Uncertainty Avoidance – Weak Uncertainty Avoidance (truth), Long-Term Orientation – Short-Term Orientation (virtue) (G. J. Hofstede et al., 2002, p. 40).

It is understood that German, Chinese, Latin American, Russian etc. cultures are different from each other; the differences can be felt in day-to-day interactions. Even, as Holmes (Holmes, 2007, p. 3) put it, '*linguistic intricacies matter*'. In many nations, including republics from the former Soviet Union, there is no difference in translation of the words 'safety' and 'security'. Therefore, the term nuclear security culture could raise some inconsistency. For example, in Russian, the term nuclear security culture was proposed to translate as 'culture of physical nuclear security' (transliterated as *kultura fizicheskoy yadernoy bezopasnosti* or *'культура физической ядерной безопасности'* – in Russian) to foster comprehension and action by the government (Holmes, 2007, p. 3). However, in my view, this translation does not fully cover the full range of the meaning that nuclear security culture entails and creates a rather limited concept. The Ukrainian version is something in between 'culture of protection' and 'security culture' (transliterated as *kultura zahyshnenosti* or *'культура захищенності'* – in Ukrainian), and is a better equivalent. Although one may argue that this is a pure matter of linguistics, the value of precise translation should not be underestimated. If the term 'culture of physical nuclear security' excludes the variety of actors responsible for security but for national guards, the 'culture of protection' and 'security culture' extrapolates applicability of the term and subsequently the responsibility to a broad range of actors. The meaningfulness of the term enlarges effectively. Therefore, we can speak of a culture among the whole chain of command and factor in the role of the public. This is especially important when we want to make greater use of the general public, the role of which, as Igor Khripunov (Khripunov, 2006, p. 39) noticed, has been underestimated and underutilised in the prevention of nuclear terrorism and raising levels of nuclear security in general.

Whereas international businesses, banks etc. try to converge or circumvent cultures by creating a corporate style, the nuclear industry, usually owned and highly regulated by the state and being to some degree secretive, is more susceptible to national cultural influences. People who work in nuclear facilities or with nuclear materials usually come from one national environment; Hofstede (1983) defines it as a '*collective mental programming*'. For example, if we take the identity dimension of culture, which '*measures the degree to which an individual is committed to an in-group such as the extended family, the firm, or the village, in individualistic societies, there is not much tie to any in-group, and everyone is in pursuit of his/her own self-interest*' (Nyaw & Ng, 1994, p. 545). Whereas, in collectivist societies, as Nyaw & Ng (1994, p. 545) admit, '*the interests of the in-group come first, even when they are at the expense of the individual's self-interest*'. Worth mentioning '*that in collectivist societies, outsiders (that is, non-group members) are viewed with greater suspicion than in individualistic societies*' (Nyaw & Ng, 1994, pp. 545-546). Therefore, some policies against the insider threat in nuclear facilities might not be well-developed in collectivist societies.

The situation with the changes to the Criminal Code of the Russian Federation for breaches of nuclear provisions, described in the previous section, can also be viewed from the prism of national culture and leadership. The changes which took place from 2000, when Vladimir Putin arrived at the helm of Russia, up to spring 2016 were characterised by the liberalization of punishment in the nuclear sphere for those who work in state positions and are dealing with nuclear materials. In Russia as well as other Eastern European countries, according to the GLOBE studies, leadership can very often be romanticised (House et al., 2004); strong leaders are accepted and even demanded by the public. Thus, trends of giving 'greater protection' to those in official state positions when misconduct occurs with nuclear/radiological materials can be explained by the strengthening of the centre of power through a system of favouritism and dependency; however, this in its turn can contribute, as we have seen in the previous section, to corruption amongst those in elite position. A GLOBE study

further elaborates that leadership behaviour in national contexts can be explained under the criteria of Power Concentration versus Decentralisation (which is referred to as Power Distance in Hofstede's works) (House et al., 2004, p. 3). Thus, in the same vein, we can also notice enlargement of the role and functions of the President – national leader – in Russia in the nuclear field as well. The Russian law '*On the of use atomic energy'* (21.11.1995) details the role of the President, who since 2007, in addition to determining the main directions of state policy in the field of nuclear energy policy and deciding on security issues, prevention and elimination of consequences of emergency situations from nuclear energy use, also approves the lists of Russian legal entities which can own nuclear facilities and nuclear materials (outlining those which may be exclusively in the federal property). Those trends generally signify power concentration in Russia to enhance the role of leadership. With this in mind, to improve nuclear security culture in Russia, as Khripunov et al. (2007, p. 104) earlier advised, it would be reasonable to involve high Russian officials in this process. For example, if President Putin made a public speech stating that nuclear security is important to national security, everyone would take this matter more seriously (Khripunov et al., 2007, p. 104). Zakariya & Kahn (Zakariya & Kahn, 2015) point out that an organization's leadership and management bear the responsibility to resolve issues related to inadequate organizational procedures or shortcomings of management. Establishing strong cultural norms, codes of behaviour and a system of enforcement are important for deterring intentional acts by organizations or individuals (Zakariya & Kahn, 2015, p. 300), and leadership is crucial.

Mandatory, regular check-ups for employees are regarded as normal security procedures in the nuclear field, however, they are not universal. When it was discovered that a young '*Moroccan-born man, who had worked in a sensitive area of the Doel* [nuclear power station] *in Belgium, Ilyass Boughalab*, *had died in the spring* [of 2014] *while fighting for the Islamic State in Syria*' (Malone & Smith, 2016), more worries appeared regarding the security and effectiveness of measures against the insider threat at Belgian nuclear sites. Masuda (2007, p. 32) emphasised that to prevent the risk of insider threat, it is necessary to acquire actively the bio-data of personnel, and to update this information regularly at each opportunity. In some societies, however, this can be seen as an intrusion into private life. If more serious vetting procedures can be introduced as a part of nuclear security culture in some countries, in others, like Japan, for example, employees in military and nuclear-related facilities reportedly do not undergo particularly close scrutiny from investigators (G. Bunn, 2000, p. 150). A Japanese expert at an IAEA conference suggested several interrelated reasons for this situation derived from specific national characteristics. Among these reasons, the expert posited that the homogeneity of the racial and cultural composition of the Japanese population, combined with strong societal norms, helps ensure that society remains relatively secure, safe and stable and therefore lessens the need for closer scrutiny of employees (G. Bunn, 2000, p. 150).

Since '*national cultures constitute the social fabric in which each individual has a place*' (G. J. Hofstede et al., 2002, p. 40), deciphering cultures can help understand the system of conceptions carried out in a particular society, so that nuclear security culture is formed taking national specifics into account. Although developing an individual nuclear security culture guidance for each country might seem an ambitious undertaking from the beginning, tailoring training programmes for a particular country might be among good starting points. Familiarisation of international consultants performing jobs for the IAEA with theory-based cross-cultural findings should help factoring them when delivering international assignments related to nuclear security. In fact, empirical evidence suggests (Bhawuk, 1998) that, among various methods of cross-cultural trainings, a theory-based cross-cultural training is among most effective ways of training which speaks for the need of further engagement with available cultural scholarship such as of Hofstede and GLOBE project. The history of the International Nuclear Security Education Network (INSEN) (Hobbs, 2015) shows that it together with International Network for Nuclear Security Training and Support Centres (NSSC Network) (Salisbury & Hobbs, 2015, p. 6) can serve as a platform for the creation of new educational and professional development materials in this area.

3.3 What other benefits we can take from studying cultural differences

Studying culture is good not only for factoring it and customising national approaches to nuclear security, but also for identifying common problems and making better use of lessons learnt guide-books. For example, absence of an effective mechanism of protection of whistle-blowers in the field of nuclear security is a global corporate problem (Larkin, 2011, pp. 263-274) and is common to many countries. Therefore, the international, community should develop a mechanism for improving it, so that it is not used as a way of revenge by disgruntled employees, helping to avoid significant breaches of security procedures and abuse/misuse of professional position that often can go unreported or unnoticed.

On a positive note, understanding specifics of national cultures can contribute to better use of motivations and granting rewards for effective protection of nuclear materials and facilities. Understanding the culture will show what type of incentives can be offered to employees in a particular societal context, what is valued within a society, such as a good word from a superior, a material incentive, or community recognition etc., since '*generous pay and benefits*

alone cannot yield' a strong security culture (Holmes, 2007, p. 4). Definitely, values such as honesty, integrity, and responsibility should be promoted among nuclear industry personnel and those performing international shipping of nuclear materials. This should be accompanied by commitment to effective equipment maintenance and procedures, as well as continuous learning and improvement. Leadership who understand the intrinsic difficulties associated with the nature of nuclear installations, facilities, promotes research and development in this area and advocates for a strong security culture is indispensable in this process.

The following model (fig.1) reflects the links between national culture, subcultures and nuclear security culture. It also stresses the necessity of instilling underlying beliefs of the importance of nuclear security and forming assumptions on the credibility of the threat. Moreover, the model recognises the potential mediation role of personal traits of the employee and shows that the influence of beliefs and traditions mainstreamed in national culture should be examined in conjunction with other factors (a principle of exteriority).

4. Conclusion

The flourishing of terrorism, together with other unaccustomed security challenges, necessitates the need to extend the scope of nuclear security and the associated culture '*beyond the traditional task of protecting weapons-usable material*' (Khripunov et al., 2007, p. 109). The increasing incidence of international terrorism worldwide, coupled with transnational criminal activities, including logistics, culminated in specific security risks for the nuclear materials and facilities. These spans from illicit international trafficking in nuclear technology and materials, to the growth of suicide terrorism and the potential for the use of radioactive materials in mass casualty attacks (Steinhäusler, 2007, p. 55), to the appearance of new cyber-threats that are difficult to track back and can be masked as an accident (Baylon et al., 2015).

Providing effective protection of nuclear facilities and materials is an expensive task and measures should be taken to ensure that it really works. Among such measures, one which is difficult to describe quantitatively since it depends on human factors but which determines the real strength of physical barriers, is nuclear security culture. Strengthening nuclear security culture is a task demanding certain efforts, but certainly, the result is worth it, especially when keeping in mind the potential consequences of a nuclear attack by terrorists on a lax security culture (M. G. Bunn et al., 2016; Khripunov et al., 2007).

This article, building on empirical data and previous analyses, has shown some traps or opportunities (in certain situations), which individuals dealing with security culture should take into account. These are belief in the threat, especially from terrorist groups and insiders, and the impact of national cultural context and subcultures (occupational groups) on nuclear security culture.

Within the last few years, security threats to the nuclear materials and activities have grown as a threat of terrorism amplified worldwide (Steinhäusler, 2007, p. 55). The recent report *Preventing Nuclear Terrorism: Continuous Improvement or Dangerous Decline?* by the well-established Belfer Center for Science and International Affairs on (M. G. Bunn et al., 2016) rightly mentioned that '*the foundation of a strong security culture is belief in the threat*'. It also emphasised that, since the Nuclear Security Summit in 2014 (the last one concluded in April 2016), '*security for nuclear materials has improved modestly – but the capabilities of some terrorist groups, particularly the Islamic State, have grown dramatically, suggesting that in the net, the risk of nuclear terrorism may be higher than it was two years ago*' (M. G. Bunn et al., 2016). Since a strong nuclear security culture is essential to sustainable nuclear security, its development must also take into account specifics of the general culture in which it is incorporated (Holgate, 2007, p. 20).

The IAEA's efforts to conceptualise nuclear security culture should continue in providing support to member states for its improvement, taking into account national specifics and potential tensions within the different occupational groups in the nuclear field. It is also important to indoctrinate that nuclear security culture is crucial, and now, with the end of the Nuclear Security Summit process, it is high time, as Holgate (Holgate, 2007, p. 20) put it before, to incorporate the concept into key documents on nuclear security with co-operation from other relevant international organisations and bodies.

5. Bibliography

Baylon, C., Brunt, R., & Livingstone, D. (2015). *Cyber Security at Civil Nuclear Facilities: Understanding the Risks*. Retrieved from London: Chatham House: https://www.chathamhouse.org/sites/files/chathamhouse/field/field_document/20151005CyberSecurityNuclearBaylonBruntLivingstone.pdf

Bhawuk, D. P. (1998). The Role of Culture Theory in Cross-Cultural Training A Multimethod Study of Culture-Specific, Culture-General, and Culture Theory-Based Assimilators. *Journal of cross-cultural psychology, 29*(5), 630-655.

Bunn, G. (2000). Raising international standards for protecting nuclear materials from theft and sabotage. *The Nonproliferation Review, 7*(2), 146-156.

Bunn, M. (2016). Belgium Highlights the Nuclear Terrorism Threat and Security Measures to Stop it. *TheWorldPost* Retrieved from http://www.huffingtonpost.com/matthew-bunn/belgium-nuclear-terrorism_b_9559006.html

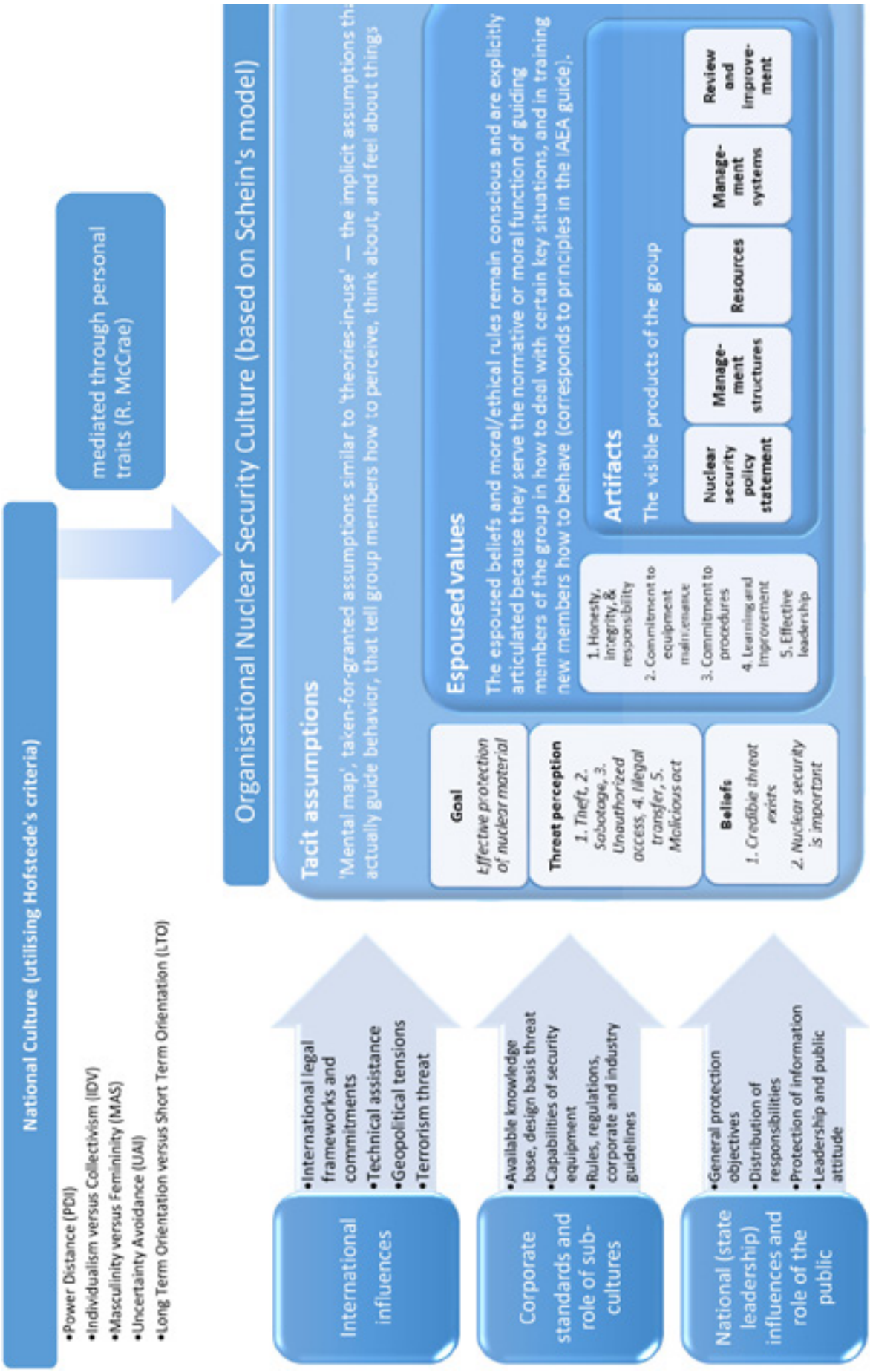

Fig. 1: Model of organisational NSC in the context of national culture and other exogenous influences *(compiled by the author based on G. Hofstede et al., 1991; IAEA, 2008, p. 7; Khripunov et al., 2004, p. 11; Schein, 2004, pp. 23-33)*

Bunn, M., & Sagan, S. D. (2014). A Worst Practices Guide to Insider Threats: Lessons from Past Mistakes. *Order, 2138*.

Bunn, M. G., Malin, M. B., Roth, N. J., & Tobey, W. H. (2016). Preventing Nuclear Terrorism: Continuous Improvement or Dangerous Decline?

Carroll, P. (2007). Security Culture: A Personal Perspective From the United Kingdom. In I. Khripunov, N. Ischenko, & J. P. Holmes (Eds.), *Nuclear Security Culture: From National Best Practices to International Standards* (Vol. 28, pp. 23-30): IOS Press.

Cooley, J. N. (2011). *Progress in evolving the State-level Concept*. Paper presented at the INMM - ESARDA - Workshop 2011 - Future directions for nuclear safeguards and verification; 16-20 Oct 2011, Aix-en-Provence (France). https://inis.iaea.org/search/search.aspx?orig_q=RN:45037242

Daly, S., Parachini, J., & Rosenau, W. (2005). *Aum Shinrikyo, Al Qaeda, and the Kinshasa Reactor: Implications of Three Case Studies for Combating Nuclear Terrorism*. Retrieved from

Downes, R., & Salisbury, D. (2016). Is Belgium's nuclear security up to scratch? *EnergyPost*.

Federal Act No. 170-FZ 'On the of use atomic energy', (21.11.1995).

Ferguson, C. D., & Potter, W. C. (2005). *The four faces of nuclear terrorism*: Routledge.

Fournier, V. (08.05.2016). New Nuclear Security Agreement will Reduce Risk of Nuclear Terrorism. Retrieved from https://www.iaea.org/newscenter/news/new-nuclear-security-agreement-will-reduce-risk-of-nuclear-terrorism

Hobbs, C. (2015). International Nuclear Security Education Network at Five Years. *1540 Compass*(9), 38-40.

Hofstede, G. (1983). The cultural relativity of organizational practices and theories. *Journal of international business studies*, 75-89.

Hofstede, G. (1984). *Culture's consequences: International differences in work-related values* (Vol. 5): Sage Publications.

Hofstede, G. (1985). The interaction between national and organizational value systems [1]. *Journal of Management Studies, 22*(4), 347-357.

Hofstede, G., Hofstede, G. J., & Minkov, M. (1991). *Cultures and organizations: Software of the mind* (Vol. 2): Citeseer.

Hofstede, G., & McCrae, R. R. (2004). Personality and culture revisited: Linking traits and dimensions of culture. *Cross-cultural research, 38*(1), 52-88.

Hofstede, G., Neuijen, B., Ohayv, D. D., & Sanders, G. (1990). Measuring Organizational Cultures: A Qualitative and Quantitative Study Across Twenty Cases. *Administrative science quarterly, 35*(2), 286-316. doi:10.2307/2393392

Hofstede, G. J., Pedersen, P., & Hofstede, G. (2002). *Exploring culture: Exercises, stories and synthetic cultures*: Nicholas Brealey Publishing.

Holgate, L. (2007). Cultural Aspects of Sustaining Nuclear Security. In I. Khripunov, N. Ischenko, & J. P. Holmes (Eds.), *Nuclear Security Culture: From National Best Practices to International Standards* (Vol. 28, pp. 17-21): IOS Press.

Holmes, J. R. (2007). Nuclear Security Culture: The Way Ahead. A Summary Report on the Proceedings. In I. Khripunov, N. Ischenko, & J. P. Holmes (Eds.), *Nuclear Security Culture: From National Best Practices to International Standards* (Vol. 28, pp. 1-6): IOS Press.

House, R. J., Hanges, P. J., Javidan, M., Dorfman, P. W., & Gupta, V. (2004). *Culture, leadership, and organizations: The GLOBE study of 62 societies*: Sage publications.

IAEA. (2.07.2014 (draft)). *Self-assessment of nuclear security culture in facilities and activities that use nuclear and/or radioactive material. Draft technical guidance*. Vienna.

IAEA. (1986) Summary Report on the Post-accident Review Meeting on the Chernobyl Accident. *INSAG Series 1* IAEA.

IAEA. (1992) The Chernobyl Accident: Updating of INSAG-1. *INSAG Series 7*: IAEA.

IAEA. (2005). *Nuclear Security - Measures to Protect Against Nuclear Terrorism. Amendment to the Convention on the Physical Protection of Nuclear Material* Retrieved from http://www.iaea.org/About/Policy/GC/GC49/Documents/gc49inf-6.pdf

IAEA. (2008) Nuclear Security Culture. Implementing Guide. *IAEA Nuclear Security Series No. 7* (pp. 37).

Kean, T. H., & Hamilton, L. H. (2004). *The 9/11 Report: The national commission on terrorist attacks upon the United States*: St. Martin's Paperbacks.

Khripunov, I. (2005). Nuclear security: Attitude check. *Bulletin of the Atomic Scientists, 61*(1), 58-64.

Khripunov, I. (2006). Educating the public about nuclear terrorist risks can help raise levels of security. *IAEA BULLETIN, 48*, 1.

Khripunov, I. (2010). Nuclear Renaissance and Security Culture. *IFANS Review, 18*(2), 95-120.

Khripunov, I. (2012). *Nuclear and Radiological Security Culture: A Post-Seoul Summit Agenda. Report of the*

Workshop "In Search of Sustainable CBRN Security Culture," held in Athens, GA, February 6-8, 2012. Retrieved from Georgia, U.S.A.:

Khripunov, I., Holmes, J., Nikonov, D., & Katsva, M. (2004). *Nuclear security culture: The case of Russia*: Center for International Trade and Security.

Khripunov, I., Ischenko, N., & Holmes, J. P. (2007). *Nuclear Security Culture: From National Best Practices to International Standards*: IOS Press.

Larkin, B. D. (2011). *Designing denuclearization: an interpretive encyclopedia* (Vol. 1): Transaction Publishers.

Malone, P., & Smith, J. R. (2016). The Islamic State's Plot to Build a Radioactive 'Dirty Bomb'. The jihadist group appears to have been looking for nuclear materials in Belgium. *ForeignPolicy*. Retrieved from http://foreignpolicy.com/2016/02/29/the-islamic-states-plot-to-build-a-radioactive-dirty-bomb/?wp_login_redirect=0

Masuda, M. (2007). Nuclear Security Culture: The Need for Universal Standard. In I. Khripunov, N. Ischenko, & J. P. Holmes (Eds.), *Nuclear Security Culture: From National Best Practices to International Standards* (Vol. 28, pp. 31-42): IOS Press.

Mowatt-Larssen, R., & Allison, G. T. (2010). *Al Qaeda Weapons of Mass Destruction threat: hype or reality?* : Belfer Center for Science and International Affairs.

Nikonov, D. (2007). Safety and Security Culture Link: Lessons from the Past. In I. Khripunov, N. Ischenko, & J. P. Holmes (Eds.), *Nuclear Security Culture: From National Best Practices to International Standards* (Vol. 28, pp. 75-81): IOS Press.

Nilsson, A. (2007). The IAEA's Perspective on Security Culture. In I. Khripunov, N. Ischenko, & J. P. Holmes (Eds.), *Nuclear Security Culture: From National Best Practices to International Standards* (Vol. 28, pp. 13-14): IOS Press.

Nyaw, M.-K., & Ng, I. (1994). A comparative analysis of ethical beliefs: A four country study. *Journal of Business Ethics, 13*(7), 543-555.

OTA. (1977). *Nuclear Proliferation and Safeguards*. Retrieved from https://www.princeton.edu/~ota/disk3/1977/7705/7705.PDF.

Packer, C. (2007). Relationship of Management Systems, Human Performance, and Security Culture. In I. Khripunov, N. Ischenko, & J. P. Holmes (Eds.), *Nuclear Security Culture: From National Best Practices to International Standards* (Vol. 28, pp. 43-53): IOS Press.

Pepper, S. E., & Bachner, K. (2014). *International Conference on Human Resource Development for Nuclear Power Programmes: Strategies for Education and Training, Networking and Knowledge Management*. Retrieved from https://www.bnl.gov/isd/documents/86220.pdf

Roth, N. J., Bunn, M. G., Malin, M. B., & Tobey, W. H. (2014). *Advancing Nuclear Security: Evaluating Progress and Setting New Goals*. Retrieved from

Salama, S., & Hansell, L. (2005). Does intent equal capability? Al-Qaeda and weapons of mass destruction. *Nonproliferation Review, 12*(3), 615-653.

Salisbury, D., & Hobbs, C. (2015). *Centers of Excellence In East Asia: Encouraging Collaborative Approaches to Nuclear Security. Policy Analysis Brief*. Retrieved from http://www.stanleyfoundation.org/publications/pab/COEPAB915.pdf

Schein, E. H. (2004). *Organizational culture and leadership* (3rd ed.). San Francisco: Jossey-Bass.

Steinhäusler, F. (2007). On the Need to Strengthen Nuclear Security Culture in View of New Security Risks. In I. Khripunov, N. Ischenko, & J. P. Holmes (Eds.), *Nuclear Security Culture: From National Best Practices to International Standards* (Vol. 28, pp. 55-62): IOS Press.

U.S.DOE. (2012). *Special Report. Inquiry into the Security Breach at the National Nuclear Security Administration's Y-12 National Security Complex*. Retrieved from http://energy.gov/ig/downloads/special-report-ig-0868

Winter, D. (2007). Security Culture in the Nuclear Field. In I. Khripunov, N. Ischenko, & J. P. Holmes (Eds.), *Nuclear Security Culture: From National Best Practices to International Standards* (Vol. 28, pp. 63-73): IOS Press.

Zakariya, N. I., & Kahn, M. (2015). Safety, security and safeguard. *Annals of Nuclear Energy, 75*, 292-302.

Success and failures of the Non-Proliferation Treaty demonstrated in history

A. Windt
Andrássy University Budapest
Pollack Mihály tér 3.
H-1088 Budapest
Hungary
E-mail: wandrasg@gmail.com

Abstract:

The Treaty on the Non-Proliferation of Nuclear Weapons (NPT) is the core of the non-proliferation regime. Because of this, determining the NPT's effectiveness is important. This essay tries to draw a conclusion on the effectiveness of the NPT. It will draw upon the historical successes and failures of the NPT in reaching the goals set out by its drafters and parties. This is done through examination of the first seven Articles of the NPT. Historical cases were elaborated to demonstrate successes and failures of the NPT in history. These include the nuclear programmes of India, Pakistan, Iraq, Iran, North Korea and South Africa. The safeguards system and export control regimes have been examined. Treaties aiming at nuclear disarmament and nuclear-weapon-free-zones have also been presented. The result is that the NPT was generally successful. Nuclear-weapon states have not transferred nuclear weapons to non-nuclear-weapon states, and the number of threshold states are kept to a minimum. A functioning safeguards system has been established and the right to peaceful use of nuclear power is mostly respected. The nuclear arms race has been stopped, and five regional treaties have banned nuclear weapons in their territory. However, the NPT failed to achieve complete nuclear disarmament, and failed to prevent some states to purse (successful or unsuccessful) nuclear weapons programme. To summarise, the NPT was able to adapt to the changing circumstances, but further revision of its effectiveness is necessary.

Keywords: nuclear, disarmament, non-proliferation, treaty, success, failure, history, safeguards

Introduction

The Treaty on the Non-Proliferation of Nuclear Weapons (NPT), opened for signature on 1 July 1968, entered into force on 5 March 1970, signalling a new phase in the history of nuclear safeguards and non-proliferation. Out of the five permanent members of the UN Security Council, three – the US, the Soviet Union and the United Kingdom – were not only among the first signatories of the treaty, but its depository states as well. China and France joined the NPT in 1992[1].

Although the NPT was not the first treaty with the goal of preventing the proliferation of nuclear weapons and material (EURATOM, Tlatelolco Treaty), it was extraordinary in its provisions. It prohibits each nuclear-weapon state (NWS, which have „exploded a weapon or other nuclear explosive device prior to 1 January, 1967")[2] to transfer nuclear weapons or other nuclear devices to non-nuclear-weapon states (NNWSs), thus preventing them from acquiring nuclear weapons themselves (Article I., NPT). Furthermore, NNWSs refrain from developing nuclear weapons, abstain from encouraging NWSs to transfer them nuclear weapons, or control over nuclear weapons (Article II, NPT). Moreover, the NPT's third most important measure defines the commitment of states to the „cessation of the nuclear arms race" and "a treaty on general and complete disarmament under strict and effective international control." (Article VI. NPT) Thus the NPT outlines a future without nuclear weapons[3].

These provisions were of utmost importance at the time, and they still are. Nuclear-weapon states and non-nuclear-weapon states have been identified and have been called upon to prevent the spread of nuclear weapons. The termination of the nuclear arms race and the wish for a future free of nuclear weapons reflected on the dangers of the Cold War, the looming Mutually Assured Destruction (MAD), the destruction of humanity through use of nuclear weapons. Furthermore, the NPT ensures "the inalienable right of all the Parties to the Treaty to develop research, production and use of nuclear energy for peaceful purposes without discrimination and in conformity with Articles I and II of this Treaty" (Art. IV., NPT)[4].

The NPT has become the core of the non-proliferation regime. It has been deemed a success. The NPT has attained near universality: as of now, there are 191 member states to the NPT[5] . It has adopted to most of the challenges throughout history, and successfully prevented the wide

[1] Armscontrol.org (29.04.2015) (DD/MM/YYYY)
[2] Article IX (3) (NPT). Iaea.org (22.05.1970), p. 4.
[3] Rockwood (2008), p. 83.; iaea.org (22.05.1970), pp. 2, 4.
[4] Iaea.org (22.05.1970), p. 3.
[5] UNODA (NPT) (24.07.2016)

spread of nuclear weapons, thus nearly achieving the prevention of horizontal proliferation.

Although the NPT outlines the framework of non-proliferation to this day, this does not mean that the NPT was a complete success. Time and time again proof emerged on the non-compliance with the treaty, namely in case of Iraq, North-Korea (and others). All four non-party states, North Korea, India, Pakistan, and Israel have developed nuclear devices themselves. The full disarmament outlined in Art. VI. has not been reached to this day. The latter is a provision with the aim of vertical non-proliferation.

This essay will try to draw a conclusion on the effectiveness of the NPT. It will draw upon the historical successes and failures of the NPT in reaching the goals set out by its drafters and parties. To do so, a goal oriented approach has been chosen, which means that, after a brief history of non-proliferation leading up to the NPT, the different Articles of the NPT will be examined. The first seven Articles have been identified by the author as the most important, because they contain all the relevant provisions of the NPT, and the others mainly focus on the Treaty itself, rather than the goal of the Treaty. Cases will be presented to support the argumentation.

The following method was used during the research: Supporting information will be gathered from the respective UN body, the IAEA; publications of think tanks and the opinions of experts on the topic. Since the development of nuclear weapons is a sensitive issue, not all relevant data is accessible. Therefore, only open access information will be used during research. Any secret data, which could potentially alter the outcome of this essay cannot be taken into account.

1. A brief history of non-proliferation before the NPT

Efforts to prevent the proliferation of nuclear weapons are as old as nuclear weapons themselves. The first two deployments ever, Hiroshima and Nagasaki showed "the dawning of the nuclear era, and the birth of the nuclear non-proliferation regime"[6]. The first idea was that the denial of technology would hinder proliferation[7]. In January 1946, the United Nations Atomic Energy Commission (UNAEC) was established, to ensure that atomic energy is only used for peaceful purposes[8]. The ambitious Baruch plan of creating "a supranational organization that would have a global monopoly in atomic energy eventually failed. Bilateral agreements on trade of nuclear technology and material have also failed (probably to preserve the nuclear monopoly of the US).

In 1949, the Soviet Union conducted its first nuclear weapons test. It was followed by the nuclear weapons test of the UK in 1952. Other states, like Belgium, Canada, France, Italy have been developing their own nuclear programs. It was clear that the non-proliferation efforts failed. However, in 1953, US. President Dwight D. Eisenhower delivered his famous "Atoms for Peace" speech. He outlined "an international organization that could serve as the repository for nuclear material from the nuclear weapons states from which the non-nuclear-weapon states could make withdrawals for peaceful purposes". This organization became known as the IAEA, tasked with the promotion of safe and peaceful use of nuclear energy and verification of the peaceful use of nuclear technology. The IAEA, an independent NGO was founded eventually on 23 October 1956, when the Statute of the IAEA was approved at the UN in New York. It entered into force on 29 July 1957.[9] As of February 2016, there are 168 member states[10].

The novelty of the IAEA was its broad rights to enforce safeguards. According to Article XII. of the IAEA Statute, the IAEA has the right to examine and approve of specialized equipment and facilities, including nuclear reactors to ensure that they would not further any military purpose, that they comply with applicable health and safety standards, that they will permit effective application of safeguards; to ask a state for operation and progress reports; to send inspectors to a state; to report non-compliance to the UN Security Council[11].

The first "safeguards system" (within the IAEA framework) was established in 1961 through the document INFCIRC/26, which was then extended in 1964 (INFCIRC/26/Add.1). It was further revised in 1965 (**INFCIRC/66**). The latter went through extensive revision in 1966 (INFCIRC/66/Rev.1) and in 1968 (INFCIRC/66/Rev.2). These were item specific agreements, which, although went through extensive evolution "to cover the ever increasing circumstances were safeguards were required", were still limited in scope, because they required safeguards only in connection to the specific items (reactors, nuclear material, conversion plants, fuel fabrication plans, etc.) listed in the agreements themselves. The Statute in itself was not legally binding however, safeguards agreements are required to ensure its application[12]. A European regional system for non-proliferation was established in 1957 under the name of EURATOM (European Atomic Energy Community) which entered into force in 1958.

In the meantime, however, two blows were dealt to the non-proliferation regime: the nuclear weapons test of France in 1960, and that of the People's Republic of China in 1964. This meant that the foregoing efforts on non-proliferation

[6] Rockwood (2008) p. 79.
[7] Ibid.
[8] Rockwood (2008) p. 80.
[9] Rockwood (2008) pp. 80-81.
[10] Iaea.org (26.02.2016)
[11] Rockwood (2008) p. 81.; Iaea.org (23.02.1989) pp. 25-29.
[12] Rockwood (2008) pp. 81-82.

were inadequate. A new system was required to ensure non-proliferation. A system with "legally binding commitments by states not to acquire or develop nuclear weapons, and a mechanism for verifying compliance with those commitments"[13].

This led to the **Tlatelolco Treaty** (Mexico), i.e. the Treaty for the Prohibition of Nuclear Weapons in Latin America and the Caribbean, and the NPT. The Parties of the Tlatelolco Treaty refrain from developing nuclear weapons, thus creating the first nuclear weapon free zone in history. The Treaty was opened for signature on 14 February 1967 in Mexico City and currently has 33 Parties. Peaceful use of nuclear energy however, is allowed. Verification is managed through the Agency for the Prohibition of Nuclear Weapons in Latin America and the Caribbean[14]. It is also likely, that the intention was not just to prevent Latin-American states to develop their own nuclear arsenal, but also to prevent other powers, mainly the USA and the SU, to station nuclear weapons in the region. In its second Protocol, the nuclear weapon states have agreed to respect the NWFZ in Latin-America, and have given a negative guarantee, meaning that they will not use or threaten with the use of nuclear weapons against the members of the Tlatelolco Treaty.[15]

The Irish Resolution (UN GA 1665 (XVI)) in 1961 and the negotiations conducted in the Eighteen Nation Committee on Disarmament paved the way for a joint draft on 11 March 1968, which has been sent to the UN General Assembly on 31 May. [16] The Text on the Treaty on the Non-Proliferation of Nuclear weapons was adopted and commended in the UN GA Resolution 2373 (XXII.), and was subsequently opened for signature[17]. France abstained in the General Assembly vote, stating that while France would not sign the Treaty, it "would behave in the future in this field exactly as the States adhering to the Treaty.[18] The Treaty was deposited in the USA, the UK and the USSR, and was signed on 1 July 1968.

2. Article I.: Nuclear-weapons states and their obligations

Article I states that: *„Each nuclear-weapon State Party to the Treaty undertakes not to transfer to any recipient whatsoever nuclear weapons or other nuclear explosive devices or control over such weapons or explosive devices directly, or indirectly; and not in any way to assist, encourage, or induce any non-nuclear-weapon State to manufacture or otherwise acquire nuclear weapons or other nuclear explosive devices, or control over such weapons or explosive devices"*[19].

This is one of the most important Articles of the NPT. It prohibits the NWSs to hand over nuclear weapons or control over these weapons to NNWSs. NWSs are defined by Article IX. Paragraph 3. as states which have "manufactured and exploded a nuclear weapon or other nuclear explosive device prior to 1 January, 1967"[20].

It is not in the interest of any of the NWSs to encourage and support proliferation. Therefore, this Article was complied with. The only blurry point to be found is the so called "nuclear sharing" between the USA and some other NATO member states. Nuclear sharing means that US nuclear weapons are stored in the territory of NATO states. Today, there are only 5 NATO members participating in a nuclear sharing agreement with the US: Belgium, Germany Italy, the Netherlands and the Turkey. There are 10-20 B-61 bombs in Belgium, 10-20 in Germany, 60-70 in Italy, 10-20 in the Netherlands and 60-70 in Turkey.[21] These are to be delivered by pilots of the states where these bombs are stationed. But the launch controls, the initiation of deploying these nuclear weapons remains in the hands of the US.[22]

It is arguable whether it is right or reasonable to maintain the nuclear capabilities of NATO, especially when these are in the form of bombs to be delivered by bombers, instead of missiles. However, it is not the aim of this essay to decide this question. It is indeed important to examine, whether the nuclear sharing is in compliance with the NPT.

It can be argued, if the other NATO members have to deliver the B-61s to target, that they have indirect control over the nuclear weapons. That would mean that the US violates Article I, and subsequently, the other 5 NATO states violate Article II. This was a focal point during the negotiations before drafting the NPT. The US had nuclear sharing agreements by the time of the negotiations. Furthermore, the US wanted a Multilateral Force (MLF), in which the NATO members would have controlled the NATO nuclear weapons together. The USSR strongly opposed this idea. The compromise reached has prohibited the creation of the MLF, but allowed the nuclear sharing agreements. The reason was that the US, with the exclusive control over the launch codes, would retain "positive control" over the NATO nuclear arsenal.[23]

Another important point is, did threshold states receive help from the NWSs to acquire nuclear weapons? The USSR has given technology and material to the DPRK.[24]

[13] Rockwood (2008) p. 83.
[14] UNODA (Tlatelolco) (24.07.2016)
[15] UNODA (Tlatelolco Protocol 2) (24.07.2016)
[16] Fas.org (24.07.2016); Rockwood (2008) p. 83
[17] Rockwood (2008) p. 83.
[18] Fas.org (24.07.2016)
[19] Iaea.org (22.05.1970), p. 2.
[20] Iaea.org (22.05.1970), p. 4.
[21] Robert S. Norris & Hans M. Kristensen (2011) US tactical nuclear weapons in Europe, 2011, Bulletin of the Atomic Scientists, 67:1, 64-73, DOI: 10.1177/0096340210393931 **p. 66.**
[22] Kamp/Remkes (24.07.2016) p. 77., 84.; Péczeli/Rózsa (2013) p. 73.
[23] Péczeli/Rózsa (2013) p. 73.
[24] NTI.org (North Korea) (04.2016)

The US has given technology and material to India.[25] However, it was never intended (or cannot be proven otherwise) that both of these superpowers wanted to encourage and support proliferation.

After the dissolution of the USSR, soviet nuclear weapons remained in the territory of Belarus, Kazakhstan and Ukraine. This unprecedented event challenged Article I (and II). However, all of the nuclear weapons in Belarus, Kazakhstan and Ukraine have either been moved to Russia or dismantled through implementation of the Lisbon Protocol[26].

Verdict: Article I of the NPT is a success. None of the NWSs have handed over nuclear weapons, or control over these to NNWSs, or encouraged proliferation. The nuclear sharing has also been justified. Those NNWSs, which have acquired nuclear weapons, have mainly used dual use items to do so, and no direct support from NWSs.

3. Article II. Non-nuclear weapons states and their obligations

Article II states that: *„Each non-nuclear-weapon State Party to the Treaty undertakes not to receive the transfer from any transferor whatsoever of nuclear weapons or other nuclear explosive devices or of control over such weapons or explosive devices directly, or indirectly; not to manufacture or otherwise acquire nuclear weapons or other nuclear explosive devices; and not to seek or receive any assistance in the manufacture of nuclear weapons or other nuclear explosive devices".*[27]

This is one of the most important Articles of the NPT. It prohibits NNWSs to receive nuclear weapons or control over these weapons from NWSs. Developing nuclear weapons is also prohibited.

This has been one of the most problematic points of the NPT. Several states sought to acquire nuclear weapons. Those, which have succeeded are: India, Israel, Pakistan, North Korea and South Africa. Iraq Iran and Libya (and probably other states) had nuclear weapons programmes, but they were fortunately unable to develop nuclear weapons themselves.

India has conducted its first peaceful nuclear test in 1974. India used dual-use items to develop its nuclear programme, and violated the peaceful-use agreements with the US. Sanctions have been introduced against India. The test "was a major contributing factor to the formation of the NSG". The first nuclear weapons test was conducted in 1998. India needed nuclear weapons to deter China and Pakistan. India currently has 90-110 warheads, and is not party to the NPT.[28]

Pakistan has conducted its first nuclear weapons test in 1998, in response to India's test. The reason for the Pakistani nuclear weapons programme was to deter India. However, Pakistan played a reactionary role to the Indian development. The Pakistani nuclear weapons programme greatly benefited from the illicit nuclear traffic network of A.Q. Khan. China has also helped Pakistan. Pakistan currently has 100-120 nuclear weapons and is not party to the NPT.[29]

Israel has never admitted to having nuclear weapons, but also never denied them. This nuclear ambiguity or opacity forms a consistent policy of Israel. In accordance with this doctrine, Israel has never officially tested a nuclear explosive. The US provided aid to the Israeli nuclear programme (Atoms for Peace) and later, France. Israel's reason to develop nuclear weapons is to deter hostile Arab states in the region, and prevent another Arab-Israeli war. Israel currently has an estimated 80 nuclear warheads and is not party to the NPT. [30]

North Korea has conducted nuclear tests four times: 2006, 2009, 2013, 2016. The soviets helped the North Korean nuclear programme by providing a reactor to the Yongbyon Nuclear Research Center, and providing plutonium reprocessing technology. North Korea has signed the NPT in 1985. In 1993, the DPRK denied access to the IAEA to some nuclear sites, which raised concerns about a military purpose nuclear programme. The DPRK has received help from the A.Q. Khan network. North Korea was the first country ever to withdraw from the NPT in 2003. The subsequent six-party-talks and international sanctions failed to prevent the DPRK from testing nuclear explosives. According to North Korea's security doctrine, Pyongyang needs nuclear weapons to deter potential aggressors like the US or South Korea. The DPRK currently has an estimated 6-8 nuclear warheads.[31]

According to President de Klerk the nuclear weapons programme of **South Africa** has run from 1974 until 1990. The sources vary on the first fully functional and complete nuclear explosive device, most of them claim it has been done as early as 1982. The arsenal was expanded throughout the years: "by 1989, South Africa possessed six warheads".

The reason for the nuclear weapons programme was to create "a deterrent to counter a perceived Soviet threat in the region". Also, Pretoria was concerned about the deployment "of Cuban forces into Angola". The country felt itself isolated because of the apartheid and nuclear

[25] NTI.org (India) (04.2015)
[26] armscontrol.org (03.2014)
[27] Iaea.org (22.05.1970), p. 2.
[28] NTI.org (India) (04.2015)
[29] NTI.org (Pakistan) (04.2016)
[30] NTI.org (Israel) (04.2016); armscontrol.org (10.2015)
[31] NTI.org (North Korea) (04.2016); armscontrol.org (10.2015)

weapons aspirations. However, in August 1988, a cease-fire agreement has been signed by South Africa, Cuba, and Angola. From then on there was no point of maintaining the South African nuclear arsenal.

In 1991, **South Africa**'s nuclear weapons have been completely dismantled. On 10 July 1991, South Africa became a member of the NPT as a NNWS. The IAEA started the verification and concluded that South Africa was free of any nuclear weapons.[32]

Although the NPT failed to prevent South Africa from acquiring nuclear weapons (because Pretoria did not join the NPT), the fact that Pretoria completely surrendered and cancelled its nuclear weapons programme willingly and voluntarily, marks an unprecedented success of the NPT and the non-proliferation regime.

Iraq has never reached the phase to acquire nuclear weapons, and has never conducted nuclear tests. Its nuclear programme started with US aid (Atoms for Peace). Concerns about a possible nuclear weapons programme of Iraq emerged in 1981, when Israel bombed the Osiraq reactor. In 1991, the IAEA uncovered undeclared nuclear material in Iraq. It became clear that Iraq, and its leader Saddam Hussein has violated the provisions of the NPT, and had a clandestine nuclear programme intended on developing nuclear weapons. This discovery happened shortly after the Gulf War. With reference to Chapter VII of the UN Charter, on the basis of UNSC Resolution 687 (1991) the Agency "undertook intrusive inspections", accessed all locations, people and information "it deemed necessary". The IAEA concluded by 1997, that the whole of Iraq's nuclear programme has been uncovered and effectively ceased. In 1998, all of the IAEA inspectors have left Iraq, because Hussein did not want to cooperate with UN inspectors. After the invasion of Iraq in 2003, the Iraq Survey Group concluded in 2004 in the Duelfer Report, that Saddam Hussein did not restart the nuclear weapons programme. [33]

Iran has also never acquired nuclear weapons, and has never conducted nuclear tests. The US helped Iran's nuclear programme (Atoms for Peace). After the Revolution in 1979, Iran's nuclear programme was frozen until the end of the war with Iraq. To deter Iraq, (and probably Israel), a nuclear weapons programme was started in the 80s. The A.Q. Khan network helped Iran in this endeavour. In 2003, Iran signed the Additional Protocol. The IAEA noted that Iran was not fully cooperative. The nuclear plant in Arak, Natanz, Esfahan and Fordow were of great concern. Sanctions have been introduced by the UNSC and western states against Iran, but Iran resumed the enrichment of uranium. Therefore, the sanctions have been introduced and increased, but negotiations have been conducted between Iran and the P5+1 (the 5 NWSs and Germany). The victory of Hassan Rohani in the presidential elections in 2013 "signalled a shift in Iran's position on nuclear negotiations" which led to an agreement between Iran and the P5+1. This agreement came to be known as the Joint Comprehensive Plan of Action, and was signed in 2015. One year after the agreement, the JCPOA has been deemed a success. It averted the creation of an Iranian nuclear device. Some sanctions have been relieved, but not those of regarding dual use items (especially the EU did not relieve those).[34]

Libya has also had a nuclear weapons programme but did not produce nuclear weapons. Although Libya signed the NPT in 1968, Libya's leader, Mu'ammar Qadhafi started a nuclear weapons programme in the 1970s. Lybia received help from the A.Q. Khan network. In 2003, Qadhafi has admitted to the country's nuclear weapons programme to the public. The programme was completely dismantled in 2004. The failure of the nuclear weapons programme was caused by its costliness and the economic sanctions crippling Libya.

Verdict: These cases make Article II. a partial success. It was indeed able to prevent further proliferation and keep the number of threshold states to a minimum. The case of South Africa, Libya and Iran show that proliferation has even been reversed. However, the fact that these countries had clandestine nuclear weapons programmes, and some were even able to produce results is concerning. India, Pakistan Israel and North Korea are not part of the NPT. Also, non-state proliferators like A.Q. Khan has not been addressed. These concerns have to be met in the future.

4. Article III.: Safeguards

The NPT makes clear that all Parties have the right for peaceful use of nuclear material (Article IV). Also, all of the states must prevent the spread of nuclear material to be used for malevolent purposes (Article I. II.). To effectively ensure both of these provisions, a new verification mechanism was required, one which had to be an improvement compared to the INFCIRC/66. to meet the new challenges and circumstances (i. e. the development of technology, new uranium mines).

In accordance with Article III.1, all NNWSs are obliged to accept safeguards "*for the exclusive purpose of verification of the fulfilment of its obligations assumed under this Treaty with a view to preventing diversion of nuclear energy from peaceful uses to nuclear weapons or other nuclear explosive devices.*"[35]

[32] NTI.org (South Africa) (09.2015)
[33] NTI.org (Iraq nuclear) (07.2015); Rockwood (2008) p. 87. NTI.org (Iraq overview) (07.2015)
[34] NTI.org (Iran) (03.2016); Brookings (14.07.2016); Zarroli (26.01.2016); Zoll.de (24.07.2016)
[35] Iaea.org (22.05.1970), pp. 2.-3.

The most important part of this Article is that only the NNWSs are obliged. This means that NWSs do not have to sign safeguards agreements with the IAEA. This is problematic, because then the NWSs are not, unlike other states, under IAEA control. It also does not apply to states not party of the NPT. That is a failure of the NPT, because the different levels of control (one state has an INFICRC/66 agreement, another a CSA, etc.) can make the realisation of the goals of the NPT difficult. Nevertheless, both NWSs and non-party states have concluded partial safeguards agreements with the IAEA. The threshold countries Cuba, India, Israel and Pakistan have concluded INFIRC/66 agreements.[36] The five NWSs have concluded INFCIRC/153 agreements (but without full scope).

In 1972, the new safeguards agreements were introduced in the document known as **INFCIRC/153**, "*The Structure and Content of Agreements between the Agency and the States required in connection with the Treaty on the Non-Proliferation of Nuclear Weapons*". Why are these new safeguards agreements better than the earlier ones? The first advantage is standardisation. The INCIRC/66 safeguards agreements were individually signed between States and the IAEA. The INFCIRC/153 outlines a template of contents which makes the rights and obligations clear and easy to control. The other advantage is the scope: Earlier, only specific nuclear items declared by the state had to be subjected to safeguards according to INFCIRC/66. The INFCIRC/153 on the other hand covers all nuclear material of the state According to Part 1, Paragraph 1 (INFCIRC/153) safeguards are to be applied "*on all source or special fissionable material in all peaceful nuclear activities within its territory, under its jurisdiction or carried out under its control anywhere*". Hence the name: Comprehensive Safeguards Agreements (**CSA**s).[37]

The NWSs have also concluded CSAs, i.e. safeguards agreements according to INFCIRC/153, but they only subjected nuclear material to safeguards which they "chose to offer to the IAEA". These agreements, which "resembled the CSAs" but had limited scope were the so called Voluntary Offer Agreements (**VOAs**). The latter could be interpreted as a success, because at least the NWSs have signed CSAs. „The chief purpose of these agreements was to encourage the non-nuclear-weapon States to accept the NPT by demonstrating that IAEA safeguards would not impede civilian nuclear activities nor place their nuclear programmes at a disadvantage in relation to those of the nuclear weapon States" [38]. But the core problem of different levels of control was not solved.

However, the "peaceful nuclear explosion" of India in 1974 made it clear that nuclear material and technology provided for peaceful purposes could be misused. This led to the increase of the depth of export controls. **Article III.2.** of the NPT states that „*each State Party to the Treaty undertakes not to provide: (a) source or special fissionable material, or (b) equipment or material especially designed or prepared for the processing, use or production of special fissionable material, to any non-nuclear-weapon State for peaceful purposes, unless the source or special fissionable material shall be subject to the safeguards required by this Article*". This meant that technology and material had to be safeguarded at the source. To comply with these measures, a group of major nuclear suppliers which played an important role in trade, convened to establish the Zangger Committee (ZAC) in 1971. Another group of major suppliers, which were parties of the Zangger Committee but not of the NPT was subsequently created. This group came to be known as the Nuclear Suppliers Group with the goal of more effectively controlling single use items ("i.e. nuclear material and other EDP").[39] These will be detailed in the next Chapter.

However, this system did not cover the entire fuel cycle. The inspected state had to agree to the routine inspection. Some nuclear material was allowed to be exempted from verification. The greatest problem of the system at the time was the fact that the system only verified which has been declared to the Agency. This was caused by bad, but accepted practice, the fear of states from the IAEA inspections, and the cautiousness of the Agency. This led to the focus of the safeguards shifting from "the absence of undeclared nuclear material or activities in the state" to "the verification of declared nuclear material. Thus correctness of a state's declarations was verified, not its completeness[40]. Although the CSAs have contained provisions on access to undeclared locations and access to all nuclear material, this was forgotten. This meant that certain "rogue states" could violate the provisions of the NPT, without any means for the IAEA to discover and handle the violation.

However, the discovery of undeclared nuclear material in Iraq, the coming-out of South Africa and the concerns about the nuclear weapons programme of the DPRK made it clear that previous safeguards measures and practice were inadequate.

The reactions were to strengthen the safeguards and export control. In 1992, the NSG has revised its guidelines and included provisions regarding dual-use items, (which could be used for both peaceful and military purposes). Also the NSG has made full-scope safeguards (CSAs) a condition for trading in items on the trigger list.[41]

In 1995, 25 years after the entry into force of the NPT, the 5th Review Conference (RevCon), also known as the

[36] IAEA (1998), p 11
[37] Rockwood (2008) p 84.; iaea.org (06.1972). p. 1.
[38] IAEA (1998) p. 2; Rockwood (2008) p. 85
[39] Rockwood (2008) p. 85. EDP: Especially Designed and Prepared for use, processing etc.
[40] Rockwood (2008) p. 86.
[41] Rockwood (2008) p. 89.

Review and Extension Conference was held. This was one of the most successful RevCons in the history of the NPT. Although a Final Declaration was not adopted, according to Article X, Para 2, the NPT was extended for an indefinite period of time. Also it paved the way for the creation of the third document on safeguards.[42] In September 1997, the **Model Additional Protocol** (AP) to the NPT was adopted, under the name of **INCIRC/540**.

The AP is considered a huge step in strengthening safeguards. It placed the entire fuel cycle under safeguards, like R&D and mines as well (Article 2/a/i, v.). It allowed access to all locations on sites (Article 2/a/iii). Furthermore, the states were obliged to provide "Information regarding the quantities, uses and locations of nuclear material exempted from safeguards" (Article 2/a/vii/a). The AP provides complementary access to the IAEA inspectors. That means access to any place on a site (Article 5/a/i); any location (Article 5/a/ii); and any decommissioned facility or decommissioned location outside facilities where nuclear material was customarily used (Article 5/a/iii). Simplified designation of Agency inspectors, visas, communications and confidentiality were also defined.[43]

Although the AP has broadened the rights of the IAEA to apply safeguards, the traditional problem remains: the different levels of control. Not all states have signed and ratified the AP yet, the AP is currently in force in 127 countries. It is a success, that all 5 NWSs have ratified the AP.[44]

Verdict: Article III can be considered a success. Most of the states are part of any of the three safeguards documents. The safeguards have prevented the wide spread of nuclear material, technology and nuclear weapons. The non-proliferation regime was able to adapt to the difficulties throughout history. The NWSs are not obliged to accept safeguards, but they still have accepted them. However, there are several problematic points. Despite safeguards, Israel, India, Pakistan and North Korea have been able to acquire nuclear weapons. It is another failure of the safeguards system, that Iraq's and South Africa's nuclear weapons programme was discovered at a late stage. The safeguards agreements are still not universal, there are still different levels of control. These issues must be addressed in the future.

5. Article IV.: Inalienable right to peaceful use

Paragraph 1 of Article IV states that: "*Nothing in this Treaty shall be interpreted as affecting the inalienable right of all the Parties to the Treaty to develop research, production and use of nuclear energy for peaceful purposes without discrimination and in conformity with Articles I and II of this Treaty*". *"All Parties to the Treaty […] participate in. the fullest possible exchange of equipment, materials and scientific and technological information for the peaceful uses of nuclear energy*" (Para 2).[45]

This article basically allows the transfer of all nuclear material and technology, to all parties, provided they do not use them for military purposes. There are numerous problems with this. First, to help ensuring the application of Articles I. II., and III., export control regimes have been introduced, to control the transfer of nuclear material and know-how. Sometimes, the export control hinders the application of Article IV. Moreover, most of the items in the trade of nuclear material are dual-use. This proves challenging, and has often meant that states denied the trade in these goods, because their nature makes them useful to violate the NPT. The reasons are mostly political reasons, which the IAEA cannot confirm. This cites resentment among developing countries, because they have the right for nuclear material.

The Coordinating Committee for Multilateral Export Controls (COCOM) was the first regime. Established in 1950, the goal of COCOM was to prevent the states of the Eastern Bloc to obtain advanced western technology. The nuclear sector was a part of COCOM, in the form of the Atomic Energy Control List. The COCOM ceased to exist in 1995, and was subsequently transformed into the Wassenaar Arrangement (WA). The goal of the WA is to promote transparency in the trade of dual use items, complement the existing export control regimes, and enhance cooperation. The Atomic Energy Control List however, has been transferred to the NSG.[46]

The Zangger Committee (ZAC, 1971) named after its Swiss chairman, Claude Zangger published its Trigger List in 1974, which governed the exports of nuclear material and know how to states non-party to the NPT (as well). Trade of items on the Trigger List would "trigger" IAEA safeguards. The Trigger List is known as the INFCIRC/209 document, and has been expanded throughout the years. The items are clarified in its annex. The Zac currently has 39 members.[47]

The Nuclear Suppliers Group (NSG) first met in 1975 and currently has 48 members. The first set of NSG guidelines governs the EDP items, the second the dual use items. The safeguards requirement, just like in the case of the ZAC, is stressed. These goals and provisions have been published in the INFCIRC/254 (1978) document. It has been amended in Warsaw, in 1992 when the dual-use items and the requirement of full scope agreements for trade were added. This is Part 2 of the INFCIRC/254. The reason for this extension was Iraq's clandestine nuclear weapons programme, which has been developed through the use of dual-use items not covered by previous export

[42] Iaea.org (RevCon) (24.07.2016)
[43] Iaea.org (AP) (09.1997) pp. 2-13.
[44] Iaea.org (Status of the AP) (22.07.2016)
[45] Iaea.org (22.05.1970), p. 3.
[46] NTI.org (COCOM) (24.07.2016); NTI.org (Wassenaar) (07.03.2016)
[47] NTI.org (ZAC) (05.04.2016)

control regimes. The new guidelines include 67 categories of dual-use items.[48]

Verdict: Article IV. can be considered a partial success. An adaptive export regime was established throughout the years, which went through extensive revision. Uncontrolled proliferation has been reduced. The problem is, that the export control regimes have been established in reaction to cases like India, Iraq etc. This means that the system is not proactive. Also, there are still cases when Article IV is not respected. The EU still denies the export of dual-use items to Iran, even after a successful Iran deal in 2015. The "inalienable right" is not universally respected, which is a weakness of the NPT.

6. Article V.: Peaceful use of nuclear explosions

According to Article V, "*Each Party to the Treaty undertakes to take appropriate measures to ensure that, […] potential benefits from any peaceful applications of nuclear explosions will be made available to non-nuclear-weapon States Party to the Treaty on a non-discriminatory basis*".[49]

It is arguable whether this article is still relevant or not. The Comprehensive Test Ban Treaty (opened for signature on 24 September 1996) has effectively prohibited all nuclear explosions. The problem is, the CTBT has not yet entered into force, because not all of the 44 States listed in its Annex 2 have ratified it yet. The DPRK, India and Pakistan have not signed the CTBT, and the US, China Egypt, Iran, Israel have not ratified it yet.[50]

Despite the failure of the CTBT (or more like the failure of the aforementioned states), the number of nuclear explosions has gradually decreased. There were treaties which aimed to limit nuclear tests. These were the Partial Test Ban Treaty, and the Threshold Test Ban Treaty. The PTBT, a multilateral treaty was signed in 1963, and banned nuclear tests in the atmosphere, outer space and under water[51]. The TTBT was signed in 1974 and ratified in 1990. It obligated the US and the USSR to limit the yield of test explosions to 150 kilotons[52]. Each NWS has a moratorium for nuclear tests (that they will refrain from nuclear tests) since the 90s[53]. Nowadays, only the DPRK conducts nuclear tests.

The only treaty specifically focusing on peaceful nuclear explosions is the Peaceful Nuclear Explosions Treaty (PNET). Signed in 1976 by Gerard Ford and Leonid Brezhnev, the PNET has allowed the so called group explosions (a number of individual explosions), which could not have an "aggregate yield exceeding 1500 kilotons" (individual explosions could still not exceed 150 kilotons)[54]. Both of them could conduct peaceful nuclear explosions outside of declared zones, (Semipalatinsk and Novaja Zemlja for the USSR, Nevada Desert for the US) where only military purpose nuclear explosions were allowed.[55] Just like the TTBT, the PNET entered into force in 1990.

The problem with nuclear explosions, is that they carry huge risks. They can cause irreversible damage to people, wildlife and the environment. This was the reason for the establishment of many regional treaties in accordance with Article VII, to prevent this damage. This was the reason for the PTBT, TTBT, PNET and the CTBT.

Verdict: This Article was a success, because the test explosions have been limited and eventually banned. This prevents further damage to people, wildlife and the environment, and places a hurdle in the way for proliferators.

7. Article VI.: Cessation of the nuclear arms race and complete nuclear disarmament

The Article VI. of the NPT contains the following provisions: "*Each of the Parties to the Treaty undertakes to pursue negotiations in good faith on effective measures relating to cessation of the nuclear arms race at an early date and to nuclear disarmament, and on a treaty on general and complete disarmament under strict and effective international control.*"[56]

This is one of the most important Articles of the NPT. It is a miracle, that, in the heat of the Cold War, the NWSs, especially the USA and the USSR could reach an agreement about the cessation of the nuclear arms race. Furthermore, a future without nuclear weapons is a goal that was unimaginable to be agreed upon before the NPT. Despite these historical agreements, Article VI. has only reached partial success.

Of these two elements, the cessation of the nuclear arms race was successful. Several treaties have been concluded in good faith to stop the vertical proliferation, the stockpiling and development of nuclear weapons. These series of treaties are the Strategic Arms Limitation Talks (SALT I and II), the Intermediate-Range and Shorter-Range Nuclear Forces Treaty (INF), and the Strategic Arms Reduction Treaty (START I).

The United States and the Soviet Union had the most nuclear weapon stockpiles. These had the potential threat of exterminating humanity in a nuclear war. To avoid this, the two states have started negotiations in 1969, which were brought to fruition on 26 May 1972, when US President Richard Nixon and Soviet Premier Leonid Brezhnev signed

[48] NTI.org (NSG) (08.03.2016)
[49] Iaea.org (22.05.1970), p. 3.
[50] NTI.org (CTBT) (08.06.2015)
[51] NTI.org (PTBT) (26.10.2011)
[52] Armscontrol.org (TTBT) (04.03.2009)
[53] Péczeli/Rózsa (2013) p. 104.
[54] Armscontrol.org (PNET) (04.04.1976)
[55] Péczeli/Rózsa (2013) p. 109.
[56] Iaea.org (22.05.1970), p. 4.

the **SALT I** Treaty in Moscow. It consists of two documents: An Interim Agreement on certain measures limiting strategic offensive arms; and the ABM Treaty on the limitation of strategic defensive systems. Parties to the Agreement were obliged not construct any more intercontinental ballistic missiles (ICBMs) and submarine-launched ballistic missiles (SLBMs). Thus the US could possess only 1054 ICBM launchers and the USSR could possess no more than 1618. Also the US was allowed to have only "*710 SLBM launchers on 44 modern ballistic missile submarines*", and the USSR was allowed to have no more than 950 SLBM launchers on 62 submarines. The Soviets were allowed to have more missiles, because of the advantage of the US in the number of nuclear strike bombers. The ABM Treaty states that there can be only two fixed deployment areas, with no more than 100-100 launchers and interceptors. Verification was managed through the national technical means (NTM) of the parties, also there was no international control. However, "no mechanisms existed to deal with non-compliance"[57]. The SALT I was the first step towards nuclear disarmament (although technically no reduction was prescribed) and the stopping of the nuclear arms race.

On 18 June 1979, another bilateral treaty between the US and the USSR was signed by Jimmy Carter and Leonid Brezhnev in Vienna, the **SALT II**. The parties agreed that they will limit the number of all strategic delivery vehicles to 2250 by 1981. Sub-limits have also been outlined: 1320 launchers of ICBMs and SLBMs equipped with multiple independently targetable re-entry vehicles (MIRV)s, air-to-surface ballistic missiles ASBMs equipped with MIRVs, and heavy bombers; 1,200 launchers of ICBMs and SLBMs equipped with MIRVs, and ASBMs equipped with MIRVs; 820 launchers of ICBMs equipped with MIRVs. Just like by the SALT I, verification was managed through the national technical means (NTM) of the parties, also there was no international control. However, "no mechanisms existed to deal with non-compliance". The SALT II has defined all types of strategic offensive arms, and has set both qualitative and quantitative limitations.[58]

On 8 December 1987, Ronald Reagan and Mikhail Gorbachev signed the "*Treaty between the United States of America and the Union of Soviet Socialist Republics on the Elimination of their Intermediate-Range and Shorter-Range Missiles*" (**Intermediate-Range Nuclear Forces Treaty – INF**) in Washington. The Treaty obligates all parties to eliminate their intermediate-range (1000 to 5500 km) and shorter-range (500 to 1000 km) missiles and their launch systems altogether. Verification is managed through data exchange and notifications through on-site inspections in each other's territory and NTM.[59] Compliance was ensured through the Special Verification Commission[60].

Before the dissolution of the USSR, the Strategic Arms Reduction Treaty was signed by George H. W. Bush and Mikhail Gorbachev on 31 July 1991. It is clear that the focus has shifted from limitation to reduction. The **START I** was the first treaty to reduce the number of strategic nuclear weapons themselves, unlike previous ones, which focused on delivery systems. It has prescribed a reduction of warheads from the 10-12,000 in 1991 to 6000 until the 7th year of entry into force (that is 5 December 2001.) Just like by the INF Treaty, verification is managed through data exchange and notifications through on-site inspections in each other's territory and NTM. [61]

It is clear that the number of nuclear weapons has increased until 1986. In this year, there were all in all 64,449 nuclear weapons[62]. This means that until this point, the SALT I and II were unsuccessful in slowing down the nuclear arms race. The INF and the START I have managed to stop the nuclear arms race.

Three more bilateral treaties have been concluded between the US and Russia on the reduction of nuclear weapons stockpiles. The first one was the failed **START II** (1993), the goal of which was to reduce the nuclear warheads to 3,000-3,500 for each party by 1 January 2003.[63] After the failed START II, the Strategic Offensive Reductions Treaty (**SORT**) was signed in 2002. The goal of SORT was to reduce the number of nuclear warheads to 1700-2200 by 31 December 2012.[64]

On 8 April 2010, the most recent agreement for nuclear arms reduction between the United States and Russia was signed by Barack Obama and Dmitry Medvedev: the **START III**, otherwise known as the **New START**. This Treaty was necessary, because the START I expired in 2009. Upon entry into force of the START III, the SORT will be terminated. The Treaty further reduces the number of warheads for the US and Russia to 1550. As far as verification is concerned, the provisions of the START I apply. The Treaty did not address Russia's concerns about the NATO Missile Shield, which has hindered negotiations.[65]

It is a relevant point that the USA and the USSR/Russia has had by far the most nuclear warheads. Nowadays, these two states are in possession of 94% of the nuclear stockpiles. This means that there can be no nuclear

[57] NTI.org (SALT I) (26.10.2011); Péczeli/Rózsa (2013) pp. 129-131.
[58] NTI.org (SALT II) (26.10.2011); Péczeli/Rózsa (2013) pp. 132-134.
[59] NTI.org (INF) (22.06.2016)
[60] Péczeli/Rózsa (2013) p. 137.
[61] NTI.org (START I) (26.10.2011); Péczeli/Rózsa (2013) pp. 137-141.
[62] Hans M. Kristensen & Robert S. Norris (2013) Global nuclear weapons inventories, 1945–2013, Bulletin of the Atomic Scientists, 69:5, 75-81, DOI: 10.1177/0096340213501363 **p. 78.**
[63] The START II has never entered into force because the US has not ratified it and withdrew from the ABM Treaty in 2002. Because of this, Russia declared the START II null and void. NTI.org (START II) (26.10.2011)
[64] NTI.org (SORT) (26.10.2011)
[65] NTI.org (New Start) (08.07.2016); Péczeli/Rózsa (2013) pp. 144-147.

disarmament, let it be partial or full, without the consent of the USA and Russia. Because of this huge difference, the other NWSs will not reduce their nuclear stockpiles unless the US and Russia do so[66].

Verdict: Article VI. is a partial success. The nuclear arms race was successfully ended.[67] The number of warheads and launch systems have been greatly reduced. Negotiations have been pursued in good faith, although not at all times (see START II and START III). Strict international control has not been achieved, on the contrary, control was left in national hands. However, the full disarmament was not achieved. This is the greatest failure of this Article. There are still many warheads (10,215)[68]. Threshold states like India, Pakistan, Israel and North-Korea have acquired nuclear weapons and do not want to renounce them just like the NWSs. None of them would renounce the nuclear deterrent and the nuclear strike-capabilities, which means that the full nuclear disarmament remains a wish never to be realised.

8. Article VII.: Regional treaties aiming at non-proliferation

The Article VII. of the NPT contains the following provisions: *„Nothing in this Treaty affects the right of any group of States to conclude regional treaties in order to assure the total absence of nuclear weapons in their respective territories."*[69]

Five regional treaties creating nuclear-weapon-free-zones (NWFZs) have been signed and ratified. These are the Tlatelolco Treaty (1967, Mexico), the Rarotonga Treaty (1985, Cook Islands), the Bangkok Treaty (1995, Thailand), the Pelindaba Treaty (1996, South Africa), Central Asian Treaty (2009, Kazakhstan).

The Tlatelolco Treaty has already been mentioned. The **Rarotonga Treaty** established the South Pacific Nuclear Free Zone. It has been signed in Rarotonga on 6 August 1985 and currently has 13 members. Just like by the Tlatelolco Treaty, the Parties of the Rarotonga Treaty refrain from developing nuclear weapons, but peaceful use of nuclear energy is allowed. It also explicitly prohibits the dumping of nuclear material into the sea within the territory of the zone. The main reason for the creation of the NWFZ in the South Pacific was to prevent the nuclear tests in the region, which put the environment, the wildlife and the people in great danger. Verification is managed through "reports and exchanges of information, consultations and review, and the application of IAEA safeguards. The Rarotonga Treaty has three Protocols, none of which has entered in force yet, because the USA has not ratified them yet.[70]

The **Bangkok Treaty** established the Southeast Asia Nuclear Weapon-Free Zone. It has been signed in Bangkok on 15 December 1995 and currently has 10 members. Just like by the Tlatelolco and the Rarotonga Treaty, the Parties of the Bangkok Treaty refrain from developing nuclear weapons, but peaceful use of nuclear energy is allowed. The parties are obliged "*not to develop, manufacture, acquire, or possess any nuclear explosive device*". Also, just like by the Rarotonga Treaty, the Bangkok Treaty explicitly prohibits the dumping of nuclear material into the sea within the territory of the zone. Verification is managed through the Commission for the Southeast Asia Nuclear Weapon-Free Zone. The Bangkok Treaty has one Protocol, but it has not yet entered into force, because none of its parties, the NWSs have signed it yet[71].

The **Pelindaba Treaty** established the African Nuclear-Weapon-Free-Zone (ANWFZ). It was signed on 11 April 1996, but it only entered into force on 15 July 2009. It has 50 Signatory States, but only 39 State Parties. The parties are obliged "not to develop manufacture, acquire, or possess any nuclear explosive device. It is also important, that all member states ensure the prohibition of stationing nuclear weapons in their territory, and the testing of these. Peaceful nuclear activities however, are allowed, provided if under IAEA safeguards, to ensure verification. The reasons for the creation of the ANWFZ are the French nuclear tests in the 60s, and the South African nuclear weapons programme. None of the three protocols of the Pelindaba Treaty has entered into force yet, because the first two were not yet ratified by the USA, and the third one was not yet signed by Spain[72].

The last regional treaty on non-proliferation which has entered into force is the **Central Asian Treaty,** otherwise known as the **Semipalatinsk Treaty**, which established the Nuclear-Weapon-Free Zone in Central Asia (CANWFZ). It has been signed in Semipalatinsk on 15 December 1995, and currently has 5 members. The goals are the same as before: The Parties refrain from developing nuclear weapons, but peaceful use of nuclear energy is allowed. The parties are obliged "*not to develop, manufacture, stockpile or otherwise acquire"* any nuclear explosive device. The reason for the creation of this NWFZ was the dissolution of the SU. The member states presumably wanted no Russian nuclear tests and weapons on their territory. The Treaty has one Protocol about the negative guarantees of the NWSs, but it has not entered into force yet, because the USA has not ratified it. The verification is much

[66] Péczeli/Rózsa (2013) p. 94.
[67] The nuclear arms race has ended quantitatively, meaning that no more nuclear warheads are being created. However, a qualitative arms race (modernisation of existing devices and equipment) is most likely continuing.
[68] Hans M. Kristensen & Robert S. Norris (2013) Global nuclear weapons inventories, 1945–2013, Bulletin of the Atomic Scientists, 69:5, 75-81, DOI: 10.1177/0096340213501363 **p. 78.**
[69] Iaea.org (22.05.1970), p. 4.
[70] UNODA (Rarotonga) (24.07.2016); Péczeli/Rózsa (2013) p. 153
[71] UNODA (Bangkok) (24.07.2016)
[72] NTI.org (Pelindaba) (15.05.2015); UNODA (Pelindaba) (24.07.2016)

stricter as of the previous treaties: All members have to sign a CSA, (INFCIRC/153), and an AP (INFCIRC/540) "*no later than 18 months after the entry into force of this Treaty*". Moreover "*each Party undertakes to apply measures of physical protection to nuclear material*" in accordance with the Convention on Physical Protection of Nuclear Material of 1987. [73]

Verdict: These Treaties are functioning, and have successfully prevented the proliferation. Together, they cover a large portion of the territory of the world, 116 states are to be found in NWFZs[74]. Thus Article VII can be declared a success. However, there were some plans of regional treaties, like establishing a NWFZ on the Arctic, in Central-Europe, in the Korean Peninsula and in the Middle-East which have failed[75]. This does not mean however, that the "*right of any group of States to conclude regional treaties"* is affected. It means that conflicting interests are likely to prevent the establishment of NWFZs. This does not affect the success of Article VII.

9. Successes and failures of the other Articles

Article VIII. Paragraph 3. states that in 5 year intervals, review conferences (RevCons) have to assure "the purposes of the Preamble and the Provisions of the NPT are being realised"[76]. The latest, the ninth RevCon was held in 2015[77].

The success and failure of the RevCons can be measured by adopting a Final Declaration with consensus. This did not happen in 1980, 1990, 1995 and 2005[78]. That would mean a partial success of Article 3. Para 3.

However, the adoption of Final Declarations does not make RevCons successful or failed. The Review and Extension Conference in 1995, held 25 years after the entry into force of the NPT was a clear success. It not only paved the way for the Additional Protocol, but has extended the legal force of the NPT, thus making Article X. Paragraph 2. a success. But a Final Declaration was not adopted.[79]

Although the withdrawal of the DPRK from the NPT in 2003 was in accordance with Article X. Para 1., this still cannot be deemed a success of the NPT.

Conclusion

This essay examined the successes and failures of the Non-Proliferation Treaty. Historical examples and developments have been used to determine the success or failure of the NPT on a case by case basis. After the presentation of the brief history of events culminating in the establishment of the NPT, the first seven articles of the NPT have been thoroughly examined. Examples regarding the successes and failures of the specific Articles have been presented. After that, the remaining, more important Articles have been examined.

As a method of research, the open-access data of the IAEA, think-tanks and experts have been used. The reason for this was the secrecy regarding nuclear weapons. It would be worth looking into this topic with the knowledge of secret data. Expansion of the research with the understanding of the motives of key people, policy makers would also be beneficial.

The key findings are the following: The NPT is the core of the international non-proliferation system. The need of averting a nuclear war and the spread of nuclear weapons and states with nuclear weapons have led to its creation. It has gone through evolution since its entry into force, facing and adapting to the new and new challenges of non-proliferation.

The NPT has lived up to its task. In other words, the NPT has been a success. It has been there for 46 years, it is still in force, and will be indefinitely. It has achieved near universality. No nuclear weapons have been handed over by the NWSs to NNWSs. The NPT has managed to keep the number of threshold states to a minimum. It was also able to reverse some cases like South Africa and Iran. A complex system of safeguards and verification has been developed and mostly implemented. The inalienable right to peaceful use has been, in the most cases respected. The number of nuclear explosions have been reduced. The nuclear arms race has been stopped. Several regional treaties banning nuclear weapons and tests have been concluded.

However, the NPT is not free of flaws. In other words, there are failures of the NPT. The greatest failure of the NPT is that it was unable to achieve complete nuclear disarmament. Also, the NPT was unable to prevent some states from developing nuclear weapons themselves. The problem of different levels of control regarding safeguards and verification make universal compliance with the NPT hard to check.

The overall effectiveness of the NPT is determined by its ability to prevent proliferation. If there are deviating interests of some states, especially the UNSC permanent members this ability is hindered. Furthermore, many threshold states have acquired nuclear weapons to deter threats to their sovereignty. If the UN was able to channel all interests and ensure a peaceful world, the chances of proliferation would be minimal. Essentially, the successes and problems of the NPT are those of the UN.

[73] UNODA (Semipalatinsk) (24.07.2016); Péczeli/Rózsa (2013) p. 157
[74] Péczeli/Rózsa (2013) p. 150.
[75] Péczeli/Rózsa (2013) p. 160-163.
[76] Iaea.org (22.05.1970), p. 4.
[77] Iaea.org (RevCon) (24.07.2016)
[78] Wan (10.03.2015)
[79] Iaea.org (RevCon) (24.07.2016), Iaea.org (22.05.1970), p. 5.

Non-proliferation is our common goal. Therefore, the NPT needs to be adapted to meet future challenges. The NPT is a good framework of non-proliferation. However, it depends on both the states and the people to determine what picture will be put into the frame.

Highlights:

- The NPT is successful but it has some flaws.
- NWSs have neither handed over nuclear weapons, nor encouraged NNWSs to acquire them.
- Most NNWs have not acquired nuclear weapons and have not pursued them. Of those which did, the case of Iraq and South Africa has been successfully solved.
- A functioning safeguards system has been created, which has adapted to historical circumstances. However, the different levels of control are still problematic.
- The inalienable right to peaceful use of nuclear power was mostly respected. Export control regimes have been created to verify peaceful use.
- Nuclear explosions have been greatly reduced.
- The nuclear arms race has been stopped, but complete nuclear disarmament was not achieved.
- Five regional treaties have banned nuclear weapons from a large portion of the world.

References

Armscontrol.org (03.2014): The Lisbon Protocol At a Glance. https://www.armscontrol.org/print/3289 (Retrieved: 24.07.2016)

Armscontrol.org (04.03.2009): Treshold Test Ban Treaty (TTBT). https://www.armscontrol.org/act/2009_03/Looking-Back_Ifft (Retrieved: 24.07.2016)

Armscontrol.org (04.04.1976): Peaceful Nuclear Explosions Treaty (PNET). https://www.armscontrol.org/documents/pnet (Retrieved: 24.07.2016)

Armscontrol.org (10.2015): Nuclear Weapons: Who Has What at a Glance https://www.armscontrol.org/factsheets/Nuclearweaponswhohaswhat (Retrieved: 24.07.2016)

Armscontrol.org (29.04.2015): Timeline of the Treaty on the Non-Proliferation of Nuclear Weapons (NPT) https://www.armscontrol.org/factsheets/Timeline-of-the-Treaty-on-the-Non-Proliferation-of-Nuclear-Weapons-NPT (Retrieved: 24.07.2016)

Brookings (14.07.2016): The Iran deal, one year out: What Brookings experts are saying. http://www.brookings.edu/blogs/markaz/posts/2016/07/14-iran-deal-anniversary-experts (Retrieved: 24.07.2016)

Fas.org (24.07.2016): Nuclear Non-Proliferation Treaty [NPT] – Background. http://fas.org/nuke/control/npt/back.htm (Retrieved: 24.07.2016)

Iaea.org (06.1972): The Structure and Content of Agreements between the Agency and the States required in connection with the Treaty on the Non-Proliferation of Nuclear Weapons (CSAs). https://www.iaea.org/sites/default/files/publications/documents/infcircs/1972/infcirc153.pdf (Retrieved: 24.07.2016)

Iaea.org (09.1997): Model Protocol Additional to the Agreement(s) between State(s) and the International Atomic Energy Agency for the Application of Safeguards. https://www.iaea.org/sites/default/files/infcirc540.pdf (Retrieved: 24.07.2016)

Iaea.org (22.05.1970): INFCIRC/140: TREATY ON THE NON-PROLIFERATION OF NUCLEAR WEAPONS. https://www.iaea.org/sites/default/files/publications/documents/infcircs/1970/infcirc140.pdf (Retrieved: 24.07.2016)

Iaea.org (22.07.2016): Status of the Additional Protocol. https://www.iaea.org/safeguards/safeguards-legal-framework/additional-protocol/status-of-additional-protocol (Retrieved: 24.07.2016)

Iaea.org (24.07.2016): NPT Review Conferences (RevCon). https://www.iaea.org/newscenter/focus/npt/npr-review-conferences (Retrieved: 24.07.2016)

Iaea.org (26.02.2016): Member States. https://www.iaea.org/about/memberstates (Retrieved: 24.07.2016)

IAEA (1998): The Evolution of the IAEA safeguards. https://www.jaea.go.jp/04/iscn/iscn_old/resource/Evolution%20of%20Safeguards%201998.pdf (Retrieved: 24.07.2016)

Kamp, Karl Heinz/Remkes, Robertus C.N. (24.07.2016): Options for NATO Nuclear Sharing Arrangements. http://www.nti.org/media/pdfs/NTI_Framework_Chpt4.pdf?_=1322701823

Kristensen, Hans M./ Norris, Robert S. (2013) Global nuclear weapons inventories, 1945–2013, Bulletin of the Atomic Scientists, 69:5, 75-81, DOI: 10.1177/0096340213501363 http://www.tandfonline.com/doi/full/10.1177/0096340213501363 (if it does not work, then http://thebulletin.org/2013/september/global-nuclear-weapons-inventories-1945-2013 (Retrieved: 24.07.2016)

Norris, Robert S./Kristensen, Hans M. (2011) US tactical nuclear weapons in Europe, 2011, Bulletin of the Atomic Scientists, 67:1, 64-73, DOI: 10.1177/0096340210393931 http://www.tandfonline.com/doi/full/10.1177/0096340210393931 (if it does not work, then http://thebulletin.org/2011/january-february/us-tactical-nuclear-weapons-europe-2011 (Retrieved: 24.07.2016)

NTI.org (03.2016): Iran country profile: Nuclear. http://www.nti.org/learn/countries/iran/nuclear/ (Retrieved: 24.07.2016)

NTI.org (04.2015): India country profile: Nuclear. http://www.nti.org/learn/countries/india/nuclear/ (Retrieved: 24.07.2016)

NTI.org (04.2016): Israel country profile: Nuclear. http://www.nti.org/learn/countries/israel/nuclear/ (Retrieved: 24.07.2016)

NTI.org (04.2016): North Korea country profile: Nuclear. http://www.nti.org/learn/countries/north-korea/nuclear/ (Retrieved: 24.07.2016)

NTI.org (04.2016): Pakistan country profile: Nuclear. http://www.nti.org/learn/countries/pakistan/nuclear/ (Retrieved: 24.07.2016)

NTI.org (05.04.2016): Zangger Committee (ZAC). http://www.nti.org/learn/treaties-and-regimes/zangger-committee-zac/ (Retrieved: 24.07.2016)

NTI.org (07.03.2016): Wassenaar Arrangement. http://www.nti.org/learn/treaties-and-regimes/wassenaar-arrangement/ (Retrieved: 24.07.2016)

NTI.org (07.2015): Iraq country profile: Nuclear. http://www.nti.org/learn/countries/iraq/nuclear/ (Retrieved: 24.07.2016)

NTI.org (07.2015): Iraq country profile: Overview. http://www.nti.org/learn/countries/iraq/ (Retrieved: 24.07.2016)

NTI.org (08.03.2016): Nuclear Suppliers Group (NSG). http://www.nti.org/learn/treaties-and-regimes/nuclear-suppliers-group-nsg/ (Retrieved: 24.07.2016)

NTI.org (08.06.2015): Comprehensive Nuclear-Test-Ban Treaty (CTBT). http://www.nti.org/learn/treaties-and-regimes/comprehensive-nuclear-test-ban-treaty-ctbt/ (Retrieved: 24.07.2016)

NTI.org (09.2015): South Africa country profile: Nuclear. http://www.nti.org/learn/countries/south-africa/nuclear/ (Retrieved: 24.07.2016)

NTI.org (15.05.2015): African Nuclear Weapon Free Zone Treaty (Pelindaba Treaty) http://www.nti.org/learn/treaties-and-regimes/african-nuclear-weapon-free-zone-anwfz-treaty-pelindaba-treaty/ (Retrieved: 24.07.2016)

NTI.org (22.06.2016): Intermediate-Range Nuclear Forces Treaty. http://www.nti.org/learn/treaties-and-regimes/treaty-between-the-united-states-of-america-and-the-union-of-soviet-socialist-republics-on-the-elimination-of-their-intermediate-range-and-shorter-range-missiles/ (Retrieved: 24.07.2016)

NTI.org (24.07.2016): Coordinating Committee for Multilateral Export Controls (COCOM). http://www.nti.org/learn/glossary/#coordinating-committee-multilateral-export-controls (Retrieved: 24.07.2016)

NTI.org (26.10.2011): Partial Test Ban Treaty (PTBT). http://www.nti.org/learn/treaties-and-regimes/treaty-banning-nuclear-test-atmosphere-outer-space-and-under-water-partial-test-ban-treaty-ptbt/ (Retrieved: 24.07.2016)

NTI.org (26.10.2011): Strategic Arms Limitation Talks (SALT I). http://www.nti.org/learn/treaties-and-regimes/strategic-arms-limitation-talks-salt-i-salt-ii/ (Retrieved: 24.07.2016)

NTI.org (26.10.2011): Strategic Arms Limitation Talks (SALT II). http://www.nti.org/learn/treaties-and-regimes/strategic-arms-limitation-talks-salt-ii/ (Retrieved: 24.07.2016)

NTI.org (26.10.2011): Strategic Arms Reduction Treaty (START I) http://www.nti.org/learn/treaties-and-regimes/treaties-between-united-states-america-and-union-soviet-socialist-republics-strategic-offensive-reductions-start-i-start-ii/ (Retrieved: 24.07.2016)

NTI.org (26.10.2011): Strategic Arms Reduction Treaty (START II) http://www.nti.org/learn/treaties-and-regimes/treaty-between-united-states-america-and-union-soviet-socialist-republics-strategic-offensive-reductions-start-ii/ (Retrieved: 24.07.2016)

NTI.org (26.10.2011): Strategic Offensive Reductions Treaty (SORT). http://www.nti.org/learn/treaties-and-regimes/strategic-offensive-reductions-treaty-sort/ (Retrieved: 24.07.2016)

Péczeli, Anna/Rózsa, N. Erzsébet (2013): Chapter 4.: Nukleáris fegyverek. In: Péczeli Anna/Rózsa, N. Erzsébet: Egy békésebb világ eszközei. Osiris Kiadó, 2013.

Rockwood, Laura (2008): Safeguards and Nonproliferation: The First Half-Century from a Legal Perspective. In: G. Janssens-Maenhout: Nuclear Safeguards and Non-Proliferation, Course Syllabus, European Communities, 2009

UNODA (24.07.2016): Additional Protocol II to the Treaty for the Prohibition of Nuclear Weapons in Latin America and the Caribbean (Tlatelolco Treaty). http://disarmament.un.org/treaties/t/tlateloco_p2/text (Retrieved: 24.07.2016)

UNODA (24.07.2016): African Nuclear Weapon Free Zone Treaty (Pelindaba Treaty) http://disarmament.un.org/treaties/t/pelindaba (Retrieved: 24.07.2016)

UNODA (24.07.2016): South Pacific Nuclear Free Zone Treaty (Rarotonga Treaty). http://disarmament.un.org/treaties/t/rarotonga (Retrieved: 24.07.2016)

UNODA (24.07.2016): Treaty for the Prohibition of Nuclear Weapons in Latin America and the Caribbean (Tlatelolco Treaty). http://disarmament.un.org/treaties/t/tlatelolco (Retrieved: 24.07.2016)

UNODA (24.07.2016): Treaty on a Nuclear-Weapon-Free-Zone in Central Asia (Semipalatinks Treaty). http://disarmament.un.org/treaties/t/canwfz (Retrieved: 24.07.2016)

UNODA (24.07.2016): Treaty on the Non-Proliferation of Nuclear Weapons. http://disarmament.un.org/treaties/t/npt (Retrieved: 24.07.2016)

UNODA (24.07.2016): Treaty on the Southeast Asia Nuclear Weapon-Free Zone (Bangkok Treaty). http://disarmament.un.org/treaties/t/bangkok (Retrieved: 24.07.2016)

Wan, Wllfred (10.03.2015): Why the NPT Review Conference Outcome Matters. http://cpr.unu.edu/why-the-npt-review-conference-outcome-matters.html (Retrieved: 24.07.2016)

Zarroli, Jim (26.01.2016): As Sanctions On Iran Are Lifted, Many U.S. Business Restrictions Remain. http://www.npr.org/sections/parallels/2016/01/26/464435805/as-sanctions-on-iran-are-lifted-many-u-s-business-restrictions-remain (Retrieved: 24.07.2016)

Zoll.de (24.07.2016): Transit of dual-use items. https://www.zoll.de/EN/Businesses/Movement-of-goods/Transit/Restrictions/Dual-use-items/dual-use-items_node.html (Retrieved: 24.07.2016)

KJ-BB-17-054-EN-N

https://esarda.jrc.ec.europa.eu